

The Higgs Triplet Model: mixing in the neutral sector,
vector-like fermions, and dark matter

Sahar Bahrami

A Thesis
In the Department
of
Physics

Presented in Partial Fulfillment of the Requirements
For the Degree of
Doctor of Philosophy (Theoretical Particle Physics) at
Concordia University
Montreal, Quebec, Canada

July 2016

©Sahar Bahrami, 2016

**CONCORDIA UNIVERSITY
SCHOOL OF GRADUATE STUDIES**

This is to certify that the thesis prepared

By: **Sahar Bahrami**

Entitled: **The Higgs Triplet Model: mixing in the neutral sector, vector-like fermions, and dark matter**

and submitted in partial fulfillment of the requirements for the degree of

DOCTOR OF PHILOSOPHY (Theoretical Particle Physics)

complies with the regulations of the University and meets the accepted standards with respect to originality and quality.

Signed by the final Examining Committee:

_____ Chair
Wei Sun

_____ External Examiner
Heather Logan

_____ External to Program
Guillame Lamoureux

_____ Examiner
Pablo Bianucci

_____ Examiner
Panagiotis Vasilopoulos

_____ Thesis Supervisor
Mariana Frank

Approved by

Pablo Bianucci, Graduate Program Director

Abstract

The Higgs Triplet Model: mixing in the neutral sector, vector-like fermions, and dark matter

Sahar Bahrami, Ph.D.

Concordia University, 2016

The inability to predict neutrino masses and the existence of Dark Matter (DM) are two essential shortcomings of the Standard Model. This thesis is a phenomenological study of a Beyond the Standard Model (BSM) scenario, Higgs Triplet Model (HTM) and effects of introducing vector-like leptons and quarks on the Higgs sector in the model. The Higgs Triplet Model provides an elegant resolution to the first problem via the seesaw mechanism. Introducing a full representation of vector-like leptons can solve the DM problem of the HTM by assigning a vector-like neutrino to be the DM candidate. As a result, two important problems in SM will be resolved.

Within this context, after a review of the main concepts, we first revisit the neutral Higgs sector of the Higgs Triplet Model. We show that, under general considerations, an unmixed neutral Higgs boson cannot have an enhanced decay branching ratio into $\gamma\gamma$ with respect to the Standard Model one, while an enhancement is possible for the mixed case, but only for the heavier of the two neutral Higgs bosons. We then analyze the implications of introducing vector-like leptons in the Higgs Triplet Model. We show that, if the vector-like leptons are allowed to be relatively light, they enhance or suppress the decay rates of loop-dominated neutral Higgs bosons decays $H \rightarrow \gamma\gamma$ and $H \rightarrow Z\gamma$, as well as alter the decay patterns of the doubly-charged Higgs bosons, modifying the restrictions on their masses. We also look at the effects of vector-like quarks (singlets, doublets or triplets) in the Higgs Triplet Model. Though the new Higgs in the model couple to leptons only, some vector-like quarks help

improve electroweak precision measurements and thus lift the mass of the doubly charged Higgs boson to within experimental limits. We also study the effects of introducing the vector-like quarks on the loop-dominated neutral Higgs decays.

We show that introducing vector-like leptons in the model also provides a resolution to the problem of Dark Matter. We investigate the invisible decay width of the Higgs boson and the electroweak precision variables, and impose restrictions on model parameters. We analyze the relic density constraint and calculate the cross sections for indirect and direct dark matter detection. With appropriate parameter restrictions, the Higgs Triplet Model with vector-like fermions is rendered completely consistent with the data.

Dedicated to my mother, Zhila

Acknowledgements

I would like to express my gratitude to the people who helped me to make this work possible.

My first and foremost thanks go to my supervisor Prof. Mariana Frank. Thank you Dr. Frank. I learned a lot from you. No matter where I go, you will be always my supervisor. I am so thankful for all your support, advice and kindness.

Thank you Dr. Champagne for the research environment that you create in the department of physics at Concordia University. I would like to thank our graduate program director, Dr. Bianucci. And I would like to thank Dr. Laszlo Kalman.

Thank you Prof. Pukhov for your time and answering my questions about MicrOmegas. Thank you Prof. Fuks for your help to solve some issues related to my FeynRules file.

Thank you Prof. Logan, Prof. Vasilopoulos and Dr. Bianucci for correcting my thesis, your painstaking efforts in reading the drafts are greatly appreciated.

Thanks to my mother for her unconditional love, care and sacrifice. And thank you Gareth for all your help.

Contribution of the Author

The original research work contained in this thesis is presented in Chapters 3 , 4 , 5 and 6. The research in Chapters 3 has been conducted in collaboration with Prof. Mariana Frank and Dr. Arbabifar and has been published in [1]. Chapters 4 , 5 and 6 are prepared in collaboration with Prof. Mariana Frank and have been published in [2-5].

In Chapters 3 , 4 , 5 and 6 , some of the analytical and all computational calculations which lead to the final results of the research as well as the production of the graphs was conducted by the author in partial fulfillment of the requirements for the degree of doctor of philosophy in the Department of Physics at Concordia University, Montreal, Quebec.

Contents

List of Figures	xii
List of Tables	xiii
List of Acronyms	xiv
List of Acronyms	xv
1 Introduction	1
1.1 Overview	1
1.2 Motivations for Looking For New Physics Beyond the Standard Model	2
1.3 Organization of this thesis	6
2 The Standard Model of Particle Physics	8
2.1 A Brief Overview of SM	8
2.1.1 The Particle Content	8
2.1.2 The Lagrangian	10
2.1.3 Electroweak Symmetry Breaking and the Higgs Mechanism	14
2.2 Higgs-Boson Physics at the LHC	17
2.2.1 Higgs-Boson Production at the LHC	17
2.2.2 Decay of the Higgs boson	18
2.2.3 Discovery of a Higgs Boson at the LHC	20
2.3 Searches for Physics Beyond the Standard Model	21
2.3.1 Vector-like Fermions	22
2.3.2 Dark Matter	23
3 Neutral Higgs Bosons in the Higgs Triplet Model	25
3.1 Introduction	25

3.2	The Higgs Triplet Model	28
3.2.1	Positivity Conditions on the Higgs potential	31
3.3	Decay rates of the neutral Higgs bosons in the HTM	32
3.3.1	Decay rates to $\gamma\gamma$	32
3.3.2	Branching ratios enhancement due to Higgs widths in HTM	35
3.3.3	Tree-level decays of the Higgs bosons into fermions and gauge bosons	36
3.4	Analysis of the decays of h and H	38
3.4.1	$\gamma\gamma$ decays for mixed neutral Higgs	39
3.4.2	Tree-level decays for Scenarios 1, 2 and 3	45
3.4.3	Predictions for H and h decay width to $Z\gamma$	46
3.5	Conclusions	49
4	Vector-like Leptons in the Higgs Triplet Model	53
4.1	Introduction	53
4.2	The Model	55
4.3	Production and Decays of the Neutral Higgs Boson	59
4.3.1	$h \rightarrow \gamma\gamma$	59
4.3.2	$h \rightarrow Z\gamma$	66
4.4	Production and Decays of the Doubly-Charged Higgs Bosons	70
4.5	Conclusions	74
5	Vector-like Quarks in the Higgs Triplet Model	78
5.1	Introduction	78
5.2	The Model	80
5.2.1	Higgs Triplet Model	80
5.2.2	Higgs Triplet Model with Vector-Like Quarks	82
5.3	Electroweak Constraints	85
5.3.1	Contributions to the S, T and U -parameters in the HTM	86
5.3.2	Vector-Like Quark contributions to the S and T parameters	91
5.3.3	Restrictions on doubly charged Higgs boson and vector-like quarks masses	92
5.4	Effect of vector quarks on $H \rightarrow \gamma\gamma$ and $H \rightarrow Z\gamma$	96
5.5	Appendix	103
5.6	Conclusions	105
6	Dark Matter in the Higgs Triplet Model	108
6.1	Introduction	108

6.2 The Higgs Triplet Model with Vector-like Leptons 112

6.3 Vector-like lepton contributions to the S and T parameters 116

6.4 Invisible decay width of the Higgs boson 120

6.5 Dark Matter Relic Density 122

6.6 Direct Detection 123

6.7 Indirect Detection 126

6.8 Detection at Particle Colliders 128

6.9 The Flux of Muons and Neutrinos from the Sun 130

6.10 Conclusions 130

7 Conclusions and Outlook 134

List of Figures

2.1	The Higgs (Mexican Hat) Potential	15
2.2	The Higgs production modes.	17
2.3	Standard Model Higgs boson decay branching ratios	19
2.4	The ATLAS upper limits on the WIMP-nucleon scattering cross section	24
3.1	Values of the singly and doubly charged Higgs masses in Scenario 1	41
3.2	Decay rates for $h \rightarrow \gamma\gamma$ and $H \rightarrow \gamma\gamma$ in Scenario 1	42
3.3	Values of the singly and doubly charged Higgs masses in Scenario 2	43
3.4	Decay rates for $h \rightarrow \gamma\gamma$ and $H \rightarrow \gamma\gamma$ in Scenario 2	44
3.5	Decay rates for $h/H \rightarrow \gamma\gamma$ in Scenario 3	45
3.6	Relative branching Ratios for $h/H \rightarrow f\bar{f}$, WW^* , ZZ^* in Scenarios 1, 2 and 3	47
3.7	Relative Branching Ratios for $h/H \rightarrow Z\gamma$ for Scenario 1 and 2	50
3.8	Relative Branching Ratios for $h/H \rightarrow Z\gamma$ in Scenario 3	51
4.1	Relative decay rate $R_{h \rightarrow \gamma\gamma}$ as a function of m'_E for various values of doubly charged Higgs bosons mass	61
4.2	Constant $R_{h \rightarrow \gamma\gamma}$ in the plane of the explicit mass terms for various values of doubly-charged Higgs bosons mass	63
4.3	Dependence of $R_{h \rightarrow \gamma\gamma}$ on the Yukawa couplings and vector-like lepton masses	64
4.4	Relative decay rate for $R_{h \rightarrow \gamma Z}$ as a function of m'_E for different values of doubly-charged Higgs masses, in the case of no mixing	68
4.5	$R_{XY} = \sigma(pp \rightarrow H^{\pm\pm}H^{\mp\mp}) \times BR(H^{\pm\pm} \rightarrow XY)$ as a function of the doubly charged Higgs boson mass for Condition 1	76
4.6	$R_{XY} = \sigma(pp \rightarrow H^{\pm\pm}H^{\mp\mp}) \times BR(H^{\pm\pm} \rightarrow XY)$ as a function of doubly charged Higgs boson mass for Condition 2	77
5.1	The contribution to the T and S parameters in the HTM	90

5.2	The allowed variation of the T parameter for the \mathcal{D}_1 and \mathcal{D}_X models	93
5.3	The contribution to the T parameter in the HTM with vector-like quarks for the \mathcal{D}_1 and \mathcal{D}_X models with the fixed values of $x_{b(t)}$	95
5.4	The contribution to the T parameter in the HTM with vector quarks for the \mathcal{D}_1 and \mathcal{D}_X models with the fixed values of the vector quark mass	97
5.5	The relative strength of the Higgs diphoton decay $R_{\gamma\gamma}$, including the restrictions of the T parameter for the \mathcal{D}_1 , \mathcal{D}_X , \mathcal{D}_Y , \mathcal{T}_X , \mathcal{D}_2 and \mathcal{U}_1 scenarios	101
5.6	The relative strength of the decay of the Higgs boson into a photon and a Z-boson, $R_{Z\gamma}$, including the restrictions of the T parameter for the \mathcal{D}_1 , \mathcal{D}_X , \mathcal{D}_Y , \mathcal{T}_X , \mathcal{D}_2 and \mathcal{U}_1 scenarios	102
6.1	The contribution to the T parameter in the HTM with vector-like leptons, as a function of the doubly charged Higgs mass and the mixing angle, for fixed values of the neutrino Yukawa coupling	119
6.2	The contribution to the T parameter in the HTM with vector-like leptons as a function of the parameters of the model	119
6.3	The invisible branching ratio of Higgs boson (BR_{inv}) in the HTM with vectorlike leptons, as functions of the dark matter mass and the neutrino Yukawa coupling	121
6.4	The correct relic density of dark matter, as a function of the dark matter mass and the neutrino Yukawa coupling in the HTM with vector-like leptons	123
6.5	The spin-dependent cross section of the nucleons in the HTM with vector-like leptons, as functions of the dark matter mass and Yukawa coupling, in the case of no mixing	125
6.6	The spin-independent (SI) cross section of nucleon, as a function of the dark matter mass and Yukawa coupling, in the case of no mixing, including the experimental constraints	127
6.7	The annihilation cross section as a function of the dark matter mass and its Yukawa coupling including the experimental constraints	129
6.8	The flux of neutrinos and muons in the HTM with vectorlike leptons, as functions of the dark matter mass and Yukawa coupling including the experimental constraints	131

List of Tables

2.1	Particle content of the SM with their gauge group representation and hypercharges.	9
2.2	Summary of the results of searches for invisible decays of the Higgs particle. . .	19
2.3	Compilation of measured signal strengths, μ and statistical significances, z , for different decay channels of the Higgs boson.	21
3.1	Experimental data from LHC and the Tevatron for the boson at 125 GeV . . .	39
4.1	Range of the ratio $R_{h \rightarrow \gamma\gamma}$, as defined in the text, for the doubly charged Higgs mass (in columns) and the neutral Higgs mixing angle $\sin \alpha$ (in rows), for Dirac vector-like lepton masses in the range $M_E, M_L \in (100 - 500)$ GeV, with $h'_E = 0.8$	65
4.2	Same as in Table 4.1, but also allowing $h'_E \in (0 - 3)$	65
4.3	Range of the ratio $R_{h \rightarrow Z\gamma}$, as defined in the text, for doubly charged Higgs mass (in columns) and neutral Higgs mixing angle $\sin \alpha$ (in rows), for Dirac vector lepton masses in the range $M_E, M_L \in (100 - 500)$ GeV, with $h'_E = 0.8$	69
4.4	Same as in Table 4.3, but also allowing $h'_E \in (0 - 3)$	69
5.1	Representations of vector-like quarks, with quantum numbers under $SU(2)_L \times U(1)_Y$.	83
5.2	Current mass lower limits on vector-like quark masses in various representations. . .	86
5.3	Mass limits on doubly charged Higgs bosons from LHC at $\sqrt{s} = 7$ TeV, $\mathcal{L} = 4.7 \text{ fb}^{-1}$. Here BP1, BP2, BP3 and BP4 stand for four CMS benchmarks in type II see-saw scenarios, obtained with branching fractions into several di-lepton combinations. . .	89
5.4	<i>Neutral current parameters f_L and f_R for vector-like quarks Z interaction.</i>	100
5.5	Couplings to the W and Z bosons	104
5.6	Couplings to the Higgs bosons	105
6.1	Representations of vector-like leptons, together with their quantum numbers under $SU(3)_C \times SU(2)_L \times U(1)_Y$	112

List of Acronyms

AMS	Alpha Magnetic Spectrometer
ATLAS	A Toroidal LHC ApparatuS
BSM	Beyond the Standard Model
CERN	European Organization for Nuclear Research
CKM	Cabibbo-Kobayashi-Maskawa
C.L	Confidence Level
CMS	Compact Muon Solenoid
CP	Charge conjugation and Parity
DESY	Deutsches Elektronen-Synchrotron
DM	Dark Matter
EW	Electroweak
Fermi-LAT	Fermi Large Area Telescope
GUT	Grand Unified Theory
HERA	Hadron Electron Ring Accelerator
HTM	Higgs Triplet Model
LEP	Large Electron-Positron Collider
LHC	Large Hadron Collider
LO	Leading Order
NLO	Next-to-Leading Order
PAMELA	Payload for Antimatter Matter Exploration and Light-nuclei Astrophysics
PDG	Particle Data Group
QCD	Quantum Chromodynamics
SD	Spin-Dependent
SI	Spin-Independent
SM	Standard Model
SSB	Spontaneous Symmetry Breaking
VBF	Vector Boson Fusion

List of Acronyms

VEV	Vacuum Expectation Value
WIMP	Weakly Interacting Massive Particle
WMAP	Wilkinson Microwave Anisotropy Probe

Chapter 1

Introduction

1.1 Overview

The Standard Model (SM) of particle physics, developed in the 1970's, which summarizes our present knowledge of the basic constituents of matter and their interactions, has been tested by many experiments over the last four decades and has been shown to successfully describe high energy particle interactions [6].

In 1967, Weinberg [7], Salam [8] and Glashow [9] formulated a successful model for electroweak interactions, which, after adding strong interactions constitutes what is now known as the SM of particle physics [10]. The quantum theory of strong interactions is described by Quantum Chromodynamics (QCD). The Standard Model is a gauge invariant quantum field theory based on the symmetry group $SU(3)_C \times SU(2)_L \times U(1)_Y$, with the colour group $SU(3)_C$ for the strong interaction between the colored quarks and with the gauge symmetry group $SU(2)_L \times U(1)_Y$ of weak left-handed isospin and hypercharge for the electroweak interaction, spontaneously broken by the Higgs mechanism [11–13]. The left handed fermions form $SU(2)_L$ doublets and the right handed fermions are $SU(2)_L$ singlets. The fermions of the theory are leptons and quarks. The photon and gluon are gauge fields which are massless. The other gauge fields acquire masses by the spontaneous breaking of gauge symmetry, via the Higgs mechanism, and become the massive W^+ , W^- , and Z^0 bosons. With the discovery of neutral currents in 1973 [14, 15], the discovery of charmonium in 1974 [16, 17], the discoveries of the W and Z^0 particles in 1983 [18, 19] and subsequent detailed measurements, the predictions of the Standard Model have been tremendously successful [20]. A remnant scalar field, the Higgs boson, is part of the physical spectrum [21, 22] and is needed to give masses to fermions,

and gauge bosons through symmetry breaking.

Spontaneous breaking of gauge symmetry was introduced into particle physics in 1964 by Englert and Brout [23], followed independently by Higgs [24, 25], and subsequently by Guralnik, Hagen and Kibble [26]. The existence of a massive scalar particle was mentioned by Higgs in [24]. Later, in another important paper [27], he derived explicitly the Feynman rules for processes involving decay of the massive Higgs boson into 2 massive vector bosons, vector-scalar scattering and scalar-scalar scattering [28].

The Higgs boson has been one of the primary scientific goals of the CMS and ATLAS detectors at the Large Hadron Collider (LHC) at CERN. On 4 July 2012, the ATLAS [6] and CMS [29] collaborations announced that the search for the Standard Model Higgs boson in proton-proton collisions with the ATLAS and CMS experiments at the LHC presented a clear evidence for the production of a neutral boson with a measured mass of near 125 GeV. The expected significance for a SM Higgs boson of that mass was 5.8 standard deviations. Although these results are consistent, within uncertainties, with expectations for the SM Higgs boson, the collection of further data will be needed to assess its nature in detail and to investigate whether the properties of the new particle imply physics beyond the SM.

1.2 Motivations for Looking For New Physics Beyond the Standard Model

The SM is the effective theory of elementary particles which is validated by a large number of experimental tests, up to a certain energy scale Λ , called the cut-off. The discovery of the Higgs boson completes the validation of the Standard Model. However there is the general belief that the SM cannot be the ultimate theory of fundamental physics since it leaves still many questions unanswered. We list here the shortcomings of the SM and some evidence for New physics Beyond the SM (BSM).

- Dark matter

It is known that approximately 5% of the matter in the Universe is formed of atoms, 27% of the total mass of our universe is made of non-luminous matter, called Dark matter (DM), that does not emit or reflect electromagnetic radiation, and the rest is dark energy. The reason researchers know DM exists is because of the gravitational effect it seems to have on visible matter. The first evidence of Dark Matter was postulated in

astrophysics¹ in a study related to the search of orbital velocities of stars in the Milky Way. Nowadays, DM evidence is confirmed by several astrophysical observations. DM is not accounted for in the SM. Although we do not know for certain how the DM came to be formed, a sizable relic abundance of weakly interacting massive particles (WIMPs) is generally expected to be produced as a by-product of our universe. WIMPs are neutral, stable or long-lived (with respect to cosmic time-scales) non-baryonic particles which are predicted by some BSM theories. Candidates for WIMPs should interact only via the weak or gravitational forces, and not through the strong force [30–33]. The study of DM in colliders is expected to become increasingly important in the current run of the LHC. With Run 2 of LHC at higher luminosity and energy, physicists will reframe what we know about BSM physics and maybe elucidate mysteries such as DM.

- Neutrino masses

Neutrinos are produced and detected by weak interactions. The SM requires neutrino to be massless. However, the experiments have provided compelling evidence for neutrino flavor oscillations caused by nonzero neutrino masses and mixing², and from cosmological observations we know that the mass scale has to be extremely small (sub-eV). Many descriptions beyond the standard models have been proposed to explain tiny neutrino masses. Whether the neutrinos are Dirac or Majorana particles is also unknown but of fundamental importance for understanding the origin of ν -masses, mixing and the underlying symmetries of particle interactions [35, 36].

- Quarks and leptons puzzles

There are three generations of quarks and leptons within the Standard Model (SM) for which we have experimental evidence. At present we don't have a good understanding of why there are three generations and so it is worth exploring the possible experimental consequences of additional fermions. Although a chiral 4th generation has already been excluded by the LHC (precisely due to the non-observation of an enhancement in the Higgs production cross-section) [37], the existence of one or more vector-like families is a perfectly valid possibility. Many theories such as string theories and D-brane theories often give rise generically to vector-like states [38, 39]. The ATLAS and CMS experiments have performed an extensive program for searches for vector-

¹Jan Oort in 1932 and Fritz Zwicky in 1933.

²Arthur MacDonald, from the Sudbury Neutrino Observatory (SNO) in Canada, and Takaaki Kajita, from the Super-Kamiokande Collaboration in Japan, are co-winners of the 2015 Nobel Prize in Physics “for the discovery of neutrino oscillations, which shows that neutrinos have mass” [34].

like fermions during LHC Run I. Other question that can be answered in BSM is that whether quarks and/or leptons consist of more fundamental particles?

- Grand Unification

The fact that the SM provides a unification between weak and electromagnetic interactions into a single electroweak theory suggests that the strong interaction should somehow be included as well. This so-called Grand Unified Theories (GUTs) would unify all non-gravitational forces into one theoretical framework, with one coupling constant governing them all. The electromagnetic coupling g_e grows as a function of energy-momentum scale μ^2 whereas the other two decrease. The various couplings might become equal at a large scale $\mu^2 = M_X^2$, where the so called unification mass M_X is of order 10^{16} GeV. The simplest and earliest BSM model, Georgi-Glashow model in 1974, incorporates both quarks and leptons into a single family [40, 41].

- Quantum gravity

The gravitational force which has profound implications for our everyday lives cannot be described within the SM. Quantum gravitational effects are expected to become relevant only at very high scales ($\Lambda = M_{Planck} = 10^{19}$ GeV) and therefore are expected to have little impact on particle physics phenomenology [42]. A general unification, unifying gravity with all three forces of Nature, has been searched for many years by several theories. The Standard Model is seen as an effective low energy theory which must be embedded in some more fundamental theory at a scale Λ . Different extensions of the SM use the effective field theory to treat this problem for example see [43–48]. Additionally, other BSM theories that intend to propose solutions to different SM issues such as the hierarchy problem or dark matter may also achieve the unification of gravity with all three forces of Nature [49].

- CP Violation

CP symmetry is the combined action of the charge conjugation (C) and parity (P) transformations. CP symmetry states that the laws of physics must be invariant under charge conjugation and change of parity i.e. CP turns the left-handed particles to right-handed anti-particles. Violation of the CP symmetry was first observed at Brookhaven National Laboratory in the 1960s in neutral particles called kaons. About 40 years later, experiments in Japan and the US found similar behaviour in another particle,

the B^0 meson. More recently, experiments at the so-called B factories and the LHCb experiment at CERN have found that the B^+ and B_s^0 mesons also demonstrate CP violation [50, 51]. The fact that CP violation permits unequal treatment of particles and anti-particles suggests that it may be responsible for the domination of matter over anti-matter in the Universe (matter/anti-matter asymmetry). From the experiments, we know that CP Violation occurs in weak interaction of quarks. Unfortunately, this is not enough to account for matter/anti-matter asymmetry. So one is forced to investigate other CP Violation mechanisms. One possibly is strong CP Violation, which has never been observed in the strong interaction, but it does not seem to have any fundamental reasons to be disallowed.³ At this point, matter/anti-matter asymmetry of the universe remains a puzzle and thus another evidence for BSM physics [54].

- The Hierarchy Problems

These are large scale separations unexplained by the SM:

- Cosmological hierarchy problem: We can rewrite the gravitational constant (G) in terms of mass (energy) called the Planck scale or Planck mass : $M_{Pl} = \frac{1}{\sqrt{G}} \simeq 10^{19}$ GeV. On the other hand, the energy scale of spontaneous symmetry breaking by the Higgs mechanism appearing in the SM is about $M_{EW} \simeq 10^2$ GeV. Why does Nature give us these extremely different energy scales?
- Gauge hierarchy problem: The hierarchy appears when we consider GUT. The GUT scale, $M_{GUT} \simeq 10^{16}$ GeV, is very large compared with the energy scale of the SM.
- The hierarchy problem of the SM Higgs sector: The hierarchy problem is the instability of the small Higgs mass. The Higgs mass receives quadratically divergent radiative corrections from self-interaction, interactions with gauge bosons and fermions i.e. the mass correction δM_H^2 grows quadratically as Λ^2 . If one takes the cut-off at the Planck energy scale: $\Lambda = M_{Planck} \simeq 10^{19}$ GeV, we will get: $\delta M_H^2 \sim M_{Planck}^2$. As the mass of the Higgs can not exceed 1 TeV (the SM observed Higgs mass is 125 GeV), this huge correction is unacceptable. In Grand Unified Theories (GUT), where $\Lambda = M_{GUT} \simeq 10^{16}$ GeV, one also gets large corrections given by $\delta M_H^2 \sim M_{GUT}^2$.

³One possible explanation was suggested by Peccei and Quinn in 1977 [52, 53]: a neutral spin-0 particle (axion) couples to quarks and cancels any strong CP Violation. The axion is a viable dark matter candidate that has not been observed yet.

- Fermionic mass hierarchy: A hierarchy is also observed in the experimental values obtained for the mass of the fermions. For instance, the ratio between the mass of lightest and heaviest charged fermions i.e. $m_{electron}/m_{top-quark}$ is of the order of 3×10^{-6} . This issue is usually known as the fermionic mass hierarchy, and it could be one more indication of new physics at the TeV scale. Experimentally, the Cabibbo-Kobayashi-Maskawa (CKM) matrix, describing intergenerational quark mixing is constrained and its parameters are defined according to the observed mass values for the fermions. It has been also realized that the CKM matrix follows a hierarchy [33, 55–58], but this remains a puzzle in the SM.

As discussed, there are many reasons to hope and expect that new particles and interactions beyond the Standard Model will be discovered in the near future. This motivates us to work on extensions of the Standard Model. Many theories have been proposed for new physics beyond the SM that address one or more of the challenges on our list. In this thesis I focus on a simple extension of the standard model the “Higgs Triplet Model” (HTM) in which a triplet scalar is added to the SM particle spectrum (while the gauge group of the SM is unchanged), providing a mechanism to give neutrino masses. We also investigate the phenomenological implications of introducing vector-like fermions in the context of the HTM, which provides the lightest vector-like neutrino as a Dark Matter candidate.

1.3 Organization of this thesis

The general structure of this thesis is as follows:

Chapter 2 provides a brief and general overview of the Standard Model of Particle Physics, focussing on the theoretical and experimental evidence which led to the prediction of the Higgs boson. The formalism detailed in this chapter will be of use when describing the structure of the model under consideration.

Chapters 3 , 4, 5 and 6 are reproduced from [1], [4], [3], and [2, 5] respectively.

In Chapter 3 , we revisit the neutral Higgs sector of the Higgs Triplet Model, where a $Y=2$ triplet scalar is added to the SM particle spectrum. We show that, contrary to previous analyses in the literature, the two neutral Higgs bosons can mix, and that if they do, only the heavier state can have an enhanced diphoton decay rate. We compared there scenarios with the data and show that one is very promising.

In Chapter 4 , we looked at the effects of vector-like leptons in the Higgs Triplet Model. They alter the decays rates of the neutral Higgs (loop dominated, in particular $\gamma\gamma$ and $Z\gamma$) and also completely alter the decay patterns of the doubly charged Higgs bosons, thus evading the experimental limits on their masses.

In Chapter 5 , we look at the effects of vector-like quarks (singlets, doublets or triplets) in the Higgs Triplet Model. Though the new Higgs bosons in the model couple to leptons only, some vector-like quarks help improve electroweak precision measurements (we identified which ones) and thus lift the mass of the doubly charged Higgs boson to within experimental limits.

In Chapter 6 , we show that introducing a full representation of vector-like leptons solves the DM problem of the Higgs Triplet Model by assigning a vector-like neutrino to be the Dark Matter (thus neutrino masses + Dark Matter, two important problems in SM are resolved). We do a complete electroweak precision analysis, and include all the Dark Matter tests. We calculate the cross section for the direct and indirect DM detection and the neutrino and muon fluxes from the Sun. We also investigate the effect of constraints from the invisible decay width of the Higgs boson and relic density on the mass and Yukawa coupling of DM. This analysis assumes that the DM candidate is light. The model is completely consistent with the present DM experimental constraints.

Finally, in the last Chapter, we conclude the Thesis by summarizing the main contributions examined in the previous chapters, and providing an outlook for future research in these areas.

Chapter 2

The Standard Model of Particle Physics

The Standard Model (SM) of fundamental particles and their interactions is one of the best tested theories in physics. In particular, up to the weak scale (of the order of a few hundreds of GeV), it has been found to be in remarkable agreement with a large set of experimental data. All the particles predicted by the SM have not only been discovered, but they also fit perfectly in the model framework. In spite of its experimental successes, it is not considered to be the final word on particle physics due to a number of limitations (mentioned in the Introduction) that the SM suffers from. This led particle theorists to study various extensions of the Standard Model. In this chapter, particular attention is given to the main aspects of the SM.

2.1 A Brief Overview of SM

2.1.1 The Particle Content

The Standard Model (SM) is formulated as a quantum field theory, based on the gauge group $SU(3)_C \times SU(2)_L \times U(1)_Y$. The particle content of the SM, with their gauge group representation and hypercharges, is summarized in Table 2.1 and include:

Three generations of fermions, the leptons :

		$SU(3)_C$	$SU(2)_L$	$U(1)_Y$
Leptons	$L^i_L = (\nu^i, l^i)$	1	2	$-\frac{1}{2}$
	l^i_R	1	1	-1
Quarks	$Q^i_L = (u^i, d^i)$	3	2	$+\frac{1}{6}$
	u^i_R	3	1	$+\frac{2}{3}$
	d^i_R	3	1	$-\frac{1}{3}$
Gluons	g	8	1	0
W bosons	W	1	3	0
B bosons	B	1	1	0
ϕ boson	ϕ	1	2	$\frac{1}{2}$

Table 2.1: Particle content of the SM with their gauge group representation and hypercharges. The index i labels the three so called generations of leptons and quarks. The L and R subscripts refer to left-handed and right-handed chiralities.

$$L^i_L = (\nu^i_L, l^i_L), \quad l^i_R, \quad (2.1)$$

where $\nu^i = \{\nu_e, \nu_\mu, \nu_\tau\}$ are the three neutral leptons (neutrinos), which interact with other particles only through the nuclear weak force, and $l^i = \{e, \mu, \tau\}$ (the electron, the muon and the tau) are the three charged leptons, with masses of about 0.5 MeV , 0.1 GeV and 1.8 GeV; while only the electron is stable, also the muon can be considered stable in the context of collider experiments due to its long lifetime ($c\tau_\mu \sim 660$ m). However since tau leptons have shorter lifetime, $c\tau_\tau \simeq 87\mu\text{m}$, they are observed only through their decay products. A lepton number is defined in each generation as the number of charged leptons, plus the number of neutrinos, minus the number of charged anti-leptons and anti-neutrinos; in the SM, lepton flavour is conserved separately for each generation, except for neutrino oscillation phenomena which conserve only the total lepton number.

The three other fermions are the quarks, up-type quarks: u (up) , c (charm) and t (top), the three down-type quarks: d (down), s (strange) and b (bottom) with electrical charges $+2/3$, $1/3$ shown as:

$$Q^i_L = (u^i_L, d^i_L), \quad u^i_R, \quad d^i_R, \quad (2.2)$$

where $u^i = \{u, c, t\}$ and $d^i = \{d, s, b\}$. The index i labels the three so called generations of leptons and quarks. The L and R subscripts refer to left-handed and right-handed chiralities.

Quarks have only been observed in hadrons, bound states of either three quarks (baryons), three anti-quarks (anti-baryons), or one quark and one anti-quark (mesons); an exception is the top quark, whose extremely short lifetime prevents the formation of bound states. Quark flavour is always conserved by strong and electromagnetic interactions, and by interactions mediated by the Z boson, but not by the weak interactions mediated by W bosons. Decays through weak interactions of hadrons composed of u , d and s quarks are characterized by long lifetimes, with values ranging from centimeters to meters, while for hadrons containing c and b quarks lifetimes are $\mathcal{O}(100 \mu\text{m})$ and $\mathcal{O}(500 \mu\text{m})$ respectively. Decays mediated by strong or electromagnetic interactions have lifetimes too short to be detectable [59]. Each fermion has an associated anti-fermion with opposite electrical charge.

The force carriers, spin 1 bosons, contain: the photon γ , mediator of the electromagnetic interactions, the eight gluons g_a ($a = 1, \dots, 8$), mediators of the strong interactions, and the three weak bosons, mediators of the weak interactions, the neutral Z^0 boson and the two charged W^\pm bosons. The gauge bosons content is therefore: $N^2 - 1 = 8$ gluon fields from the adjoint of $SU(3)_C$ and 3 $W_\mu^i, i = 1, 2, 3$, from the adjoint of $SU(2)_L$, and 1 B_μ from $U(1)_Y$. The fields W_μ^i and B_μ mix to form the massive W^\pm and Z^0 gauge bosons and the massless photon.

Finally, there is a scalar Higgs boson field, also interacting with fermions and gauge bosons through weak interactions. The Higgs boson doesn't interact with γ and g_a , that is why they are massless. The quarks interact with all the gauge vector bosons including γ , W^\pm , Z , g_a and the Higgs. Leptons interact with all the gauge vector bosons except gluons as they do not experience strong interactions. Neutrinos participate exclusively in the weak interactions. The photon, γ , interacts with only W^\pm , charged leptons and quarks. The Z interacts with the W^\pm , leptons, quarks and the Higgs boson. The W^\pm interact with the Z , γ , leptons, quarks, Higgs boson and themselves. The eight gluons g_a interact with only the quarks and among themselves [60].

2.1.2 The Lagrangian

The Lagrangian of the SM (\mathcal{L}_{SM}) can be divided into four different parts,

$$\mathcal{L}_{\text{SM}} = \mathcal{L}_{\text{YM}} + \mathcal{L}_{\text{ferm}} + \mathcal{L}_{\text{Higgs}} + \mathcal{L}_{\text{Yuk}}, \quad (2.3)$$

which will be discussed one by one in the following. The Yang-Mills part \mathcal{L}_{YM} describes the dynamic behaviour of the gauge fields and is defined as,

$$\mathcal{L}_{\text{YM}} = -\frac{1}{4}W_{\mu\nu}^i W^{\mu\nu i} - \frac{1}{4}G_{\mu\nu}^a G^{\mu\nu a} - \frac{1}{4}B_{\mu\nu} B^{\mu\nu}, \quad (2.4)$$

where

$$W_{\mu\nu}^i = \partial_\mu W_\nu^i - \partial_\nu W_\mu^i - g\varepsilon^{ijk}W_\mu^j W_\nu^k, \quad i, j, k = 1, 2, 3,$$

$$B_{\mu\nu} = \partial_\mu B_\nu - \partial_\nu B_\mu,$$

$$G_{\mu\nu}^a = \partial_\mu G_\nu^a - \partial_\nu G_\mu^a - g_s f^{abc}G_\mu^b G_\nu^c, \quad a, b, c = 1, \dots, 8,$$

are the field-strength tensors of the gauge fields : W_μ^i ($i = 1, 2, 3$) for the $SU(2)_L$ group of the weak isospin I_W^i , B_μ for the $U(1)_Y$ of weak hypercharge Y_W , and G_μ^a for the $SU(3)_C$ of colour. The respective gauge couplings of these groups are denoted g , g' , and g_s , ε^{ijk} is the anti-symmetric tensor, and f^{abc} are the structure constants of the $SU(3)_C$ group.

The interaction of the gauge fields with the fermions is encoded in

$$\mathcal{L}_{\text{ferm}} = \bar{L}^i iD_\mu \gamma^\mu L^i + \bar{e}_R^i iD_\mu \gamma^\mu e_R^i + \bar{Q}^i iD_\mu \gamma^\mu Q^i + \bar{u}_R^i iD_\mu \gamma^\mu u_R^i + \bar{d}_R^i iD_\mu \gamma^\mu d_R^i \quad (2.5)$$

The covariant derivative is given as

$$D_\mu = \partial_\mu - igI_W^i W_\mu^i - ig'Y_W B_\mu + ig_s T_c^a G_\mu^a, \quad (2.6)$$

where I_W^i , Y_W , and T_c^a are the generators of the respective gauge groups. In detail, $I_W^i = \sigma_i/2$ (with the Pauli matrices $\sigma_i/2$) for the left-handed $SU(2)_L$ doublets and $I_W^i = 0$ for the right-handed singlets, the weak hypercharge Y_W is related to the relative electric charge Q by the Gell-Mann-Nishijima relation $Q = I_W^3 + Y_W/2$, and $T_c^a = \lambda_a/2$ ($\lambda_a =$ Gell-Mann matrices) for $SU(3)_C$ quark triplets and $T_c^a = 0$ for the leptons. In quantum electrodynamics, we identify the photon field A_μ and the Z -boson field Z_μ as linear combinations of W_μ^3 and B_μ obtained by the rotation

$$\begin{pmatrix} Z_\mu \\ A_\mu \end{pmatrix} = \begin{pmatrix} c_W & -s_W \\ s_W & c_W \end{pmatrix} \begin{pmatrix} W_\mu^3 \\ B_\mu \end{pmatrix} \quad (2.7)$$

with the weak mixing angle θ_W and coupling constant e fixed by

$$\cos \theta_W = c_W = \sqrt{1 - s_W^2} = \frac{g}{\sqrt{g^2 + g'^2}}, \quad e = \frac{gg'}{\sqrt{g^2 + g'^2}}, \quad (2.8)$$

The fields $W^\pm = (W_\mu^1 \mp iW_\mu^2)/\sqrt{2}$ correspond to the charged weak gauge bosons W^\pm of charge $\pm e$.

The Higgs Lagrangian is composed of the kinetic term and the Higgs potential as

$$\mathcal{L}_{Higgs} = |D^\mu \Phi|^2 - V_{SM} \quad V_{SM} = -\mu^2(\Phi^\dagger \Phi) + \lambda_1(\Phi^\dagger \Phi)^2. \quad (2.9)$$

The Higgs doublet field Φ can be parameterized in terms of the real physical Higgs field H and the unphysical Goldstone boson fields Φ^+ and χ , which are complex and real respectively, as

$$\Phi = \begin{pmatrix} \Phi^+ \\ \Phi^0 = \frac{1}{\sqrt{2}}(v + H + i\chi) \end{pmatrix}, \quad (2.10)$$

where $v = 246$ GeV is the vacuum expectation value (VEV) of $\sqrt{2}\Phi^0$.

Inserting the parametrisation Eq. (2.10) of Φ and the covariant derivative Eq. (2.6) with $I_{W,\Phi}^i = \sigma_i/2$, $Y_{W,\Phi} = 1$, $T_c^a = 0$ into the Higgs Lagrangian Eq. (2.9) and dropping the Goldstone bosons, we find

$$\mathcal{L}_{Higgs} = \frac{1}{2}(\partial_\mu H)^2 + \frac{g^2}{4}(v + H)^2 W_\mu^+ W^{\mu,-} + \frac{g^2}{8c_W^2}(v + H)^2 Z_\mu Z^\mu + \frac{\mu^2}{2}(v + H)^2 - \frac{\lambda}{16}(v + H)^4, \quad (2.11)$$

which contains mass terms for the corresponding weak gauge bosons W^\pm and Z as well as for the Higgs boson H , as

$$M_W = \frac{gv}{2}, \quad M_Z = \frac{M_W}{c_W}, \quad M_H = \sqrt{2\mu^2}, \quad (2.12)$$

The Higgs particle is also responsible for the masses of quarks and leptons through Yukawa couplings to the Higgs particle. The Yukawa interactions for the SM quarks and leptons are

$$\mathcal{L}_{Yuk} = -(y_l)^{ij} \bar{L}_L^i \Phi l_R^j - (y_d)^{ij} \bar{Q}_L^i \Phi d_{jR} - (y_u)^{ij} \bar{Q}_L^i \sigma^2 \Phi^* u_R^j + h.c., \quad (2.13)$$

where the various y^{ij} s are Yukawa coupling constants. By taking the following basis transformations:

$$\begin{aligned} u_R^i &\longrightarrow (V_u)^{ij} u_R^j, & d_R^i &\longrightarrow (V_d)^{ij} d_R^j, & l_R^i &\longrightarrow (V_l)^{ij} l_R^j, \\ Q_L^i &= \begin{pmatrix} u_L^i \\ d_L^i \end{pmatrix} \longrightarrow \begin{pmatrix} (V_u)^{ij} u_L^j \\ (V_d)^{ij} d_L^j \end{pmatrix} = (V_u)^{ij} \begin{pmatrix} u_L^j \\ V_{CKM} d_L^j \end{pmatrix}, \\ L_L^i &= \begin{pmatrix} \nu_L^i \\ l_L^i \end{pmatrix} \longrightarrow (V_l)^{ij} \begin{pmatrix} \nu_L^j \\ l_L^j \end{pmatrix}. \end{aligned} \quad (2.14)$$

where V_{CKM} is the Cabibbo-Kobayashi-Maskawa matrix [61–63] which determines to what extent quarks can interact across different generations :

$$V_{CKM} = V_u^\dagger V_d = \begin{pmatrix} V_{ud} & V_{us} & V_{ub} \\ V_{cd} & V_{cs} & V_{cb} \\ V_{td} & V_{ts} & V_{tb} \end{pmatrix}. \quad (2.15)$$

It can be parameterized by three mixing angles and a CP-violating phase:

$$V_{CKM} = \begin{pmatrix} c_{12}c_{13} & s_{12}c_{13} & s_{13}e^{-i\delta} \\ -s_{12}c_{23} - c_{12}s_{23}s_{13}e^{i\delta} & c_{12}c_{23} - s_{12}s_{23}s_{13}e^{i\delta} & s_{23}c_{13} \\ s_{12}s_{23} - c_{12}s_{23}s_{13}e^{i\delta} & -c_{12}s_{23} - s_{12}c_{23}s_{13}e^{i\delta} & c_{23}c_{13} \end{pmatrix}, \quad (2.16)$$

where $s_{ij} = \sin \theta_{ij}$, $c_{ij} = \cos \theta_{ij}$ and δ is the phase responsible for all CP-violating phenomena in flavor-changing processes in the SM. We can rewrite the V_{CKM} using the Wolfenstein parameterization [64–66]:

$$V_{CKM} = \begin{pmatrix} 1 - \lambda^2 & \lambda & A\lambda^3(\rho - i\eta) \\ -\lambda & 1 - \lambda^2 & A\lambda^2 \\ A\lambda^3(1 - \rho - i\eta) & -A\lambda^2 & 1 \end{pmatrix},$$

where λ , A , ρ and η are the Wolfenstein parameters. The unitarity of the CKM matrix imposes:

$$\sum_i U_{ij}U_{ik}^* = \delta_{jk} \quad \text{and} \quad \sum_j U_{ij}U_{kj}^* = \delta_{ik}. \quad (2.17)$$

After some algebra, we can rewrite the Lagrangian in Eq (2.13) , as :

$$\begin{aligned} \mathcal{L}_{Yuk} = & -y_d^j \bar{u}_L^i V_{CKM}^{ij} d_R^j \Phi^+ - y_d^i \bar{d}_L^i d_R^i \Phi^0 - y_u^i \bar{u}_L^i u_R^i (\Phi^0)^* - y_u^j \bar{d}_L^i (V_{CKM}^{ij})^\dagger u_R^j (\Phi^+)^* \\ & - y_l^i \bar{\nu}_L^i l_R^i \Phi^+ - y_l^i \bar{l}_L^i l_R^i \Phi^0 + h.c., \end{aligned} \quad (2.18)$$

where y_u^i , y_d^i , and y_l^i are the diagonal elements of the corresponding diagonalized Yukawa matrices. They are given by the expression

$$y_f^i = \sqrt{2} \frac{m_f^i}{v}. \quad (2.19)$$

Therefore the generated fermion masses are proportional to the doublet VEV, $m_f^i \propto v$. Also note that since there are no right-handed neutrinos ν_R^i in the SM, the neutrinos cannot acquire masses in this way and consequently, they remain massless [67–69].

The SM is a gauge theory, meaning that its Lagrangian is invariant under continuous symmetry group of local transformations of the fields. This locality allows the parameters of the transformation to depend on each point x in space-time, whereas for a global symmetry the transformation is the same for all x . An important aspect of the SM is the Higgs Mechanism. It turns out that it is impossible to simply insert the mass terms of the gauge bosons (W^\pm and Z^0) into the Lagrangian and still respect gauge symmetry. And since left-handed and right-handed fermions transform differently under $SU(2)_L \times U(1)_Y$ gauge transformations, naive fermion-mass terms $\propto (\bar{\Psi}_{fL}\Psi_{fR} + \bar{\Psi}_{fR}\Psi_{fL})$ for a fermion f are also ruled out by gauge invariance. A solution to both of these problems is provided by the Higgs-Brout-Englert-Guralnik-Hagen-Kibble mechanism of spontaneous symmetry breaking (SSB), or the Higgs Mechanism for short, in which the Lagrangian undergoes SSB, losing part of its full symmetry by introducing a scalar field which develops a non-symmetric ground state. As a result, a massless gauge boson will absorb a would-be-Goldstone boson to acquire a mass. Fermions also can get mass by coupling to the scalar field in a gauge invariant way [13, 67, 68].

2.1.3 Electroweak Symmetry Breaking and the Higgs Mechanism

In this section, we discuss two important aspects of the SM: spontaneous symmetry breaking (SSB) and Higgs Mechanism. This process will be illustrated by an example [54]. Suppose we take a vector field A_μ with the Proca Lagrangian describing a particle of spin 1 and mass m_A :

$$\mathcal{L} = -\frac{1}{16\pi}F^{\mu\nu}F_{\mu\nu} - \frac{1}{4\pi} \frac{m_{AC}}{\hbar} A^\mu A_\mu, \quad (2.20)$$

where $F_{\mu\nu} \equiv \partial_\mu A_\nu - \partial_\nu A_\mu$, where A_μ is the gauge field which changes according to the rule

$$A_\mu \longrightarrow A_\mu + \partial_\mu \lambda, \quad (2.21)$$

in coordination with the local phase transformation

$$\Psi \longrightarrow e^{i\theta(x)}\Psi. \quad (2.22)$$

Since $F^{\mu\nu}$ is invariant under Eq (2.21), but $A^\mu A_\mu$ is not, then evidently the new field must be massless ($m_A = 0$), otherwise the invariance will be lost. While the photon and gluons are massless, the W^\pm and Z^0 are not. SSB and Higgs mechanism are procedures to modify the gauge theory to explain massive gauge fields.

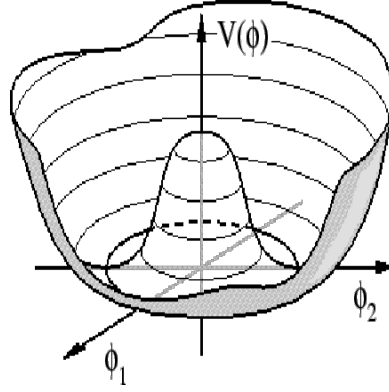


Figure 2.1: The Higgs (Mexican Hat) Potential

Suppose we have the following Lagrangian for two fields ϕ_1 and ϕ_2 :

$$\mathcal{L} = \frac{1}{2}(\partial_\mu \phi_1)(\partial^\mu \phi_1) + \frac{1}{2}(\partial_\mu \phi_2)(\partial^\mu \phi_2) + \frac{1}{2}\mu^2(\phi_1^2 + \phi_2^2) - \frac{1}{4}\lambda^2(\phi_1^2 + \phi_2^2)^2. \quad (2.23)$$

The potential energy function is

$$\mathcal{U} = -\frac{1}{2}\mu^2(\phi_1^2 + \phi_2^2) + \frac{1}{4}\lambda^2(\phi_1^2 + \phi_2^2)^2, \quad (2.24)$$

and the minima lie on a circle of radius $\frac{\mu}{\lambda}$ (Fig. 2.1) : $\phi_{1_{min}}^2 + \phi_{2_{min}}^2 = \frac{\mu^2}{\lambda^2}$ with the chosen ground states (the states with minimum energy or the vacuum) : $\phi_{1_{min}} = \frac{\mu}{\lambda}$; $\phi_{2_{min}} = 0$. The vacuum expectation value (VEV) $\phi_{1_{min}}$ of the Higgs field is the crucial quantity that gives mass to the gauge boson A_μ . For the Feynman calculations, a perturbation procedure, we start from the ground states and treat the fields as fluctuations about that state.

We introduce new fields, η and ξ , which are the fluctuations about this vacuum state: $\eta \equiv \phi_1 - \frac{\mu}{\lambda}$ and $\xi \equiv \phi_2$. Rewriting the Lagrangian in terms of these new field variables, we find

$$\mathcal{L} = \left[\frac{1}{2}(\partial_\mu \eta)(\partial^\mu \eta) - \mu^2 \eta^2 \right] + \left[\frac{1}{2}(\partial_\mu \xi)(\partial^\mu \xi) \right] - \left[\mu\lambda(\eta^3 + \eta\xi^2) + \frac{1}{4}\lambda^2(\eta^4 + \xi^4 + 2\eta^2\xi^2) \right] + \frac{\mu^4}{4\lambda^2}. \quad (2.25)$$

The first term is a free Klein-Gordon Lagrangian for the field η which acquires a mass: $m_\eta = \sqrt{2}\frac{\mu}{\hbar c}$. The second term is a free Lagrangian for the field ξ , which is massless($m_\xi = 0$). We call this massless scalar particle ‘‘Goldstone boson’’. In this form the Lagrangian does not look symmetrical at all. In order to eliminate the Goldstone boson, we will apply the idea of SSB to the case of local gauge invariance.

The Lagrangian in Eq. (2.23) can be written more compactly if we combine the two real fields, ϕ_1 and ϕ_2 , into a single complex field : $\phi \equiv \phi_1 + i\phi_2$. We can make the system invariant

under local gauge transformations Eq. (2.22) by introducing a massless gauge field A_μ , using covariant derivatives

$$D_\mu = \partial_\mu + i \frac{q}{\hbar c} A_\mu. \quad (2.26)$$

The Lagrangian in Eq. (2.23) becomes

$$\begin{aligned} \mathcal{L} = & \left[\frac{1}{2} (\partial_\mu \eta) (\partial^\mu \eta) - \mu^2 \eta^2 \right] + \left[\frac{1}{2} (\partial_\mu \xi) (\partial^\mu \xi) \right] + \left[-\frac{1}{16\pi} F^{\mu\nu} F_{\mu\nu} + \frac{1}{2} \left(\frac{q\mu}{\hbar c \lambda} \right)^2 A_\mu A^\mu \right] \\ & + \left\{ \left(\frac{q}{\hbar c} \right) (\eta (\partial_\mu \xi) - \xi (\partial_\mu \eta)) A^\mu + \frac{\mu}{\lambda} \left(\frac{q}{\hbar c} \right)^2 \eta (A_\mu A^\mu) \right. \\ & + \frac{1}{2} \left(\frac{q}{\hbar c} \right)^2 (\eta^2 + \xi^2) (A_\mu A^\mu) - \lambda \mu (\eta^3 + \eta \xi^2) - \frac{1}{4} \lambda^2 (\eta^4 + 2\eta^2 \xi^2 + \xi^4) \left. \right\} \\ & + \left(\frac{q\mu}{\hbar c \lambda} \right) (\partial_\mu \xi) A^\mu + \left(\frac{\mu^2}{2\lambda} \right)^2. \end{aligned} \quad (2.27)$$

So the free gauge field A_μ has acquired a mass:

$$m_A = 2\sqrt{\pi} \frac{q\mu}{\lambda c^2}, \quad (2.28)$$

However, we still have that unwanted Goldstone boson ($\phi_2 = \xi$). In order to transform this field away, we write Eq. (2.22) in terms of its real and imaginary parts,

$$\phi \longrightarrow \phi' = (\cos \theta + i \sin \theta) (\phi_2 + i \phi_1), \quad (2.29)$$

we see that picking

$$\theta = -\tan\left(\frac{\phi_2}{\phi_1}\right), \quad (2.30)$$

will render ϕ' real. The gauge field A_μ will transform accordingly (Eq. (2.21), but the Lagrangian will take the same form in terms of the new field variables as it did in terms of the old ones. The only difference is that ξ is now zero. In this particular gauge, the Lagrangian (Eq. (2.27) reduces to

$$\begin{aligned} \mathcal{L} = & \left[\frac{1}{2} (\partial_\mu \eta) (\partial^\mu \eta) - \mu^2 \eta^2 \right] + \left[-\frac{1}{16\pi} F^{\mu\nu} F_{\mu\nu} + \frac{1}{2} \left(\frac{q\mu}{\hbar c \lambda} \right)^2 A_\mu A^\mu \right] \\ & + \left[\frac{\mu}{\lambda} \left(\frac{q}{\hbar c} \right)^2 \eta (A_\mu A^\mu) + \frac{1}{2} \left(\frac{q}{\hbar c} \right)^2 \eta^2 (A_\mu A^\mu) - \lambda \mu \eta^3 - \frac{1}{4} \lambda^2 \eta^4 \right] + \left(\frac{\mu^2}{2\lambda} \right)^2. \end{aligned} \quad (2.31)$$

So we have eliminated the Goldstone boson; we are left with a single massive scalar η (the Higgs particle) and a massive gauge field A_μ .

This mechanism is the famous Higgs mechanism, obtained by combining of local gauge invariance and spontaneous symmetry breaking. According to the SM, the Higgs mechanism is responsible for the masses of the weak interaction gauge bosons (W^\pm and Z^0).

2.2 Higgs-Boson Physics at the LHC

2.2.1 Higgs-Boson Production at the LHC

Since the Higgs-boson couplings to all particles are proportional to the masses of these particles, Higgs-boson production processes predominantly arise from diagrams involving heavy particles. At the proton-proton collider LHC the Higgs boson is produced in several processes. Feynman diagrams for the dominant production mechanisms with their expected number of events at LHC are shown in Fig. 2.2. The dominant production process of SM Higgs bosons at the LHC is gluon fusion ($gg \rightarrow H$). Although the massless gluons do not couple directly to the Higgs, production is via triangular quark loops. This process is dominated by the contribution of the top-quark loop. The second-highest rate after gluon fusion is (weak)

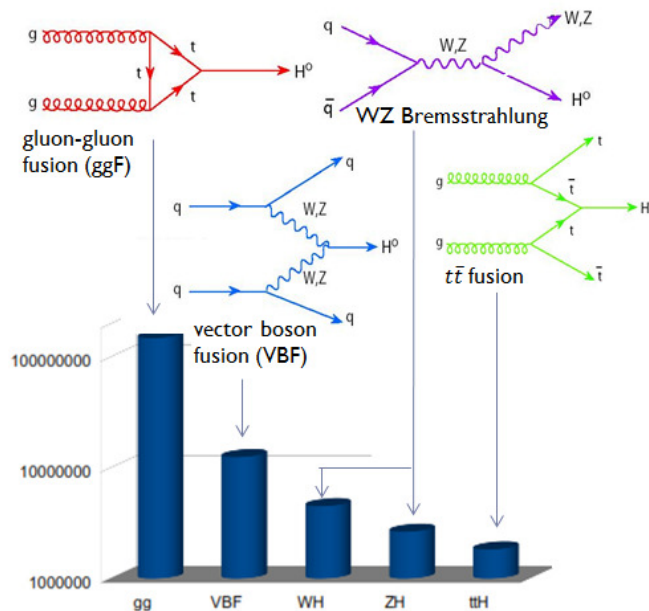


Figure 2.2: The Higgs production modes with their expected number of events at HL-LHC with $\int L dt = 3000 \text{ fb}^{-1}$. This figure is reproduced from [70].

vector-boson fusion (VBF). Either one or both of the incoming quarks can also be replaced by anti-quarks, but the qq initial state gives the largest contribution for proton-proton collisions. A less prominent production mode is through WZ bremsstrahlung. Higgs strahlung in association with top quark pairs or $t\bar{t}$ fusion ($t\bar{t}H$ with $H \rightarrow b\bar{b}$) is an important channel, allowing for a direct measurement of the Yukawa coupling between top quark and Higgs boson, but it

has a very low production cross section. The associated Higgs production with a $b\bar{b}$ pair plays a minor role in the SM. This production process can be significantly enhanced, however, in extensions of the SM, such as supersymmetric or two-Higgs-doublet models.

2.2.2 Decay of the Higgs boson

Standard Model decay channels

The LHC search program for the SM Higgs boson comprised five main decay channels: the decay into (1) W bosons ($H \rightarrow W^+W^-$), (2) Z bosons ($H \rightarrow ZZ$), (3) Photons ($H \rightarrow \gamma\gamma$), (4) b -quarks ($H \rightarrow b\bar{b}$) and (5) τ -leptons ($H \rightarrow \tau^+\tau^-$). The Higgs branching ratio of each decay channel as a function of its expected mass are shown in Fig. 2.3 as given by the LHC Higgs Cross Section Working Group [71]. For a Higgs boson mass of about 125 GeV, the Higgs boson phenomenology within the SM is particularly rich, since many different decay modes are potentially detectable. In this area, the search is dominated by bosonic modes, where Higgs decays to W^+W^- and ZZ . Within the W^+W^- channel, purely leptonic ($H \rightarrow W^+W^- \rightarrow l\nu l\nu$) and semi-leptonic ($H \rightarrow W^+W^- \rightarrow l\nu qq$) decay modes are being analysed at the LHC. The decay of the Higgs boson to a pair of Z bosons has also been very attractive due to the production of a very clean signal. The Z boson decay to $4l$ leads to very small background. The decay mode of $H \rightarrow ZZ \rightarrow llqq$ is also being searched. For lower masses, the most important channels are $b\bar{b}$, $\tau^+\tau^-$ and $\gamma\gamma$ [33, 67, 69, 72]. In spite of the small rate for the decays to $\gamma\gamma$, these decays have low background and good mass resolution.

Non-standard decay channels

The main decay and production properties of Higgs boson are consistent with a Standard Model Higgs boson. It may however have other decay channels beyond those predicted by the Standard Model.

Among non-standard decays and of great interest are invisible decays into stable particles that do not interact with the detector. The discovery of the Higgs particle has raised the question of its couplings to Dark Matter and how it could be used to further try to reveal DM existence at colliders, using the Higgs boson as a portal to Dark Matter. If kinematically accessible and with a sufficiently large coupling to the Higgs boson, Dark Matter particles would manifest

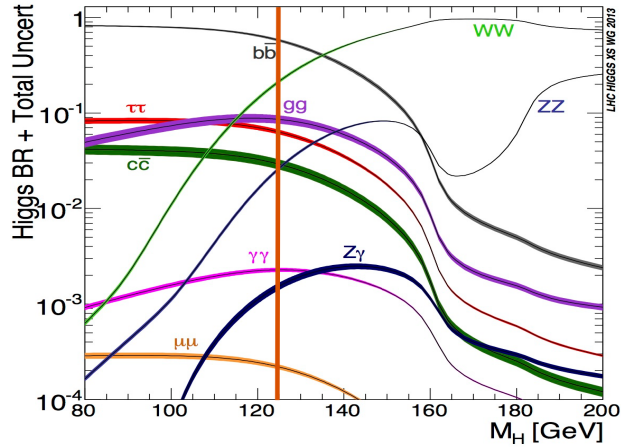


Figure 2.3: Standard Model Higgs boson decay branching ratios. This figure is reproduced from [71] (125 GeV bar by me).

themselves as invisible decays of the Higgs boson, thus strongly motivating searches for these. The results of searches for invisible decays of the Higgs particle are reported in Table 2.2. Results can be interpreted in terms of 95% CL limit on the invisible branching fraction for a Standard Model production cross section or as the ratio of the product of the Higgs production cross section times the Higgs invisible branching fraction to its SM expectation [36]. Invisible decay width of the Higgs boson will be discussed more in Section 6.4.

	ATLAS	CMS
$W, Z \rightarrow \text{fatjet}, H \rightarrow \text{inv.}$	1.6 (2.2)	–
$Z \rightarrow \ell^+ \ell^-, H \rightarrow \text{inv.}$	65% (84%)	75% (91%)
$Z \rightarrow b\bar{b}, H \rightarrow \text{inv.}$	–	1.8 (2.0)
VBF $H \rightarrow \text{inv.}$	–	69% (53%)

Table 2.2: Summary of the results of searches for invisible decays of the Higgs particle. The results in parentheses are the expected exclusions. This table is reproduced from [36].

Furthermore, additional structure of the BSMs can modify SM-like Higgs production and

decay processes via different couplings and via new sources for higher-order contributions leading to new production and decay modes and in general to a new Higgs phenomenology. For instance, for the loop-induced processes of Higgs production in gluon fusion and Higgs boson decay into a pair of photons or gluons, the impact of additional particles in the loop would be particularly important [59, 67, 72, 73]. In this thesis, the loop-dominated decays $H \rightarrow \gamma\gamma$ and $H \rightarrow Z\gamma$ in HTM with and without additional vector-like fermions will be discussed.

2.2.3 Discovery of a Higgs Boson at the LHC

In summer 2012, the ATLAS and CMS experiments observed an excess of events near $M_H = 125.09 \pm 0.24$ GeV in the $H \rightarrow ZZ^* \rightarrow 4l$ and $H \rightarrow \gamma\gamma$ channels. The final results of Run 1 from studies by the ATLAS and CMS collaborations on the signal strength μ and the significance z are summarised in Table 2.3. They are based on the full Run 1 data set, corresponding to an integrated luminosity of nearly 5 fb^{-1} recorded at $\sqrt{s} = 7$ TeV and of about 20 fb^{-1} at $\sqrt{s} = 8$ TeV. The ATLAS numbers are given for a Higgs boson mass of 125.36 GeV, whereas for the CMS experiment the results are quoted at the best-fit values.

Apart from the observed signal, we may have additional Higgs bosons provided that the Higgs sector consists of more than one single doublet, as in the SM. Several types of searches for additional Higgs bosons have been performed at the LHC, for instance for charged Higgs bosons H^\pm , which also appear in models with an extended Higgs sector [1, 59, 67, 72].

Recently, the ATLAS and CMS collaborations have reported [81, 82] on a search for new physics using high mass diphoton events in proton-proton collisions at a center-of-mass energy of $\sqrt{s} = 13$ TeV, with invariant mass larger than 200 GeV. The largest deviation from the background-only hypothesis was found in a broad region around 750 GeV, with a local significance of about 3.6σ and 2.6σ in the respective experiments. The diphoton resonance around 750 GeV, may be explained by scalars in the extension of the SM. This can be a tantalizing hint of the new physics beyond the Standard Model, however more events and analyses are needed to ascertain what the state is.

Channel	Signal strength and significance values			
	ATLAS		CMS	
	μ	z	μ	z
$H \rightarrow ZZ$	$1.44^{+0.34+0.21}_{-0.31-0.11}$	8.1	$0.93^{+0.26+0.13}_{-0.23-0.09}$	6.8
$H \rightarrow \gamma\gamma$	$1.17 \pm 0.23^{+0.16}_{-0.11}$	5.2	$1.14 \pm 0.21^{+0.09+0.13}_{-0.05-0.09}$	5.7
$H \rightarrow W^+W^-$	$1.09^{+0.16+0.17}_{-0.15-0.14}$	6.1	$0.72^{+0.20}_{-0.18}$	4.3
$H \rightarrow \tau^+\tau^-$	$1.43^{+0.27+0.33}_{-0.26-0.27}$	4.5	0.78 ± 0.27	3.2
$VH \rightarrow H \rightarrow b\bar{b}$	$0.5 \pm 0.3 \pm 0.2$	1.4	1.0 ± 0.5	2.1

Table 2.3: Compilation of measured signal strengths, $\mu = \frac{\sigma_{obs}}{\sigma_{SM}}$, and statistical significances, z , for different decay channels of the Higgs boson. If two or more errors are indicated, the first is statistical, the second is the experimental systematic error, and the third one represents theoretical uncertainties. This table is reproduced from [67, 74–80].

2.3 Searches for Physics Beyond the Standard Model

In the previous sections, we have shown why the SM of particle physics is one of the most successful theories in physics, which explains with great accuracy the experimental data we have so far. However, there are several theoretical issues and pieces of experimental evidence for physics that is not described by the SM (as explained in the introduction), which led theorists to believe there could be new physics at a TeV scale. As the collider at the current energy frontier, the LHC is in a unique position to look for signals of BSM physics. Searching for BSMs constitutes a major fraction of the experimental programme at the LHC.

It is impossible to cover all possible extensions of the SM in the LHC programme by a

search with a dedicated experimental analysis. Fortunately, it is often possible to recast a single analysis as a search for particles in very different models. Additionally, different extensions of the SM have been proposed by theorists, aiming to treat shortcomings in the SM. Among various possibilities, the Higgs Triplet Model is a prime candidate for new physics since it includes a clear explanation of the neutrino masses which will be described in detail in Chapter 3. Since an extension of the SM via additional vector-like fermions is not ruled out experimentally and this can provide a Dark Matter candidate, introducing vector-like fermions in BSMs like HTM can shed light on two unresolved issues of the SM i.e. neutrino masses and existence of Dark Matter, as shown in Chapter 6.

2.3.1 Vector-like Fermions

One of the most straightforward extensions of the SM is the inclusion of vector-like fermion generation(s). Vector-like fermions are characterized by having left- and right-handed components transforming in the same way under the symmetry group of the theory and the couplings for the right-handed components are the same as the left-handed ones. For this reason their mass terms appear explicitly in the Lagrangian, $\overline{\Psi}_L \Psi_R$, are not forbidden by any symmetry and so the masses of such fermions could be much larger than the electroweak (EW) scale. Furthermore the masses of the quarks could be very different from those of the leptons [2, 3, 37, 39, 83–85].

The ATLAS and CMS experiments have performed an extensive program of searches for vector-like fermions during LHC Run I. For example, the ATLAS collaboration has performed a search for pair production of vector-like quarks, both vector-like up-type (T) and down-type (B), as well as four-top-quark production using pp collision data at $\sqrt{s} = 8$ TeV corresponding to an integrated luminosity of 20.3 fb^{-1} . The observed lower limits on the T quark mass range between 715 GeV and 950 GeV and are the most stringent constraints to date. For $B\overline{B}$ production, the observed lower limits on the B quark mass range between 575 GeV and 813 GeV. The 95% Confidence Level (CL) observed lower limits on vector-like T and B quarks masses are for all possible values of the branching ratios into three decay modes: $T \rightarrow Wb, Zt, Ht$ and $B \rightarrow Wt, Zb, Hb$ [86].

No official limits on vector-like leptons have been obtained so far by the LHC detector collaborations. The current bounds on vector-like leptons quoted by the Particle Data Group (PDG) come from the LEP e^+e^- collider experiments. Assuming a heavy charged lepton decaying to $W\nu$ with the 100% branching fraction, the lower bound on its mass is 100.8 GeV.

Relaxing that assumption could lead to different limits, but in any case the upper bound ~ 100 GeV survives [37, 87, 88].

One of the important consequences of introducing vector-like leptons and quarks in theoretical models is improving electroweak precision and mass restrictions, which will be discussed in Chapter 4 and 5, respectively [2, 4].

2.3.2 Dark Matter

Strong evidence for the incompleteness of the SM also comes from the observation of non-baryonic Dark Matter (DM) in our universe. DM has not yet been observed in particle physics experiments. If any non-gravitational interactions between DM and SM particles exists, particles of DM could be produced at the LHC. Since DM particles themselves do not produce signals in the LHC detectors, one way to observe them is when they are produced in association with a visible SM particle. Many theories predict DM particles to be light enough to be produced at the LHC. If they were created at the LHC, they would escape through the detectors unnoticed. However, they would carry away energy and momentum, so physicists could infer their existence from the amount of energy and momentum missing after a collision [89, 90].

As the SM does not contain any DM candidates, a great deal of effort has gone into providing viable candidates, or alternative BSM scenarios. For models which do not have natural candidates, we usually consider the simplest additions to the SM that can account for DM e.g., a scalar, a fermion, or a vector, singlets, or doublets under $SU(2)_L$, etc. [2]. The most popular class of models explaining the cosmological observations contains DM that is a weakly interacting massive particle (WIMP). WIMPs that have a mass close to the EW scale and couplings similar to the weak coupling constant will produce the correct DM remnant density.

Many experiments seek to find evidence of DM either through direct or indirect DM searches. Direct searches look for energy deposited within a detector by the DM particles in the dark halo of the Milky Way. WIMPs can potentially scatter through collisions with nuclei through both spin-independent (SI) and spin-dependent (SD) interactions. For SI, cross sections are proportional to the square of the atomic mass of the target nuclei. The cross sections for SD scattering, in contrast, are proportional to the spin of the target nucleus. The current experimental sensitivity to SD scattering is far below that of SI interactions. Another major class of DM searches are indirect detection experiments which attempt to find the products

from WIMP annihilations, including gamma rays, neutrinos, positrons, electrons, and anti-protons. These searches are sensitive to interactions with all SM particles [30, 31]. If the WIMPs interact with quarks via a heavy mediator, they could also be pair produced in collider events. Fig. 2.4 shows the latest ATLAS results [91], on DM pair production in association with a γ for SI and SD interactions, compared to various DM searches. The search extends the limit on the scattering cross section into the low mass region $m < 10$ GeV where the astroparticle experiments have less sensitivity.

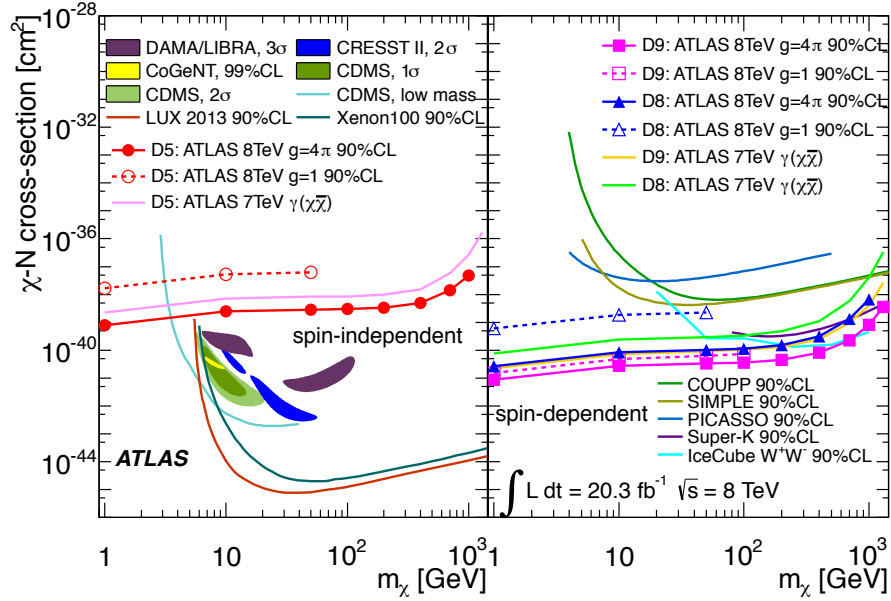


Figure 2.4: The ATLAS upper limits at 90 % C.L. on the WIMP-nucleon (χ -N) scattering cross section as a function of DM mass (m_χ) for spin independent (left) and spin dependent (right) interactions in pp collision with $\sqrt{s} = 8$ TeV and 20.3 fb^{-1} . Also shown are results from various Dark Matter search experiments. This figure is reproduced from [91].

ATLAS and CMS organized a forum, the ATLAS-CMS Dark Matter Forum, to establish a general agreement on the use of the simplified theoretical models for early Run-2 searches with the participation of experts on DM theories [89]. During the upcoming Run 2 of the LHC with almost doubled beam energy, most of the limits described in Run 1 will certainly be improved significantly, unless new phenomena show up [67].

Chapter 3

Neutral Higgs Bosons in the Higgs Triplet Model

Abstract

We revisit the neutral Higgs sector of the Higgs Triplet Model, with non-negligible mixing in the CP-even Higgs sector. We examine the possibility that one of the Higgs boson states is the particle observed at the LHC at 125 GeV, and the other is either the small LEP excess at 98 GeV; or the CMS excess at 136 GeV; or that the neutral Higgs bosons are (almost) degenerate and have both mass 125 GeV. We show that, under general considerations, an (unmixed) neutral Higgs boson cannot have an enhanced decay branching ratio into $\gamma\gamma$ with respect to the Standard Model one. An enhancement is however possible for the mixed case, but only for the heavier of the two neutral Higgs bosons, and not for mass-degenerate Higgs bosons. At the same time the branching ratios into WW^* , ZZ^* , $b\bar{b}$ and $\tau^+\tau^-$ are similar to the Standard Model, or reduced. We correlate the branching ratios of both Higgs states into $Z\gamma$ to those into $\gamma\gamma$ for the three scenarios. The mixed neutral sector of the Higgs triplet model exhibits some features which could distinguish it from other scenarios at the LHC.

3.1 Introduction

The hunt for the Higgs boson in the Standard Model (SM) and beyond has been given a big boost with the recently discovered resonance at $\simeq 125 - 126$ GeV, observed by ATLAS [6]

and CMS [29] at 5σ . While this particle resembles in most features the SM Higgs boson, the data hints of enhancements in its decay rate to $\gamma\gamma$ (although this signal is, at about 2σ , not sufficiently statistically secure), as well as depressed rates into $\tau^+\tau^-$ and WW^* , which could hint at extended symmetries. The signals are also consistent with the findings at the Tevatron [92]. If the $\gamma\gamma$ signals persist with more statistics, they would be an encouraging sign of physics beyond the Standard Model (BSM). This possibility has already inspired many explorations in literature [93–106]. The Higgs boson decay into $\gamma\gamma$ is loop induced and thus, sensitive to new physics contributions. The simplest explanation would be the presence of a charged boson in the loop, most likely a charged Higgs boson which appears in most BSM scenarios. In addition, if taken at face value, the suppression of the leptonic decay modes could be an indication that the neutral boson observed is not a pure SM state, but a mixed state, in which the other component has depressed couplings to leptons.

There are additional hints that more than one Higgs boson might have been observed. For instance, CMS observes an additional excess in the $\gamma\gamma$ and $\tau\tau$ channels at ~ 136 GeV [107, 108], which also seems to provide a best fit to the Tevatron data [109]. Additionally, LEP has observed an excess in $e^+e^- \rightarrow Zb\bar{b}$ near ~ 98 GeV [110, 111]. This has lead several authors [112–117] to investigate the possibility that the data could be fit by not one but two Higgs bosons— or two degenerate, or nearly degenerate, Higgs bosons [118, 119].

Motivated by these observations, we investigate one of the simplest extensions of the SM, the Higgs Triplet Model (HTM) with nontrivial mixing in the neutral sector. We probe whether the CP-even Higgs states can explain the signal at 125 GeV, and either the additional state at 98 GeV, or the one at 136 GeV. The HTM has two important ingredients lacking in the SM. First, it provides an explanation for small neutrino masses [120, 121] through the seesaw mechanism [122]: even if the boson at the LHC turns out to be completely consistent with the SM boson, the SM leaves the question of neutrino masses unresolved. Second, the model includes in its Higgs spectrum one singly charged and doubly charged boson, making loop enhancements of decays into $\gamma\gamma$ possible.

The neutral Higgs sector of the HTM has been studied previously [123–136]. Various authors have provided analyses showing the $\gamma\gamma$ signal suppressed with respect to the SM [129, 133]. An exception to this is in Ref. [137], where it was shown that in the case where the triple boson coupling is negative, the decay rates to $\gamma\gamma$ are enhanced.

But most of the authors have considered the HTM for the case in which the mixing of the CP-even neutral bosons is negligible, with the exception of in Ref. [138], where the mixing is

assumed to be maximal. For negligible mixing, the neutral boson visible at LHC is SM-like (a neutral component of a doublet Higgs representation) with the same tree-level couplings to fermions and gauge bosons, but which also couples to singly and doubly charged Higgs bosons, possibly a source of enhancement for the $\gamma\gamma$ signal. The production cross sections and decays to $f\bar{f}$, WW^* and ZZ^* are unchanged with respect to the SM. Should these rates be different, new particles must be added to the model to provide a viable explanation [139].

We revisit the model for the case where the mixing is non-negligible, and both states are mixtures of doublet and triplet Higgs representations. We study the tree-level and loop-induced ($\gamma\gamma$ and $Z\gamma$) decays of the two bosons for the case in which $m_{H_1} = 125$ GeV, $m_{H_2} = 136$ GeV (motivated by the CMS data); for the case where $m_{H_1} = 98$ GeV, $m_{H_2} = 125$ GeV (motivated by the LEP excess); and for the case where the two Higgs are degenerate in mass and $m_{H_1} = m_{H_2} = 125$ GeV, which is motivated by the case where there is a single boson observed at the LHC. We do not assume specific mixing, but rather study the variation in all parameters due to mixing and comment on the case where the mixing is negligible as a limiting case. We consider deviations from unity of ratios of branching ratios in the HTM (with H_1, H_2 Higgs bosons) versus the SM (with Φ Higgs boson):

$$R_{H_1, H_2 \rightarrow XX} = \frac{[\sigma(gg \rightarrow H_1, H_2) \times BR(H_1, H_2 \rightarrow XX)]_{HTM}}{[\sigma(gg \rightarrow \Phi) \times BR(\Phi \rightarrow XX)]_{SM}} \quad (3.1)$$

with $XX = \gamma\gamma, f\bar{f}, ZZ^*, WW^*$, and predict the rate for $Z\gamma$, as the correlation between this decay and $\gamma\gamma$ would be a further test of the structure of the model.

This Chapter is organized as follows: in Section 6.2 we summarize the main features of the HTM, paying particular attention to the neutral Higgs sector, and outline the conditions on the relevant parameters. In Section 3.3 we present expressions for the decay width of the neutral Higgs bosons, as well as give general analytic expressions for the decay rates, for both $\gamma\gamma$ in Section 3.3.1 and, following examination of the effect of the total width difference between the Higgs boson in SM and in the HTM in Section 3.3.2, the tree-level decays to $f\bar{f}$, WW^* and ZZ^* in Section 3.3.3. We follow in Section 3.4 with numerical analysis for the decays of the bosons in scenarios inspired by the experimental data. In Section 3.4.3 we show predictions for the same parameter space for the decays of the neutral Higgs bosons to $Z\gamma$, another indicator of extra charged particles in the model.

3.2 The Higgs Triplet Model

We describe the Higgs Triplet Model (HTM), which has been recently the topic extensive studies [129–134]. The HTM is based on the same gauge symmetry group as the SM, $SU(2)_L \times U(1)_Y$. The only difference is the addition of one triplet field Δ with hypercharge $Y = 1$ and the lepton number $L = 2$ to the SM Higgs sector, which already contains one isospin doublet field Φ with hypercharge $Y = 1/2$. The relevant terms in Lagrangian are:

$$\mathcal{L}_{\text{HTM}} = \mathcal{L}_{\text{kin}} + \mathcal{L}_Y - V(\Phi, \Delta), \quad (3.2)$$

where \mathcal{L}_{kin} , \mathcal{L}_Y and $V(\Phi, \Delta)$ are the kinetic term, Yukawa interaction and the scalar potential, respectively. The kinetic term of the Higgs fields is

$$\mathcal{L}_{\text{kin}} = (D_\mu \Phi)^\dagger (D^\mu \Phi) + \text{Tr}[(D_\mu \Delta)^\dagger (D^\mu \Delta)], \quad (3.3)$$

with

$$D_\mu \Phi = \left(\partial_\mu + i\frac{g}{2}\tau^a W_\mu^a + i\frac{g'}{2}B_\mu \right) \Phi, \quad D_\mu \Delta = \partial_\mu \Delta + i\frac{g}{2}[\tau^a W_\mu^a, \Delta] + ig'B_\mu \Delta, \quad (3.4)$$

the covariant derivatives for the doublet and triplet Higgs fields. The Yukawa interaction for the Higgs fields is

$$\mathcal{L}_Y = - \left[\bar{Q}_L^i Y_d^{ij} \Phi d_R^j + \bar{Q}_L^i Y_u^{ij} \tilde{\Phi} u_R^j + \bar{L}_L^i Y_e^{ij} \Phi e_R^j + \text{h.c.} \right] + h_{ij} \bar{L}_L^i \tau_2 \Delta L_L^j + \text{h.c.}, \quad (3.5)$$

where $\tilde{\Phi} = i\tau_2 \Phi^*$, $Y_{u,d,e}$ are 3×3 complex matrices, and h_{ij} is a 3×3 complex symmetric Yukawa matrix. The most general Higgs potential involving the doublet Φ and triplet Δ is given by

$$\begin{aligned} V(\Phi, \Delta) = & m^2 \Phi^\dagger \Phi + M^2 \text{Tr}(\Delta^\dagger \Delta) + [\mu \Phi^T i\tau_2 \Delta^\dagger \Phi + \text{h.c.}] + \lambda_1 (\Phi^\dagger \Phi)^2 \\ & + \lambda_2 [\text{Tr}(\Delta^\dagger \Delta)]^2 + \lambda_3 \text{Tr}[(\Delta^\dagger \Delta)^2] + \lambda_4 (\Phi^\dagger \Phi) \text{Tr}(\Delta^\dagger \Delta) + \lambda_5 \Phi^\dagger \Delta \Delta^\dagger \Phi, \end{aligned} \quad (3.6)$$

where m and M are the Higgs bare masses, μ is the lepton number violating parameter, and λ_1 - λ_5 are Higgs coupling constants. We assume all the parameters to be real. The scalar fields Φ and Δ can be written as:

$$\Phi = \begin{bmatrix} \varphi^+ \\ \frac{1}{\sqrt{2}}(\varphi + v_\Phi + i\chi) \end{bmatrix}, \quad \Delta = \begin{bmatrix} \frac{\Delta^+}{\sqrt{2}} & \Delta^{++} \\ \frac{1}{\sqrt{2}}(\delta + v_\Delta + i\eta) & -\frac{\Delta^+}{\sqrt{2}} \end{bmatrix}, \quad (3.7)$$

where v_Φ and v_Δ are the VEVs of the doublet Higgs field and the triplet Higgs field, with $v^2 \equiv v_\Phi^2 + 2v_\Delta^2 \simeq (246 \text{ GeV})^2$. The electric charge is defined as $Q = I_3 + Y$, with I_3 the third component of the $SU(2)_L$ isospin.

Minimizing the potential with respect to the VEVs v_Φ , v_Δ yields expressions for m, M in terms of the other coefficients in the model. The mass matrices for the Higgs bosons are diagonalized by unitary matrices, yielding physical states for the singly charged, the CP-odd, and the CP-even neutral scalar sectors, respectively:

$$\begin{aligned} \begin{pmatrix} \varphi^\pm \\ \Delta^\pm \end{pmatrix} &= \begin{pmatrix} \cos \beta_\pm & -\sin \beta_\pm \\ \sin \beta_\pm & \cos \beta_\pm \end{pmatrix} \begin{pmatrix} w^\pm \\ H^\pm \end{pmatrix}, & \begin{pmatrix} \chi \\ \eta \end{pmatrix} &= \begin{pmatrix} \cos \beta_0 & -\sin \beta_0 \\ \sin \beta_0 & \cos \beta_0 \end{pmatrix} \begin{pmatrix} z \\ A \end{pmatrix}, \\ \begin{pmatrix} \varphi \\ \delta \end{pmatrix} &= \begin{pmatrix} \cos \alpha & -\sin \alpha \\ \sin \alpha & \cos \alpha \end{pmatrix} \begin{pmatrix} h \\ H \end{pmatrix}, \end{aligned} \quad (3.8)$$

where the mixing angles in the same sectors are given by

$$\begin{aligned} \tan \beta_\pm &= \frac{\sqrt{2}v_\Delta}{v_\Phi}, & \tan \beta_0 &= \frac{2v_\Delta}{v_\Phi}, \\ \tan 2\alpha &= \frac{v_\Delta}{v_\Phi} \frac{2v_\Phi^2(\lambda_4 + \lambda_5) - 4M_\Delta^2}{2v_\Phi^2\lambda_1 - M_\Delta^2 - 2v_\Delta^2(\lambda_2 + \lambda_3)}. \end{aligned} \quad (3.9)$$

where $M_\Delta^2 \equiv \frac{v_\Phi^2 \mu}{\sqrt{2}v_\Delta}$. There are seven physical mass eigenstates $H^{\pm\pm}$, H^\pm , A , H and h , in addition to the three Goldstone bosons G^\pm and G^0 which give mass to the gauge bosons. The masses of the physical states are expressed in terms of the parameters in the Lagrangian as

$$m_{H^{++}}^2 = M_\Delta^2 - v_\Delta^2 \lambda_3 - \frac{\lambda_5}{2} v_\Phi^2, \quad (3.10)$$

$$m_{H^+}^2 = \left(M_\Delta^2 - \frac{\lambda_5}{4} v_\Phi^2 \right) \left(1 + \frac{2v_\Delta^2}{v_\Phi^2} \right), \quad (3.11)$$

$$m_A^2 = M_\Delta^2 \left(1 + \frac{4v_\Delta^2}{v_\Phi^2} \right), \quad (3.12)$$

$$m_h^2 = 2v_\Phi^2 \lambda_1 \cos^2 \alpha + [M_\Delta^2 + 2v_\Delta^2(\lambda_2 + \lambda_3)] \sin^2 \alpha + \left[\frac{2v_\Delta}{v_\Phi} M_\Delta^2 - v_\Phi v_\Delta (\lambda_4 + \lambda_5) \right] \sin 2\alpha, \quad (3.13)$$

$$m_H^2 = 2v_\Phi^2 \lambda_1 \sin^2 \alpha + [M_\Delta^2 + 2v_\Delta^2(\lambda_2 + \lambda_3)] \cos^2 \alpha - \left[\frac{2v_\Delta}{v_\Phi} M_\Delta^2 - v_\Phi v_\Delta (\lambda_4 + \lambda_5) \right] \sin 2\alpha, \quad (3.14)$$

Conversely, the six parameters μ and λ_1 - λ_5 in the Higgs potential can be written in terms of

the physical scalar masses, the mixing angle α and doublet and triplet VEVs v_Φ and v_Δ :

$$\mu = \frac{\sqrt{2}v_\Delta}{v_\Phi^2} M_\Delta^2 = \frac{\sqrt{2}v_\Delta}{v_\Phi^2 + 4v_\Delta^2} m_A^2, \quad (3.15)$$

$$\lambda_1 = \frac{1}{2v_\Phi^2} (m_h^2 \cos^2 \alpha + m_H^2 \sin^2 \alpha), \quad (3.16)$$

$$\lambda_2 = \frac{1}{2v_\Delta^2} \left[2m_{H^{++}}^2 + v_\Phi^2 \left(\frac{m_A^2}{v_\Phi^2 + 4v_\Delta^2} - \frac{4m_{H^+}^2}{v_\Phi^2 + 2v_\Delta^2} \right) + m_H^2 \cos^2 \alpha + m_h^2 \sin^2 \alpha \right], \quad (3.17)$$

$$\lambda_3 = \frac{v_\Phi^2}{v_\Delta^2} \left(\frac{2m_{H^+}^2}{v_\Phi^2 + 2v_\Delta^2} - \frac{m_{H^{++}}^2}{v_\Phi^2} - \frac{m_A^2}{v_\Phi^2 + 4v_\Delta^2} \right), \quad (3.18)$$

$$\lambda_4 = \frac{4m_{H^+}^2}{v_\Phi^2 + 2v_\Delta^2} - \frac{2m_A^2}{v_\Phi^2 + 4v_\Delta^2} + \frac{m_h^2 - m_H^2}{2v_\Phi v_\Delta} \sin 2\alpha, \quad (3.19)$$

$$\lambda_5 = 4 \left(\frac{m_A^2}{v_\Phi^2 + 4v_\Delta^2} - \frac{m_{H^+}^2}{v_\Phi^2 + 2v_\Delta^2} \right). \quad (3.20)$$

The parameters of the model are restricted by the values of the W and Z masses are obtained at tree level

$$m_W^2 = \frac{g^2}{4} (v_\Phi^2 + 2v_\Delta^2), \quad m_Z^2 = \frac{g^2}{4 \cos^2 \theta_W} (v_\Phi^2 + 4v_\Delta^2), \quad (3.21)$$

and the electroweak ρ parameter defined at tree level

$$\rho \equiv \frac{m_W^2}{m_Z^2 \cos^2 \theta_W} = \frac{1 + \frac{2v_\Delta^2}{v_\Phi^2}}{1 + \frac{4v_\Delta^2}{v_\Phi^2}}. \quad (3.22)$$

As the experimental value of the ρ parameter is near unity, v_Δ^2/v_Φ^2 is required to be much smaller than unity at the tree level, justifying the expansions in Eqs. (3.26), (3.27), (3.28). Note that the smallness of v_Δ/v_Φ insures that the mixing angles β_\pm and β_0 are close to 0, while α remains undetermined. Finally, small Majorana neutrino masses, proportional to the lepton number violating coupling constant μ , are generated by the Yukawa interaction of the triplet field

$$(m_\nu)_{ij} = \sqrt{2} h_{ij} v_\Delta = h_{ij} \frac{\mu v_\Phi^2}{M_\Delta^2}. \quad (3.23)$$

If $\mu \ll M_\Delta$ the smallness of the neutrino masses are explained by the type II seesaw mechanism. This condition constrains the size of $h_{ij} v_\Delta$ by relating it to the neutrino mass. The smallness of v_Δ yields approximate relationships among the masses:

$$m_{H^+}^2 - m_{H^{++}}^2 \simeq m_A^2 - m_{H^+}^2 \simeq \frac{\lambda_5}{4} v_\Phi^2, \quad (3.24)$$

$$m_H^2 \simeq m_A^2 (\simeq M_\Delta^2), \quad (3.25)$$

which are valid to $\mathcal{O}(v_\Delta^2/v_\Phi^2)$. We can further simplify, for the parameters $\lambda_2, \lambda_3, \lambda_4$ in terms of λ_5 , the neutral Higgs masses and the mixing angle:

$$\lambda_2 = -\lambda_5 + \frac{1}{2v_\Delta^2} \sin^2 \alpha (m_h^2 - m_H^2) + 2\frac{m_H^2}{v_\Phi^2} + \mathcal{O}\left(\frac{v_\Delta^2}{v_\Phi^2}\right), \quad (3.26)$$

$$\lambda_3 = \lambda_5 + \mathcal{O}\left(\frac{v_\Delta^2}{v_\Phi^2}\right), \quad (3.27)$$

$$\lambda_4 = -\lambda_5 + \frac{m_h^2 - m_H^2}{2v_\Delta v_\Phi} \sin 2\alpha + 2\frac{m_H^2}{v_\Phi^2} + \mathcal{O}\left(\frac{v_\Delta^2}{v_\Phi^2}\right), \quad (3.28)$$

which must be consistent with conditions on the Higgs potential.

3.2.1 Positivity Conditions on the Higgs potential

The parameters in the Higgs potential are not arbitrary, but subjected to several conditions. These have been thoroughly analyzed in [130–132], and we summarize their results briefly. Positivity requirement in the singly and doubly charged Higgs mass sectors (for $v_\Delta > 0$) are:

$$\mu > 0; \quad \mu > \frac{\lambda_5 v_\Delta}{2\sqrt{2}}; \quad \mu > \frac{\lambda_5 v_\Delta}{\sqrt{2}} + \sqrt{2} \frac{\lambda_3 v_\Delta^3}{v_\Phi^2}, \quad (3.29)$$

while, for the requirement that the potential is bounded from below, the complete set of conditions are:

$$\lambda_1 > 0; \quad \lambda_2 + \lambda_3 > 0; \quad \lambda_2 + \frac{\lambda_3}{2} > 0; \quad (3.30)$$

$$\lambda_4 + \sqrt{4\lambda_1(\lambda_2 + \lambda_3)} > 0; \quad \lambda_4 + \sqrt{4\lambda_1\left(\lambda_2 + \frac{\lambda_3}{2}\right)} > 0; \quad (3.31)$$

$$\lambda_4 + \lambda_5 + \sqrt{4\lambda_1(\lambda_2 + \lambda_3)} > 0; \quad \lambda_4 + \lambda_5 + \sqrt{4\lambda_1\left(\lambda_2 + \frac{\lambda_3}{2}\right)} > 0. \quad (3.32)$$

Note that from the expressions in Eq. (3.15) and (3.16), some conditions are automatically satisfied, such as positivity of μ and λ_1 . Positivity of $\lambda_2 + \lambda_3$ and $\lambda_2 + \frac{\lambda_3}{2}$ are consistent with the requirements of the square root in Eq. (3.31) and (3.32) being real. From all of these conditions, the last expressions in Eq. (3.31) and (3.32) would restrict possible enhancements in the $h, H \rightarrow \gamma\gamma$ decay.

Before we proceed with the detailed analysis, some general comments are in order. As shown in Ref. [129], and as we show in detail in the next section, for $\sin \alpha = 0$, the coupling between h and the doubly charged Higgs is strictly proportional to λ_4 . If λ_4 is positive (negative),

the contribution of the doubly charged Higgs bosons is subtracted from (added to) the W boson contribution, which is dominant, resulting in a suppression (enhancement) of the $\gamma\gamma$ branching ratio. The contribution for the singly charged Higgs bosons is significantly smaller, but follows the same general pattern. Note that if $\alpha = 0$, $\lambda_2 = \lambda_4$. Thus it is inconsistent to assume $\lambda_2 > 0$, while $\lambda_4 < 0$. Moreover, for $\sin \alpha = 0$,

$$\lambda_4 = -\lambda_5 + 2\frac{m_H^2}{v_\Phi^2} = -2\left(\frac{m_H^2}{v_\Phi^2} - \frac{m_{H^{++}}^2}{v_\Phi^2}\right) + 2\frac{m_H^2}{v_\Phi^2} = 2\frac{m_{H^{++}}^2}{v_\Phi^2}, \quad (3.33)$$

and thus λ_4 cannot be negative, preventing an enhancement of $R_{\gamma\gamma}$ for the unmixed neutral Higgs boson h due to the presence of the singly and doubly-charged Higgs in the loop.

Thus the only possibility in which there could be some enhancement in the decay to $\gamma\gamma$ is the case in which there is some mixing between the two states Φ^0 and Δ^0 , and both states are responsible for some of the signals observed at the LHC, Tevatron and LEP, an alternative which we investigate in the remainder of this work. We continue to call the two mixed states h and H , with the convention that, when $\alpha \rightarrow 0$, these states correspond to the unmixed states Φ^0 (neutral doublet) and Δ^0 (neutral triplet), respectively. We take a different point of view from previous analyses. We make no assumption about the mixing but express all parameters as functions of α , the mixing angle in the neutral (CP-even) Higgs sector, as in Eqs. (3.24), (3.25), (3.26), (3.27) and (3.28).

3.3 Decay rates of the neutral Higgs bosons in the HTM

3.3.1 Decay rates to $\gamma\gamma$

In this section we present the analytic expressions for the decays of the neutral bosons. The detailed numerical analysis and comparison with the LHC, Tevatron and LEP data follows in the next section. We concentrate first on the decays to $\gamma\gamma$, as, in spite of the small rate, these decays are very promising, as the two-photon invariant mass $M_{\gamma\gamma}$ can be reconstructed to $\mathcal{O}(1\%)$ accuracy. Indeed both CMS and ATLAS have their most accurate data for this channel. We allow arbitrary mixing in the neutral sector and discuss the restrictions on the parameters in the Higgs sector imposed by the data, as well as by the conditions on the potential, and investigate the consequences for the decay of both neutral Higgs bosons in the HTM.

First consider Eqs. (3.26), (3.27), (3.28), for $\sin \alpha \neq 0$. As $\lambda_2 + \lambda_3 > 0$, this requires $m_h^2 > m_H^2$,

that is the state that in the limit $\sin \alpha = 0$ is the Higgs doublet state is heavier than the state that in the limit $\sin \alpha = 0$ is the Higgs triplet state. Unlike for the state with $\alpha = 0$, $\lambda_2 \neq \lambda_4$, more precisely

$$\lambda_4 = \lambda_2 - \frac{m_h^2 - m_H^2}{2v_\Delta^2} \sin \alpha \sin(\alpha - \beta_0) \simeq \lambda_2 - \frac{m_h^2 - m_H^2}{2v_\Delta^2} \sin^2 \alpha. \quad (3.34)$$

The decay rates of the Higgs bosons in the HTM are defined in terms of the decay of the Higgs boson in the SM (denoted as Φ) as

$$\begin{aligned} R_{h,H \rightarrow \gamma\gamma} &\equiv \frac{\sigma_{\text{HTM}}(gg \rightarrow h, H \rightarrow \gamma\gamma)}{\sigma_{\text{SM}}(gg \rightarrow \Phi \rightarrow \gamma\gamma)} = \frac{[\sigma(gg \rightarrow h, H) \times BR(h, H \rightarrow \gamma\gamma)]_{\text{HTM}}}{[\sigma(gg \rightarrow \Phi) \times BR(\Phi \rightarrow \gamma\gamma)]_{\text{SM}}} \\ &= \frac{[\sigma(gg \rightarrow h, H) \times \Gamma(h, H \rightarrow \gamma\gamma)]_{\text{HTM}}}{[\sigma(gg \rightarrow \Phi) \times \Gamma(\Phi \rightarrow \gamma\gamma)]_{\text{SM}}} \times \frac{[\Gamma(\Phi)]_{\text{SM}}}{[\Gamma(h, H)]_{\text{HTM}}}, \end{aligned} \quad (3.35)$$

where the ratios of cross section rates by gluon fusion are

$$\frac{[\sigma(gg \rightarrow h)]_{\text{HTM}}}{[\sigma(gg \rightarrow \Phi)]_{\text{SM}}} = \cos^2 \alpha; \quad \frac{[\sigma(gg \rightarrow H)]_{\text{HTM}}}{[\sigma(gg \rightarrow \Phi)]_{\text{SM}}} = \sin^2 \alpha. \quad (3.36)$$

We present first the decay widths of h to $\gamma\gamma$:

$$\begin{aligned} [\Gamma(h \rightarrow \gamma\gamma)]_{\text{HTM}} &= \frac{G_F \alpha^2 m_h^3}{128 \sqrt{2} \pi^3} \left| \sum_f N_c^f Q_f^2 g_{hff} A_{1/2}(\tau_f^h) + g_{hWW} A_1(\tau_W^h) \right. \\ &\quad \left. + \tilde{g}_{hH^\pm H^\mp} A_0(\tau_{H^\pm}^h) + 4\tilde{g}_{hH^{\pm\pm} H^{\mp\mp}} A_0(\tau_{H^{\pm\pm}}^h) \right|^2. \end{aligned} \quad (3.37)$$

The couplings of h to the vector bosons and fermions are as follows:

$$g_{h\bar{t}t} = \cos \alpha / \cos \beta_\pm; \quad g_{hWW} = \cos \alpha + 2 \sin \alpha v_\Delta / v_\Phi, \quad (3.38)$$

and the scalar trilinear couplings are parametrized as follows:

$$\tilde{g}_{hH^{++}H^{--}} = \frac{m_W}{gm_{H^{\pm\pm}}^2} g_{hH^{++}H^{--}}; \quad \tilde{g}_{hH^+H^-} = \frac{m_W}{gm_{H^\pm}^2} g_{hH^+H^-}, \quad (3.39)$$

with the following explicit expressions in terms of the parameters of the scalar potential, Eq. (4.5):

$$g_{hH^{++}H^{--}} = 2\lambda_2 v_\Delta \sin \alpha + \lambda_4 v_\Phi \cos \alpha, \quad (3.40)$$

$$\begin{aligned} g_{hH^+H^-} &= \frac{1}{2} \left\{ \left[4v_\Delta (\lambda_2 + \lambda_3) \cos^2 \beta_\pm + 2v_\Delta \lambda_4 \sin^2 \beta_\pm - \sqrt{2} \lambda_5 v_\Phi \cos \beta_\pm \sin \beta_\pm \right] \sin \alpha \right. \\ &\quad \left. + \left[4\lambda_1 v_\Phi \sin \beta_\pm^2 + (2\lambda_4 + \lambda_5) v_\Phi \cos^2 \beta_\pm + (4\mu - \sqrt{2} \lambda_5 v_\Delta) \cos \beta_\pm \sin \beta_\pm \right] \cos \alpha \right\}. \end{aligned} \quad (3.41)$$

These couplings become, in terms of the masses and mixing, for the trilinear coupling of the neutral and doubly charged Higgs to h ,

$$\tilde{g}_{hH^{++}H^{--}} \simeq \frac{v_\Phi^2}{2m_{H^{++}}^2} \left\{ \frac{m_h^2 - m_H^2}{v_\Delta v_\Phi} \sin \alpha + \left(2\frac{m_H^2}{v_\Phi^2} - \lambda_5 \right) \cos(\alpha - \beta_0) \right\}, \quad (3.42)$$

$$\tilde{g}_{hH^+H^-} \simeq \frac{v_\Phi^2}{2m_{H^+}^2} \left\{ \frac{m_h^2 - m_H^2}{v_\Delta v_\Phi} \sin \alpha + \left(2\frac{m_H^2}{v_\Phi^2} - \frac{\lambda_5}{2} \right) \cos(\alpha - \beta_0) \right\}. \quad (3.43)$$

We obtain similar expressions for the neutral boson H :

$$\begin{aligned} \Gamma(H \rightarrow \gamma\gamma) &= \frac{G_F \alpha^2 m_H^3}{128\sqrt{2}\pi^3} \left| \sum_f N_c Q_f^2 g_{Hff} A_{1/2}(\tau_f^H) + g_{HWW} A_1(\tau_W^H) \right. \\ &\quad \left. + \tilde{g}_{HH^\pm H^\mp} A_0(\tau_{H^\pm}^H) + 4\tilde{g}_{HH^{\pm\pm} H^{\mp\mp}} A_0(\tau_{H^{\pm\pm}}^H) \right|^2. \end{aligned} \quad (3.44)$$

The couplings of H to the vector bosons and fermions relative to the values in the SM are as follows:

$$g_{H\bar{t}t} = -\sin \alpha / \cos \beta_\pm; \quad g_{HWW} = -\sin \alpha + 2 \cos \alpha v_\Delta / v_\Phi, \quad (3.45)$$

The scalar trilinear couplings are parametrized similar to those for h :

$$\tilde{g}_{HH^{++}H^{--}} = \frac{m_W}{gm_{H^{\pm\pm}}^2} g_{HH^{++}H^{--}}; \quad \tilde{g}_{HH^+H^-} = \frac{m_W}{gm_{H^\pm}^2} g_{HH^+H^-}, \quad (3.46)$$

with the following explicit expressions in terms of the parameters of the scalar potential (these can be obtained from the expressions for h , with the replacements $\cos \alpha \rightarrow -\sin \alpha$, $\sin \alpha \rightarrow \cos \alpha$):

$$g_{HH^{++}H^{--}} = 2\lambda_2 v_\Delta \cos \alpha - \lambda_4 v_\Phi \sin \alpha, \quad (3.47)$$

$$\begin{aligned} g_{HH^+H^-} &= \frac{1}{2} \left\{ \left[4v_\Delta (\lambda_2 + \lambda_3) \cos^2 \beta_\pm + 2v_\Delta \lambda_4 \sin^2 \beta_\pm - \sqrt{2}\lambda_5 v_\Phi \cos \beta_\pm \sin \beta_\pm \right] \cos \alpha \right. \\ &\quad \left. - \left[4\lambda_1 v_\Phi \sin \beta_\pm^2 + (2\lambda_4 + \lambda_5) v_\Phi \cos^2 \beta_\pm + (4\mu - \sqrt{2}\lambda_5 v_\Delta) \cos \beta_\pm \sin \beta_\pm \right] \sin \alpha \right\}, \end{aligned} \quad (3.48)$$

we obtain

$$\tilde{g}_{HH^{++}H^{--}} \simeq -\frac{v_\Phi^2}{2m_{H^{++}}^2} \left(2\frac{m_H^2}{v_\Phi^2} - \lambda_5 \right) \sin(\alpha - \beta_0) \quad (3.49)$$

$$\tilde{g}_{HH^+H^-} \simeq -\frac{v_\Phi^2}{2m_{H^+}^2} \left(2\frac{m_H^2}{v_\Phi^2} - \frac{\lambda_5}{2} \right) \sin(\alpha - \beta_0) \quad (3.50)$$

We define throughout $\tau_i^h = m_h^2/4m_i^2$, $\tau_i^H = m_H^2/4m_i^2$ ($i = f, W, H^\pm, H^{\pm\pm}$). The loop functions A_1 (for the W boson) and $A_{1/2}$ (for the fermions, f) are given as

$$A_0(\tau) = -[\tau - f(\tau)]\tau^{-2}, \quad (3.51)$$

$$A_{1/2}(\tau) = -\tau^{-1} [1 + (1 - \tau^{-1}) f(\tau^{-1})], \quad (3.52)$$

$$A_1(\tau) = 1 + \frac{3}{2}\tau^{-1} + 4\tau^{-1} \left(1 - \frac{1}{2}\tau^{-1}\right) f(\tau^{-1}). \quad (3.53)$$

These function are similarly defined for H , with the change $h \rightarrow H$, and the function $f(\tau)$ is given by :

$$f(\tau) = \begin{cases} \arcsin^2 \sqrt{\tau} & \tau \leq 1 \\ -\frac{1}{4} \left[\log \frac{1 + \sqrt{1 - \tau^{-1}}}{1 - \sqrt{1 - \tau^{-1}}} - i\pi \right]^2 & \tau > 1. \end{cases} \quad (3.54)$$

Second, note that the contribution from the loop with $H^{\pm\pm}$ in Eq.(3.37) is enhanced relative to the contribution from H^\pm by a factor of four at the amplitude level. All couplings are evaluated to $\mathcal{O}(\frac{v_\Delta^2}{v_\Phi^2})$. However, for all relevant parameter space the effect of β_0 is negligible ($\tan \beta_0 = \frac{2v_\Delta}{v_\Phi}$), and we can assume with no loss of generality that $\beta_0 \simeq 0$. Third, as m_H is the lightest of the two Higgs states (and we would wish to associate it with one of the observed bosons), λ_5 is constrained to be negative, otherwise the singly and doubly charged Higgs bosons would be unacceptably light. Fourth, inspection of the analytic expressions indicate that for all of the parameter space, the reduced couplings $\tilde{g}_{hH^{++}H^{--}}$ and $\tilde{g}_{hH^{++}H^{--}}$ are positive [as $\alpha \in (0, \pi/2)$], while $\tilde{g}_{HH^{++}H^{--}}$ and $\tilde{g}_{HH^{++}H^{--}}$ are negative. This means that we expect that, from trilinear couplings alone, $R(h \rightarrow \gamma\gamma)$ could be enhanced with respect to the SM over a region of the parameter space, while $R(H \rightarrow \gamma\gamma)$ will be suppressed over all of the parameter space.

3.3.2 Branching ratios enhancement due to Higgs widths in HTM

Our considerations for relative branching ratios are affected by the fact that the total width of the Higgs boson in the HTM is not the same as in the SM. The widths are the same as those in the SM for h in the limit $\sin \alpha \rightarrow 0$. However, for $\alpha \neq 0$ we must take into account the relative widths factors

$$\frac{[\Gamma(\Phi)]_{SM}}{[\Gamma(h, H)]_{HTM}} = \frac{[\Gamma(\Phi \rightarrow \sum_f f\bar{f}) + \Gamma(\Phi \rightarrow WW^*) + \Gamma(\Phi \rightarrow ZZ^*)]_{SM}}{[\Gamma(h, H \rightarrow \sum_f f\bar{f}) + \Gamma(h, H \rightarrow WW^*) + \Gamma(h, H \rightarrow ZZ^*) + \Gamma(h, H \rightarrow \nu\nu)]_{HTM}}. \quad (3.55)$$

We expect this to enhance the relative signal strength, as roughly

$$\frac{[\Gamma(\Phi)]_{SM}}{[\Gamma(h)]_{HTM}} \simeq \frac{1}{\cos^2 \alpha} \left[1 - \frac{[\Gamma(h \rightarrow \nu\nu)]_{HTM}}{[\Gamma(\Phi)]_{SM}} \right]; \quad \frac{[\Gamma(\Phi)]_{SM}}{[\Gamma(H)]_{HTM}} \simeq \frac{1}{\sin^2 \alpha} \left[1 - \frac{[\Gamma(H \rightarrow \nu\nu)]_{HTM}}{[\Gamma(\Phi)]_{SM}} \right].$$

In the detailed numerical analysis, we highlight the relative width enhancement to illustrate its importance.

3.3.3 Tree-level decays of the Higgs bosons into fermions and gauge bosons

The largest branching ratio of a Higgs boson with mass of 125 GeV would be into $b\bar{b}$. Unfortunately, this channel is very difficult to observe at the LHC as the continuum background exceeds the signal by roughly eight orders of magnitude. The decay into $\tau^+\tau^-$ is also problematic, because of the low velocity of the Higgs boson, which makes the reconstruction of $m_{\tau\tau}$ difficult. Although observation of the decays to fermions is problematic, more statistics and combining LHC and Tevatron results will improve data. Thus we include the predictions of the model here.

The decays to the gauge bosons are more promising, but there are also some issues that need to be resolved in interpreting the data there. The decay to $W^\pm W^\mp$ has a large rate, but once one of the W bosons decay leptonically, the Higgs mass is hard to reconstruct, and the analysis relies on angular correlations. The two W bosons are produced with opposite polarization, and as W bosons are purely left-handed the two leptons prefer to move in the same rather than in opposite directions. On the positive side, the backgrounds are electroweak, and thus small. The Higgs decay into ZZ , with further decay into four muons is referred to as the “golden channel”. This is because the m_{4l} is easy to reconstruct. The limitations are the leptonic branching ratio of the Z and sharp drop in the off-shell Higgs branching ratio.

We show, for completeness, the relative decay branching ratios of the neutral bosons h and H into fermions, as well as into gauge bosons, compared to the SM ones. The decay rates for h can be expressed as

$$\Gamma(h \rightarrow f\bar{f}) = \sqrt{2}G_F \frac{m_h m_f^2}{8\pi} N_c^f \beta \left(\frac{m_f^2}{m_h^2} \right)^3 \cos^2 \alpha, \quad (3.56)$$

$$\Gamma(h \rightarrow \nu\nu) = \Gamma(h \rightarrow \nu^c \bar{\nu}) + \Gamma(h \rightarrow \bar{\nu}^c \nu) = \sum_{i,j=1}^3 S_{ij} |h_{ij}|^2 \frac{m_h}{4\pi} \sin^2 \alpha, \quad (3.57)$$

The second decay is of the form $h \rightarrow$ invisible, as it shows only as missing energy. It does not exist for a SM Higgs boson, and it is not a good signature for detection at the LHC. Fortunately, this decay width is small, even for $\sin \alpha = 1$, as the couplings h_{ij} must be small to generate small neutrino masses. But as these decays are tree-level, we include them in the total width consideration.

The decay rate of the Higgs boson h decaying into the gauge boson pair VV ($V = W$ or Z) is given by

$$\Gamma(h \rightarrow VV) = \frac{|\kappa_V(h)|^2 m_h^3}{128\pi m_V^4} \delta_V \left[1 - \frac{4m_V^2}{m_h^2} + \frac{12m_V^4}{m_h^4} \right] \beta \left(\frac{m_V^2}{m_h^2} \right), \quad (3.58)$$

where $\delta_W = 2$ and $\delta_Z = 1$, and where $\kappa_V(h)$ are the couplings of the Higgs h with the vector bosons:

$$\kappa_W(h) = \frac{ig^2}{2} (v_\phi \cos \alpha + 2v_\Delta \sin \alpha), \quad (3.59)$$

$$\kappa_Z(h) = \frac{ig^2}{2 \cos^2 \theta_W} (v_\phi \cos \alpha + 4v_\Delta \sin \alpha). \quad (3.60)$$

The decay rates of the three body decay modes are

$$\Gamma(h \rightarrow VV^*) = \frac{3g_V^2 |\kappa_V(h)|^2 m_h}{512\pi^3 m_V^2} \delta_{V'} F\left(\frac{m_V^2}{m_h^2}\right), \quad (3.61)$$

where $\delta_{W'} = 1$ and $\delta_{Z'} = \frac{7}{12} - \frac{10}{9} \sin^2 \theta_W + \frac{40}{27} \sin^4 \theta_W$, and where the function $F(x)$ is given as

$$\begin{aligned} F(x) &= -|1-x| \left(\frac{47}{2}x - \frac{13}{2} + \frac{1}{x} \right) + 3(1-6x+4x^2) |\log \sqrt{x}| \\ &+ \frac{3(1-8x+20x^2)}{\sqrt{4x-1}} \arccos \left(\frac{3x-1}{2x^{3/2}} \right). \end{aligned} \quad (3.62)$$

The decay rates for H can be expressed as

$$\Gamma(H \rightarrow f\bar{f}) = \sqrt{2} G_F \frac{m_H m_f^2}{8\pi} N_c^f \beta \left(\frac{m_f^2}{m_H^2} \right)^3 \sin^2 \alpha, \quad (3.63)$$

$$\Gamma(H \rightarrow \nu\nu) = \Gamma(H \rightarrow \nu^c \bar{\nu}) + \Gamma(H \rightarrow \bar{\nu}^c \nu) = \sum_{i,j=1}^3 S_{ij} |h_{ij}|^2 \frac{m_H}{4\pi} \cos^2 \alpha, \quad (3.64)$$

with the second expression for the decay $H \rightarrow$ invisible.

As before, we can write general formulas for the decay rates of the Higgs boson decaying into the gauge boson V pair ($V = W$ or Z) are given by

$$\Gamma(H \rightarrow VV) = \frac{|\kappa_V(H)|^2 m_H^3}{128\pi m_V^4} \delta_V \left[1 - \frac{4m_V^2}{m_H^2} + \frac{12m_V^4}{m_H^4} \right] \beta \left(\frac{m_V^2}{m_H^2} \right), \quad (3.65)$$

where $\delta_W = 2$ and $\delta_Z = 1$ and where $\kappa_V(H)$ are the couplings of the Higgs H with the vector bosons:

$$\kappa_W(H) = \frac{ig^2}{2} (-v_\phi \sin \alpha + 2v_\Delta \cos \alpha), \quad (3.66)$$

$$\kappa_Z(H) = \frac{ig^2}{2 \cos^2 \theta_W} (-v_\phi \sin \alpha + 4v_\Delta \cos \alpha). \quad (3.67)$$

The decay rates of the three body decay modes are

$$\Gamma(H \rightarrow VV^*) = \frac{3g_V^2 |\kappa_V(H)|^2}{512\pi^3 m_V^2} m_H \delta_{V'} F\left(\frac{m_V^2}{m_H^2}\right), \quad (3.68)$$

where $\delta_{W'} = 1$ and $\delta_{Z'} = \frac{7}{12} - \frac{10}{9} \sin^2 \theta_W + \frac{40}{27} \sin^4 \theta_W$, and where the function $F(x)$ is given in Eq. (3.62).

3.4 Analysis of the decays of h and H

We proceed by evaluating the branching ratios into photons of both h and H in three scenarios, motivated by existing data. We summarize the experimental constraints for the state at 125 GeV in Table 3.1, and list the additional properties of the Higgs bosons specific to each Scenario.

- Scenario 1 (the LHC/CMS Scenario): $m_H = 125$ GeV, $m_h = 136$ GeV. In this scenario we require, for the state h at 136 GeV, in addition to the conditions in Table 3.1, that $R(h \rightarrow \gamma\gamma) = 0.45 \pm 0.3$, $R(h \rightarrow ZZ^*) \leq 0.2$, and $R(h \rightarrow \tau\tau) < 1.8$, in agreement with the excess observed by CMS.
- Scenario 2 (the LEP/LHC Scenario): $m_H = 98$ GeV, $m_h = 125$ GeV. In this scenario we require $0.1 < R(H \rightarrow b\bar{b}) < 0.25$ in agreement with the excess in e^+e^- at LEP, and for h , the conditions from Table 3.1.
- Scenario 3 (almost degenerate ATLAS and CMS Scenario): the two CP-even neutral Higgs bosons H and h are (almost) degenerate and have both mass of about 125 GeV. In this case, we sum over the relative width $R(h)$ and $R(H)$ of both bosons and compare with the signal at 125 GeV with the conditions from Table 3.1.

Additionally, we also comment on the case in which one of the Higgs states is the one seen at the LHC at 125 GeV, and the other has escaped detection. Throughout the analysis, we impose no restrictions on the mixing and express all the masses and couplings as a function of $\sin \alpha$ and the mass splitting parameter λ_5 .

<i>Experiment</i>	$R_{\gamma\gamma}^{exp}$	$R_{ZZ^*}^{exp}$	$R_{WW^*}^{exp}$	R_{bb}^{exp}	$R_{\tau\tau}^{exp}$
(1) CMS 7+8 TeV	1.56 ± 0.43	0.7 ± 0.44	0.6 ± 0.4	0.12 ± 0.70	-0.18 ± 0.75
(2) ATLAS 7+8 TeV	1.9 ± 0.5	1.3 ± 0.6	–	–	–
(3) CDF and D0	3.6 ± 2.76	–	0.32 ± 0.83	1.97 ± 0.71	–

Table 3.1: Experimental data from LHC and the Tevatron for the boson at 125 GeV.

3.4.1 $\gamma\gamma$ decays for mixed neutral Higgs

Scenario 1

We study the implications on the parameter space of the HTM if the lightest Higgs boson is the one observed at the LHC, with the mild $\gamma\gamma$ excess at CMS being due to a second Higgs boson at 136 GeV. Setting these values for the h and H masses, we plot the masses of the singly and doubly charged Higgs in Fig. 3.1 as functions of λ_5 . The graphs justify our expectations, based on analytical results, that λ_5 must be negative, yielding the ordering $m_{H^{++}} > m_{H^+} > m_H$. These graphs also give the values of the charged Higgs masses for different λ_5 values, to be used in the explorations of $R(\gamma\gamma)$. As $\lambda_4 + \lambda_5 + \sqrt{4\lambda_1(\lambda_2 + \frac{\lambda_3}{2})} > 0$, we checked the relationship between the λ 's for $\lambda_5 < 0$ and found that the inequality is satisfied over the whole parameter space. Before proceeding with the analysis, we note that we are dealing with a very different parameter space than for $\alpha = 0$. The states are now mixed significantly: the state H that in the limit $\alpha \rightarrow 0$ is neutral triplet Higgs boson is lighter than the state h that in the limit $\alpha \rightarrow 0$ is neutral doublet Higgs boson, and the ordering of mass states is opposite to that favored for $\alpha = 0$ [133], that is in our model $m_{H^{++}} > m_{H^+} > m_H$.

In order to proceed with the analysis of Higgs decays, we must set reasonable, but not overconservative limits on doubly charged boson masses. The strongest limits on the doubly charged boson masses come from ATLAS [140] and CMS [141], from $pp \rightarrow H^{\pm\pm}H^{\mp\mp}$. At ATLAS, assuming a branching ratio of 100% into left-handed leptonic final states, masses of less than 409 GeV, 375 GeV and 398 GeV are excluded, for Yukawa couplings of $h_{ij} > 3 \times 10^{-6}$, for final states $e^\pm e^\pm$, $e^\pm \mu^\pm$ and $\mu^\pm \mu^\pm$, respectively. These confirm, and are slightly more stringent than the Tevatron measurements [142–144]. Separate searches were performed for $q\bar{q} \rightarrow \gamma^*, Z^* \rightarrow H^{\pm\pm}H^{\mp\mp}$ and $q'\bar{q} \rightarrow W^* \rightarrow H^{\pm\pm}H^{\mp\mp}$. For cases where the final state has one or two τ^\pm leptons, the limits are weaker, 350 GeV and 200 GeV, respectively [145]. However, most of these limits have been obtained for complete dominance of the leptonic decays (which

is the case for $v_\Delta < 10^{-4}$ GeV) and degeneracy of the triplet scalars. In this Chapter, we assume $v_\Delta \sim \mathcal{O}(1 \text{ GeV})$, for which the $H^{\pm\pm} \rightarrow W^\pm W^\pm$ dominates [146–148]. The scenario in which the doubly charged Higgs decay predominantly into two same-sign vector bosons has been explored, and it was shown that the LHC running at 8 or 14 TeV would be able to detect such a boson with a mass of ~ 180 GeV. Additionally, for the case where $m_{H^{\pm\pm}} > m_{H^\pm}$, as it is in this case, the decay $H^{\pm\pm} \rightarrow H^\pm W^\pm$ can be dominant over a large range of v_Δ [136]. In view of all these considerations, we wish to keep our analysis as general as possible so we consider m_{H^\pm} as low as 110 GeV, and $m_{H^{\pm\pm}}$ as low as 150 GeV. From Fig. 3.1 this requires that λ_5 is negative, and from the figure, if $|\lambda_5| > 1/2$, $m_{H^{++}} > 175$ GeV and $m_{H^+} > 150$ GeV.

We present next the plots for the relative signal strength (with respect to the SM one) of $R_{h \rightarrow \gamma\gamma}$ and $R_{H \rightarrow \gamma\gamma}$ as a function of $\sin \alpha$, for various values of λ_5 . For each value of λ_5 , we obtain m_{H^+} and $m_{H^{++}}$, and introduce these values into calculation of the branching ratios. The plots are in Fig. 3.2, top for h , bottom for H , at the left, without width corrections, and at the right, including width corrections. Increasing the absolute value of λ_5 increases the charged Higgs masses and depresses the relative ratio of decay into $\gamma\gamma$. While the decay of the heavier Higgs boson (at 136 GeV) can be enhanced significantly or suppressed with respect to the SM, fulfilling the constraint $R(h \rightarrow \gamma\gamma) = 0.45 \pm 0.3$ for several λ_5 values, the lighter boson signal is always reduced with respect to the SM. Thus, H cannot be the boson observed at the LHC with mass of 125 GeV, confirming our analytical considerations, and this scenario is disfavored by the present LHC data.

Scenario 2

We now proceed to analyze the implications on the parameter space of the HTM if the lightest Higgs boson is the 2.3σ signal excess observed at LEP at 98 GeV, while the heavier Higgs boson is the boson observed at the LHC at 125 GeV. Setting these values for the h and H masses, we plot the masses of the singly and doubly charged Higgs in Fig. 3.3 as functions of λ_5 (singly charged at the left, doubly charged at the right). Again, in this scenario λ_5 is constrained to be negative, yielding the ordering $m_{H^{++}} > m_{H^+} > m_H$. From the figure, $|\lambda_5| > 1/2$, $m_{H^{++}} > 160$ GeV and $m_{H^+} > 130$ GeV. The values of the charged Higgs masses for different λ_5 values, shown in Fig. 3.3 are then used in the explorations of $R(\gamma\gamma)$.

We present the plots for the relative signal strength (with respect to the SM one) of $R_{h \rightarrow \gamma\gamma}$ and $R_{H \rightarrow \gamma\gamma}$ as a function of $\sin \alpha$, for various values of λ_5 in Fig. 3.4, on the top row for h , and

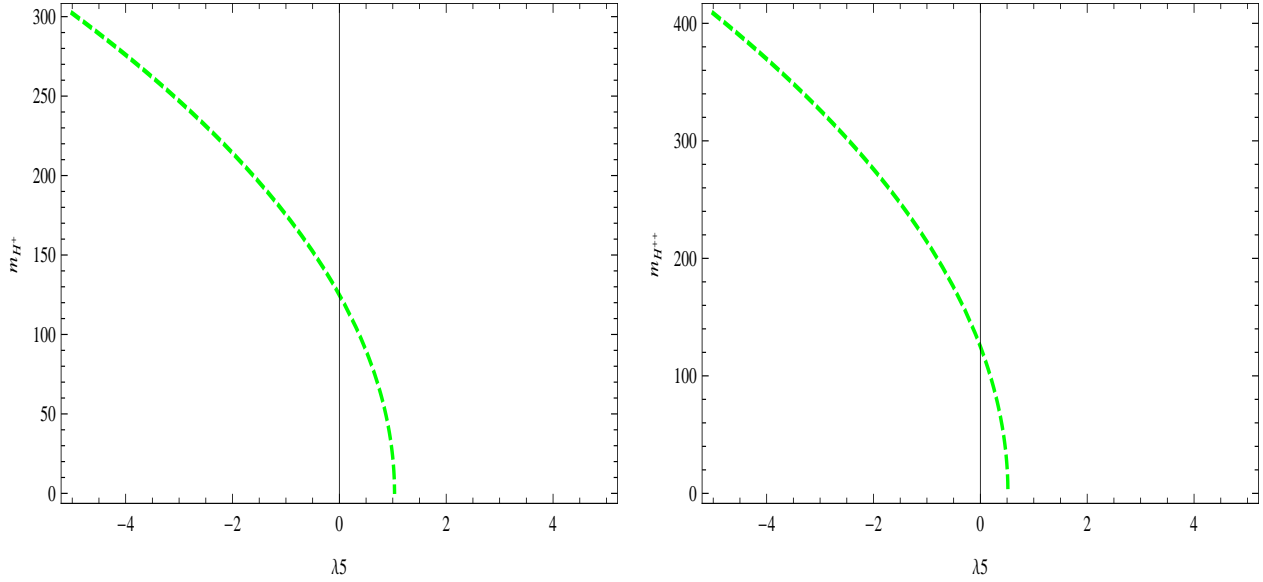


Figure 3.1: Values of the singly charged (left panel) and doubly charged Higgs masses (right panel) in Scenario 1, with the parameter $\lambda_5 \approx \frac{4}{v_\Phi^2}(m_H^2 - m_{H^+}^2) \approx \frac{4}{v_\Phi^2}(m_{H^+}^2 - m_{H^{++}}^2)$.

the bottom one for H . The left panels show the relative $\gamma\gamma$ widths uncorrected for relative width differences and the right-handed panels include the total width corrections. While the decay of the heavier Higgs boson (at 125 GeV) can be enhanced significantly with respect to the SM, the lighter boson signal is always reduced with respect to the SM. If the charged Higgs bosons are relatively light, the angle for which the enhancement is about a factor of 1.5-2 times the SM value is about $\sin \alpha \simeq 0.2$ for $\lambda_5 = -1/2$, about $\sin \alpha \simeq 0.35$ for $\lambda_5 = -1$, about $\sin \alpha \simeq 0.5$ for $\lambda_5 = -3/2$, and in a range $\sin \alpha \simeq 0.6 - 0.9$ for $\lambda_5 = -2$. For the latter case, $m_{H^{++}} = 260$ GeV and $m_{H^+} = 200$ GeV. For all of the parameter ranges where $h \rightarrow \gamma\gamma$ is enhanced, the width of the other neutral Higgs boson $H \rightarrow \gamma\gamma$ is suppressed and thus this Higgs boson would escape detection. This feature is general: as long as h is the boson observed at 125 GeV, and H lies below, the decay to $H \rightarrow \gamma\gamma$ would be suppressed with respect to a SM Higgs boson of the same mass, and H would escape detection. Thus this scenario would survive even if the LEP e^+e^- excess at 98 GeV does not. The details of the exact enhancements depend on the mass splittings, but the enhancements of $h \rightarrow \gamma\gamma$ themselves appear to be fairly robust.

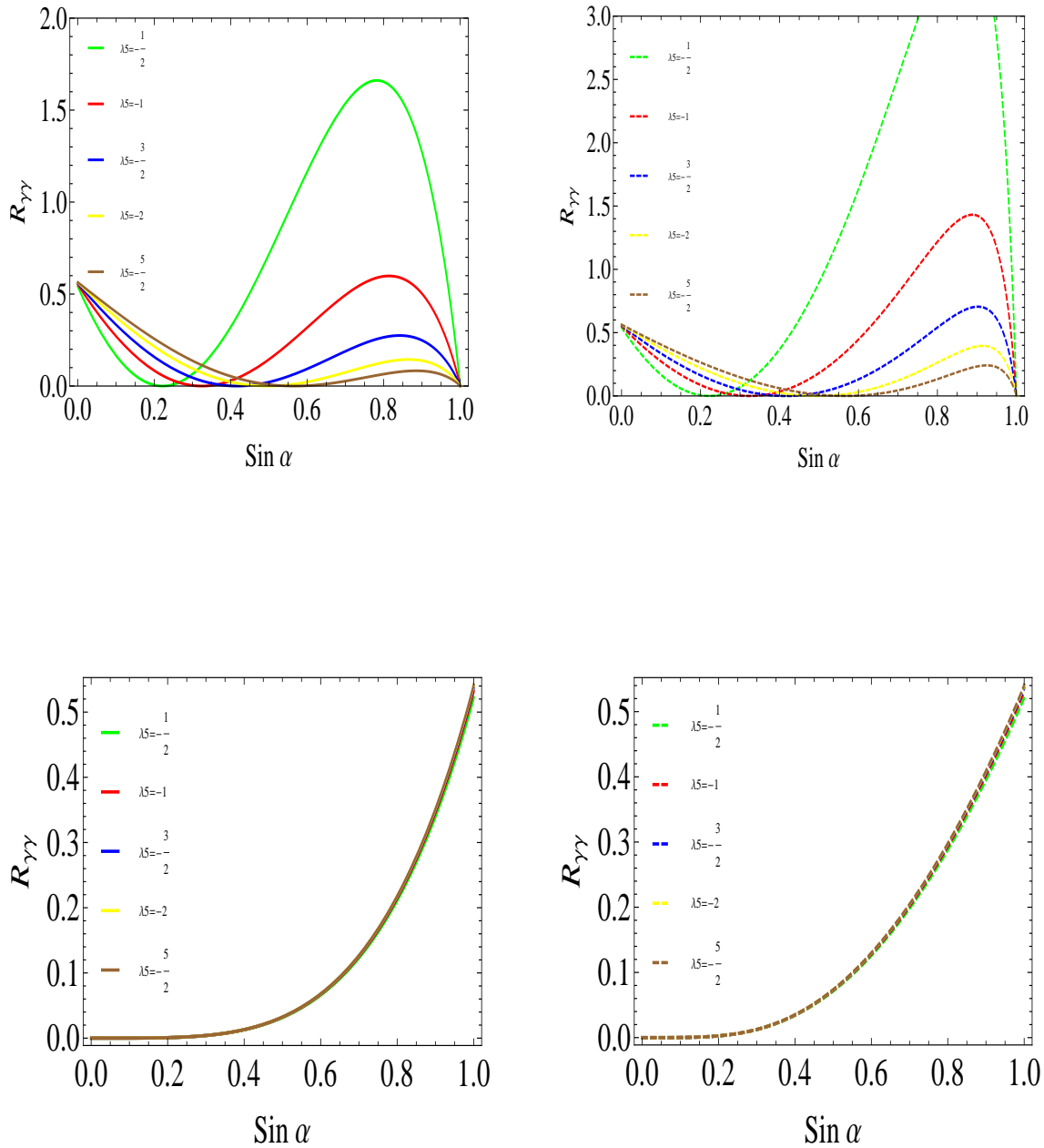


Figure 3.2: Decay rates for $h \rightarrow \gamma\gamma$ (top row) and $H \rightarrow \gamma\gamma$ (bottom row) as a function of $\sin \alpha$ in Scenario 1, for different values of the parameter λ_5 . The left-handed panels show the relative widths uncorrected for relative width differences; the right-handed panels include the total width corrections.

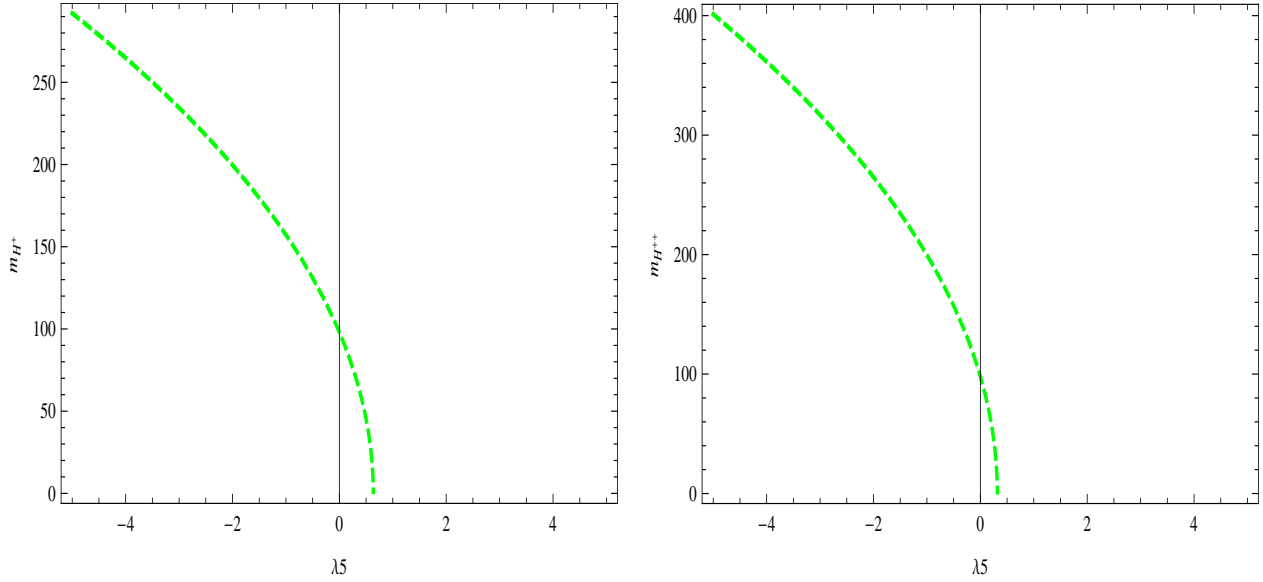


Figure 3.3: Values of the singly charged (left panel) and doubly charged Higgs masses (right panel) in Scenario 2, with the parameter $\lambda_5 = \frac{4}{v_\Phi^2}(m_H^2 - m_{H^+}^2) \approx \frac{4}{v_\Phi^2}(m_{H^+}^2 - m_{H^{++}}^2)$.

Scenario 3

Finally, we look at the implications of the case where the only Higgs boson is the one observed at 125 GeV, that is h and H are nearly degenerate¹. We call this boson h/H . In that case we have, for the ratio of the number of events in the HTM versus the SM:

$$R_{XX} = R_{h \rightarrow XX} + R_{H \rightarrow XX}. \quad (3.69)$$

The values of the masses of the singly and doubly charged Higgs as functions of λ_5 remain the same as in Fig. 3.3 (as they depend only on the H mass). The plots for the relative signal strength (with respect to the SM one) of $R_{h/H \rightarrow \gamma\gamma}$ as a function of $\sin \alpha$, for various values of λ_5 , are shown in Fig. 3.5 in the left panel, for the relative $\gamma\gamma$ widths uncorrected for relative width differences, in the right-handed panels including the total width corrections. At first glance, the results are rather surprising. One would expect that the enhancement from $h \rightarrow \gamma\gamma$ will add to the reduction from $H \rightarrow \gamma\gamma$ resulting in a perhaps more evenly varying signal, but enhanced with respect to the SM. The fact that this is not the case is apparent from Eq. (3.41). In the degenerate mass case the term in λ_4 proportional to $m_h^2 - m_H^2$ cancels exactly, and thus from the point of view of the decay into $\gamma\gamma$, scenario 3 reproduces exactly the results

¹In that case the pseudoscalar A will also have mass 125 GeV, but given the $\beta_0 \simeq 0$ mixing angle in that sector, it will decay invisibly into two neutrinos, not altering the visible branching ratios.

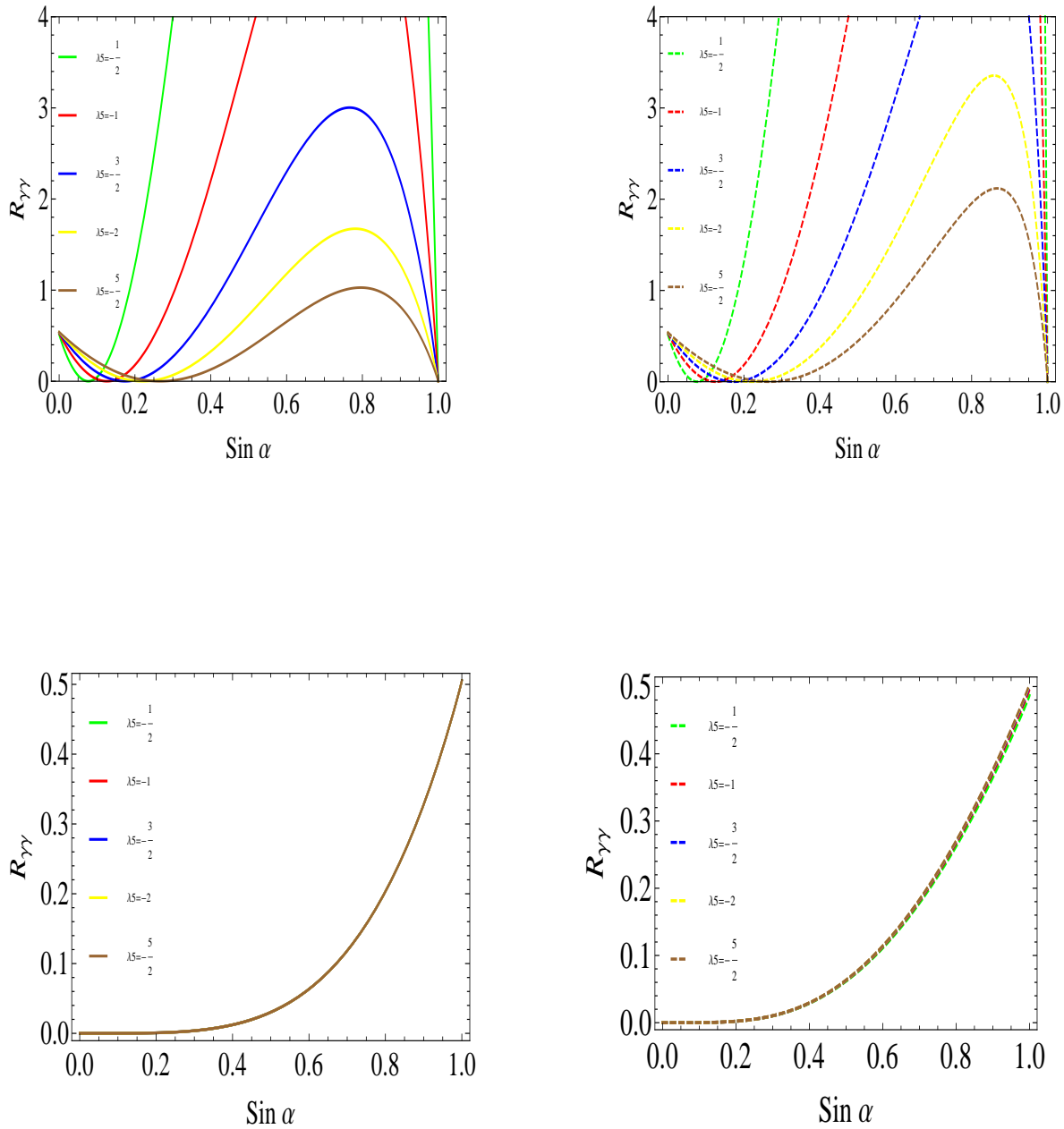


Figure 3.4: Decay rates for $h \rightarrow \gamma\gamma$ (top row) and $H \rightarrow \gamma\gamma$ (bottom row) as a function of $\sin \alpha$ in Scenario 2, for different values of the parameter λ_5 . The left-handed panels show the relative widths uncorrected for relative width differences, the right-handed panels include the total width corrections.

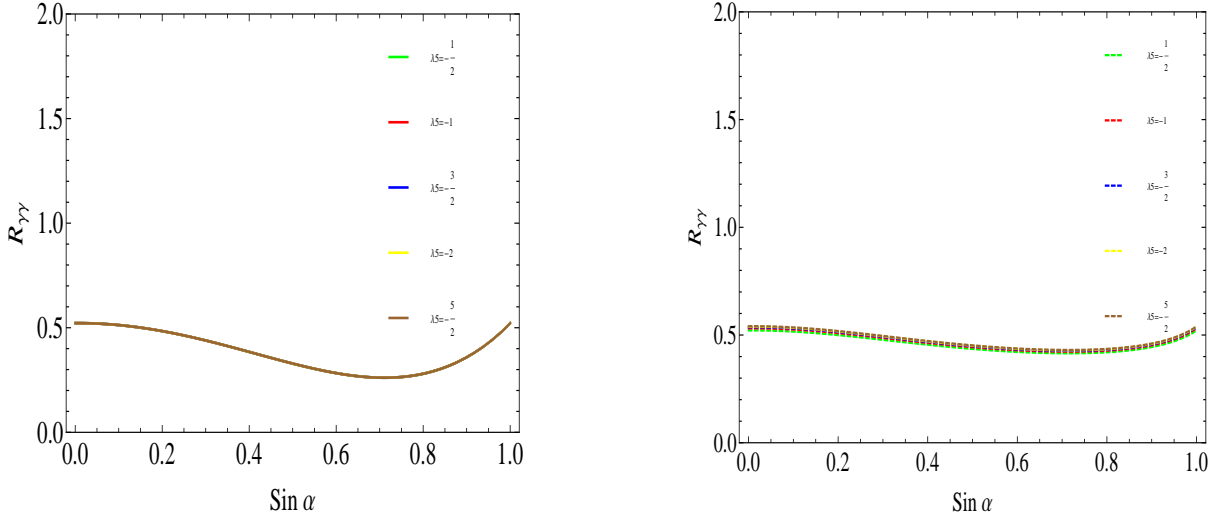


Figure 3.5: Decay rates for $h/H \rightarrow \gamma\gamma$ as a function of $\sin \alpha$, for different values of the parameter λ_5 in Scenario 3. The left-handed panel shows the relative widths uncorrected for relative width differences, the right-handed panel includes the total width corrections.

for the unmixed case (with $\sin \alpha = 0$), see Eq. (3.34), and is approximately independent of α . Indeed for most of the parameter space, terms in $m_h^2 \cos^2 \alpha + m_H^2 \sin^2 \alpha \rightarrow m_{h/H}^2$, and the same for $\cos \alpha \leftrightarrow \sin \alpha$. We checked that the reduction in the $\gamma\gamma$ signal holds for masses approximately degenerate (within 3-5 GeV),² while the signal is enhanced for mass splittings of more than 8 – 10 GeV.

3.4.2 Tree-level decays for Scenarios 1, 2 and 3

We conclude this section with an analysis of the tree-level decays ($f\bar{f}$, WW^* , ZZ^*) of the neutral Higgs bosons in the three scenarios. More precise measurements of these decays, combined with the $\gamma\gamma$, would constrain the model, as all decays rates depend on very few parameters. In Fig. 3.6 we plot the tree level decays, for all scenarios, with and without width correction. Note that without correcting for the width, the relative branching ratios are mass independent (thus the same for scenarios 1 and 2) but they depend on whether the boson is h or H . All the tree-level branching ratios are suppressed with respect to the same ones in the SM and independent of λ_5 , while the width-corrected relative decay width are very similar

²This may be relevant as ATLAS and CMS do not agree completely on the mass of the discovered boson.

for scenarios 1 and 2, and thus we show only one. For values of the angles α for which the relative branching ratio to $\gamma\gamma$ falls within the allowed range, the tree-level branching ratios for scenarios 1 and 2 can lie anywhere between 0.05 and 0.9. Thus more precise measurements of these ratios would give an indication of the value of the mixing ($\sin \alpha$), which will pick up a definite value of the mass splittings, allowing for a prediction of $m_{H^{++}}$ and m_{H^+} . In particular, for scenario 2, which is favored by the measurements of $h \rightarrow \gamma\gamma$ branching ratios, the decays of $H \rightarrow f\bar{f}$ obey $0.1 < R(H \rightarrow b\bar{b}) < 0.25$ in the region $0.5 < \sin \alpha < 0.7$, thus overlapping with regions allowed by the $\gamma\gamma$ constraints for $\lambda_5 = -3/2$ and -2 . The tree-level graphs for scenario 3, both with and without width correction, show that these branching ratios are very close to the SM ones, and relatively independent of $\sin \alpha$, reproducing as before the case for unmixed neutral Higgs bosons. The high branching ratio into $b\bar{b}$ and $\tau^-\tau^+$ is achieved *only* accompanied by a significant reduction in the $\gamma\gamma$ branching ratio. At present, this scenario is disfavored by the measurements at the LHC of $\gamma\gamma$ widths.

3.4.3 Predictions for H and h decay width to $Z\gamma$

As a further test of the implications of the HTM with nontrivial mixing, we evaluate the loop mediated Higgs decay $h, H \rightarrow Z\gamma$. In the SM the decay $\Phi \rightarrow Z\gamma$ is similar to the one for $\gamma\gamma$, but with a smaller rate and a further reduced branching ratio of $Z \rightarrow \mu^+\mu^-$ (or e^+e^-). Like the decay to $\gamma\gamma$, it is sensitive to the presence of charged particles in the loop, and is affected by both their charge and weak isospin. Thus deviations from the SM value could signify beyond the Standard Model physics. The SM contribution for a Higgs state at 125 GeV is very small, $[\Gamma(\Phi \rightarrow Z\gamma)]_{SM} \simeq 6 \times 10^{-6}$ GeV, yielding a branching ratio of about 1.5×10^{-3} [149], comparable to that of $\Phi \rightarrow \gamma\gamma$. The SM contributions from the W boson and top quark, and the HTM from the additional charged scalars to the decay rate of h, H are given by [13, 112]³

$$\begin{aligned} \Gamma(\Phi \rightarrow Z\gamma)_{SM} &= \frac{G_F^2 M_W^2 m_h^3 \alpha}{64\pi^4} \left(1 - \frac{M_Z^2}{m_\Phi^2}\right)^3 |\mathcal{A}_{SM}|^2, \\ \Gamma(h \rightarrow Z\gamma)_{HTM} &= \frac{G_F^2 M_W^2 m_h^3 \alpha}{64\pi^4} \left(1 - \frac{M_Z^2}{m_h^2}\right)^3 \left| \mathcal{A}_W(h) + \mathcal{A}_t(h) - 2\mathcal{A}_0^{H^+}(h) - 4\mathcal{A}_0^{H^{++}}(h) \right|^2, \end{aligned} \quad (3.70)$$

³Please note that the formula for the branching ratios into Z gamma have been taken from [150–153] and the corresponding figures have been corrected from [1].

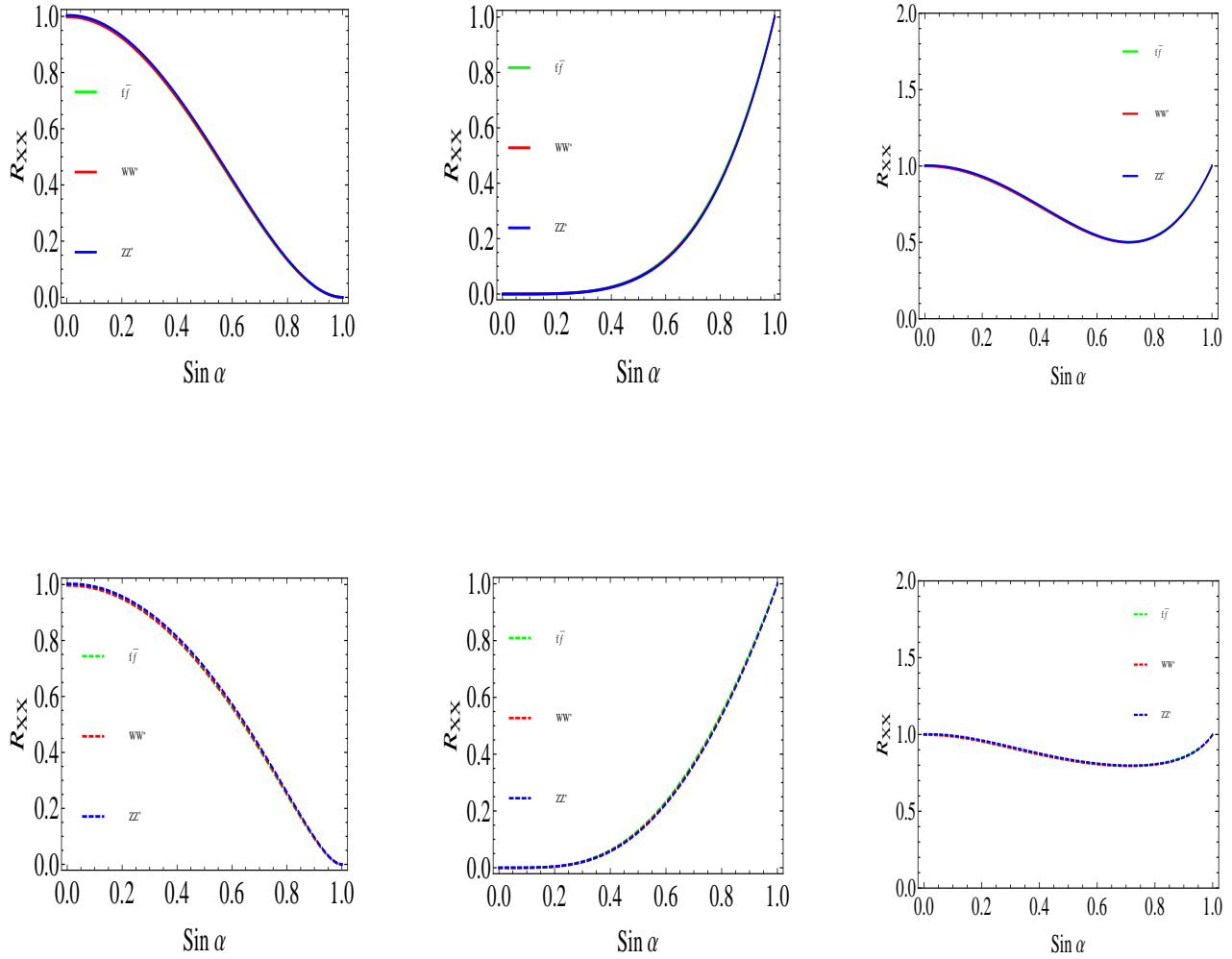


Figure 3.6: Relative branching Ratios for $h \rightarrow f\bar{f}$, WW^* , ZZ^* in scenarios 1 and 2 (left column), for $H \rightarrow f\bar{f}$, WW^* , ZZ^* for scenarios 1 and 2 (middle column), and for $h, H \rightarrow f\bar{f}$, WW^* , ZZ^* in Scenario 3 (right column) as a function of the mixing angle in the neutral sector. The top row shows the relative ratios without width corrections, the lower row, including the width corrections.

where

$$\begin{aligned}
\mathcal{A}_{SM} &= \cos \theta_W A_1(\tau_W^\Phi, \sigma_W) + 2N_c \frac{Q_t(1 - 2Q_t \sin^2 \theta_W)}{\cos \theta_W} A_{1/2}(\tau_t^\Phi, \sigma_t) , \\
\mathcal{A}_W(h) + \mathcal{A}_t(h) &= \\
g_{hWW} \cos \theta_W A_1(\tau_W^h, \sigma_W) + g_{ht\bar{t}} \frac{2N_c Q_t(1 - 2Q_t \sin^2 \theta_W)}{\cos \theta_W} A_{1/2}(\tau_t^h, \sigma_t) , \\
\mathcal{A}_0^{H^+}(h) &= \sin \theta_W g_{ZH^+H^-} \tilde{g}_{hH^+H^-} A_0(\tau_{H^+}^h, \sigma_{H^+}) , \\
\mathcal{A}_0^{H^{++}}(h) &= \sin \theta_W g_{ZH^{++}H^{--}} \tilde{g}_{hH^{++}H^{--}} A_0(\tau_{H^{++}}^h, \sigma_{H^{++}}) , \tag{3.71}
\end{aligned}$$

where $\tau_i^h = 4m_i^2/m_h^2$, $\sigma_i = 4m_i^2/M_Z^2$, $g_{ZH^{++}H^{--}} = 2 \cot 2\theta_W$, $g_{ZH^+H^-} = -\tan \theta_W$, g_{hWW} is given by Eq. (3.38), and $\tilde{g}_{hH^{++}H^{--}}$ and $\tilde{g}_{hH^+H^-}$ are given by Eqs. (3.39). The loop functions are given by

$$\begin{aligned}
A_1(\tau, \sigma) &= 4(3 - \tan^2 \theta_W) I_2(\tau, \sigma) + [(1 + 2\tau^{-1}) \tan^2 \theta_W - (5 + 2\tau^{-1})] I_1(\tau, \sigma) , \\
A_{1/2}(\tau, \sigma) &= I_1(\tau, \sigma) - I_2(\tau, \sigma) , \\
A_0(\tau, \sigma) &= I_1(\tau, \sigma) , \tag{3.72}
\end{aligned}$$

where

$$\begin{aligned}
I_1(\tau, \sigma) &= \frac{\tau\sigma}{2(\tau - \sigma)} + \frac{\tau^2\sigma^2}{2(\tau - \sigma)^2} [f(\tau^{-1}) - f(\sigma^{-1})] + \frac{\tau^2\sigma}{(\tau - \sigma)^2} [g(\tau^{-1}) - g(\sigma^{-1})] , \\
I_2(\tau, \sigma) &= -\frac{\tau\sigma}{2(\tau - \sigma)} [f(\tau^{-1}) - f(\sigma^{-1})] , \tag{3.73}
\end{aligned}$$

where $f(\tau)$ is given in Eq. (3.54), and

$$g(\tau^{-1}) = \sqrt{\tau - 1} \arcsin \sqrt{\tau^{-1}} \quad \text{for } \tau > 1. \tag{3.74}$$

The decay of $H \rightarrow \gamma\gamma$ can be evaluated as before, using the same formulas, with the replacements $h \rightarrow H$, $m_h \rightarrow m_H$:

$$\Gamma(H \rightarrow Z\gamma)_{HTM} = \frac{G_F^2 M_W^2 m_H^3 \alpha}{64\pi^4} \left(1 - \frac{M_Z^2}{m_H^2}\right)^3 \left| \mathcal{A}_W(H) + \mathcal{A}_t(H) - 2\mathcal{A}_0^{H^+}(H) - 4\mathcal{A}_0^{H^{++}}(H) \right|^2 , \tag{3.75}$$

where

$$\begin{aligned}
\mathcal{A}_W(H) + \mathcal{A}_t(H) &= \\
g_{HWW} \cos \theta_W A_1(\tau_W^H, \sigma_W) + g_{Ht\bar{t}} 2N_c \frac{Q_t(1 - 2Q_t \sin^2 \theta_W)}{\cos \theta_W} A_{1/2}(\tau_t^H, \sigma_t) , \\
\mathcal{A}_0^{H^+}(H) &= \sin \theta_W g_{ZH^+H^-} \tilde{g}_{HH^+H^-} A_0(\tau_{H^+}^H, \sigma_{H^+}) , \\
\mathcal{A}_0^{H^{++}}(H) &= \sin \theta_W g_{ZH^{++}H^{--}} \tilde{g}_{HH^{++}H^{--}} A_0(\tau_{H^{++}}^H, \sigma_{H^{++}}) , \tag{3.76}
\end{aligned}$$

where $\tau_i^H = 4m_i^2/m_H^2$, $\sigma_i = 4m_i^2/M_Z^2$, g_{HWW} is given in Eq. (3.45), and $\tilde{g}_{HH^{++}H^{--}}$ and $\tilde{g}_{HH^+H^-}$ are given by Eqs. (3.46).

Comparison with the SM predictions lead to the modification factor $R_{Z\gamma}$ for the $h, H \rightarrow Z\gamma$ decay rate width

$$\begin{aligned} R_{h,H \rightarrow Z\gamma} &\equiv \frac{\sigma_{\text{HTM}}(gg \rightarrow h, H \rightarrow Z\gamma)}{\sigma_{\text{SM}}(gg \rightarrow \Phi \rightarrow Z\gamma)} \\ &= \frac{[\sigma(gg \rightarrow h, H) \times \Gamma(h, H \rightarrow Z\gamma)]_{\text{HTM}}}{[\sigma(gg \rightarrow \Phi) \times \Gamma(\Phi \rightarrow Z\gamma)]_{\text{SM}}} \times \frac{[\Gamma(\Phi)]_{\text{SM}}}{[\Gamma(h, H)]_{\text{HTM}}}. \end{aligned} \quad (3.77)$$

In Fig. 3.7 we plot the relative width factor $R_{Z\gamma}$ as a function of the scalar mixing $\sin \alpha$ for scenarios 1 and 2, and for various mass splittings in the charged sector. One can see that the model predicts only one enhanced signal for $h \rightarrow Z\gamma$ in scenario 2. For the lighter H no enhancement is observed in $Z\gamma$. A measurement of the rare decay into $Z\gamma$ could thus serve as a confirmation of this scenario in HTM.

For scenario 3, the HTM predicts no enhancement over the SM. The results are shown in Fig 3.8 where we only plot the relative branching ratios corrected for the width. The variations with $\sin \alpha$ are very small, and more pronounced for the uncorrected relative width, overall similar to those for $\gamma\gamma$, and indicative of the effects of the charged Higgs bosons in the loop.

3.5 Conclusions

We presented a comprehensive analysis of the decay ratios of the CP-even neutral Higgs bosons in the HTM, when the bosons mix with arbitrary angle α . Of the bare states in the model, one is the usual neutral component of the SM Higgs doublet, the other is the neutral component of a Higgs triplet, introduced to provide neutrino masses. We studied the ratios of production and decay of the Higgs in this model at tree and one-loop level, relative to the ones in the SM. We have shown that, in the case where the two Higgs bosons do not mix, positivity conditions on the scalar potential forbid an enhancement of the branching ratio into $\gamma\gamma$. Allowing for arbitrary mixing, these conditions require that h (the neutral Higgs that is the corresponding SM one in the no mixing limit) is heavier than H . We have also shown that, if the Higgs bosons are allowed to mix nontrivially, the relative branching ratio into $\gamma\gamma$ of h with respect to the SM Higgs can be enhanced, and that, for all these cases, the singly charged Higgs boson is lighter than the doubly charged boson, and both are heavier than H .

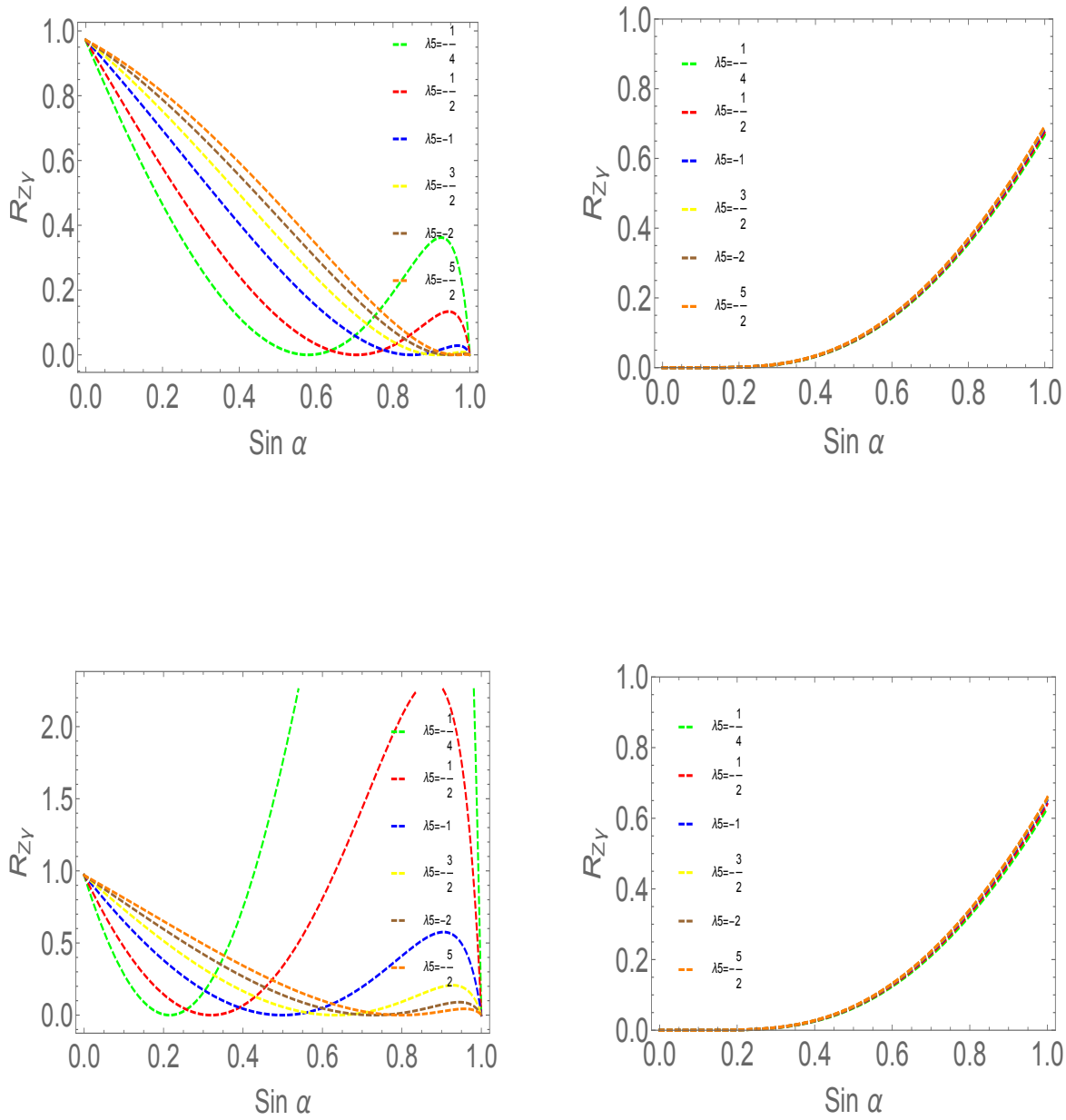


Figure 3.7: Relative Branching Ratios for $h \rightarrow Z\gamma$ (left column) and $H \rightarrow Z\gamma$ (right column) with width corrections for Scenario 1 (upper row), and Scenario 2 (lower row) as a function of $\sin \alpha$, for various λ_5 values.

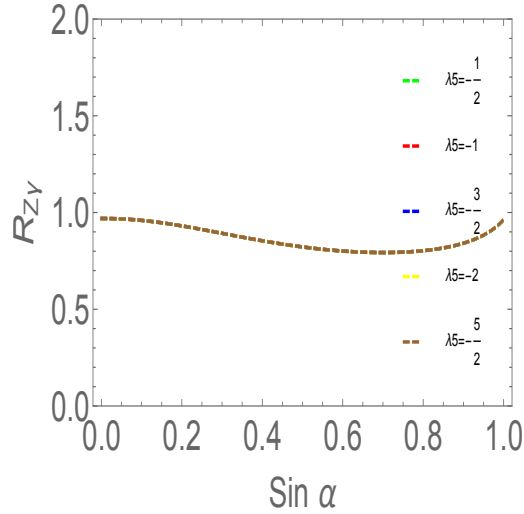


Figure 3.8: Relative Branching Ratios for $h/H \rightarrow Z\gamma$ in Scenario 3 as a function of $\sin \alpha$, for various λ_5 values.

This is a very different scenario from the unmixed one, where h is the lighter neutral Higgs, and the doubly charged Higgs bosons are lighter than the singly charged Higgs, who in turn are lighter than the neutral triplet H .

We allowed the mixing angle α to vary and expressed all the couplings in the Higgs potential as a function of this angle, and of the square-mass splitting λ_5 . We analyzed three scenarios. The first one, where H is the boson observed at 125 GeV and h is the CMS excess at 136 GeV, is disfavored by the data, as the branching ratio of $H \rightarrow \gamma\gamma$ is always reduced with respect to SM expectations. However, scenario 2, where h is the boson observed at 125 GeV, and H the excess observed in e^+e^- at LEP at 98 GeV, is favored by the data, and consistent with all other measurements. This scenario can also explain a lighter Higgs H that is missed by colliders because of significantly reduced decay into $\gamma\gamma$. In both of these scenarios the tree-level decay rates of h and H are reduced with respect to the SM. Should such a reduction survive more precise measurements, scenario 2 looks very promising. The case where the two neutral bosons are (almost) degenerate resembles very much the unmixed neutral case. The relative branching ratio into $\gamma\gamma$ is suppressed, and even if the tree-level decays are at the same level as expected in the SM, this scenario is disfavored at present by the LHC measurements.

We have tested all scenarios with the decay $h, H \rightarrow Z\gamma$ and we find only one significant enhancement in scenario 2, for h . This scenario shows enhancements in $\gamma\gamma$ for the boson at 125 GeV; and no enhancement for scenario 3, in which the two Higgs bosons are (almost) degenerate. As this branching ratio is also sensitive to the extra charged particles in the model, a precise measurement could shed some light on the structure of the model.

In conclusion, the power to discriminate the SM Higgs boson from Higgs bosons in extended models depends critically on differentiating their couplings and decays. We have shown that a very simple model, in which only one extra (triplet) Higgs representation is added to the SM to allow for neutrino masses, shows promise in being able to explain the present data at LHC, and indicated how, with more precise data, this Higgs sector can be validated or ruled out.

Chapter 4

Vector-like Leptons in the Higgs Triplet Model

Abstract

We analyze the phenomenological implications of introducing vector-like leptons on the Higgs sector in the HTM. We impose only a parity symmetry which disallows mixing between the new states and the ordinary leptons. If the vector-like leptons are allowed to be relatively light, they enhance or suppress the decay rates of loop-dominated neutral Higgs bosons decays $h \rightarrow \gamma\gamma$ and $h \rightarrow Z\gamma$, and affect their correlation. An important consequence is that, for light vector-like leptons, the decay patterns of the doubly charged Higgs boson will be altered, modifying the restrictions on their masses. We study the implications for signals at the LHC, for both $\sqrt{s} = 7$ TeV and for 13 TeV, and show that doubly charged boson decays into same-sign vector leptons could be observed.

4.1 Introduction

With the discovery of the Standard Model (SM) Higgs-like scalar at the LHC [29, 154], the SM particle content seems complete. In particular, the mass and couplings of the neutral Higgs boson seem to disfavor an additional chiral generation of quarks and leptons [155, 156]. However, additional vector-like fermions, in which an SM generation is paired with another one of opposite chirality, and with identical couplings, are less constrained, as there is no quadratic contribution to their masses. These states appear as natural extensions of the SM particle

content in theories with warped or universal extra dimensions, as Kaluza-Klein excitations of the bulk field [157–163], in non-minimal supersymmetric extensions of the SM [164–170], in composite Higgs models [171–179], in Little Higgs Model [180–185] and in gauged flavor groups [186–189]. Vector-like fermions have identical left- and right-handed couplings and can have masses which are not related to their couplings to the Higgs bosons [190]. Depending on the dominant decay mode, the limits on new vector-like fermions range from $\sim 100 - 600$ GeV [191, 192], rendering them observable at the LHC.

Vector-like quarks can modify both the production and decays of the Higgs boson at the LHC, while vector-like leptons do not carry $SU(3)_c$ charge and can only modify the decay patterns of the Higgs. Study of the latter would be a sensitive probe for new physics. The lepton states contribute to self-energy diagrams for electroweak gauge boson masses and precision observables, and consistent limits on their masses and mixings have been obtained [97, 193–195].

Vector-like leptons have been studied in the context of the SM [97, 196–210], but less so for models beyond the SM, where they can also significantly alter the phenomenology of the model. In the SM, introducing heavy fermions provides a contribution of the same magnitude and sign as that of the top quark and interferes destructively with the dominant W -contribution, reducing the $h \rightarrow \gamma\gamma$ rate with respect to its SM value. Recent studies indicate that cancellations between scalar and fermionic contributions allow a wide range of Yukawa and mass mixings among vector states [139, 211]. An investigation of vector-like leptons in the two Higgs doublet model [139, 211] showed that the presence of additional Higgs bosons alleviates electroweak precision constraints. Introducing vector leptons into supersymmetry [212] can improve vacuum stability and enhance the diphoton rate by as much as 50%, while keeping new particle masses above 100 GeV and preserving vacuum stability conditions.

In this chapter, we investigate vector leptons in the context of the Higgs Triplet Model (HTM). We do not deal with LHC phenomenology (pair production and decay) of the extra leptons, which has been discussed extensively in the literature [167, 213, 214], choosing instead to focus on signature features of this model. We have previously shown that in the Higgs Triplet Model, enhancement of the $h \rightarrow \gamma\gamma$ rate is possible only for the case where the doublet and triplet neutral Higgs fields mix considerably [1]. We extend our analysis to include additional vector-like leptons in the model and investigate how these affect the Higgs diphoton decay rate, with or without significant mixing in the neutral Higgs sector. Originally, both CMS

and ATLAS experiments at LHC observed an enhancement of the Higgs diphoton rate, while the diboson rates ($h \rightarrow WW^*, ZZ^*$) have been roughly consistent with SM expectations. At present CMS observes $\sigma(pp \rightarrow h) \times BR(h \rightarrow \gamma\gamma) = 0.77 \pm 0.27$ times the SM rate, while ATLAS observes $\sigma(pp \rightarrow h) \times BR(h \rightarrow \gamma\gamma) = 1.55_{-0.28}^{+0.33}$ times the SM rate [215–218]. Given these numbers, it is possible that either the SM value will be proven correct, or a modest enhancement will persist. A further test of the SM is the correlation of the decay $h \rightarrow Z\gamma$ with one for $h \rightarrow \gamma\gamma$. We also include the prediction for the vector-like lepton effect on branching ratio of $h \rightarrow Z\gamma$ and comment on the relationship with the diphoton decay.

We have an additional reason to investigate the effects of vector-like leptons in the Higgs Triplet Model. The model includes doubly charged Higgs bosons, predicted by most models to be light. Being pair produced, the doubly charged Higgs bosons are assumed to decay into a pair of leptons with the same electric charge, through Majorana-type interactions [140, 141]. Assuming a branching fraction of 100% decays into leptons, *i.e.*, neglecting possible decays into W -boson pairs, the doubly charged Higgs mass has been constrained to be larger than about 450 GeV, or more, depending on the decay channel. However, if the vector leptons are light enough, which they can be, the doubly charged Higgs bosons can decay into them and thus evade the present collider bounds on their masses. We investigate this possibility in the second part of this chapter.

This Chapter is organized as follows. We introduce the Higgs Triplet Model with vector leptons in Section 6.2. In Section 4.3 we analyze the effect of the vector-like leptons on the decays of the neutral Higgs bosons, and discuss the constraints on the parameter space coming from requiring agreement with present LHC data. We include both loop-dominated decays, $h \rightarrow \gamma\gamma$ in 4.3.1, and $h \rightarrow Z\gamma$ in 4.3.2. In Section 4.4 we analyze the effect of the vector-like leptons on the production and decay mechanisms of the doubly-charged Higgs at the LHC.

4.2 The Model

The Higgs Triplet Model has been studied previously in Ref. [123–134, 219–222]. Here we concentrate on the effect of extending the model by incorporating additional vector-like leptons. For the purpose of this analysis, vector-like quarks either do not exist, or are much heavier and decouple from the spectrum. The model contains a vector-like fourth generation of leptons, namely the $SU(2)_L$ left-handed lepton doublets $L'_L = (\nu'_L, e'_L)$, right-handed

charged and neutral lepton singlets, ν'_R and e'_R , and the mirror right-handed lepton doublets, $L''_R = (\nu''_R, e''_R)$ and left-handed charged and neutral lepton singlets ν''_L and e''_L . The vector-like leptons have the following quantum numbers under $SU(3)_C \times SU(2)_L \times U(1)_Y$:

$$\begin{aligned} L'_L &= (\mathbf{1}, \mathbf{2}, -1/2), & L''_R &= (\mathbf{1}, \mathbf{2}, -1/2), & e'_R &= (\mathbf{1}, \mathbf{1}, -1), \\ e''_L &= (\mathbf{1}, \mathbf{1}, -1), & \nu'_R &= (\mathbf{1}, \mathbf{1}, 0), & \nu''_L &= (\mathbf{1}, \mathbf{1}, 0), \end{aligned} \quad (4.1)$$

with the electric charge given by $Q = T_3 + Y$, where T_3 the weak isospin. The Lagrangian density of this model is:

$$\mathcal{L}_{\text{HTM}} = \mathcal{L}_{\text{kin}} + \mathcal{L}_Y + \mathcal{L}_{\text{VL}} - V(\Phi, \Delta), \quad (4.2)$$

where \mathcal{L}_{kin} , \mathcal{L}_Y , \mathcal{L}_{VL} and $V(\Phi, \Delta)$ are the kinetic term, Yukawa interaction for the ordinary SM fermions, the mass and Yukawa interaction for the vector-like leptons, and the scalar potential, respectively. The Yukawa interactions for the ordinary SM leptons are [1]

$$\mathcal{L}_Y = - [\bar{L}_L^i h_e^{ij} \Phi e_R^j + \text{h.c.}] - [h_{ij} \bar{L}_L^{ic} i\tau_2 \Delta L_L^j + \text{h.c.}], \quad (4.3)$$

where $\tilde{\Phi} = i\tau_2 \Phi^*$, h_e is a 3×3 complex matrix, and h_{ij} is a 3×3 complex symmetric Yukawa matrix. Additionally, with the vector-like family of leptons as defined above, the vector-like lepton part of the Lagrangian density is

$$\begin{aligned} \mathcal{L}_{\text{VL}} &= - [M_L \bar{L}'_L L''_R + M_E e'_R e''_L + M_\nu \bar{\nu}'_R \nu''_L + \frac{1}{2} M'_\nu \bar{\nu}'_R{}^c \nu'_R + \frac{1}{2} M''_\nu \bar{\nu}''_L{}^c \nu''_L + h'_E (\bar{L}'_L \Phi) e'_R \\ &\quad + h''_E (\bar{L}''_R \Phi) e''_L + h'_\nu (\bar{L}'_L \tau \Phi^\dagger) \nu'_R + h''_\nu (\bar{L}''_R \tau \Phi^\dagger) \nu''_L + h'_{ij} \bar{L}'_L{}^c i\tau_2 \Delta L'_L + h''_{ij} \bar{L}''_R{}^c i\tau_2 \Delta L''_R \\ &\quad + \lambda^i_E (\bar{L}'_L \Phi) e^i_R + \lambda^i_L (\bar{L}'_L \Phi) e^i_R + \lambda'_{ij} \bar{L}'_L{}^c i\tau_2 \Delta L'_L + \lambda''_{ij} \bar{L}''_R{}^c i\tau_2 \Delta L''_R + \text{h.c.}] \end{aligned} \quad (4.4)$$

where we include explicit mass terms, Yukawa interactions among vector-like leptons, and Yukawa interactions between vector-like leptons and ordinary leptons. The scalar potential is

$$\begin{aligned} V(\Phi, \Delta) &= m^2 \Phi^\dagger \Phi + M^2 \text{Tr}(\Delta^\dagger \Delta) + [\mu \Phi^T i\tau_2 \Delta^\dagger \Phi + \text{h.c.}] + \lambda_1 (\Phi^\dagger \Phi)^2 \\ &\quad + \lambda_2 [\text{Tr}(\Delta^\dagger \Delta)]^2 + \lambda_3 \text{Tr}[(\Delta^\dagger \Delta)^2] + \lambda_4 (\Phi^\dagger \Phi) \text{Tr}(\Delta^\dagger \Delta) + \lambda_5 \Phi^\dagger \Delta \Delta^\dagger \Phi, \end{aligned} \quad (4.5)$$

with m and M the Higgs bare masses, μ the lepton-number violating parameter, and λ_1 - λ_5 the Higgs coupling constants. The expressions for the λ_1 - λ_5 parameters in terms of Higgs masses are given in Chapter 3.

The electroweak gauge symmetry is broken by the VEVs of the neutral components of the doublet and triplet Higgs fields,

$$\langle \Phi^0 \rangle = v_\Phi / \sqrt{2}, \quad \langle \Delta^0 \rangle = v_\Delta / \sqrt{2}. \quad (4.6)$$

where Φ and Δ are the doublet Higgs field and the triplet Higgs field, with $v^2 \equiv v_\Phi^2 + 2v_\Delta^2 = (246 \text{ GeV})^2$. Higgs masses and coupling constants in the presence of nontrivial mixing in the neutral sector have been obtained previously [1].

One can invoke new symmetries to restrict the interaction of the vector leptons with each other or with the ordinary leptons, or disallow the presence of bare mass terms in the Lagrangian. For instance,

1. If an additional $U(1)$ symmetry is present under which the primed, double primed and the ordinary leptons have different charges, this would forbid explicit masses M_L , M_E , M_ν and M'_ν from the Lagrangian. Vector-like leptons would get masses only through couplings to the Higgs doublet fields [210, 223].
2. If one imposes a symmetry under which all the new $SU(2)_L$ singlet fields are odd, while the new $SU(2)_L$ doublets are even, this forces all Yukawa couplings involving new leptons to vanish, $h'_E = h''_E = h'_\nu = h''_\nu = h'_{ij} = h''_{ij} = 0$, and the masses arise only from explicit terms in the Lagrangian [97].
3. Finally one can impose a new parity symmetry which disallows mixing between the ordinary leptons and the new vector-like lepton fields, under which all the new fields are odd, while the ordinary leptons are even [224], i.e., such that $\lambda^i_E = \lambda^i_L = \lambda'_{ij} = \lambda'_{ij} = \lambda''_{ij} = 0$; alternatively one might choose these couplings to be very small.

In this analysis the focus will be on Higgs decays. We investigate the model subjected to symmetry conditions 3; as we would like to neglect mixing between the ordinary and the new vector-like leptons. When allowed, stringent constraints exist on the masses and couplings with ordinary leptons. New vector-like leptons are ruled out when they mediate flavor-changing neutral current processes, generate SM neutrino masses or contribute to neutrinoless double beta decay. Recent studies of models which allow mixing between the ordinary leptons and the new ones exist [223, 224], but restrictions from lepton-flavor-violating decays either force the new leptons to be very heavy $M_L, M_E \sim 10 - 100 \text{ TeV}$, or reduce the branching ratio for $h \rightarrow \tau^+\tau^-$, $\mu^+\mu^-$ and $h \rightarrow \gamma\gamma$ decays to 30-40% of the SM prediction, neither of which are desirable features for our purpose here. In the Higgs Triplet Model, distinguishing signals would be provided by lighter vector-like leptons. Since imposing no mixing between ordinary and new leptons allows new lepton masses to be as light as $\sim 100 \text{ GeV}$ —perhaps without a reduction in the Higgs diphoton branching ratio— we investigate this scenario here. In addition, we also investigate the effect of imposing condition 1, that is, requiring the explicit mass terms in the Lagrangian to be 0.

In the charged sector, the 2×2 mass matrix \mathcal{M}_E is defined as [97, 210]

$$(E'_L \ e''_L)(\mathcal{M}_E) \begin{pmatrix} e'_R \\ E''_R \end{pmatrix}, \quad \text{with} \quad \mathcal{M}_E = \begin{pmatrix} m'_E & M_L \\ M_E & m''_E \end{pmatrix}, \quad (4.7)$$

where $m'_E = h'_E v_\Phi / \sqrt{2}$ and $m''_E = h''_E v_\Phi / \sqrt{2}$, with v_Φ the VEV of the neutral component of the Higgs doublet. The mass matrix can be diagonalized as follows:

$$V_L^\dagger \mathcal{M}_E V_R = \begin{pmatrix} M_{E_1} & 0 \\ 0 & M_{E_2} \end{pmatrix}. \quad (4.8)$$

The mass eigenvalues are

$$M_{E_1, E_2}^2 = \frac{1}{2} \left[(M_L^2 + m'_E{}^2 + M_E^2 + m''_E{}^2) \pm \sqrt{X^2 + Y^2} \right], \quad (4.9)$$

with

$$\begin{aligned} X &= (M_L^2 + m'_E{}^2 - M_E^2 - m''_E{}^2), \\ Y &= 2(m''_E M_L + m'_E M_E). \end{aligned} \quad (4.10)$$

By convention, $M_{E_1} > M_{E_2}$. For simplicity we assume that the lepton Yukawa couplings h'_E and h''_E are real so that the transformations that diagonalize the mass matrix are real orthogonal matrices:

$$V_L = \begin{pmatrix} \cos \theta_L & \sin \theta_L \\ -\sin \theta_L & \cos \theta_L \end{pmatrix}, \quad (4.11)$$

$$V_R = \begin{pmatrix} \cos \theta_R & \sin \theta_R \\ -\sin \theta_R & \cos \theta_R \end{pmatrix}. \quad (4.12)$$

The angles $\theta_{L,R}$ are given by

$$\tan \theta_L = \frac{m''_E M_L + m'_E M_E}{M_{E_2}^2 - M_L^2 - m'_E{}^2}, \quad (4.13)$$

$$\tan \theta_R = \frac{m'_E M_L + m''_E M_E}{M_{E_2}^2 - M_L^2 - m''_E{}^2}. \quad (4.14)$$

The eigenstates of the vector-like lepton mixing matrix enter in the evaluation of $h \rightarrow \gamma\gamma$ and $h \rightarrow Z\gamma$ in the next section.

4.3 Production and Decays of the Neutral Higgs Boson

The presence of the vector leptons affects the loop-dominated decays of the neutral Higgs, $h \rightarrow \gamma\gamma$ and $h \rightarrow Z\gamma$, and possible relationships between them. In the Higgs Triplet Model, singly and doubly charged bosons also enter in the loops, creating a different dynamic than in the SM. We analyze these decays in turn, and look for possible correlations between them.

4.3.1 $h \rightarrow \gamma\gamma$

Recently, the Higgs Triplet Model has received renewed interest because of attempts to reconcile the excess of events in $h \rightarrow \gamma\gamma$ observed at the LHC over those predicted by the SM. Such an enhancement hints at the presence of additional particles—singlets under $SU(3)_C$, but charged under $U(1)_{\text{em}}$ —which affect only the loop-dominated decay branching ratio, while leaving the production cross section and tree-level decays largely unchanged. Vector-like leptons are prime candidates for such particles, so we study their contribution to the Higgs decay. The decay width $h \rightarrow \gamma\gamma$ is

$$[\Gamma(h \rightarrow \gamma\gamma)]_{HTM} = \frac{G_F \alpha^2 m_h^3}{128 \sqrt{2} \pi^3} \left| \sum_f N_c^f Q_f^2 g_{hff} A_{1/2}(\tau_f^h) + g_{hWW} A_1(\tau_W^h) + \tilde{g}_{hH^\pm H^\mp} A_0(\tau_{H^\pm}^h) \right. \\ \left. + 4\tilde{g}_{hH^{\pm\pm} H^\mp} A_0(\tau_{H^{\pm\pm}}^h) + \frac{\mu_{E_1} g_{hff}}{M_{E_1}} A_{1/2}(\tau_{E_1}^h) + \frac{\mu_{E_2} g_{hff}}{M_{E_2}} A_{1/2}(\tau_{E_2}^h) \right|^2, \quad (4.15)$$

with M_{E_1}, M_{E_2} given in Eq. (6.13), and where the loop functions for spin-0, spin-1/2 and spin-1 are given by:

$$A_0(\tau) = -[\tau - f(\tau)] \tau^{-2}, \quad (4.16)$$

$$A_{1/2}(\tau) = -\tau^{-1} [1 + (1 - \tau^{-1}) f(\tau^{-1})], \quad (4.17)$$

$$A_1(\tau) = 1 + \frac{3}{2}\tau^{-1} + 4\tau^{-1} \left(1 - \frac{1}{2}\tau^{-1}\right) f(\tau^{-1}), \quad (4.18)$$

and the function $f(\tau)$ is given by :

$$f(\tau) = \begin{cases} \arcsin^2 \sqrt{\tau} & 0 < \tau \leq 1 \\ -\frac{1}{4} \left[\log \frac{1 + \sqrt{1 - \tau^{-1}}}{1 - \sqrt{1 - \tau^{-1}}} - i\pi \right]^2 & \tau > 1, \end{cases} \quad (4.19)$$

with $\tau_i^h = \frac{m_h^2}{4m_i^2}$, and m_i is the mass of the particle running in the loop [97]. In Eq. (5.33) the first contribution is from the top quark, the second is from the W boson, the third is from

the singly charged Higgs boson, the fourth is from the doubly charged Higgs boson, and the last two are from the vector-like leptons. We use the following expressions for the couplings of the Higgs bosons with charged vector-like leptons:

$$\begin{aligned}\mu_{E_1} &= -\cos\theta_L \cos\theta_R (m'_E \tan\theta_R + m''_E \tan\theta_L) \\ \mu_{E_2} &= \cos\theta_L \cos\theta_R (m'_E \tan\theta_L + m''_E \tan\theta_R)\end{aligned}\quad (4.20)$$

The couplings of h to the vector bosons and fermions are as follows:

$$g_{hff} = \cos\alpha / \cos\beta_{\pm}; \quad g_{hWW} = \cos\alpha + 2\sin\alpha v_{\Delta}/v_{\Phi}, \quad (4.21)$$

with $ff = t\bar{t}, E_1\bar{E}_1, E_2\bar{E}_2$ and the scalar trilinear couplings are parametrized as follows

$$\begin{aligned}\tilde{g}_{hH^{++}H^{--}} &= \frac{m_W}{gm_{H^{\pm\pm}}^2} \left[2\lambda_2 v_{\Delta} \sin\alpha + \lambda_4 v_{\Phi} \cos\alpha \right], \\ \tilde{g}_{hH^+H^-} &= \frac{m_W}{2gm_{H^{\pm}}^2} \left\{ \left[4v_{\Delta}(\lambda_2 + \lambda_3) \cos^2\beta_{\pm} + 2v_{\Delta}\lambda_4 \sin^2\beta_{\pm} - \sqrt{2}\lambda_5 v_{\Phi} \cos\beta_{\pm} \sin\beta_{\pm} \right] \sin\alpha \right. \\ &\quad \left. + \left[4\lambda_1 v_{\Phi} \sin\beta_{\pm}^2 + (2\lambda_4 + \lambda_5)v_{\Phi} \cos^2\beta_{\pm} + (4\mu - \sqrt{2}\lambda_5 v_{\Delta}) \cos\beta_{\pm} \sin\beta_{\pm} \right] \cos\alpha \right\}.\end{aligned}\quad (4.22)$$

Since the new leptons do not affect the Higgs production channels, the effect on the diphoton search channel at the LHC is expressed by the ratio (signal strength)

$$\begin{aligned}R_{h\rightarrow\gamma\gamma} &\equiv \frac{\sigma_{\text{HTM}}(gg \rightarrow h \rightarrow \gamma\gamma)}{\sigma_{\text{SM}}(gg \rightarrow \Phi \rightarrow \gamma\gamma)} = \frac{[\sigma(gg \rightarrow h) \times BR(h \rightarrow \gamma\gamma)]_{\text{HTM}}}{[\sigma(gg \rightarrow \Phi) \times BR(\Phi \rightarrow \gamma\gamma)]_{\text{SM}}} \\ &= \frac{[\sigma(gg \rightarrow h) \times \Gamma(h \rightarrow \gamma\gamma)]_{\text{HTM}}}{[\sigma(gg \rightarrow \Phi) \times \Gamma(\Phi \rightarrow \gamma\gamma)]_{\text{SM}}} \times \frac{[\Gamma(\Phi)]_{\text{SM}}}{[\Gamma(h)]_{\text{HTM}}},\end{aligned}\quad (4.23)$$

where Φ is the SM neutral Higgs boson and where the ratio of the cross sections by gluon fusion is

$$\frac{\sigma_{\text{HTM}}(gg \rightarrow h \rightarrow \gamma\gamma)}{\sigma_{\text{SM}}(gg \rightarrow \Phi \rightarrow \gamma\gamma)} = \cos^2\alpha. \quad (4.24)$$

Here α is the mixing angle in the CP-even neutral sector:

$$\begin{pmatrix} \varphi \\ \delta \end{pmatrix} = \begin{pmatrix} \cos\alpha & -\sin\alpha \\ \sin\alpha & \cos\alpha \end{pmatrix} \begin{pmatrix} h \\ H \end{pmatrix}, \quad (4.25)$$

with

$$\tan 2\alpha = \frac{v_{\Delta}}{v_{\Phi}} \frac{2v_{\Phi}^2(\lambda_4 + \lambda_5) - 4v_{\Phi}^2\mu/\sqrt{2}v_{\Delta}}{2v_{\Phi}^2\lambda_1 - v_{\Phi}^2\mu/\sqrt{2}v_{\Delta} - 2v_{\Delta}^2(\lambda_2 + \lambda_3)}. \quad (4.26)$$

In Chapter 3 we investigated the Higgs boson decay branching ratio into $\gamma\gamma$ with respect to the SM— assuming that the lightest Higgs boson is the 2.3σ signal excess observed at the

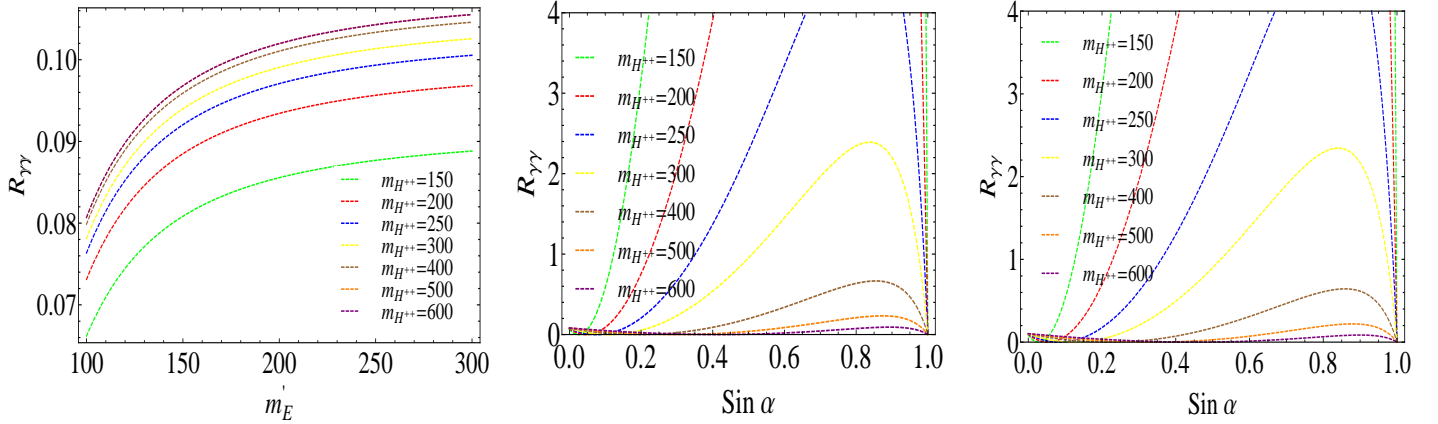


Figure 4.1: Relative decay rate $R_{h \rightarrow \gamma\gamma}$ in the limit $M_L = M_E = 0$ (left panel) as a function of $m'_E = m''_E$, for $\sin \alpha = 0$, as a function of $\sin \alpha$ for $m'_E = m''_E = 100$ GeV (middle panel), and as a function of $\sin \alpha$ for $m'_E = m''_E = 200$ GeV (right panel). The colored-coded curves correspond to different values of doubly charged Higgs masses, given in the attached panels in GeV.

LEP at 98 GeV, while the heavier Higgs boson is the boson observed at the LHC at 125 GeV— in a Higgs Triplet Model without vector-like leptons, and found that this is the only scenario which allows for an enhancement of the $h \rightarrow \gamma\gamma$ branching fraction. We thus set the values 125 GeV and 98 GeV for the h and H masses, respectively, and adjust the parameters $\lambda_1 - \lambda_5$ accordingly.

Vector-like lepton masses and mixing parameters depend on M_L and M_E , the explicit mass parameters in the Lagrangian; and h'_E, h''_E , the vector-like leptons Yukawa parameters. In the limit of vanishing Dirac mass terms M_L and M_E , the prefactors $\frac{\mu_{E_i}}{M_{E_i}}$ in Eq. (5.33) go to 1. It then follows that there is destructive interference between the dominant W - boson contribution and the charged leptons loops [97]. In this limit, despite possible enhancement from singly and doubly charged Higgs bosons in the loop, we find a large suppression of the diphoton rate. We present the plots for the relative signal strength of $R_{h \rightarrow \gamma\gamma}$, defined in Eq. (5.34) as a function of $m'_E = m''_E$ (or equivalently $h'_E = h''_E$), for various values of doubly charged Higgs bosons mass in the left panel of Fig. 4.1, for $\sin \alpha = 0$. Clearly, for this case (no mixing) the decay of the h is suppressed significantly with respect to the value in the SM over the whole region of the parameter space in m'_E .

Allowing mixing in the neutral Higgs sector changes the relative contributions of the charged

Higgs to the diphoton decay. We show decay rates for $h \rightarrow \gamma\gamma$ as a function of $\sin\alpha$ for different values of doubly charged Higgs boson mass, assuming $m'_E = m''_E = 100$ GeV (and 200 GeV), in the middle and right panels of Fig. 4.1, respectively. Considerations for relative branching ratios are affected by the fact that the total width of Higgs boson in the HTM for $\sin\alpha \neq 0$ is not the same as in the SM. The relative widths factor is

$$\frac{[\Gamma(h)]_{HTM}}{[\Gamma(\Phi)]_{SM}} = \frac{[\Gamma(h \rightarrow \sum_f f\bar{f}) + \Gamma(h \rightarrow WW^*) + \Gamma(h \rightarrow ZZ^*) + \Gamma(h \rightarrow \nu\nu)]_{HTM}}{[\Gamma(\Phi \rightarrow \sum_f f\bar{f}) + \Gamma(\Phi \rightarrow WW^*) + \Gamma(\Phi \rightarrow ZZ^*)]_{SM}}. \quad (4.27)$$

The plots in Fig. 4.1 correspond to symmetry condition 1 in Section 4.2, that is, $M_L = M_E = 0$.

However, if mixing with SM leptons is forbidden, but the vector-like leptons are still allowed to mix with each other, the prefactors μ_{E_i}/M_{E_i} in Eq. (5.33) are not 1, and can modify the Higgs diphoton decay. In the next plots we investigate the effect of nonzero mass parameters M_L and M_E , for fixed values of the Yukawa couplings. In Fig. 4.2 we present the contour plots of constant $R_{h \rightarrow \gamma\gamma}$ for $h'_E = h''_E = 0.8$ in the plane of the explicit mass terms M_L and M_E , for various values of doubly charged Higgs bosons mass and $\sin\alpha$. The contours are labeled by the value of $R_{h \rightarrow \gamma\gamma}$. The vector-like lepton masses are restricted to values for which [210] $M_{E_2} \geq 62.5$ GeV, where $M_{E_{1,2}}$ are given in Eq. (6.13). The plots indicate that it is difficult to obtain any significant enhancement of the ratio $R_{h \rightarrow \gamma\gamma}$ for $\sin\alpha = 0$, and this does not depend on the chosen values for the doubly charged Higgs mass; however for $\sin\alpha \neq 0$, enhancements are possible for various values of $m_{H^{\pm\pm}}$. In Fig. 4.3 we investigate the dependence of $R_{h \rightarrow \gamma\gamma}$ on the Yukawa couplings and vector-like lepton masses. We show contour plots for fixed $R_{h \rightarrow \gamma\gamma}$ in a $h'_E - M_L$ plane, with $h'_E = h''_E$ and $M_L = M_E$, for various values of $\sin\alpha$ and doubly charged Higgs boson masses. Enhancements are possible here for all values of $\sin\alpha$, but while for $\sin\alpha = 0$ the decay $h \rightarrow \gamma\gamma$ is enhanced for large vector-like lepton masses and Yukawa couplings, for $\sin\alpha \neq 0$ we observe enhancements for light vector-like lepton masses and small Yukawa couplings.

If we wish to study the light vector-like leptons parameter space where $h \rightarrow \gamma\gamma$ is enhanced, $\sin\alpha \neq 0$ is preferred. The enhancement is affected by mixing in the vector-like lepton sector, the various values for doubly charged Higgs bosons mass and the values of $\sin\alpha$.

As the plots cover only a limited range of the parameter space, in the Tables below we give the ranges for the values of the ratio $R_{h \rightarrow \gamma\gamma}$ for the various scenarios. In Table 4.1, we fix the value of the Yukawa coupling to $h'_E = 0.8$, allow the vector-like lepton masses to vary in

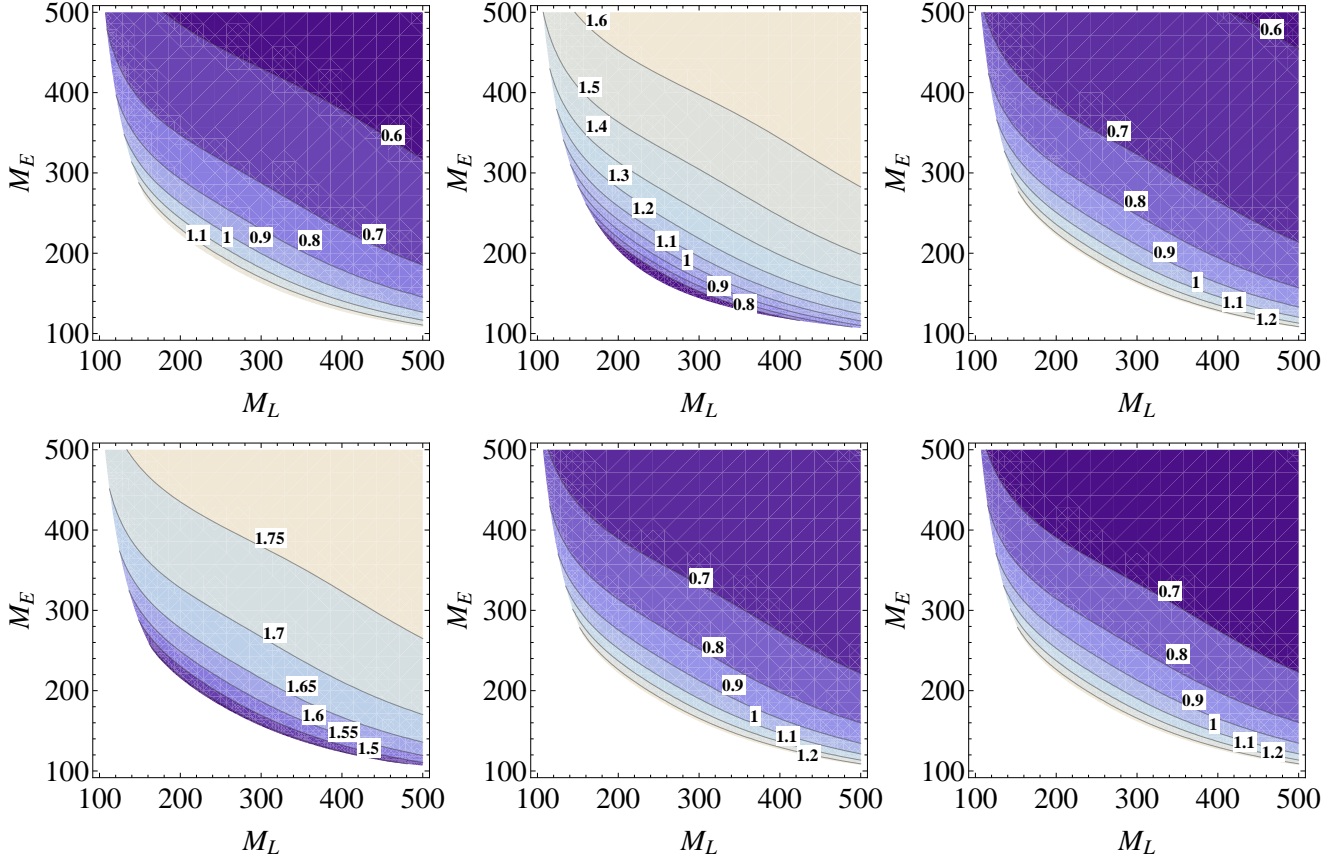


Figure 4.2: Contour plots of constant $R_{h \rightarrow \gamma\gamma}$ for mass terms M_E and M_L , for $h'_E = h''_E = 0.8$ and combinations of doubly charged Higgs boson masses and $\sin \alpha$: (upper left panel) $m_{H^{\pm\pm}} = 150$ GeV, $\sin \alpha = 0$; (upper middle panel) $m_{H^{\pm\pm}} = 150$ GeV, $\sin \alpha = 0.2$; (upper right panel) $m_{H^{\pm\pm}} = 300$ GeV, $\sin \alpha = 0$; (lower left panel) $m_{H^{\pm\pm}} = 300$ GeV, $\sin \alpha = 0.9$; (lower middle panel) $m_{H^{\pm\pm}} = 500$ GeV, $\sin \alpha = 0$; (lower right panel) $m_{H^{\pm\pm}} = 600$ GeV, $\sin \alpha = 0$.

the (100-500) GeV range, and show the values for $R_{h \rightarrow \gamma\gamma}$ for different values of $\sin \alpha$ and the doubly charged Higgs mass. We note that the relative branching ratios are very sensitive to the values of both the doubly charged Higgs mass and $\sin \alpha$. Enhancements in the branching ratio of $h \rightarrow \gamma\gamma$ are possible for light values of $m_{H^{\pm\pm}} \leq 300$ GeV, and are much more pronounced at large $\sin \alpha$. Note that for $\sin \alpha = 0$, the result is independent of $m_{H^{\pm\pm}}$, in agreement with the results obtained in Chapter 3. The reason is the following. In Eq. (4.22), for $\sin \alpha = 0$, the coupling between neutral and doubly charged Higgs is

$$\tilde{g}_{hH^{++}H^{--}} = \frac{m_W}{gm_{H^{\pm\pm}}^2} \left[\lambda_4 v_\Phi \right] = \frac{m_W}{gm_{H^{\pm\pm}}^2} \left[2 \frac{m_{H^{\pm\pm}}^2}{v_\Phi^2} v_\Phi \right] = 2 \frac{m_W}{gv_\Phi}, \quad (4.28)$$

where we used the expression for λ_4 from Ref. [1], which is independent of $m_{H^{\pm\pm}}$. In Table 4.2 we allow— in addition to mass variations,— variations in the Yukawa coupling $h'_E \in (0 - 3)$.

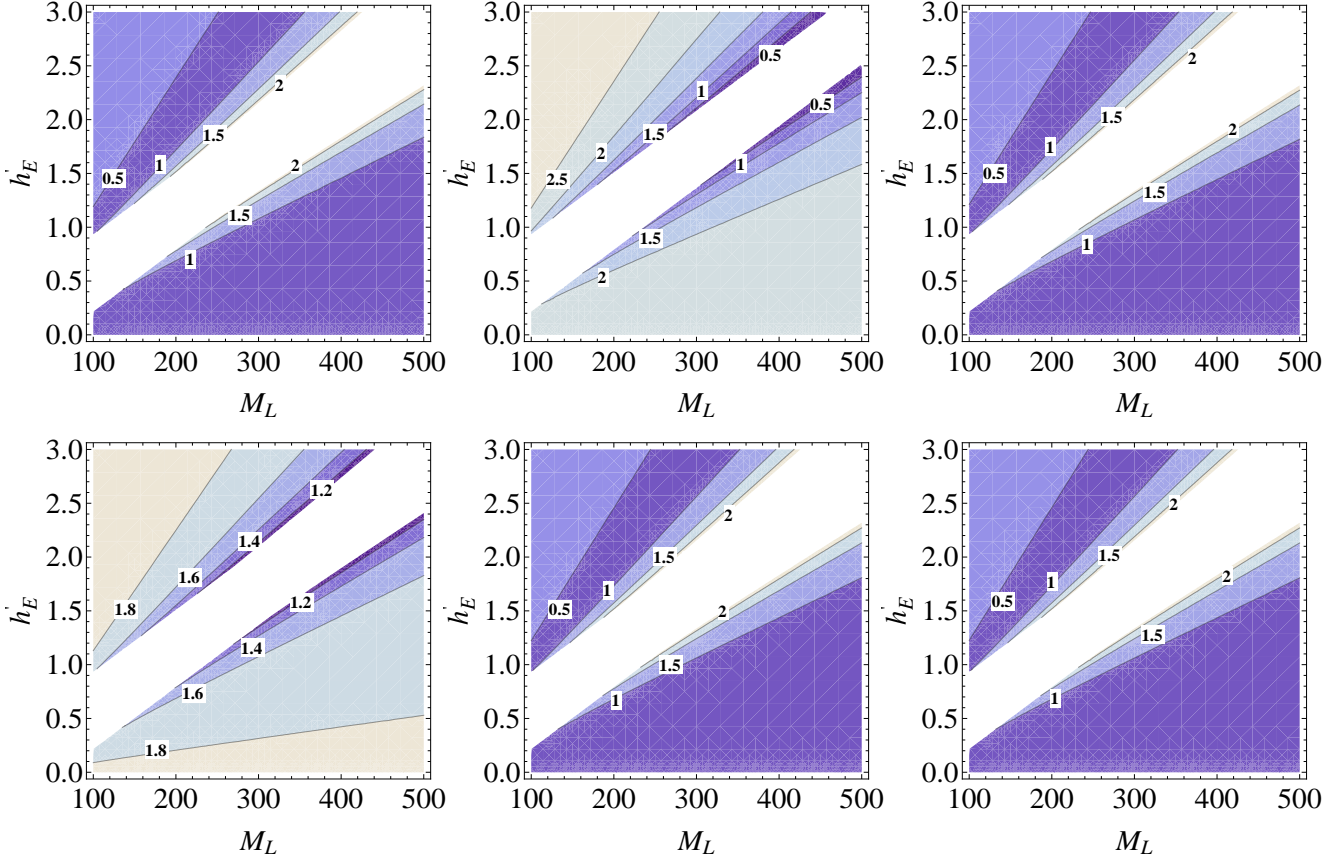


Figure 4.3: Contour plots of constant $R_{h \rightarrow \gamma\gamma}$ for mass terms M_L and $h'_E = h''_E$, for various doubly-charged Higgs boson masses and $\sin \alpha$: (upper left panel) $m_{H^{\pm\pm}} = 200$ GeV, $\sin \alpha = 0$; (upper middle panel) $m_{H^{\pm\pm}} = 200$ GeV, $\sin \alpha = 0.4$; (upper right panel) $m_{H^{\pm\pm}} = 300$ GeV, $\sin \alpha = 0$; and (lower left panel) $m_{H^{\pm\pm}} = 300$ GeV, $\sin \alpha = 0.9$; (lower middle panel) $m_{H^{\pm\pm}} = 500$ GeV, $\sin \alpha = 0$; (lower right panel) $m_{H^{\pm\pm}} = 600$ GeV, $\sin \alpha = 0$.

This means allowing both explicit (Dirac) masses and additional contributions by electroweak symmetry breaking, m'_E, m''_E . The dependence on the Yukawa coupling h'_E is much weaker than on $\sin \alpha$ or on $m_{H^{\pm\pm}}$.

However, one can see from the Tables that modest enhancements of the ratio $R_{h \rightarrow \gamma\gamma}$ are possible for $\sin \alpha = 0$ for large vector-like leptons Yukawa couplings, unlike in the case of the triplet model without vector-like leptons. This would then be a clear distinguishing feature, namely enhancements of the decay $h \rightarrow \gamma\gamma$ in the absence of mixing in the neutral sector. The absence of mixing would manifest itself in observing tree-level decays ($h \rightarrow b\bar{b}, \tau^+\tau^-, ZZ^*$ and WW^*) identical to those in the SM. There seems to be a minimum value of $R_{h \rightarrow \gamma\gamma}$ for $\sin \alpha = 0.1$, where the contribution from the doubly charged Higgs bosons is important for

Table 4.1: Range of the ratio $R_{h \rightarrow \gamma\gamma}$, as defined in the text, for the doubly charged Higgs mass (in columns) and the neutral Higgs mixing angle $\sin \alpha$ (in rows), for Dirac vector-like lepton masses in the range $M_E, M_L \in (100 - 500)$ GeV, with $h'_E = 0.8$.

$R_{\gamma\gamma}$	$m_{H^{\pm\pm}} = 150$ GeV	200 GeV	250 GeV	300 GeV	500 GeV	600 GeV
$\sin \alpha = 0$	0.6 – 1.2	0.6 – 1.2	0.6 – 1.2	0.6 – 1.2	0.6 – 1.2	0.6 – 1.2
$\sin \alpha = 0.1$	0.02 – 0.08	0.05 – 0.23	0.2 – 0.5	0.3 – 0.7	0.5 – 1	0.6 – 1
$\sin \alpha = 0.2$	0.8 – 1.6	0.02 – 0.14	0.01 – 0.08	0.1 – 0.3	0.4 – 0.8	0.5 – 0.9
$\sin \alpha = 0.3$	4 – 5.2	0.2 – 0.9	0.02 – 0.12	0.01 – 0.04	0.25 – 0.55	0.3 – 0.7
$\sin \alpha = 0.4$	9 – 10.75	1.4 – 2.2	0.1 – 0.5	0.02 – 0.08	0.15 – 0.35	0.25 – 0.55
$\sin \alpha = 0.5$	16 – 18	3.2 – 4.2	0.6 – 1.2	0.05 – 0.3	0.06 – 0.22	0.15 – 0.35
$\sin \alpha = 0.6$	24 – 26.5	5.6 – 6.8	1.4 – 2.1	0.25 – 0.7	0.01 – 0.08	0.06 – 0.2
$\sin \alpha = 0.7$	32.5 – 34.5	8.2 – 9.4	2.4 – 3.1	0.7 – 1.1	0.002 – 0.008	0.02 – 0.08
$\sin \alpha = 0.8$	38.5 – 40.75	10.4 – 11.4	3.4 – 4.1	1.2 – 1.65	0.005 – 0.045	0.001 – 0.006
$\sin \alpha = 0.9$	36.2 – 37.4	10.2 – 10.9	3.7 – 4.1	1.5 – 1.75	0.04 – 0.1	0.005 – 0.02

Table 4.2: Same as in Table 4.1, but also allowing $h'_E \in (0 - 3)$.

$R_{\gamma\gamma}$	$m_{H^{\pm\pm}} = 150$ GeV	200 GeV	250 GeV	300 GeV	500 GeV	600 GeV
$\sin \alpha = 0$	0.5 – 2	0.5 – 2	0.5 – 2	0.5 – 2	0.5 – 2	0.5 – 2
$\sin \alpha = 0.1$	0.05 – 0.3	0.1 – 0.6	0.2 – 1	0.2 – 1.4	0.5 – 1.75	0.5 – 2
$\sin \alpha = 0.2$	0.5 – 2	0.1 – 0.4	0.05 – 0.3	0.1 – 0.7	0.25 – 1.5	0.25 – 1.75
$\sin \alpha = 0.3$	2 – 6	0.5 – 1	0.1 – 0.4	0.05 – 0.2	0.2 – 1.2	0.2 – 1.4
$\sin \alpha = 0.4$	6 – 11	1 – 2.5	0.2 – 0.6	0.05 – 0.3	0.2 – 0.8	0.2 – 1
$\sin \alpha = 0.5$	14 – 18	2 – 4	0.5 – 1.5	0.2 – 0.4	0.1 – 0.5	0.2 – 0.8
$\sin \alpha = 0.6$	20 – 26	4 – 7	0.5 – 2.5	0.25 – 0.75	0.05 – 0.25	0.1 – 0.5
$\sin \alpha = 0.7$	30 – 36	7 – 10	1.5 – 3.5	0.25 – 1.25	0.01 – 0.07	0.05 – 0.2
$\sin \alpha = 0.8$	36 – 40	9 – 12	2.5 – 4	0.5 – 1.75	0.02 – 0.08	0.01 – 0.04
$\sin \alpha = 0.9$	35 – 38	9.5 – 11	3.2 – 4.2	1.2 – 1.8	0.05 – 0.1	0.01 – 0.04

small doubly charged masses and counters the contribution from the vector-like leptons. This is a suppression of the branching ratio for $h \rightarrow \gamma\gamma$, which is due to the fact that the vector-like lepton contribution interacts destructively with the dominant W^\pm contribution. As a general feature, $R_{h \rightarrow \gamma\gamma}$ increases when we lower the doubly charged Higgs mass and increase $\sin \alpha$. This rules out part of the parameter space. For instance, for $m_{H^{\pm\pm}} = 150$ GeV, the mixing cannot be larger than $\sin \alpha = 0.2$, and for $m_{H^{\pm\pm}} = 200$ GeV, mixings larger than $\sin \alpha \geq 0.5$ are ruled out. If the value of $m_{H^{\pm\pm}}$ is increased to 500–600 GeV, only modest enhancements are possible, and only for $\sin \alpha = 0$, for vector-like lepton explicit masses in the 100–500 GeV range and $h'_E = 0.8$. Increasing the vector-like leptons Yukawa coupling increases the overall ratio $R_{h \rightarrow \gamma\gamma}$.

4.3.2 $h \rightarrow Z\gamma$

In most models, the $h \rightarrow \gamma\gamma$ and $h \rightarrow Z\gamma$ partial decay widths are correlated or anticorrelated, though usually the enhancement/suppression in the $Z\gamma$ channel is much smaller compared to that in the $\gamma\gamma$ channel. However, as in models with new loop contributions to $h \rightarrow \gamma\gamma, Z\gamma$, a sensitivity to both is expected; we study the correlation between the two here, in the presence of vector-like leptons. An investigation of the branching ratio of $h \rightarrow Z\gamma$ is also further justified by the recent results from CMS and ATLAS [225, 226], which indicate branching fractions consistent with the SM expectation at 1σ in the Higgs boson h mass region at 95% C.L. The decay width for $h \rightarrow Z\gamma$ is given by [150–153]:

$$\begin{aligned}
[\Gamma(h \rightarrow Z\gamma)]_{HTM} &= \frac{\alpha G_F^2 m_W^2 m_h^3}{64\pi^4} \left(1 - \frac{m_Z^2}{m_h^2}\right)^3 \left| \frac{1}{c_W} \sum_f 2N_c^f Q_f (I_3^f - 2Q_f s_W^2) g_{hff} A_{1/2}^h(\tau_f^h, \tau_f^Z) \right. \\
&+ \frac{(I_3^E - 2Q_E s_W^2)(2Q_E)}{c_W} \left[\frac{\mu_{E_1} g_{hff}}{M_{E_1}} A_{1/2}^h(\tau_{E_1}^h, \tau_{E_1}^Z) + \frac{\mu_{E_2} g_{hff}}{M_{E_2}} A_{1/2}^h(\tau_{E_2}^h, \tau_{E_2}^Z) \right] \\
&+ c_W g_{hWW} A_1^h(\tau_W^h, \tau_W^Z) - 2s_W \tilde{g}_{hH^\pm H^\mp} g_{ZH^\pm H^\mp} A_0^h(\tau_{H^\pm}^h, \tau_{H^\pm}^Z) \\
&\left. - 4s_W \tilde{g}_{hH^{\pm\pm} H^\mp} g_{ZH^{\pm\pm} H^\mp} A_0^h(\tau_{H^{\pm\pm}}^h, \tau_{H^{\pm\pm}}^Z) \right|^2, \tag{4.29}
\end{aligned}$$

where $\tau_i^h = 4m_i^2/m_h^2$, $\tau_i^Z = 4m_i^2/m_Z^2$ (with $i = f(\equiv t), E_1, E_2, W, H^\pm, H^{\pm\pm}$), and the loop-factors are given by

$$\begin{aligned}
A_0^h(\tau_h, \tau_Z) &= I_1(\tau^h, \tau^Z), \\
A_{1/2}^h(\tau^h, \tau^Z) &= I_1(\tau^h, \tau^Z) - I_2(\tau^h, \tau^Z), \\
A_1^h(\tau^h, \tau^Z) &= 4(3 - \tan^2 \theta_W) I_2(\tau^h, \tau^Z) + [(1 + 2\tau^{h-1}) \tan^2 \theta_W - (5 + 2\tau^{h-1})] I_1(\tau^h, \tau^Z).
\end{aligned} \tag{4.30}$$

The functions I_1 and I_2 are given by

$$\begin{aligned}
 I_1(\tau^h, \tau^Z) &= \frac{\tau^h \tau^Z}{2(\tau^h - \tau^Z)} + \frac{\tau^{h2} \tau^{Z2}}{2(\tau^h - \tau^Z)^2} [f(\tau^{h-1}) - f(\tau^{Z-1})] \\
 &+ \frac{\tau^{h2} \tau^Z}{(\tau^h - \tau^Z)^2} [g(\tau^{h-1}) - g(\tau^{Z-1})], \\
 I_2(\tau^h, \tau^Z) &= -\frac{\tau^h \tau^Z}{2(\tau^h - \tau^Z)} [f(\tau^{h-1}) - f(\tau^{Z-1})],
 \end{aligned} \tag{4.31}$$

where the function $f(\tau)$ is defined in Eq. (4.19), and the function $g(\tau)$ is defined as

$$g(\tau) = \begin{cases} \sqrt{\tau^{-1} - 1} \sin^{-1}(\sqrt{\tau}), & (\tau < 1) \\ \frac{1}{2} \sqrt{1 - \tau^{-1}} \left[\log \left(\frac{1 + \sqrt{1 - \tau^{-1}}}{1 - \sqrt{1 - \tau^{-1}}} \right) - i\pi \right], & (\tau \geq 1). \end{cases} \tag{4.32}$$

In Eq. (5.36) we list, in order, the ordinary leptons, vector leptons, W boson, singly charged Higgs, and doubly charged Higgs contribution. The scalar couplings $g_{hf\bar{f}}$ and $g_{hW^+W^-}$ are given in Eq. (4.21), and the scalar trilinear couplings $\tilde{g}_{hH^\pm H^\mp}$ and $\tilde{g}_{hH^{\pm\pm}H^\mp}$ are given in Eq. (4.22). The remaining couplings in Eq. (5.36) are given by

$$g_{ZH^+H^-} = -\tan \theta_W, \quad g_{ZH^{++}H^{--}} = 2 \cot 2\theta_W. \tag{4.33}$$

We proceed to perform a similar analysis as in Sec. 4.3.1. We show first the variation of the branching ratio $h \rightarrow Z\gamma$ with the mass $m'_E = m''_E$, for various values of the doubly charged Higgs masses, for the case of no mixing in the neutral sector, $\sin \alpha = 0$ (shown in the left panel of Fig. 4.4), and as a function of the mixing angle $\sin \alpha$ for $m'_E = 100$ GeV, and $m'_E = 200$ GeV, in the middle and right panels of Fig. 4.4, respectively. We have chosen the same parameter values as in Fig. 4.1 for comparison. It is clear that the branching ratio into $Z\gamma$ is fairly independent of both m'_E and $m_{H^{\pm\pm}}$ and is always just below the SM expectations. Note that the severe suppression seen in $h \rightarrow \gamma\gamma$ for $\sin \alpha = 0$ (Fig. 4.1, left panel) does not occur here, and the results of the left panel of Fig. 4.4 are consistent with the data at LHC.

But the variation with the mixing angle α is pronounced, and the branching ratio can reach almost twice its SM value for $\sin \alpha \sim 0.8$. However—correlated with our predictions from Sec. 4.3.1 and LHC measurements for $R_{h \rightarrow \gamma\gamma}$ —the parameter space corresponding to an enhanced $h \rightarrow Z\gamma$, for both $m'_E = 100$ GeV and 200 GeV, for doubly charged Higgs mass $m_{H^{\pm\pm}} = 150$ GeV is ruled out. For all other values considered, the value for $R_{h \rightarrow Z\gamma}$ is close to or below the SM expectations. This is a general prediction of the model.

For a large range of parameter space, the decay $h \rightarrow Z\gamma$ can be suppressed significantly with respect to the SM. We plot signal strength for $h \rightarrow Z\gamma$ as a function of $\sin \alpha$ for different

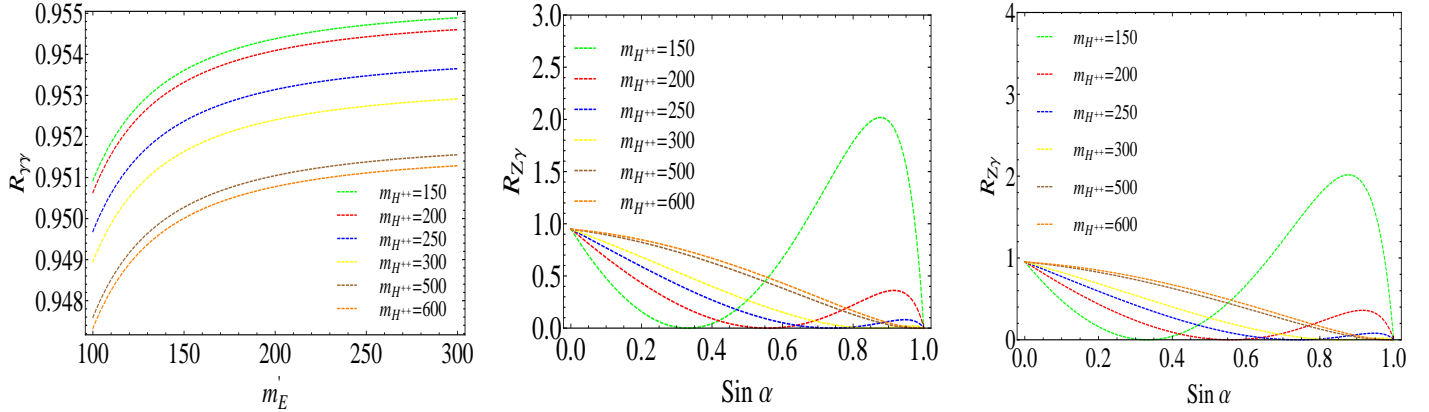


Figure 4.4: Signal strength for $R_{h \rightarrow \gamma Z}$ as a function of $m'_E = m''_E$ for different values of doubly-charged Higgs masses, in the case of no mixing, i.e., $\sin \alpha = 0$ (left panel); and as a function of $\sin \alpha$ for $m'_E = m''_E = 100$ GeV (middle panel), and $m'_E = m''_E = 200$ GeV (right panel). The colored-coded curves correspond to different values of doubly-charged Higgs masses, given in the attached panels in GeV.

values of doubly charged Higgs boson mass, assuming $m'_E = m''_E = 100$ GeV and 200 GeV in the middle and right panels of Fig. 4.4, respectively. Again, considerations for signal strength are affected by the fact that the total width of Higgs boson in the HTM is not the same as in the SM. The widths are the same as those in the SM for h for $\sin \alpha = 0$, while for $\sin \alpha \neq 0$ we take into account the relative widths factors, Eq.(4.27).

In Tables 4.3 and 4.4 we present the explicit ranges of $R_{h \rightarrow Z\gamma}$ for varying M_E, M_L and for a range of h'_E parameters. We choose a fixed value for $h'_E = 0.8$ in Table 4.3, as this is the preferred choice from other analyses [97, 210], and to facilitate a comparison with Table 4.1. A comparison of Tables 4.1 and 4.3 shows that the decay $h \rightarrow Z\gamma$ is far more stable against variations in masses and values for $\sin \alpha$ than $h \rightarrow \gamma\gamma$, making it a less sensitive indicator for the presence of vector-like lepton states.

In Table 4.4 we also allow variations in the Yukawa coupling $h'_E \in (0 - 3)$. As before this amounts to allowing both explicit masses and contributions from electroweak symmetry breaking, m'_E, m''_E , to vector-like lepton masses. A comparison of the Tables 4.3 and 4.4 indicates that the results are not very sensitive to variations in the Yukawa coupling h'_E or the vector-like lepton mass parameters M_E, M_L . However, the relative branching ratios are very sensitive to values of $\sin \alpha$. While the branching ratio into $Z\gamma$ is almost always

suppressed with respect to its SM value, there is a small region of the parameter space—with a light $H^{\pm\pm}$ and $\sin\alpha \simeq 0.7 - 0.9$ —where enhancement is possible; however as discussed before, this region is ruled out by constraints from $h \rightarrow \gamma\gamma$ measurement, Table 4.2. Note that for $\sin\alpha = 0$ the branching ratio is (as before) independent of the mass of $H^{\pm\pm}$ and is about the same as in the SM.

Table 4.3: Range of the ratio $R_{h \rightarrow Z\gamma}$, as defined in the text, for doubly charged Higgs mass (in columns) and neutral Higgs mixing angle $\sin\alpha$ (in rows), for Dirac vector lepton masses in the range $M_E, M_L \in (100 - 500)$ GeV, with $h'_E = 0.8$.

$R_{Z\gamma}$	$m_{H^{\pm\pm}} = 150$ GeV	200 GeV	250 GeV	300 GeV	500 GeV	600 GeV
$\sin\alpha = 0$	0.96 – 1	0.96 – 1	0.96 – 1	0.96 – 1	0.96 – 1	0.96 – 1
$\sin\alpha = 0.1$	0.48 – 0.51	0.68 – 0.72	0.78 – 0.82	0.83 – 0.87	0.91 – 0.94	0.92 – 0.96
$\sin\alpha = 0.2$	0.16 – 0.18	0.44 – 0.47	0.6 – 0.63	0.69 – 0.73	0.83 – 0.87	0.85 – 0.89
$\sin\alpha = 0.3$	0.01 – 0.015	0.24 – 0.26	0.43 – 0.45	0.55 – 0.58	0.74 – 0.78	0.78 – 0.81
$\sin\alpha = 0.4$	0.03 – 0.04	0.09 – 0.10	0.27 – 0.3	0.41 – 0.43	0.63 – 0.66	0.68 – 0.71
$\sin\alpha = 0.5$	0.25 – 0.26	0.01 – 0.02	0.14 – 0.16	0.27 – 0.29	0.52 – 0.54	0.56 – 0.59
$\sin\alpha = 0.6$	0.64 – 0.66	0.005 – 0.006	0.05 – 0.06	0.15 – 0.17	0.39 – 0.41	0.43 – 0.46
$\sin\alpha = 0.7$	1.18 – 1.21	0.07 – 0.08	0.005 – 0.007	0.06 – 0.07	0.25 – 0.27	0.3 – 0.32
$\sin\alpha = 0.8$	1.76 – 1.78	0.21 – 0.22	0.008 – 0.01	0.009 – 0.011	0.13 – 0.14	0.17 – 0.18
$\sin\alpha = 0.9$	1.98 – 1.99	0.35 – 0.36	0.06	0.004 – 0.005	0.03 – 0.04	0.05 – 0.06

Table 4.4: Same as in Table 4.3, but also allowing $h'_E \in (0 - 3)$.

$R_{Z\gamma}$	$m_{H^{++}} = 150$ GeV	200 GeV	250 GeV	300 GeV	500 GeV	600 GeV
$\sin\alpha = 0$	0.94 – 1.04	0.94 – 1.04	0.94 – 1.04	0.94 – 1.04	0.94 – 1.04	0.94 – 1.04
$\sin\alpha = 0.1$	0.47 – 0.54	0.66 – 0.74	0.76 – 0.84	0.8 – 0.9	0.92 – 0.98	0.9 – 1
$\sin\alpha = 0.2$	0.16 – 0.2	0.43 – 0.49	0.6 – 0.7	0.68 – 0.74	0.82 – 0.9	0.8 – 0.9
$\sin\alpha = 0.3$	0.01 – 0.018	0.23 – 0.27	0.42 – 0.47	0.54 – 0.6	0.74 – 0.8	0.76 – 0.84
$\sin\alpha = 0.4$	0.03 – 0.05	0.09 – 0.12	0.27 – 0.31	0.4 – 0.5	0.63 – 0.68	0.67 – 0.73
$\sin\alpha = 0.5$	0.23 – 0.27	0.01 – 0.02	0.14 – 0.17	0.27 – 0.3	0.51 – 0.56	0.56 – 0.61
$\sin\alpha = 0.6$	0.6 – 0.7	0.001 – 0.009	0.05 – 0.07	0.15 – 0.18	0.38 – 0.42	0.43 – 0.47
$\sin\alpha = 0.7$	1.16 – 1.22	0.07 – 0.08	0.004 – 0.008	0.06 – 0.08	0.26 – 0.28	0.3 – 0.33
$\sin\alpha = 0.8$	1.73 – 1.79	0.2 – 0.23	0.006 – 0.01	0.008 – 0.01	0.13 – 0.15	0.17 – 0.18
$\sin\alpha = 0.9$	1.95 – 2	0.34 – 0.36	0.06 – 0.07	0.004 – 0.005	0.03 – 0.04	0.05 – 0.06

4.4 Production and Decays of the Doubly-Charged Higgs Bosons

The discovery of the doubly charged Higgs bosons would be one of the most striking signals of physics beyond SM, and a clear signature for the Higgs Triplet model. From theoretical expectations, the decay modes of $H^{\pm\pm}$ depend on the value of the VEV of the neutral triplet Higgs component, v_Δ . When $v_\Delta \leq 0.1$ MeV, the dominant decay mode of $H^{\pm\pm}$ is into lepton pairs. If $v_\Delta \gg 0.1$ MeV, the main decay modes of $H^{\pm\pm}$ are into $W^{\pm(\star)}W^{\pm(\star)1}$, and into $H^\pm W^{\pm(\star)}$, if kinematically allowed.

We briefly summarize the results of the experimental constraints on doubly charged bosons. Searches for $H^{\pm\pm}$ were performed at Large Electron Positron Collider (LEP) [152, 227–229], the Hadron Electron Ring Accelerator (HERA) [230, 231] and the Tevatron [143–145, 232]. The most up-to-date bounds have been recently derived by ATLAS and CMS collaborations at the LHC. Assuming a Drell-Yan-like pair production, these collaborations have looked for long-lived doubly charged states, and after analyzing 5 fb^{-1} of LHC collisions at a center-of-mass energy $\sqrt{s} = 7$ TeV and 18.8 fb^{-1} of collisions at $\sqrt{s} = 8$ TeV, they constrained the masses to lie above 685 GeV [140, 141, 233, 234]. The assumption is that the doubly charged Higgs bosons decay 100% into a pair of leptons with the same electric charge through Majorana-type interactions [140, 141], thus neglecting possible decays into W -boson pairs, which is shown to alter the pattern of $H^{\pm\pm}$ branching fractions [147, 235]. In this chapter, we allow decays into $W^\pm W^\pm$ bosons, and also include the decays into vector leptons, which, if light enough, would modify the decays of the doubly charged Higgs bosons further. We take $v_\Delta = 1$ GeV throughout our considerations².

The main production mode for doubly charged Higgs bosons $H^{\pm\pm}$ is the pair production $pp \rightarrow \gamma^*, Z^* \rightarrow H^{\pm\pm} H^{\mp\mp}$ and the associated production $pp \rightarrow W^{\pm*} \rightarrow H^{\pm\pm} H^\mp$. The production cross sections for both the vector boson fusion $qQ \rightarrow q'Q' H^{\pm\pm}$, and the associated weak boson production $qQ \rightarrow W^{\pm*} \rightarrow H^{\pm\pm} W^\mp$ are proportional to v_Δ^2 and much less significant for $v_\Delta \ll v_\Phi$.

At hadron colliders the partonic cross section for the leading order (LO) production cross

¹ For the present analysis, the mass of the doubly charged Higgs boson will be such that decays into on-shell W^\pm pairs are kinematically allowed.

²This value of v_Δ is small enough to satisfy electroweak precision conditions, but large enough to allow decay into gauge boson and charged Higgs [1, 123–134, 219–222].

section for a doubly charged Higgs boson pair is

$$\hat{\sigma}_{LO}(q\bar{q} \rightarrow H^{\pm\pm}H^{\mp\mp}) = \frac{\pi\alpha^2}{9Q^2}\beta^3 \left[4e_q^2 + \frac{2e_q v_q v_{H^{\pm\pm}}(1 - M_Z^2/Q^2) + (v_q^2 + a_q^2)v_{H^{\pm\pm}}^2}{(1 - M_Z^2/Q^2)^2 + M_Z^2\Gamma_Z^2/Q^4} \right], \quad (4.34)$$

where we defined

$$v_q = \frac{2I_{3q} - 4e_q \sin^2 \theta_W}{\sin 2\theta_W}, \quad a_q = \frac{2I_{3q}}{\sin 2\theta_W}, \quad v_{H^{\pm\pm}} = \frac{2I_{3H^{\pm\pm}} - 4 \sin^2 \theta_W}{\sin 2\theta_W},$$

with I_{3i} the third component of the isospin for left-handed particle i , $Q^2 = \hat{s}$ the square of the partonic center-of-mass energy, $\beta = \sqrt{1 - 4m_{H^{\pm\pm}}^2/Q^2}$, and α the QED coupling constant evaluated at scale Q . The hadronic cross section is obtained by convolution with the parton density functions of the proton

$$\sigma_{LO}(pp \rightarrow H^{\pm\pm}H^{\mp\mp}) = \int_{\tau_0}^1 d\tau \sum_q \frac{d\mathcal{L}^{q\bar{q}}}{d\tau} \hat{\sigma}_{LO}(Q^2 = \tau s), \quad (4.35)$$

where $\mathcal{L}^{q\bar{q}}$ is the parton luminosity and $\tau_0 = 4m_{H^{\pm\pm}}^2/s$ (s is the total energy squared at the LHC). The cross section for pair-production, including Next-to-leading order (NLO) corrections, has been evaluated in Ref. [236].

Depending on mass parameters in the model, the doubly charged Higgs boson can decay into lepton pairs, including vector leptons, W^\pm pairs, or $H^\pm W^\pm$ states. In the Higgs triplet model, the decay rate for $H^{\pm\pm}$ into leptons is

$$\Gamma(H^{\pm\pm} \rightarrow l_i^\pm l_j^\pm) = S_{ij} |h_{ij}|^2 \frac{m_{H^{\pm\pm}}}{4\pi} \left(1 - \frac{m_i^2}{m_{H^{\pm\pm}}^2} - \frac{m_j^2}{m_{H^{\pm\pm}}^2} \right) \left[\lambda \left(\frac{m_i^2}{m_{H^{\pm\pm}}^2}, \frac{m_j^2}{m_{H^{\pm\pm}}^2} \right) \right]^2, \quad (4.36)$$

where m_i is the mass of the i th lepton ($i = e, \mu$ or τ) and $S_{ij} = 1(1/2)$ for $i \neq j$, ($i = j$). Similarly the decay rate of $H^{\pm\pm}$ into fourth generation vector-like leptons is, if kinematically allowed

$$\Gamma(H^{\pm\pm} \rightarrow E_i^\pm E_j^\pm) = S_{ij} \left[|h'_{E_i E_j}|^2 + |h''_{E_i E_j}|^2 \right] \frac{m_{H^{\pm\pm}}}{4\pi} \left(1 - \frac{m_{E_i}^2}{m_{H^{\pm\pm}}^2} - \frac{m_{E_j}^2}{m_{H^{\pm\pm}}^2} \right) \left[\lambda \left(\frac{m_{E_i}^2}{m_{H^{\pm\pm}}^2}, \frac{m_{E_j}^2}{m_{H^{\pm\pm}}^2} \right) \right]^2, \quad (4.37)$$

with M_{E_i} the mass eigenvalue from Eq. (6.13). In addition, we include the decay rates of $H^{\pm\pm}$ into $W^\pm W^\pm$ and $W^\pm H^\pm$:

$$\Gamma(H^{\pm\pm} \rightarrow W^\pm W^\pm) = \frac{g^4 v_\Delta^2 m_{H^{\pm\pm}}^3}{64\pi m_W^4} \left(1 - \frac{4m_W^2}{m_{H^{\pm\pm}}^2} + \frac{12m_W^4}{m_{H^{\pm\pm}}^4} \right) \beta \left(\frac{m_W^2}{m_{H^{\pm\pm}}^2} \right) \quad (4.38)$$

$$\Gamma(H^{\pm\pm} \rightarrow W^\pm H^\pm) = \frac{g^2 m_{H^{\pm\pm}}^3}{16\pi m_W^2} \cos^2 \beta_\pm \left[\lambda \left(\frac{m_W^2}{m_{H^{\pm\pm}}^2}, \frac{m_{H^\pm}^2}{m_{H^{\pm\pm}}^2} \right) \right]^{3/2}, \quad (4.39)$$

where $\cos \beta_{\pm} \simeq 1$ is the mixing angle in the singly charged Higgs sector and

$$\beta(x) = \sqrt{1 - 4x}, \quad \lambda(x, y) = 1 + x^2 + y^2 - 2xy - 2x - 2y. \quad (4.40)$$

We investigate the branching ratios of $H^{\pm\pm}$ in two distinct parameter regions:

- Condition 1: when $H^{\pm\pm} \rightarrow W^{\pm}H^{\pm}$ is not kinematically allowed, $H^{\pm\pm}$ decays into leptons and W^{\pm} pairs only:

$$BR(X_i^{\pm}X_j^{\pm}) = \frac{\Gamma(H^{\pm\pm} \rightarrow X_i^{\pm}X_j^{\pm})}{\Gamma_1(H^{\pm\pm})}, \quad \text{where } X_i = l_i^{\pm}, E_i^{\pm}, W^{\pm}, \quad (4.41)$$

with the total width for Condition 1 being

$$\Gamma_1(H^{\pm\pm}) = \Gamma(H^{\pm\pm} \rightarrow l_i^{\pm}l_j^{\pm}) + \Gamma(H^{\pm\pm} \rightarrow E_i^{\pm}E_j^{\pm}) + \Gamma(H^{\pm\pm} \rightarrow W^{\pm}W^{\pm}).$$

- Condition 2: when $H^{\pm\pm} \rightarrow W^{\pm}H^{\pm}$ is kinematically allowed,³ $H^{\pm\pm}$ is able to decay into charged Higgs and gauge bosons as well,

$$\begin{aligned} BR(X_i^{\pm}X_j^{\pm}) &= \frac{\Gamma(H^{\pm\pm} \rightarrow X_i^{\pm}X_j^{\pm})}{\Gamma_2(H^{\pm\pm})} \quad \text{where } X_i = l_i^{\pm}, E_i^{\pm}, W^{\pm}, \quad \text{and} \\ BR(W^{\pm}H^{\pm}) &= \frac{\Gamma(H^{\pm\pm} \rightarrow H^{\pm}W^{\pm})}{\Gamma_2(H^{\pm\pm})}, \end{aligned} \quad (4.42)$$

with the total decay width for Condition 2 being

$$\Gamma_2(H^{\pm\pm}) = \Gamma(H^{\pm\pm} \rightarrow l_i^{\pm}l_j^{\pm}) + \Gamma(H^{\pm\pm} \rightarrow E_i^{\pm}E_j^{\pm}) + \Gamma(H^{\pm\pm} \rightarrow W^{\pm}W^{\pm}) + \Gamma(H^{\pm\pm} \rightarrow H^{\pm}W^{\pm}).$$

In what follows, we wish to analyze the decay patterns of $H^{\pm\pm}$ and present plots of the production cross section times the branching fractions for large regions of the allowed parameter space, for the LHC operating at both $\sqrt{s} = 7$ TeV (where analyses of the existing data still continue) and at $\sqrt{s} = 13$ TeV (the next energy frontier).⁴ To cover a wide range of parameter space, we distinguish two cases for each condition, depending on the vector-like lepton masses. We set the Yukawa coupling of the vector-like leptons with the doublet Higgs bosons to be $h'_E = h''_E = 0.8$ for both cases, and impose symmetry condition 3, that is, we only disallow mixing of vector-like and ordinary leptons:

- Case A corresponds to very light vector-like leptons: $M_E = M_L = 205$ GeV. For this case we obtain for the mass eigenvalues, $M_{E_1} = 344.2$ GeV, $M_{E_2} = 65.8$ GeV, the latter of which is close to the allowed minimum.

³In this version of the HTM, the doubly charged Higgs boson is always heavier than the singly charged one [1].

⁴Cross section and branching ratios at $\sqrt{s} = 8$ TeV and 14 TeV are practically indistinguishable from those at 7 TeV and 13 TeV, respectively

- Case B corresponds to intermediate-mass vector leptons: $M_E = 400$ GeV, $M_L = 300$ GeV. For this case we obtain for the mass eigenvalues, $M_{E_1} = 498$ GeV, $M_{E_2} = 202$ GeV.

In Fig. 4.5 we show plots corresponding to Condition 1 (when the decay $H^{\pm\pm} \rightarrow W^\pm H^\pm$ is not kinematically allowed), with Case A in the top row and Case B in the bottom row. We plot $R_{XY} = \sigma(pp \rightarrow H^{\pm\pm} H^{\mp\mp}) \times BR(H^{\pm\pm} \rightarrow XY)$ with X, Y as specified in the attached panels, as functions of the doubly charged masses. In evaluating the cross sections we have included the NLO correction factor $K \simeq 1.25$, as calculated in Ref. [236]. On the left and right sides of the figure we show the results for $\sqrt{s} = 7$ TeV and $\sqrt{s} = 13$ TeV, respectively. We set $h'_{EE} = h''_{EE} = 0.1$ and $h_{ij} = 0.01$ throughout. Similar graphs would be obtained with smaller values of h'_{EE} and h''_{EE} , but the values of R_{EE} would be correspondingly reduced. We have chosen to investigate the cross section times branching ratios for intermediate to high values of the doubly charged Higgs mass (400-1200 GeV), as in this region the decay into vector leptons becomes relevant. If the masses of the vector leptons are low, the doubly charged Higgs boson decays significantly into them; in particular, the decay into the two lightest vector leptons E_2 becomes dominant, and can reach 80-90% when kinematically allowed (in the $m_{H^{\pm\pm}} > 200$ GeV region for $M_{E_2} = 65.8$ GeV, Case A) and overwhelms the other decay modes, which are now below 5%. The branching ratio into $W^\pm W^\mp$ is important for doubly charged masses below the threshold for pair production of vector leptons $m_{H^{\pm\pm}} < 400$ GeV, and becomes negligible for $m_{H^{\pm\pm}} > 700$ GeV.

The difference between the figures at $\sqrt{s} = 7$ TeV and $\sqrt{s} = 13$ TeV is in the total cross section for pair production of doubly charged bosons, which is expected to be $\simeq 1.5$ fb at $\sqrt{s} = 7$ TeV and $\simeq 8$ fb at $\sqrt{s} = 13$ TeV (for $m_{H^{\pm\pm}} = 400$ GeV). The integrated luminosity was taken to be $\mathcal{L} = 10 \text{ fb}^{-1}$ [128].

The difference between Case A and Case B in this figure are threshold effects. For Case B, $m_{H^{\pm\pm}} > 400$ GeV for decay into pairs of E_2 states, as $M_{E_2} = 202$ GeV; otherwise the branching ratios are the same. Had we chosen smaller doubly charged Higgs couplings with vector leptons, $h'_{EE} \simeq 0.01$, the branching ratios into ordinary leptons, vector leptons, and W^\pm pairs would become comparable for $m_{H^{\pm\pm}} \geq 600$ GeV.

In Fig. 4.6 we plot the same quantities for Condition 2 (when $H^{\pm\pm} \rightarrow W^\pm H^\pm$ is kinematically allowed), with Case A in the top row and Case B in the bottom row, for $\sqrt{s} = 7$ TeV on the left-hand side and $\sqrt{s} = 13$ TeV on the right-hand side. The decay pattern is very different here, and it is dominated by the decay $H^{\pm\pm} \rightarrow W^\pm H^\pm$. For a vector lepton coupling to the

doubly charged Higgs set to $h'_{EE} = h''_{EE} = 0.1$, the decay into $H^\pm W^\pm$ dominates throughout the parameter space where it is kinematically allowed and can reach a branching fraction of over 90%, while the decay into vector leptons can have branching ratios of up to 25%. Again, the decay rates into W^\pm boson pairs and ordinary leptons are below 1%, and the only difference between Case A and Case B are, as in Fig. 4.5, threshold effects. The dominance of the decay mode $H^{\pm\pm} \rightarrow W^\pm H^\pm$ persists, and is even more evident for smaller couplings with vector leptons, $h'_{EE} \simeq 0.01$.

4.5 Conclusions

An extension of the SM via additional vector-like leptons is not ruled out experimentally, and has been shown to provide a dark matter candidate. In models beyond the SM, the vector-like leptons can alter not only the phenomenology of the Higgs, but also that of other additional particle representations predicted by the models. We provide an example within the Higgs Triplet Model, where we showed that, in the absence of triplet-doublet Higgs mixing in the neutral sector ($\sin \alpha = 0$), there is no enhancement of the rate of decay of $h \rightarrow \gamma\gamma$ in this model with respect to the SM expectation.

Introducing vector-like leptons does not affect any of the tree-level decays or the production of the neutral Higgs boson observed at the LHC. However, loop decays into electroweak particles, such as $h \rightarrow Z\gamma$ and $h \rightarrow \gamma\gamma$ would be affected. We show that, for the no-mixing scenario ($\sin \alpha = 0$) the decay rates into $\gamma\gamma$ and $Z\gamma$ do not depend on the doubly charged Higgs mass, and thus without the additional vector-like leptons, these decays would be unchanged from the SM expectations. With vector-like leptons modest enhancements or suppressions are possible, most notably for $h \rightarrow \gamma\gamma$, where for large Yukawa couplings the rate of decays could even double. Under the same circumstances, the decay width for $h \rightarrow Z\gamma$ remains practically unchanged from its SM value. The model thus presents a mechanism for enhancing one loop-decay and not the other, which seems to be consistent with the LHC data (so far).

If $\sin \alpha \neq 0$, the effect of the doubly charged Higgs bosons is felt for both $h \rightarrow \gamma\gamma$ and $h \rightarrow Z\gamma$, most spectacularly so for very light $m_{H^{\pm\pm}} = 150$ GeV, which is ruled out for $\sin \alpha \neq 0$. Parameter-space regions where light doubly charged Higgs masses (200-250 GeV), *and* significant mixing in the neutral sector coexist are disfavored. In general, there are many parameter combinations for which the decay $h \rightarrow \gamma\gamma$ is enhanced, but few for an enhanced $h \rightarrow Z\gamma$, and these regions are ruled out by the branching ratio for $h \rightarrow \gamma\gamma$. However, if

the decay $h \rightarrow \gamma\gamma$ is (modestly) enhanced, while $h \rightarrow Z\gamma$ is the same as the SM prediction to 1σ , small mixing angles and light doubly charged Higgs bosons $m_{H^{\pm\pm}} \lesssim 300$ GeV are preferred. The fact that there are no regions of the parameter space consistent with present measurements of the signal strength for $h \rightarrow \gamma\gamma$ and an enhanced rate for $h \rightarrow Z\gamma$ is a feature of this model, valid over the whole explored range of the parameter space. Other than this, there are no definite correlations or anticorrelations between these two loop-dominated decays.

The intermediate mass doubly charged Higgs boson can decay into light vector-like leptons, which would alter its decay profile significantly. We explored this possibility and found that, if the singly charged Higgs mass is such that the decay $H^{\pm\pm} \rightarrow W^\pm H^\pm$ is not kinematically accessible, dominant branching ratios into vector leptons, if kinematically accessible, are expected for triplet Yukawa couplings $h'_{EE} = 0.1$. If and where the decay $H^{\pm\pm} \rightarrow W^\pm H^\pm$ is kinematically accessible, its corresponding branching ratio is the largest, while the branching fraction into vector-like leptons could reach 20-25% for $h'_{EE} = 0.1$. Under both these circumstances, the decay patterns of the doubly charged Higgs bosons are changed, raising the hope that they can be found at masses around 200-600 GeV. The analyses presented here show that the cross section times branching ratios into vector-like leptons is significant enough to considerably alter the decay patterns of the doubly charged boson, and at $\sqrt{s} = 13$ TeV these decay modes would be observable at the LHC—with cross sections times branching ratios of the order of several femtobarns (fb)—and may be a promising way to discover vector-like leptons.

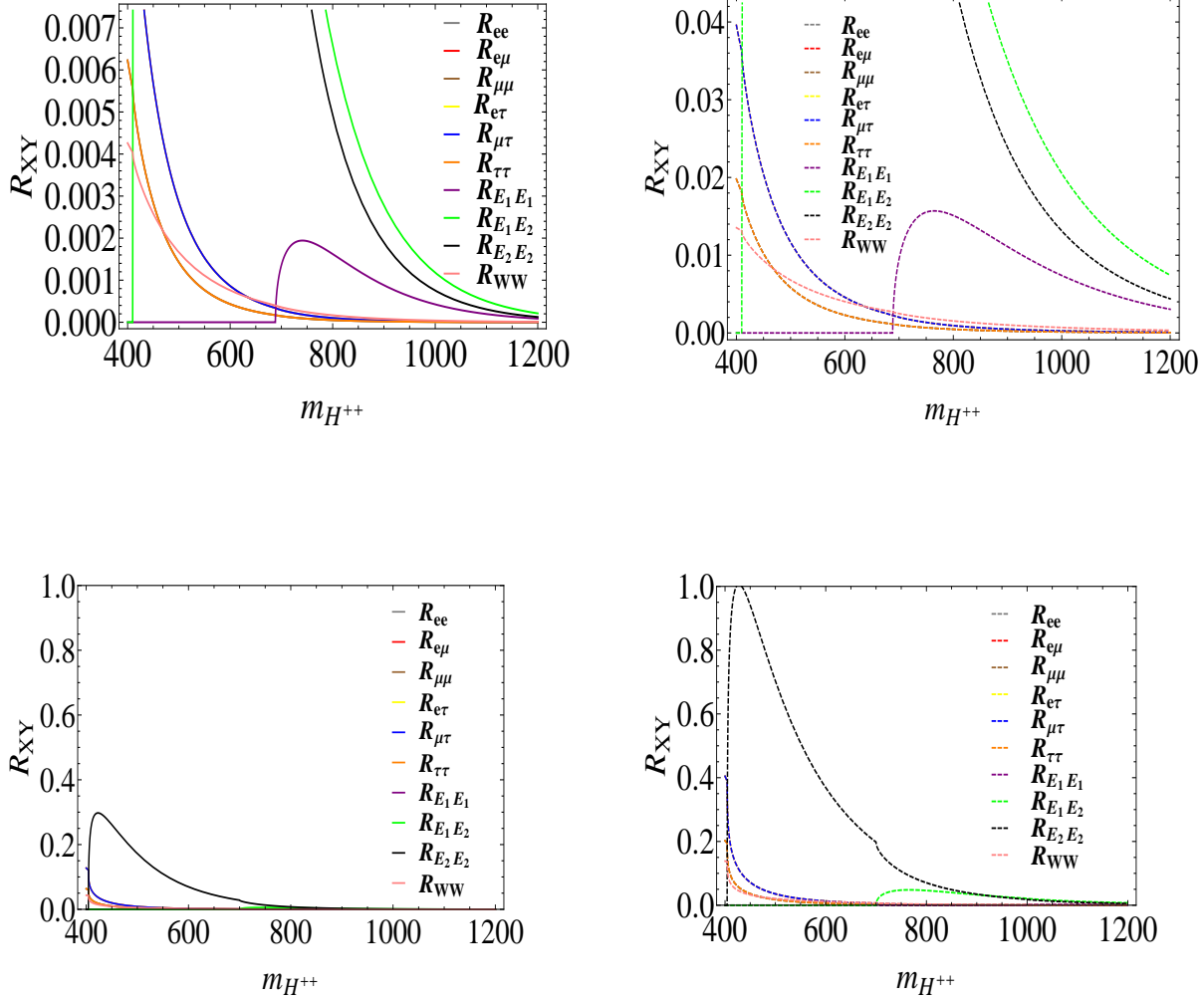


Figure 4.5: $R_{XY} = \sigma(pp \rightarrow H^{\pm\pm}H^{\mp\mp}) \times BR(H^{\pm\pm} \rightarrow XY)$, in fb, as a function of doubly charged Higgs boson mass at $\sqrt{s} = 7$ TeV (left panel) and $\sqrt{s} = 13$ TeV (right panel), for Condition 1 (when $H^{\pm\pm} \rightarrow W^{\pm}H^{\pm}$ is not kinematically allowed). The upper and lower panels depict the values for Case A and Case B, respectively. Cross sections include the QCD NLO correction factor $K \sim 1.25$. Throughout we take $h'_{EE} = h''_{EE} = 0.1$ and $h_{ij} = 0.01$.

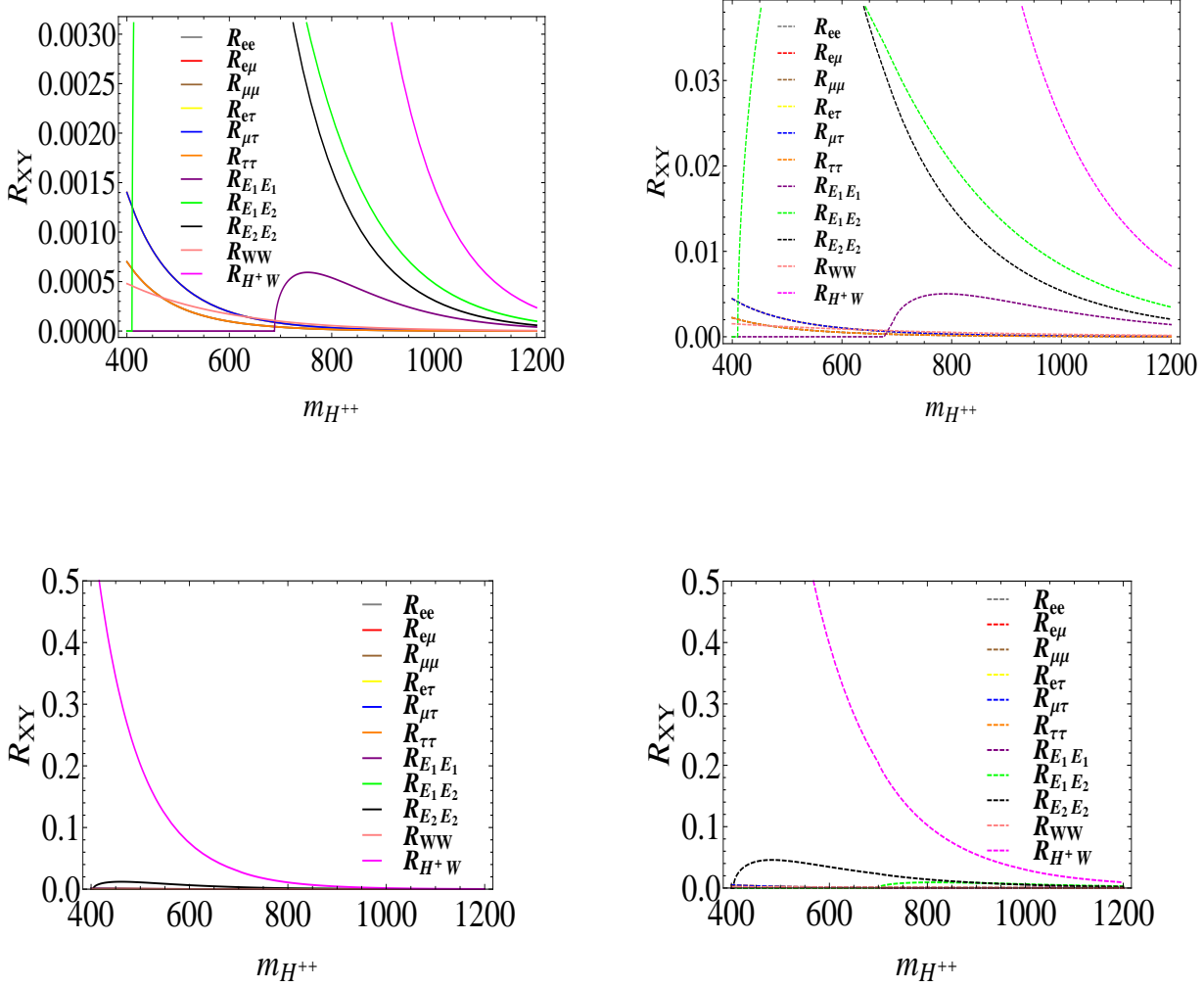


Figure 4.6: Same as Fig 4.5, but for Condition 2 (when $H^{\pm\pm} \rightarrow W^\pm H^\pm$ is kinematically allowed).

Chapter 5

Vector-like Quarks in the Higgs Triplet Model

Abstract

We analyze the effects of introducing vector-like quarks in the HTM. In this scenario, the model contains, in addition to the SM particle content, one triplet Higgs representation, and a variety of vector-like quark states, including singlet, doublet, and triplet states. We investigate the electroweak precision variables and impose restrictions on model parameters. We show that, for some representations, introducing vector-like quarks significantly alters the constraints on the mass of the doubly charged Higgs boson, bringing it in closer agreement with present experimental constraints. We also study the effects of introducing the vector-like quarks on neutral Higgs phenomenology, in particular on the loop-dominated decays $H \rightarrow \gamma\gamma$ and $H \rightarrow Z\gamma$, and the restrictions they impose on the parameter space.

5.1 Introduction

The Standard Model (SM) of particle physics has received a big boost of confidence from the LHC Higgs data [29, 154], as the discovery of the Higgs boson completes the model and as the model appears so far to satisfy most, if not all, experimental constraints. Yet the SM fails to answer some fundamental questions, from both the theoretical and the experimental sides. Extensions of the SM resolve some of these questions, and while their predictions can overlap with the SM for phenomena where SM fits the experimental data, they can also resolve some

conflicts of the SM with the data where such discrepancies exist. For instance, supplementing the SM by an additional complex Higgs triplet representation resolves naturally the origin of the neutrino mass [120–122, 237] and the existence of dark matter [238–241], and provides an explanation for the excess in the Higgs decay into two photons [1].

In addition to scalar fields, the SM can be extended by additional fermionic particles. Some of the simplest extensions would include an additional pair of chiral fermions, mimicking the already-existing fermion representations. However such models are all but ruled out by the Higgs data. An exception to this may be provided by including such additional representations in the Higgs Triplet Model (HTM) with nontrivial mixing between the neutral CP-even Higgs states [242], but even there the parameter space is under significant pressure and may be ruled out by data from the LHC operating at 13 TeV. The addition of nonchiral fermionic representations, such as vector-like quarks and/or vector-like leptons, is much less constrained. Vector-like fermions, which decay into SM fermions and a gauge boson or a Higgs particle, are predicted by extra-dimensional models [243], little Higgs models [181, 184, 244], heterotic string and string D-brane theories [245, 246] and by some composite Higgs models [176, 247, 248]. Vector-like fermions do not acquire mass through Yukawa couplings, they only affect the loop-dominated Higgs decay, and they may provide a better fit to the LHC Higgs data [249]. A great deal of literature is dedicated to analyses of vector fermions in the SM [170, 194, 250–254], as well as in model-independent scenarios [255, 256].

In general, fewer studies involve introducing vector fermions into specific non-SM models. Supplementing these models by additional vector fermion states can alleviate some of the restrictions on the parameters in these scenarios. For instance, adding vector leptons in the two Higgs doublet model [211] alleviates electroweak precision constraints. In supersymmetry, vector leptons can improve vacuum stability and enhance the Higgs-to-diphoton rate by as much as 50% [212].

In Chapter 4 we showed that, if light enough, vector-like leptons introduced into the Higgs triplet Model modify *both* the decay rates of the neutral Higgs boson into two photons, *and* the decay patterns and branching ratios of the doubly charged Higgs bosons. In this chapter, we extend our study to a carefully general consideration of the theoretical and phenomenological implications of additional vector-like quark states in the HTM. The effects of the vector-like quarks in the Higgs Triplet Model on the Higgs decays have been investigated before in Ref. [139], where the authors showed that for some values of the couplings between the Higgs boson and the vector-like quarks, the decay $H \rightarrow \gamma\gamma$ can be enhanced. Our approach

here is very different than theirs. We specify the possible hypercharge assignments for the new quarks and then allow their masses and couplings to be free parameters. We study cases in which vector-like states couple to the gauge fields and mix weakly with SM quarks of the third generation only, to avoid flavor violation problems. We investigate the precision electroweak constraints due to their presence in the HTM and the impact of vector-like states on the Higgs branching fractions, particularly into two photons and into $Z\gamma$. Unlike vector-like leptons, vector-like quarks affect *both* the production cross section and the decay rates of the Higgs bosons. We present numerical results which restrict the masses and mixings of the new vector-like quarks and which have implications for future vector-like fermion searches. We also revisit the implications of their inclusion for doubly charged Higgs states.

This chapter is organized as follows. In the next section Sec. 5.2 we summarize the basics features of the Higgs triplet Model without (in 5.2.1) and with (in 5.2.2) vector-like quarks. We define the representations, as well as masses and mixing parameters. We proceed by examining the electroweak precision constraints in Sec. 5.3 in the HTM, again without (5.3.1) and with (5.3.2) vector-like quarks. In the same section, we present a numerical analysis on the restrictions coming from the oblique parameters on the masses of the doubly charged Higgs bosons, and on the masses and mixing parameters with third generation quarks for the vector-like quarks, in 5.3.3. These restrictions are then applied to evaluation of the relative (with respect to the SM) branching ratios for $H \rightarrow \gamma\gamma$ and $H \rightarrow Z\gamma$ in Sec. 5.4. Some definition of our parameters are included in the Appendix 5.5.

5.2 The Model

5.2.1 Higgs Triplet Model

The HTM has been studied extensively in [130–132, 134, 220]. The symmetry group is the same as that in the SM, $SU(2)_L \times U(1)_Y$, but one triplet field Δ with hypercharge $Y = 1$ is added to the SM Higgs sector, which already contains one isospin doublet field Φ with hypercharge $Y = 1/2$. The Higgs fields are given by:

$$\Phi = \begin{bmatrix} \varphi^+ \\ \frac{1}{\sqrt{2}}(\varphi + v_\Phi + i\chi) \end{bmatrix}, \quad \Delta = \begin{bmatrix} \frac{\Delta^+}{\sqrt{2}} & \Delta^{++} \\ \frac{1}{\sqrt{2}}(\delta + v_\Delta + i\eta) & -\frac{\Delta^+}{\sqrt{2}} \end{bmatrix}, \quad (5.1)$$

where v_Φ and v_Δ are the VEVs of the doublet Higgs field and the triplet Higgs field, with $v^2 \equiv v_\Phi^2 + 2v_\Delta^2 \simeq (246 \text{ GeV})^2$. The Higgs potential involving the doublet Φ and triplet Δ

is

$$\begin{aligned}
V(\Phi, \Delta) &= m^2 \Phi^\dagger \Phi + M_t^2 \text{Tr}(\Delta^\dagger \Delta) + [\mu \Phi^T i \tau_2 \Delta^\dagger \Phi + \text{h.c.}] + \lambda_1 (\Phi^\dagger \Phi)^2 \\
&+ \lambda_2 [\text{Tr}(\Delta^\dagger \Delta)]^2 + \lambda_3 \text{Tr}[(\Delta^\dagger \Delta)^2] + \lambda_4 (\Phi^\dagger \Phi) \text{Tr}(\Delta^\dagger \Delta) + \lambda_5 \Phi^\dagger \Delta \Delta^\dagger \Phi, \quad (5.2)
\end{aligned}$$

with parameters (all assumed real), m and M_t the Higgs bare masses, μ the lepton-number violating parameter, and λ_1 - λ_5 , the Higgs coupling constants. The scalar potential in Eq. (6.5) induces mixing among the physical states for the singly charged, the CP-odd, and the CP-even neutral scalar sectors, respectively:

$$\begin{aligned}
\begin{pmatrix} \varphi^\pm \\ \Delta^\pm \end{pmatrix} &= \begin{pmatrix} \cos \beta_\pm & -\sin \beta_\pm \\ \sin \beta_\pm & \cos \beta_\pm \end{pmatrix} \begin{pmatrix} w^\pm \\ H^\pm \end{pmatrix}, & \begin{pmatrix} \chi \\ \eta \end{pmatrix} &= \begin{pmatrix} \cos \beta_0 & -\sin \beta_0 \\ \sin \beta_0 & \cos \beta_0 \end{pmatrix} \begin{pmatrix} z \\ A \end{pmatrix}, \\
\begin{pmatrix} \varphi \\ \delta \end{pmatrix} &= \begin{pmatrix} \cos \alpha & -\sin \alpha \\ \sin \alpha & \cos \alpha \end{pmatrix} \begin{pmatrix} h \\ H \end{pmatrix}, \quad (5.3)
\end{aligned}$$

with mixing angles given by

$$\begin{aligned}
\tan \beta_\pm &= \frac{\sqrt{2}v_\Delta}{v_\Phi}, & \tan \beta_0 &= \frac{2v_\Delta}{v_\Phi}, \\
\tan 2\alpha &= \frac{v_\Delta}{v_\Phi} \frac{2v_\Phi^2(\lambda_4 + \lambda_5) - 4M_\Delta^2}{2v_\Phi^2\lambda_1 - M_\Delta^2 - 2v_\Delta^2(\lambda_2 + \lambda_3)}. \quad (5.4)
\end{aligned}$$

The CP-even Higgs states which mix with the angle α are given, in terms of the couplings in the scalar potential, by

$$m_h^2 = 2v_\Phi^2 \lambda_1 \cos^2 \alpha + [M_\Delta^2 + 2v_\Delta^2(\lambda_2 + \lambda_3)] \sin^2 \alpha + \left[\frac{2v_\Delta}{v_\Phi} M_\Delta^2 - v_\Phi v_\Delta (\lambda_4 + \lambda_5) \right] \sin 2\alpha, \quad (5.5)$$

$$m_H^2 = 2v_\Phi^2 \lambda_1 \sin^2 \alpha + [M_\Delta^2 + 2v_\Delta^2(\lambda_2 + \lambda_3)] \cos^2 \alpha - \left[\frac{2v_\Delta}{v_\Phi} M_\Delta^2 - v_\Phi v_\Delta (\lambda_4 + \lambda_5) \right] \sin 2\alpha, \quad (5.6)$$

where we defined $M_\Delta^2 \equiv \frac{v_\Phi^2 \mu}{\sqrt{2}v_\Delta}$. Note that, while the mixing angles in the charged and CP-odd sectors are constrained to be small by the hierarchy of the VEVs, the same is not necessarily the case for α . In fact, as we have previously shown, if and only if α is allowed to be nonzero, yielding significant mixing in the CP-even neutral sector, the decay of one of the neutral Higgs bosons into two photons can be enhanced [1]. The parameters of the model are restricted by the values of the W and Z masses and the electroweak ρ parameter, defined at

tree level

$$\begin{aligned}
 m_W^2 &= \frac{g^2}{4}(v_\Phi^2 + 2v_\Delta^2), & m_Z^2 &= \frac{g^2}{4\cos^2\theta_W}(v_\Phi^2 + 4v_\Delta^2), \\
 \rho &\equiv \frac{m_W^2}{m_Z^2\cos^2\theta_W} = \frac{1 + \frac{2v_\Delta^2}{v_\Phi^2}}{1 + \frac{4v_\Delta^2}{v_\Phi^2}}, & & (5.7)
 \end{aligned}$$

insuring the smallness of v_Δ/v_Φ . The parameters of the model are further restricted by the smallness of the Majorana neutrino masses, proportional to the lepton number violating coupling constant μ

$$(m_\nu)_{ij} = \sqrt{2}h_{ij}v_\Delta = h_{ij}\frac{\mu v_\Phi^2}{M_\Delta^2}, \quad (5.8)$$

requiring $\mu \ll M_\Delta$ for the smallness of the neutrino masses to be explained by the type II seesaw mechanism.

In Ref. [4] has been shown that introducing vector-like leptons in the model can significantly alter the decay patterns of the doubly charged Higgs bosons and thus modify the experimental bounds on their masses. We adopt here the same model parameters, and allow $\sin\alpha$ to vary, set $m_h = 125$ GeV and $m_H = 98$ GeV. We proceed by introducing vector-like quarks and study their effects in the HTM.

5.2.2 Higgs Triplet Model with Vector-Like Quarks

In considering addition of vector-like leptons to the Higgs Triplet Model in Ref. [4], the representations considered included $SU(2)_L$ lepton doublets, right-handed charged and neutral vector singlets and their mirror images. Our assumption was that the vector-like leptons can be light, and then introduced a parity symmetry which forbade mixing between the new vector-like fields (odd under this symmetry) and the ordinary leptons (even under the same symmetry). This insured that flavor, stringently constrained in ordinary lepton decays, was not violated.

Introduction of vector-like quarks imposes different constraints on the HTM, and thus the scenarios presented here would be qualitatively different from those introduced in Ref. [4]. First, vector-like quarks affect both the production and decay of the Higgs bosons at the LHC. Second, flavor violation is less constrained in the quark sector, allowing the new vector-like states to mix weakly with the third family of ordinary quarks. In this subsection we introduce vector-like quarks into the model, and in the next section we study their effects. We first classify the vector-like quarks in terms of multiplets of $SU(2)_L \times U(1)_Y$, then proceed

by writing gauge invariant interactions for each. The new states interact with the Higgs states through Yukawa interactions. The allowed multiplet states for the vector-like quarks, together with their nomenclature, are listed in Table 5.1 [170, 194, 250–254]. The first two representations are U -like and D -like singlets, the next three are doublets (one SM-like, two non-SM like), and the last two are triplets. The various representations are distinguished by their $SU(2)_L$ and hypercharge quantum numbers.

Table 5.1: Representations of vector-like quarks, with quantum numbers under $SU(2)_L \times U(1)_Y$.

Name	\mathcal{U}_1	\mathcal{D}_1	\mathcal{D}_2	\mathcal{D}_X	\mathcal{D}_Y	\mathcal{T}_X	\mathcal{T}_Y
Type	Singlet	Singlet	Doublet	Doublet	Doublet	Triplet	Triplet
	T	B	$\begin{pmatrix} T \\ B \end{pmatrix}$	$\begin{pmatrix} X \\ T \end{pmatrix}$	$\begin{pmatrix} B \\ Y \end{pmatrix}$	$\begin{pmatrix} X \\ T \\ B \end{pmatrix}$	$\begin{pmatrix} T \\ B \\ Y \end{pmatrix}$
$SU(2)_L$	1	1	2	2	2	3	3
Y	2/3	-1/3	1/6	7/6	-5/6	2/3	-1/3

In these representations, Yukawa and the relevant interaction terms between the vector-like quarks and SM quarks are [257]

$$\begin{aligned}
\mathcal{L}_{SM} &= -y_u \bar{q}_L H^c u_R - y_d \bar{q}_L H d_R, \\
\mathcal{L}_{\mathcal{U}_1, \mathcal{D}_1} &= -\lambda_u \bar{q}_L H^c U_{1R} - \lambda_d \bar{q}_L H D_{1R} - M \bar{U}_L U_R - M \bar{D}_L D_R, \\
\mathcal{L}_{\mathcal{D}_2} &= -\lambda_u \bar{D}_{2L} H^c u_R - \lambda_d \bar{D}_{2L} H d_R - M \bar{D}_{2L} D_{2R}, \\
\mathcal{L}_{\mathcal{D}_X, \mathcal{D}_Y} &= -\lambda_u \bar{D}_{XL} H u_R - \lambda_d \bar{D}_{YL} H^c d_R - M \bar{D}_{XL} D_{XR} - M \bar{D}_{YL} D_{YR}, \\
\mathcal{L}_{\mathcal{T}_X, \mathcal{T}_Y} &= -\lambda_u \bar{q}_L \tau^a H^c \mathcal{T}_{XR}^a - \lambda_d \bar{q}_L \tau^a H \mathcal{T}_{YR}^a - M \bar{\mathcal{T}}_{XL} \mathcal{T}_{XR} - M \bar{\mathcal{T}}_{YL} \mathcal{T}_{YR}. \tag{5.9}
\end{aligned}$$

After the spontaneous symmetry breaking, the Yukawa interactions generate mixing between the SM quarks and the vector-like quarks at tree level. The singlet vector-like quark and the triplet vector-like quark exhibit similar mixing patterns, while the doublet vector-like quark has a different mixing pattern [257]. To avoid conflicts with low energy experimental data, we consider that the vector-like quarks mix with the third generation of SM quarks only.

The mass matrix for the mixing between m_t and m_T can be diagonalized by two mixing matrices:

$$V_L^u = \begin{pmatrix} \cos \theta_L^u & \sin \theta_L^u \\ -\sin \theta_L^u & \cos \theta_L^u \end{pmatrix}, \quad V_R^u = \begin{pmatrix} \cos \theta_R^u & \sin \theta_R^u \\ -\sin \theta_R^u & \cos \theta_R^u \end{pmatrix}, \tag{5.10}$$

for the singlet or triplet vector-like quark, such that

$$\begin{pmatrix} \cos \theta_L^u & -\sin \theta_L^u \\ \sin \theta_L^u & \cos \theta_L^u \end{pmatrix} \begin{pmatrix} \frac{y_u v}{\sqrt{2}} & x_t \\ 0 & M \end{pmatrix} \begin{pmatrix} \cos \theta_R^u & \sin \theta_R^u \\ -\sin \theta_R^u & \cos \theta_R^u \end{pmatrix} = \begin{pmatrix} m_t & 0 \\ 0 & m_T \end{pmatrix}, \quad (5.11)$$

where $m_T \geq M \geq m_t$. Similar relations hold for m_b and m_B . The relations between the tree-level input parameters and the mixing angles and masses are given by [258]:

$$\begin{aligned} \frac{y_u^2 v^2}{2} &= m_t^2 \left(1 + \frac{x_t^2}{M^2 - m_t^2} \right) \\ m_T^2 &= M^2 \left(1 + \frac{x_t^2}{M^2 - m_t^2} \right), \\ \sin \theta_L^{u,d} &= \frac{M x_{t(b)}}{\sqrt{(M^2 - m_{t(b)}^2)^2 + M^2 x_{t(b)}^2}} \\ \sin \theta_R^{u,d} &= \frac{m_{t(b)} x_{t(b)}}{\sqrt{(M^2 - m_{t(b)}^2)^2 + M^2 x_{t(b)}^2}}, \end{aligned} \quad (5.12)$$

where $x_t = \frac{\lambda_u v}{\sqrt{2}}$ and $x_b = \frac{\lambda_d v}{\sqrt{2}}$. For the case of doublets, the diagonalization can be carried out in a similar way:

$$\begin{pmatrix} \cos \theta_L^u & -\sin \theta_L^u \\ \sin \theta_L^u & \cos \theta_L^u \end{pmatrix} \begin{pmatrix} \frac{y_u v}{\sqrt{2}} & 0 \\ x & M \end{pmatrix} \begin{pmatrix} \cos \theta_R^u & \sin \theta_R^u \\ -\sin \theta_R^u & \cos \theta_R^u \end{pmatrix} = \begin{pmatrix} m_t & 0 \\ 0 & m_T \end{pmatrix}. \quad (5.13)$$

The relations between the parameters are the same, except that the formulas for the left- and right-handed mixing angles are interchanged:

$$\begin{aligned} \sin \theta_L^{u,d} &= \frac{m_{t(b)} x_{t(b)}}{\sqrt{(M^2 - m_{t(b)}^2)^2 + M^2 x_{t(b)}^2}}, \\ \sin \theta_R^{u,d} &= \frac{M x_{t(b)}}{\sqrt{(M^2 - m_{t(b)}^2)^2 + M^2 x_{t(b)}^2}}. \end{aligned} \quad (5.14)$$

We use the shorthand notations $s_L^{u,d} \equiv \sin \theta_L^{u,d}$ and $c_L^{u,d} \equiv \cos \theta_L^{u,d}$. Note that in the \mathcal{T}_X triplet model, the two mixing angles are related to each other by $x_b = \sqrt{2}x_t$. In the \mathcal{T}_Y model, for bottom sector $x_b = -x_t$ and for the top the same formulas as in other case apply, with $x_t \rightarrow \sqrt{2}x_t$ [257, 258]. All multiplets thus involve at least one mixing angle. These mixed states will be used to express interactions with the Higgs and gauge bosons and constrain those interactions. The mixing of a b quark with a heavy vector-like B quark modifies the $Zb\bar{b}$ coupling at the tree level, while the mixing between a t quark with a heavy vector-like T

modifies the $Wb\bar{t}$ vertex. We compute both of these, using analytical expressions. In the \mathcal{D}_1 model¹, the strongest tree level bound comes from correction to $Zb_L\bar{b}_L$ coupling:

$$\delta R_b = 2R_b(1 - R_b) \frac{\delta g_{ZbL}}{\delta g_{ZbL}^{SM}}, \quad (5.15)$$

where

$$\delta g_{ZbL}^{SM} = 1 - \frac{2}{3} \sin^2 \theta_W, \quad \delta g_{ZbL} = s_L^{d2}. \quad (5.16)$$

Here g_{ZbL}^{SM} is the Z -boson coupling to the left-handed b quark in the SM, R_b is defined as $\frac{\Gamma(Z \rightarrow b\bar{b})}{\Gamma(Z \rightarrow \text{hadrons})}$, with its SM value $R_b = 0.21578_{-0.0008}^{+0.0005}$ [257]. Electroweak measurements constraints for the deviation δR_b due to the new physics effects are $\delta R_b = 0.00051 \pm 0.00066$ [88], and experimental restrictions [259] are $[Zb\bar{b}]_{\text{exp}} = 0.21629 \pm 0.00066$. The relevant couplings for the models analyzed are included in the Appendix.

In the \mathcal{D}_X model, the tree level bound comes from the left-handed $Wb\bar{t}$ coupling:

$$\frac{\delta g_W}{\delta g_W^{SM}} = c_L^u - 1. \quad (5.17)$$

We allow a variation of $\pm 20\%$ [258]. Experimental searches for vector-like quarks have set mass limits on some of the representations. We summarize up-to-date restrictions in Table 5.2 below. Current experimental bounds depend critically on the details of the models and assumptions about branching ratios. However, the vector-like quarks could have escaped detection so far by prompt decays, and even relaxed limits on the mixing between top and vector-like top quarks can avoid the present experimental bounds [252]. In what follows we shall make conservative assumptions about the masses, but discuss possible consequences of having lighter masses.

5.3 Electroweak Constraints

The Peskin-Takeuchi parameters S , T and U [274] are commonly used to constrain and characterize new physics, as a means to comparing its predictions with the electroweak precision data. They can be calculated perturbatively in any model from the gauge boson propagator

¹These corrections are scenario dependent. More general formulas have appeared elsewhere [258].

Table 5.2: Current mass lower limits on vector-like quark masses in various representations.

Vector-like quark type	Mass Limits	Channel	Models
m_T	656 GeV [260, 261]	100% bW	$\mathcal{U}_1, \mathcal{D}_X, \mathcal{T}_X, \mathcal{T}_Y$
	625 GeV [262], 750 GeV [263]	100% tZ	$\mathcal{U}_1, \mathcal{D}_2, \mathcal{D}_X, \mathcal{T}_X, \mathcal{T}_Y$
	570 GeV [264], 740 GeV [265]	100% bW	$\mathcal{U}_1, \mathcal{D}_2, \mathcal{D}_X, \mathcal{T}_X, \mathcal{T}_Y$
	540-607 GeV [266], 850 GeV [267]	100% tH	$\mathcal{U}_1, \mathcal{D}_2, \mathcal{D}_X, \mathcal{T}_X, \mathcal{T}_Y$
	687-782 GeV [268], 540 GeV [269]	bW, tZ, tH	$\mathcal{U}_1, \mathcal{D}_2, \mathcal{D}_X, \mathcal{T}_X, \mathcal{T}_Y$
	640-790 GeV [267]	bW, tH	$\mathcal{U}_1, \mathcal{D}_2, \mathcal{D}_X, \mathcal{T}_X, \mathcal{T}_Y$
m_B	800 GeV [270], 720 GeV [269]	100% Wt	$\mathcal{D}_1, \mathcal{D}_2, \mathcal{D}_Y, \mathcal{T}_X, \mathcal{T}_Y$
	680-700 GeV [271], 645 GeV [272]	100% bZ	$\mathcal{D}_1, \mathcal{D}_2, \mathcal{D}_Y, \mathcal{T}_X, \mathcal{T}_Y$
	582-732 GeV [271], 590 GeV [269]	bZ, tW, bH	$\mathcal{D}_1, \mathcal{D}_2, \mathcal{D}_Y, \mathcal{T}_X, \mathcal{T}_Y$
m_X	770 GeV [273]	100% tW	$\mathcal{D}_X, \mathcal{T}_X$
m_Y	656 GeV [268]	100% bW	$\mathcal{D}_Y, \mathcal{T}_Y$

functions, and are defined as [275]:

$$\begin{aligned}
S &= 16\pi \text{Re} \left[\bar{\Pi}_{T,\gamma}^{3Q}(m_Z^2) - \bar{\Pi}_{T,Z}^{33}(0) \right], \\
T &= \frac{4\sqrt{2}G_F}{\alpha_e} \text{Re} \left[\bar{\Pi}_T^{33}(0) - \bar{\Pi}_T^{11}(0) \right], \\
U &= 16\pi \text{Re} \left[\bar{\Pi}_{T,Z}^{33}(0) - \bar{\Pi}_{T,W}^{11}(0) \right],
\end{aligned} \tag{5.18}$$

where the gauge boson two-point functions are defined as $\bar{\Pi}_{T,V}^{AB}(p^2) = \frac{\bar{\Pi}_T^{AB}(p^2) - \bar{\Pi}_T^{AB}(m_V^2)}{p^2 - m_V^2}$, and $\alpha_e \equiv \alpha_e(m_Z^2)$. The current experimental bounds defining $\Delta T = T - T_{\text{SM}}$, $\Delta S = S - S_{\text{SM}}$ and considering $\Delta U = 0$, are $\Delta S = 0.05 \pm 0.09$, $\Delta T = 0.08 \pm 0.07$ [134, 220]. In our considerations we allow for a more conservative deviation for the ΔT parameter between -0.2 and 0.4 [258].

5.3.1 Contributions to the S, T and U -parameters in the HTM

The explicit expressions for the S, T and U parameters for the HTM, including the extra Higgs representation, but without the vector-like quarks, are

$$\begin{aligned}
S_{HTM} &= 16\pi \text{Re} \left[\Pi_{HTM,\gamma}^{3Q}(m_Z^2) - \Pi_{HTM,Z}^{33}(0) \right], \\
T_{HTM} &= \frac{4\sqrt{2}G_F}{\alpha_e} \text{Re} \left[\Pi_{HTM}^{33}(0) - \Pi_{HTM}^{11}(0) \right], \\
U_{HTM} &= 16\pi \text{Re} \left[\Pi_{HTM,Z}^{33}(0) - \Pi_{HTM,W}^{11}(0) \right].
\end{aligned} \tag{5.19}$$

where $\Pi_{\text{HTM}}^{AB}(p^2)$ are the gauge boson two-point functions in the Higgs Triplet Model. The coupling factors are $\hat{g}_Z = \frac{\hat{g}}{\cos \theta_W}$, so

$$\begin{aligned}\Pi_{\text{HTM}}^{3Q}(p^2) &= \frac{\Pi^{Z\gamma}(p^2)}{\sin \theta_W \cos \theta_W \hat{g}_Z^2} + \frac{\Pi^{\gamma\gamma}(p^2)}{\cos^2 \theta_W \hat{g}_Z^2}, \\ \Pi_{\text{HTM}}^{33}(p^2) &= \frac{\Pi^{ZZ}(p^2)}{\hat{g}_Z^2} + \frac{2 \sin \theta_W \Pi^{Z\gamma}(p^2)}{\cos \theta_W \hat{g}_Z^2} + \frac{\sin^2 \theta_W \Pi^{\gamma\gamma}(p^2)}{\cos^2 \theta_W \hat{g}_Z^2}, \\ \Pi_{\text{HTM}}^{11}(p^2) &= \frac{1}{\cos^2 \theta_W \hat{g}_Z^2} \Pi_{\text{HTM}}^{WW},\end{aligned}\tag{5.20}$$

evaluated at physical momentum transfers scales $p^2 = 0, m_Z^2, m_W^2$.

In the HTM with and without vector-like quarks, the S parameter is far less restricted by the parameters of the model, and does not pose difficulties in any of the models listed in Table 5.1. While we shall plot the dependence of both S and T parameters on the variables of the HTM, we give the explicit results for the T parameter only.

The W -boson two-point function in the HTM is ² [134, 220] :

$$\begin{aligned}\Pi_{\text{HTM}}^{WW}(p^2) &= \frac{g^2}{16\pi^2} \left\{ g^2 \left[\left(\frac{v_\phi}{2} c_\alpha + v_\Delta s_\alpha \right)^2 B_0(p^2, m_h, m_W) + \left(-\frac{v_\phi}{2} s_\alpha + v_\Delta c_\alpha \right)^2 B_0(p^2, m_H, m_W) \right] \right. \\ &+ 2v_\Delta^2 B_0(p^2, m_{H^{\pm\pm}}, m_W) + \frac{c_{\beta_\pm}^2}{2c_W^2} v_\Delta^2 B_0(p^2, m_{H^\pm}, m_W) \\ &+ \frac{1}{c_W^2} \left[\frac{v_\phi}{2} s_W^2 c_{\beta_\pm} + \frac{v_\Delta}{\sqrt{2}} (1 + s_W^2) s_{\beta_\pm} \right]^2 B_0(p^2, m_Z, m_W) \left. + \frac{e^2}{4} (v_\phi^2 + 2v_\Delta^2) B_0(p^2, 0, m_W) \right. \\ &+ \frac{1}{4} \left[(c_\alpha s_{\beta_\pm} - \sqrt{2} s_\alpha c_{\beta_\pm})^2 B_5(p^2, m_{H^\pm}, m_h) + (c_\alpha c_{\beta_\pm} + \sqrt{2} s_\alpha s_{\beta_\pm})^2 B_5(p^2, m_W, m_h) \right. \\ &+ (s_\alpha s_{\beta_\pm} + \sqrt{2} c_\alpha c_{\beta_\pm})^2 B_5(p^2, m_{H^\pm}, m_H) + (s_\alpha c_{\beta_\pm} - \sqrt{2} c_\alpha s_{\beta_\pm})^2 B_5(p^2, m_W, m_H) \\ &+ (s_{\beta_0} s_{\beta_\pm} + \sqrt{2} c_{\beta_0} c_{\beta_\pm})^2 B_5(p^2, m_{H^\pm}, m_A) + (s_{\beta_0} c_{\beta_\pm} - \sqrt{2} c_{\beta_0} s_{\beta_\pm})^2 B_5(p^2, m_W, m_A) \\ &+ \left. \left. (-c_{\beta_0} s_{\beta_\pm} + \sqrt{2} s_{\beta_0} c_{\beta_\pm})^2 B_5(p^2, m_{H^\pm}, m_Z) + (c_{\beta_0} c_{\beta_\pm} + \sqrt{2} s_{\beta_0} s_{\beta_\pm})^2 B_5(p^2, m_W, m_Z) \right] \right. \\ &\left. + c_{\beta_\pm}^2 B_5(p^2, m_{H^{\pm\pm}}, m_{H^\pm}) + s_{\beta_\pm}^2 B_5(p^2, m_{H^{\pm\pm}}, m_W) \right\}.\end{aligned}\tag{5.21}$$

²In the models with only doublet fields and singlets, the electroweak rho parameter is predicted to be one at the tree level. However, since the HTM predicts $\rho \neq 1$, a new input parameter ($\sin^2 \theta_W$) has to be introduced in addition to the usual three input parameters such as (α_{em}, G_F, m_Z) to describe the electroweak parameters [134, 220].

The photon two-point function is calculated as:

$$\begin{aligned} \Pi_{\text{HTM}}^{\gamma\gamma}(p^2) &= \frac{e^2}{16\pi^2} \left[\frac{g^2}{2} (v_\phi^2 + 2v_\Delta^2) B_0(p^2, m_W, m_W) + 4B_5(p^2, m_{H^{\pm\pm}}, m_{H^{\pm\pm}}) \right. \\ &\quad \left. + B_5(p^2, m_{H^\pm}, m_{H^\pm}) + B_5(p^2, m_W, m_W) \right]. \end{aligned} \quad (5.22)$$

The Z -boson two-point function in the HTM is

$$\begin{aligned} \Pi_{\text{HTM}}^{ZZ}(p^2) &= \frac{g_Z^2}{16\pi^2} \left\{ m_Z^2 [(c_{\beta_0} c_\alpha + 2s_{\beta_0} s_\alpha)^2 B_0(p^2, m_h, m_Z) + (c_{\beta_0} s_\alpha - 2s_{\beta_0} c_\alpha)^2 B_0(p^2, m_H, m_Z)] \right. \\ &\quad \left. + m_W^2 [2c_{\beta_\pm}^2 s_{\beta_\pm}^2 B_0(p^2, m_{H^\pm}, m_W) + 2(s_W^2 + s_{\beta_\pm}^2)^2 B_0(p^2, m_{G^\pm}, m_W)] \right\} \\ &\quad + \frac{g_Z^2}{64\pi^2} \left[4(c_W^2 - s_W^2)^2 B_5(p^2, m_{H^{\pm\pm}}, m_{H^{\pm\pm}}) + (c_W^2 - s_W^2 - c_{\beta_\pm}^2)^2 B_5(p^2, m_{H^\pm}, m_{H^\pm}) \right. \\ &\quad + (c_W^2 - s_W^2 - s_{\beta_\pm}^2)^2 B_5(p^2, m_{G^\pm}, m_{G^\pm}) + 2s_{\beta_\pm}^2 c_{\beta_\pm}^2 B_5(p^2, m_{H^\pm}, m_{G^\pm}) \\ &\quad + (2c_\alpha c_{\beta_0} + s_\alpha s_{\beta_0})^2 B_5(p^2, m_H, m_A) + (2s_\alpha c_{\beta_0} - c_\alpha s_{\beta_0})^2 B_5(p^2, m_h, m_A) \\ &\quad \left. + (s_\alpha c_{\beta_0} - 2c_\alpha s_{\beta_0})^2 B_5(p^2, m_H, m_{G^0}) + (c_\alpha c_{\beta_0} + 2s_\alpha s_{\beta_0})^2 B_5(p^2, m_h, m_{G^0}) \right]. \end{aligned} \quad (5.23)$$

The photon- Z -boson mixing is calculated as:

$$\begin{aligned} \Pi_{\text{HTM}}^{Z\gamma}(p^2) &= \frac{g^2 s_W}{16\pi^2 c_W} \left\{ \frac{g^2}{2} \sqrt{v_\phi^2 + 2v_\Delta^2} \left[v_\phi s_W^2 c_{\beta_\pm} + \sqrt{2} v_\Delta (1 + s_W^2) s_{\beta_\pm} \right] B_0(p^2, m_W, m_W) \right. \\ &\quad - 2(c_W^2 - s_W^2) B_5(p^2, m_{H^{\pm\pm}}, m_{H^{\pm\pm}}) - \frac{1}{2} (c_W^2 - s_W^2 - c_{\beta_\pm}^2) B_5(p^2, m_{H^\pm}, m_{H^\pm}) \\ &\quad \left. - \frac{1}{2} (c_W^2 - s_W^2 - s_{\beta_\pm}^2) B_5(p^2, m_W, m_W), \right. \end{aligned} \quad (5.24)$$

where we used the short-hand notation for the Higgs mixing angles $s(c)_\alpha \equiv \sin(\cos)\alpha$, $s(c)_{\beta_0} \equiv \sin(\cos)\beta_0$, $s(c)_{\beta_\pm} \equiv \sin(\cos)\beta_\pm$, and for $s(c)_W \equiv \sin(\cos)\theta_W$. Here m_{G^\pm} and m_{G^0} are the masses of the Nambu-Goldstone bosons G^\pm and G^0 , respectively, which in the 't Hooft-Feynman gauge are the same as the corresponding gauge boson masses i.e. $m_{G^\pm} = m_W$ and $m_{G^0} = m_Z$. The $B_0 - B_5$ functions are listed in [275].

In Fig. 5.1 we show the dependence of the T and S parameters on the doubly charged Higgs mass, for $v_\Delta = 1$ GeV, for the minimum mixing in the neutral sector, $\sin \alpha = 0$, in the left panel, and maximum mixing, $\sin \alpha = 1$, in the right panel. The vertical axes are chosen to indicate the experimental limits. The figure shows that while the S parameter agrees with experimental constraints over the whole parameter space, the T parameter is very sensitive to the doubly charged Higgs mass and, if constrained to lie in the allowed range, an upper bound on $m_{H^{\pm\pm}}$ of ~ 266 GeV is required, for the case of no mixing in the neutral CP-even Higgs sector. The bound is slightly raised for $\sin \alpha = 1$ (maximal mixing), but not significantly (upper bound on $m_{H^{\pm\pm}}$ of ~ 280 GeV). Varying the triplet VEV v_Δ does not affect the results

significantly. These results agree with previous studies [134, 220] and represent a potential problem for the HTM, as they are in apparent conflict with the experimental limits on the doubly charged mass, as summarized below.

The mass of doubly charged Higgs boson $m_{H^{\pm\pm}}$ has been constrained by the Large Electron Positron Collider (LEP) [152, 227, 229], the Hadron Electron Ring Accelerator (HERA) [230, 231] and the Tevatron [143–145, 232]. Some restrictions have been obtained independently of the decay modes of the boson. Particularly, if $m_{H^{\pm\pm}}$ is less than half of the Z -boson mass, the new decay mode $Z \rightarrow H^{\pm\pm}H^{\mp\mp}$ will open. From the precise measurement of total decay width of the Z -boson $\Gamma_Z^{NP} < 3$ MeV (95% C.L.) [88], and the partial decay width into a doubly charged boson pair, a lower mass bound $m_{H^{\pm\pm}} > 42.9$ GeV at 95% C.L. can be obtained.

The most up-to-date mass bounds have been obtained through the direct searches at the LHC. The ATLAS Collaboration has looked for doubly charged Higgs bosons via pair production in the same sign dilepton final states, based on the data sample corresponding to an integrated luminosity of 4.7 fb^{-1} at $\sqrt{s} = 7$ TeV. We summarize the results obtained in the different two-lepton modes in Table 5.3 below. Taken at face value, these limits raise doubts about the existence of a light doubly charged Higgs boson.

Table 5.3: Mass limits on doubly charged Higgs bosons from LHC at $\sqrt{s} = 7$ TeV, $\mathcal{L} = 4.7 \text{ fb}^{-1}$. Here BP1, BP2, BP3 and BP4 stand for four CMS benchmarks in type II see-saw scenarios, obtained with branching fractions into several di-lepton combinations.

Decay mode	CMS combined limit at 95% [141]	ATLAS combined limit at 95% [140]
100% e^+e^+	444 GeV	409 GeV
100% $e^+\mu^+$	453 GeV	375 GeV
100% $e^+\tau^+$	373 GeV	–
100% $\mu^+\mu^+$	459 GeV	398 GeV
100% $\mu^+\tau^+$	375 GeV	–
100% $\tau^+\tau^+$	204 GeV	–
BP1	383 GeV	–
BP2	408 GeV	–
BP3	403 GeV	–
BP4	400 GeV	–

However, the generality and range of validity of these constraints have been questioned by several authors. Other decay modes for $H^{\pm\pm}$ such as those into $W^\pm W^\pm$ pairs become domi-

nant under some conditions, namely for $v_\Delta \gtrsim 10^{-4}$ GeV and close to or above WW threshold (this is the case here, as we take $v_\Delta = 1$ GeV, and $m_{H^{\pm\pm}} \gtrsim 200$ GeV) [147, 235, 276]. Using the ATLAS result (with 4.7 fb^{-1} integrated luminosity at $\sqrt{s} = 7$ TeV) from the search of doubly charged bosons by the lepton-pair decay, these authors [147, 235, 276] obtain a lower limit for the doubly charged boson mass of 60 GeV at the 95% C.L., reevaluated to be 85 GeV for an integrated luminosity of 20 fb^{-1} . Thus it is reasonable to allow the LHC limits to be used with caution, and prudent not to restrict the masses too much, as this may limit our analysis. We thus allow the doubly-charged bosons also to be light $m_{H^{\pm\pm}} \gtrsim 100$ GeV.

Still, we assume that the window for observing a light doubly charged Higgs boson is fairly narrow, and it would be desirable that a viable model should be able to accommodate heavier masses for these bosons. In the next section, we shall see that the upper bounds on doubly charged masses from precision electroweak constraints are raised by introducing vector-like quarks.

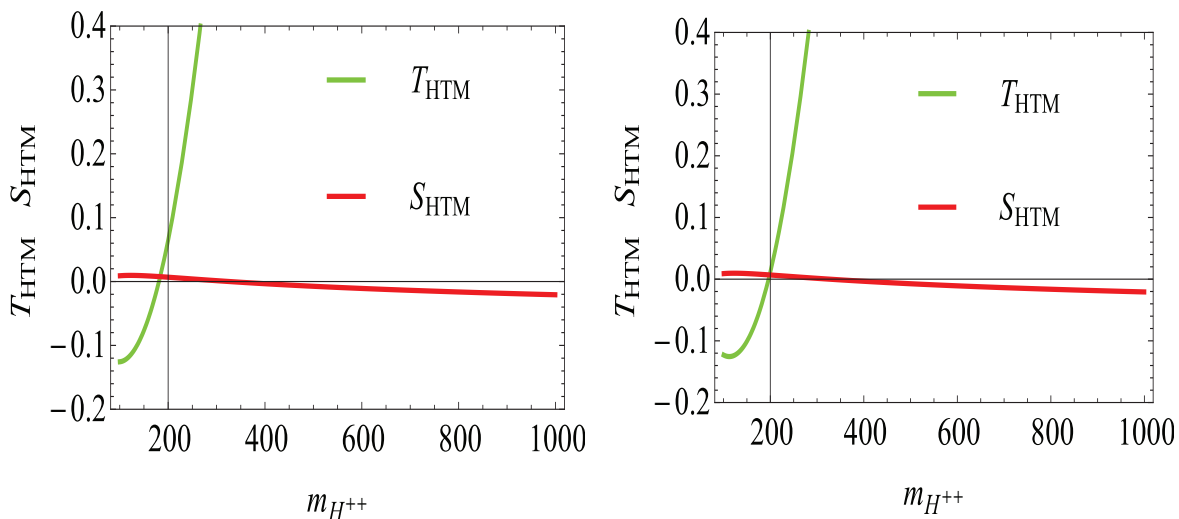


Figure 5.1: The contribution to the T and S parameters in the HTM, as a function of the doubly charged Higgs mass, (left) for $\sin \alpha = 0$, (right) for $\sin \alpha = 1$. We take $v_\Delta = 1$ GeV and indicate the allowed regions for ΔT .

5.3.2 Vector-Like Quark contributions to the S and T parameters

The oblique correction parameter S for vector-like quarks is [277]:

$$\begin{aligned}
S = & \frac{N_c}{2\pi} \left\{ \sum_{\alpha} \sum_i [(|V_{\alpha i}^L|^2 + |V_{\alpha i}^R|^2) \Psi_+(y_{\alpha}, y_i) + 2\text{Re}(V_{\alpha i}^L V_{\alpha i}^{R*}) \Psi_-(y_{\alpha}, y_i)] \right. \\
& - \sum_{\beta < \alpha} [(|U_{\alpha\beta}^L|^2 + |U_{\alpha\beta}^R|^2) \chi_+(y_{\alpha}, y_{\beta}) + 2\text{Re}(U_{\alpha\beta}^L U_{\alpha\beta}^{R*}) \chi_-(y_{\alpha}, y_{\beta})] \\
& \left. - \sum_{j < i} [(|D_{ij}^L|^2 + |D_{ij}^R|^2) \chi_+(y_i, y_j) + 2\text{Re}(D_{ij}^L D_{ij}^{R*}) \chi_-(y_i, y_j)] \right\} \quad (5.25)
\end{aligned}$$

where the functions $\chi_{+(-)}$ are defined as

$$\begin{aligned}
\chi_+(y_1, y_2) & \equiv \frac{y_1 + y_2}{2} - \frac{(y_1 - y_2)^2}{3} + \left[\frac{(y_1 - y_2)^3}{6} - \frac{1}{2} \frac{y_1^2 + y_2^2}{y_1 - y_2} \right] \ln \frac{y_1}{y_2} + \frac{y_1 - 1}{6} f(y_1, y_1) \\
& + \frac{y_2 - 1}{6} f(y_2, y_2) + \left[\frac{1}{3} - \frac{y_1 + y_2}{6} - \frac{(y_1 - y_2)^2}{6} \right] f(y_1, y_2), \\
\chi_-(y_1, y_2) & \equiv -\sqrt{y_1 y_2} \left[2 + (y_1 - y_2 - \frac{y_1 + y_2}{y_1 - y_2}) \ln \frac{y_1}{y_2} + \frac{f(y_1, y_1) + f(y_2, y_2)}{2} - f(y_1, y_2) \right], \quad (5.26)
\end{aligned}$$

and the function f is:

$$f(y_1, y_2) \equiv \begin{cases} -2\sqrt{\Delta} \left(\arctan \frac{y_1 - y_2 + 1}{\sqrt{\Delta}} - \arctan \frac{y_1 - y_2 - 1}{\sqrt{\Delta}} \right) & \Delta > 0 \\ 0 & \Delta = 0 \\ \sqrt{-\Delta} \ln \frac{y_1 + y_2 - 1 + \sqrt{-\Delta}}{y_1 + y_2 - 1 - \sqrt{-\Delta}} & \Delta < 0, \end{cases} \quad (5.27)$$

where $\Delta = -1 - y_1^2 - y_2^2 + 2y_1 + 2y_2 + 2y_1 y_2$. The functions Ψ_+ and Ψ_- are defined by

$$\begin{aligned}
\Psi_+(y_{\alpha}, y_i) & \equiv \frac{22y_{\alpha} + 14y_i}{9} - \frac{1}{9} \ln \frac{y_{\alpha}}{y_i} + \frac{11y_{\alpha} + 1}{18} f(y_{\alpha}, y_{\alpha}) + \frac{7y_i - 1}{18} f(y_i, y_i), \\
\Psi_-(y_{\alpha}, y_i) & \equiv -\sqrt{y_{\alpha} y_i} \left[4 + \frac{f(y_{\alpha}, y_{\alpha}) + f(y_i, y_i)}{2} \right]. \quad (5.28)
\end{aligned}$$

The oblique correction parameter T for vector-like quarks is:

$$\begin{aligned}
T = & \frac{N_c}{16\pi s_W^2 c_W^2} \left\{ \sum_{\alpha} \sum_i [(|V_{\alpha i}^L|^2 + |V_{\alpha i}^R|^2) \theta_+(y_{\alpha}, y_i) + 2\text{Re}(V_{\alpha i}^L V_{\alpha i}^{R*}) \theta_-(y_{\alpha}, y_i)] \right. \\
& - \sum_{\beta < \alpha} [(|U_{\alpha\beta}^L|^2 + |U_{\alpha\beta}^R|^2) \theta_+(y_{\alpha}, y_{\beta}) + 2\text{Re}(U_{\alpha\beta}^L U_{\alpha\beta}^{R*}) \theta_-(y_{\alpha}, y_{\beta})] \\
& \left. - \sum_{j < i} [(|D_{ij}^L|^2 + |D_{ij}^R|^2) \theta_+(y_i, y_j) + 2\text{Re}(D_{ij}^L D_{ij}^{R*}) \theta_-(y_i, y_j)] \right\}, \quad (5.29)
\end{aligned}$$

where $V_{\alpha i}^{L,R}$, $U_{\alpha\beta}^{L,R}$ and $D_{ij}^{L,R}$ are listed in Appendix. We adopted the convention of using Greek letters to denote up-type quarks and Latin ones to denote down-type quarks. Here $N_c = 3$ is the number of colours, and the functions $\theta_{+(-)}$ are defined as

$$\begin{aligned}\theta_+(y_1, y_2) &\equiv y_1 + y_2 - \frac{2y_1y_2}{y_1 - y_2} \ln \frac{y_1}{y_2}, \\ \theta_-(y_1, y_2) &\equiv 2\sqrt{y_1y_2} \left(\frac{y_1 + y_2}{y_1 - y_2} \ln \frac{y_1}{y_2} - 2 \right),\end{aligned}\tag{5.30}$$

where $y_i = \frac{m_i^2}{m_Z^2}$ [277]. As in the HTM without vector-like quarks, the S -parameter does not impose any restrictions on the parameter space of the model. We concentrate on the T parameter. As explicit expressions exist for the T parameter in some models [257], we do not include them all. We are interested in the case in which the contributions from vector-like quarks are of opposite signs to those from the extra states in the HTM, and thus allow to relax the severe constraint on the doubly charged Higgs mass discussed in the previous section. In Fig. 5.2, we show the contribution to the T parameter in two of the models, \mathcal{D}_1 , \mathcal{D}_X . We have chosen these models since these are the only ones which yield contributions to the T parameter which can be negative, interfering destructively with those coming from the particle content of the HTM. As shown in Fig. 5.2, the T parameter in these models is negative in a small region, restricting the upper bound on $m_{H^{\pm\pm}}$ to ~ 400 GeV in the \mathcal{D}_X and \mathcal{D}_1 models. The rest of the models from Table 5.1 not shown in Fig. 5.2 give always a positive contribution to the T parameter and thus, when added to the HTM contribution, the restrictions on the doubly charged Higgs mass worsen.

5.3.3 Restrictions on doubly charged Higgs boson and vector-like quarks masses

We investigate further the \mathcal{D}_1 and \mathcal{D}_X models, where the negative contributions to the T parameter are significant. For the specific models under study, we give explicit expressions

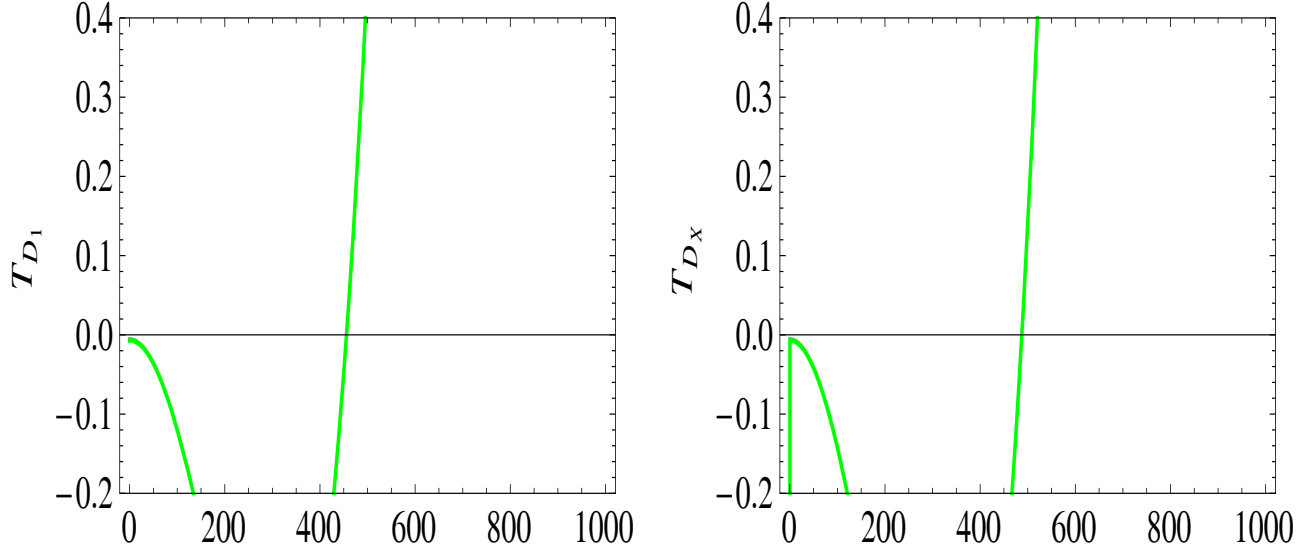


Figure 5.2: The allowed variation of the T parameter with $x_{t(b)}$, as defined in the text, for models \mathcal{D}_1 (left panel), \mathcal{D}_X (right panel). We chose $M = 800$ GeV for both plots.

for the T parameter³:

$$\begin{aligned}
\Delta T_{\mathcal{D}_1} &= \frac{3}{16\pi s_W^2 c_W^2} \left[s_L^{d2} \theta_+(y_t, y_B) - s_L^{d2} \theta_+(y_t, y_b) - c_L^{d2} s_L^{d2} \theta_+(y_b, y_B) \right], \\
\Delta T_{\mathcal{D}_X} &= \frac{3}{16\pi s_W^2 c_W^2} \left[s_L^{u2} \theta_+(y_T, y_b) - s_L^{u2} \theta_+(y_t, y_b) + (s_L^{u2} + s_R^{u2}) \theta_+(y_t, y_X) \right. \\
&\quad + (c_L^{u2} + c_R^{u2}) \theta_+(y_T, y_X) + 2s_L^u s_R^u \theta_-(y_t, y_X) + 2c_L^u c_R^u \theta_-(y_T, y_X) \\
&\quad \left. - (4c_L^{u2} s_L^{u2} + c_R^{u2} s_R^{u2}) \theta_+(y_t, y_T) - (4c_L^u s_L^u c_R^u s_R^u) \theta_-(y_t, y_T) \right]. \tag{5.31}
\end{aligned}$$

For a given physics model, the predictions for the T parameter consist of the sum of the vector-quark contributions and the nonvanishing SM remainders, when the Higgs mass (m_h) and top mass (m_t) differ from those used for the SM reference. The dependence of T on the latter two parameters is then approximated by the one-loop terms

$$\Delta T_{h,t} \sim -\frac{3}{16\pi c_W^2} \ln \frac{m_h^2}{m_{h,\text{ref}}^2} + \frac{3}{16\pi s_W^2 c_W^2} \ln \frac{m_t^2 - m_{t,\text{ref}}^2}{m_Z^2}. \tag{5.32}$$

The m_t dependence is often neglected [278]. Assuming the Higgs mass is 125 GeV and its reference value $m_{h,\text{ref}} = 120$ GeV [257], we added the two sources (vector-like quark contributions and the correction coming from the Higgs mass deviation from its reference value) to the T parameter in the HTM.

³Explicit expressions for model \mathcal{D}_X appear in [257], but we include it here, and add expressions for model \mathcal{D}_1 for completeness.

Motivated by T parameter contributions to \mathcal{D}_1 and \mathcal{D}_X models from vector-like quarks which are of opposite sign from the contributions in the HTM, we proceed to analyze restrictions on the doubly charged Higgs mass when we add the singlet B vector-like quark in \mathcal{D}_1 scenario or the singlet T vector-like quark in the non-SM vector-like doublet in the \mathcal{D}_X scenario, to the particle content of the Higgs Triplet Model. In Fig. 5.3 we show the effects on the T parameter as a contour in an $m_{H^{\pm\pm}} - M$ plane. The upper panels correspond to the \mathcal{D}_1 model and the lower to the \mathcal{D}_X model. The left (right) panels correspond to no mixing (maximal mixing) in the neutral Higgs sector, *i. e.*, between h and H . In both models, it is clear that the presence of the mixing relaxes the constraints on the doubly charged mass from restrictions on the T parameter, though generally by less than 10%. In the \mathcal{D}_1 model, for vector-like quark masses $M = 800$ GeV, the maximum doubly charged mass value allowed is $m_{H^{\pm\pm}} = 338$ GeV, reached for $x_b = 270$ GeV for $\sin \alpha = 0$, while for $\sin \alpha = 1$, the maximum doubly charged mass value allowed is $m_{H^{\pm\pm}} = 355$ GeV, for $x_b = 270$ GeV. In the plots for the \mathcal{D}_1 model we include restrictions from $Zb\bar{b}$ decay, while in the plots for the \mathcal{D}_X model we include restrictions from Wtb vertex.

In the \mathcal{D}_X scenario, for $M = 800$ GeV, the maximum doubly charged mass value allowed is $m_{H^{\pm\pm}} = 363$ GeV, when $x_t = 300$ GeV for $\sin \alpha = 0$, while for $\sin \alpha = 1$, the maximum doubly charged mass value allowed is $m_{H^{\pm\pm}} = 370$ GeV, for $x_t = 300$ GeV. The contour plots indicate the values for the T parameter, as shown in the figure inserts. For all plots, we selected the particular value for $x_{t(b)}$ to correspond to the largest upper limit for doubly charged Higgs mass, as seen in Fig. 5.4.

We note that, in the \mathcal{D}_1 model, for the chosen values of x_b , the mass range for the vector-like quarks is not restricted by either the T parameter or by $Zb\bar{b}$, while in the \mathcal{D}_X model Wtb constrains vector-like quarks to be $M \geq 606$ GeV, in agreement with conservative bounds from Table 5.2. We note that our most relaxed constraints for the doubly charged mass are obtained for $M = 305$ GeV. In the \mathcal{D}_X model for $\sin \alpha = 0(1)$ the upper limit is $m_{H^{++}} = 397(412)$ GeV, while in the \mathcal{D}_1 model for $\sin \alpha = 0(1)$ the upper limit is $m_{H^{++}} = 392(410)$ GeV.

We are interested in restriction on vector-like quark parameters M and $x_{b(t)}$, which have further implications for doubly charged Higgs boson masses, as we shall discuss.

Lower bounds on the masses of the vector-like quarks have been obtained under various scenarios [170, 194, 250–254]. But in the HTM, masses of these states are more restricted by electroweak constraints. Fig. 5.4 shows the dependence of T parameter and its restriction as a contour plot in the $m_{H^{\pm\pm}} - x_b$ plane for models \mathcal{D}_1 , in the left-side panels and \mathcal{D}_X in the

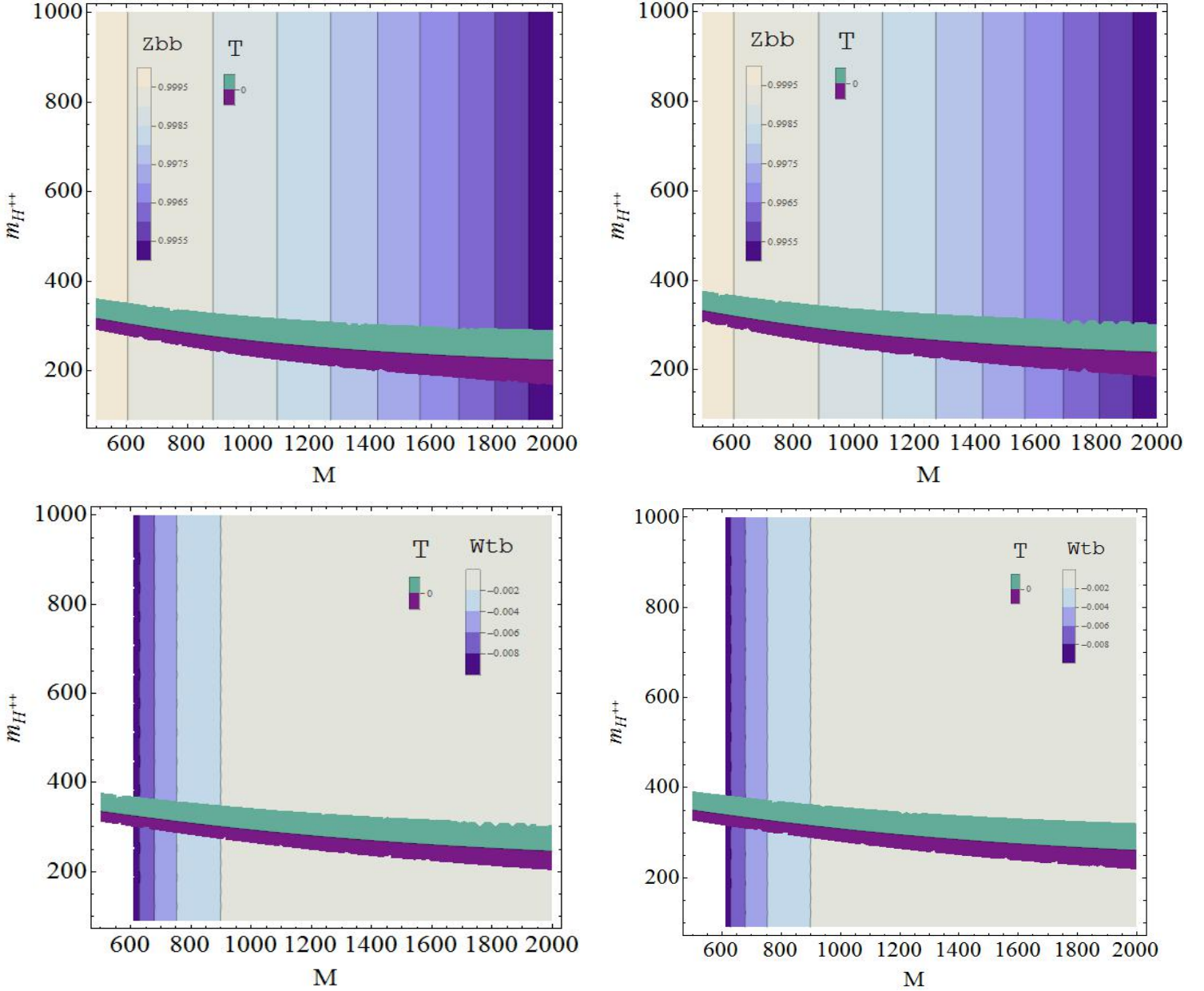


Figure 5.3: Contour graphs showing the contribution to the T parameter in the HTM with vector-like quarks, as functions of the doubly charged Higgs mass $m_{H^{\pm\pm}}$ and the vector-like quark mass M , for fixed values of $x_{b(t)}$. We show (upper left panel) the \mathcal{D}_1 model with $x_b = 270$ GeV, $\sin \alpha = 0$, (upper right panel) the \mathcal{D}_1 model with $x_b = 270$ GeV, $\sin \alpha = 1$, (lower left panel) the \mathcal{D}_X model with $x_t = 300$ GeV, $\sin \alpha = 0$, (lower right panel) the \mathcal{D}_X model with $x_t = 300$ GeV, $\sin \alpha = 1$.

right-side panels, for vector-like quark masses $M = 800$ GeV. The upper panels are for no mixing in neutral Higgs boson sector, $\sin \alpha = 0$, while the lower panels represent the maximal mixing case, $\sin \alpha = 1$. In this case, the tree-level decay $Z \rightarrow b\bar{b}$ imposes a lower bound on the x_b parameter, $x_b \geq 117$ GeV, for scenario \mathcal{D}_1 , and this limit is the same from restrictions on positive and negative deviations in δR_b . The plot for the \mathcal{D}_X model in Fig. 5.4 indicates that Wtb does not impose similar restrictions on x_t .

The mixing parameter $x_{b(t)}$ is also restricted by the T parameter, as shown in Fig. 5.4. In the \mathcal{D}_1 model with vector-like quark mass $M = 800$ (1000) GeV, the maximum x_b allowed is $x_b = 503$ (538) GeV, while in the \mathcal{D}_X model for $M = 800$ (1000) GeV, the upper limit for x_t is $x_t = 525$ (553) GeV.

We note that Fig. 5.4 also indicates the constraints on the doubly charged mass, as a function of $x_{b(t)}$, for fixed values of vector-like quark mass parameter M , from restrictions on the T parameter. In the \mathcal{D}_1 model, for $\sin \alpha = 0$, the maximum doubly charged mass value allowed is $m_{H^{\pm\pm}} = 338$ (329) GeV, for $M = 800$ (1000) GeV, while for $\sin \alpha = 1$, the maximum doubly charged mass value allowed is $m_{H^{\pm\pm}} = 355$ (343) GeV. In the plots for the \mathcal{D}_1 model we include restrictions from $Zb\bar{b}$ decay, which set lower limits on x_b but seems not to affect $m_{H^{\pm\pm}}$. In the \mathcal{D}_X scenario, for $\sin \alpha = 0$, the maximum doubly charged mass value allowed is $m_{H^{\pm\pm}} = 359$ (345) GeV, for $M = 800$ (1000) GeV, respectively, while for $\sin \alpha = 1$, the maximum doubly charged mass value allowed is $m_{H^{\pm\pm}} = 370$ (360) GeV. Again the Wtb vertex does not limit x_t or $m_{H^{\pm\pm}}$.

To summarize, experimental constraints on Wtb impose restrictions on M in the \mathcal{D}_X scenario, while leaving x_t free; while in the \mathcal{D}_1 scenario $Zb\bar{b}$ imposes restrictions on x_b while leaving M unconstrained.

5.4 Effect of vector quarks on $H \rightarrow \gamma\gamma$ and $H \rightarrow Z\gamma$

The production and decays of the vector-like quarks will proceed in the same way as in the SM, and this was explored extensively before. However, what could be different are effects on the loop-induced decays $H \rightarrow \gamma\gamma$ and $H \rightarrow Z\gamma$, through interplays of contributions of additional particles in the loop, in our case charged and doubly charged Higgs bosons and vector-like quarks. So in this section, we study vector-like quarks contribution to the Higgs

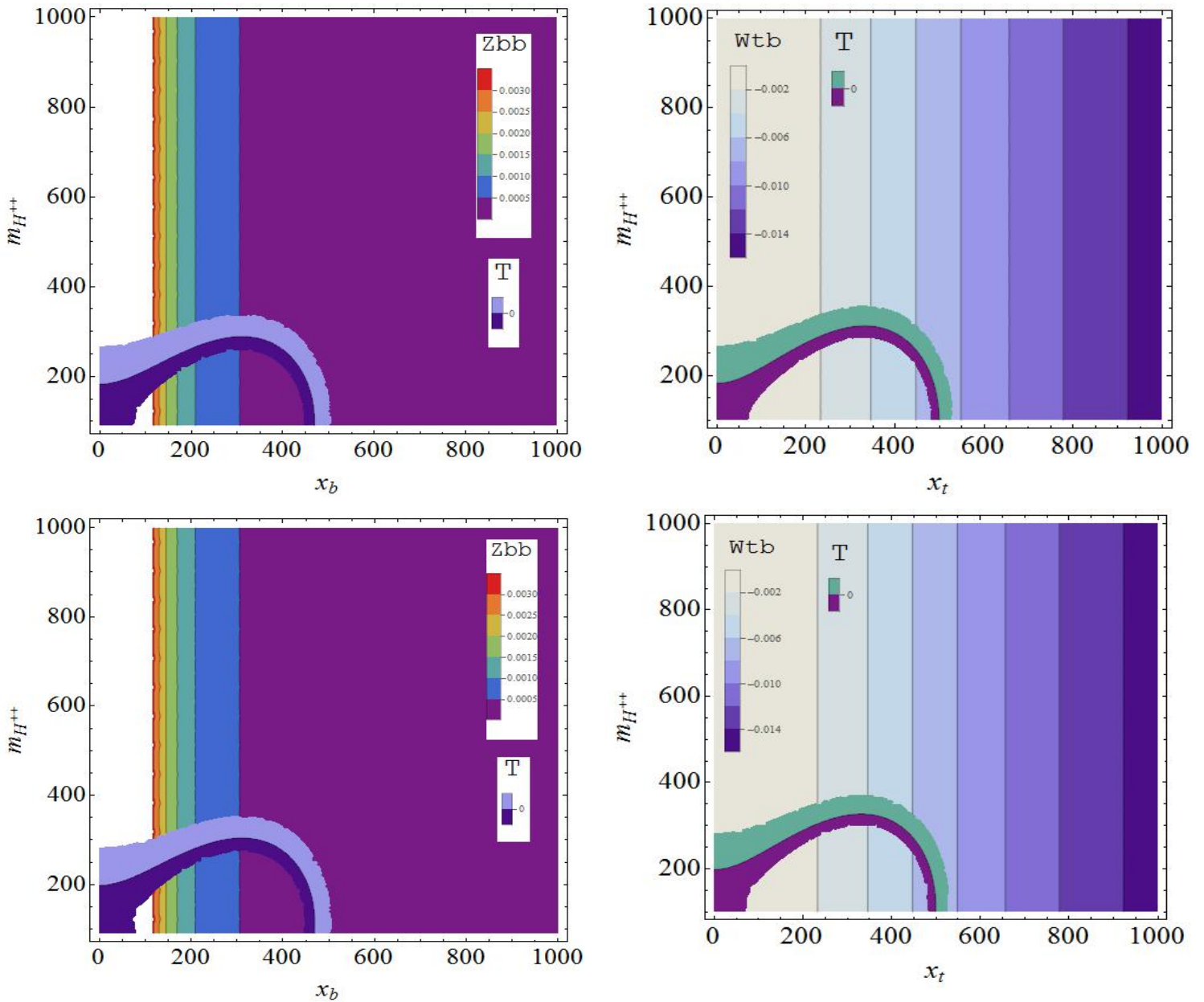


Figure 5.4: Contour graphs showing the contribution to the T parameter in the HTM with vector quarks, as functions of the doubly charged Higgs mass $m_{H^{\pm\pm}}$ and x_b , x_t , for fixed values of the vector quark mass $M = 800$ GeV. We choose (upper left panel), scenario \mathcal{D}_1 , $\sin \alpha = 0$, (upper right panel), scenario \mathcal{D}_X , $\sin \alpha = 0$, (lower left panel), scenario \mathcal{D}_1 , $\sin \alpha = 1$, (lower right panel), scenario \mathcal{D}_X , $\sin \alpha = 1$. We allow for the T parameter between -0.2 and 0.4 .

decay in the HTM. The decay width $h \rightarrow \gamma\gamma$ is

$$\begin{aligned} [\Gamma(h \rightarrow \gamma\gamma)]_{HTM} &= \frac{G_F \alpha^2 m_h^3}{128 \sqrt{2} \pi^3} \left| \sum_f N_c^f Q_f^2 g_{hff} A_{1/2}(\tau_f^h) + g_{hWW} A_1(\tau_W^h) + \tilde{g}_{hH^\pm H^\mp} A_0(\tau_{H^\pm}^h) \right. \\ &\quad \left. + 4\tilde{g}_{hH^{\pm\pm} H^{\mp\mp}} A_0(\tau_{H^{\pm\pm}}^h) + \sum_q \frac{Y_{qq} Q_q^2 N_c^f g_{hff}}{m_q} A_{1/2}(\tau_q^h) \right|^2, \end{aligned} \quad (5.33)$$

where the sum runs over $q = t, T$ for up-type quarks and over b, B for down-type ones. The value for m_T is given in Eq. (5.12), and the loop functions for spin 0, spin 1/2 and spin 1 have appeared in Section (3.3). For this, and for the couplings of h to the vector bosons and fermions, and the scalar trilinear couplings we use the same expressions as in Section (3.3). The couplings of the Higgs bosons with vectorlike quarks (Y_{qq}) appearing in Eq. (5.33) are listed in Section (5.5).

The new quarks effect on the diphoton search channel at the LHC is expressed by the ratio

$$R_{\gamma\gamma} = \frac{[\sigma(gg \rightarrow h) \times \Gamma(h \rightarrow \gamma\gamma)]_{HTM}}{[\sigma(gg \rightarrow \Phi) \times \Gamma(\Phi \rightarrow \gamma\gamma)]_{SM}} \times \frac{[\Gamma(\Phi)]_{SM}}{[\Gamma(h)]_{HTM}}, \quad (5.34)$$

where Φ is the SM neutral Higgs boson. We neglect the contribution of the b quark. The ratio of the production cross sections by gluon fusion is

$$\frac{\sigma_{HTM}(gg \rightarrow h)}{\sigma_{SM}(gg \rightarrow \Phi)} = \left[g_{hff} + \frac{\sum_q \frac{Y_{qq} g_{hff}}{m_q} A_{1/2}(\tau_q^h)}{A_{1/2}(\tau_t^h)} \right]^2. \quad (5.35)$$

As in Chapter 3, we set the values 125 GeV and 98 GeV for the h and H masses respectively, and adjust the parameters $\lambda_1 - \lambda_5$ accordingly. The relative widths factor is as defined in Chapter 4. Previously, in Ref. [139], couplings of the vector-like quarks in the Higgs potential were assumed to be arbitrary, and thus the $gg \rightarrow H$ production rate could be reduced to 20% of the SM value. In our considerations, vector quark couplings are restricted from the mixing matrices Eq. (5.11) and Eq. (5.13), and we relate the couplings in the Higgs potential to the Higgs masses [1].

Our numerical investigations agree with those in Ref. [253, 254]. In both the loops for Higgs production through gluon fusion, and in the loops for Higgs diphoton decay, the contributions of the vector-like quarks are very small. This effect is stronger than expected by decoupling, and arise also from small couplings of the new quarks, given in Section 5.5. The couplings of the new quarks to the Higgs bosons is limited by the trace of the mixing matrix for both

singlet or triplet and for doublet representations, which must equal 1 [253, 254]. Even for varying $M \in (500 - 2000)$ GeV and $x_{b(t)} \in (0 - 1000)$ GeV, the variation in $R_{\gamma\gamma}$ is less than 10%, and thus below the precision of the current measurements at the LHC.

The decay rates $R_{\gamma\gamma}$ and $R_{Z\gamma}$ depend sensitively on $\sin\alpha$ and $m_{H^{\pm\pm}}$. We investigate this dependence in the context of the HTM model with vector-like quarks, because, although the vector-like quarks do not explicitly modify the diphoton and Z -photon decays, they affect the parameter space of $\sin\alpha - m_{H^{\pm\pm}}$ through restrictions on the T parameter, and thus they *indirectly* affect the decays.

The results of our analyses are shown in Fig. 5.5. In purple, we draw contour plots for the T parameter restrictions, while values for $R_{\gamma\gamma}$ are shown in multicolor contours. We have drawn plots for scenarios (in order, from the top, left to right side): \mathcal{D}_1 , \mathcal{D}_X , \mathcal{D}_Y , \mathcal{T}_X , \mathcal{D}_2 , \mathcal{U}_1 , but we omit plots for scenario \mathcal{T}_Y , for brevity and because for this model the allowed range for $m_{H^{\pm\pm}}$ for the parameters chosen is the smallest. The differences in the contours for $R_{\gamma\gamma}$ between models are negligible: however, what differs amongst models are restrictions on the values of the doubly charged Higgs boson mass.

For the model \mathcal{D}_1 (top left panel), $R_{\gamma\gamma}$ can take values between 0.5 and 4.5, but the mass $m_{H^{\pm\pm}}$ is restricted to lie in a band (260 – 354) GeV; while for scenario \mathcal{D}_X (middle top panel), $R_{\gamma\gamma}$ can take values between 0.5 and 4, but the mass $m_{H^{\pm\pm}}$ is restricted to lie in a band (282 – 373) GeV. For the other scenarios, $R_{\gamma\gamma}$ can take values between 0.5 and 5, but the mass $m_{H^{\pm\pm}}$ is restricted to lie in a band (100 – 280) GeV for the \mathcal{D}_2 model, in (100 – 284) GeV for the \mathcal{D}_Y model, in (100 – 275) GeV for the \mathcal{T}_X model, and in (100 – 280) GeV for the \mathcal{U}_1 model. The restriction on the mass of the doubly charged Higgs boson is thus what differentiates these models.

We note also that, as in HTM without additional fermions, for $\sin\alpha = 0$ the Higgs diphoton decay *cannot* be enhanced with respect to its SM value. This confirms the analyses in Chapters 3 and 4. The relative branching ratios $R_{\gamma\gamma}$ are very sensitive to values of $\sin\alpha$. In the allowed regions of $m_{H^{\pm\pm}}$ bands, the angle for which the enhancement in the diphoton decay is 1.5 – 3.5 times the SM value is $\sin\alpha \in (-0.95, -0.13)$ and $(0.57, 0.96)$ in the \mathcal{D}_1 model and $\sin\alpha \in (-0.96, -0.17)$ and $(0.7, 0.96)$ in the \mathcal{D}_X model. In the \mathcal{D}_2 model an enhancement of $R_{\gamma\gamma}$ of 1.5 – 3.5 is obtained for a large range of both positive $\sin\alpha \in (0.6, 0.97)$ and negative values $\sin\alpha \in (-0.95, -0.15)$, and the same holds for the other models, \mathcal{D}_Y , \mathcal{T}_X , \mathcal{U}_1 and \mathcal{T}_Y . As a general feature, $R_{\gamma\gamma}$ is more enhanced at negative values of $\sin\alpha$. In all the plots we chose $M = 800$ GeV and values for x_t and x_b consistent with a large allowed parameter range

for $m_{H^{\pm\pm}}$. For the \mathcal{D}_1 model, the plots are for $x_b = 300$ GeV, above the required minimum, while for model \mathcal{D}_X , the plots are for $x_t = 300$ GeV, consistent with the previous section. For other models, the restrictions for x_b and x_t are much relaxed, and we have chosen $x_b = 20$ GeV and $x_t = 50$ GeV, as in previous studies [257, 258]. An exception is model \mathcal{T}_Y , where in order to have a $-0.2 \leq \Delta T \leq 0.4$, $x_t < 24$ GeV, and the mass range for the doubly charged Higgs boson (which is maximum 147 GeV for this x_t) increases with decreasing x_t (for instance the maximum reaches 267 GeV for $x_t = 10$ GeV).

In general, for heavier M and lighter $x_{t(b)}$, we can obtain a slightly higher upper band for mass of doubly charged Higgs bosons. The exceptions are the \mathcal{T}_Y model, as mentioned above, and \mathcal{D}_1 and \mathcal{D}_X models, where higher upper limits for $m_{H^{\pm\pm}}$ are obtained for lighter vector-like quark masses M .

The decay width for $h \rightarrow Z\gamma$ is given by [150, 153, 279, 280]:

$$\begin{aligned}
[\Gamma(h \rightarrow Z\gamma)]_{HTM} &= \frac{\alpha G_F^2 m_W^2 m_h^3}{64\pi^4} \left(1 - \frac{m_Z^2}{m_h^2}\right)^3 \left| \frac{1}{c_W} \sum_f 2N_c^f Q_f (I_3^f - 2Q_f s_W^2) g_{hff} A_{1/2}^h(\tau_f^h, \tau_f^Z) \right. \\
&+ \frac{1}{c_W} \sum_q 2N_c^f Q_q (I_3^q - 2Q_q s_W^2) \frac{Y_{qq}}{m_q} g_{hff} A_{1/2}^h(\tau_q^h, \tau_q^Z) \\
&+ c_W g_{hWW} A_1^h(\tau_W^h, \tau_W^Z) - 2s_W \tilde{g}_{hH^\pm H^\mp} g_{ZH^\pm H^\mp} A_0^h(\tau_{H^\pm}^h, \tau_{H^\pm}^Z) \\
&\left. - 4s_W \tilde{g}_{hH^{\pm\pm} H^{\mp\mp}} g_{ZH^{\pm\pm} H^{\mp\mp}} A_0^h(\tau_{H^{\pm\pm}}^h, \tau_{H^{\pm\pm}}^Z) \right|^2, \tag{5.36}
\end{aligned}$$

where the sum runs over $q = t, T$ for up-type quarks and over b, B for down-type ones and $\tau_i^h = 4m_i^2/m_h^2$, $\tau_i^Z = 4m_i^2/m_Z^2$, with $i = t, T, b, B, W, H^\pm, H^{\pm\pm}$. $I_3^f = \pm\frac{1}{2}$ is the weak isospin of top and bottom quarks, while for vector-like quarks $I_3^F = I_3^f + f_L = f_R$, with $F = T, B$, and f_L, f_R depend on the vector-like quark representation [281], and are listed in Table 5.4. The loop-factors and couplings have been given before, and we use the expressions in Section

Table 5.4: Neutral current parameters f_L and f_R for vector-like quarks Z interaction.

Name		\mathcal{U}_1	\mathcal{D}_1	\mathcal{D}_2	\mathcal{D}_X	\mathcal{D}_Y	\mathcal{T}_X	\mathcal{T}_Y
Type		Singlet	Singlet	Doublet	Doublet	Doublet	Triplet	Triplet
T	f_L	-1/2		0	-1		-1/2	+1/2
	f_R	0		+1/2	-1/2		0	+1
B	f_L		+1/2	0		+1	-1/2	+1/2
	f_R		0	-1/2		1/2	-1	0

4.3. The decay rates for $R_{Z\gamma}$ depend on $\sin \alpha$ and $m_{H^{\pm\pm}}$, though the variation is much milder

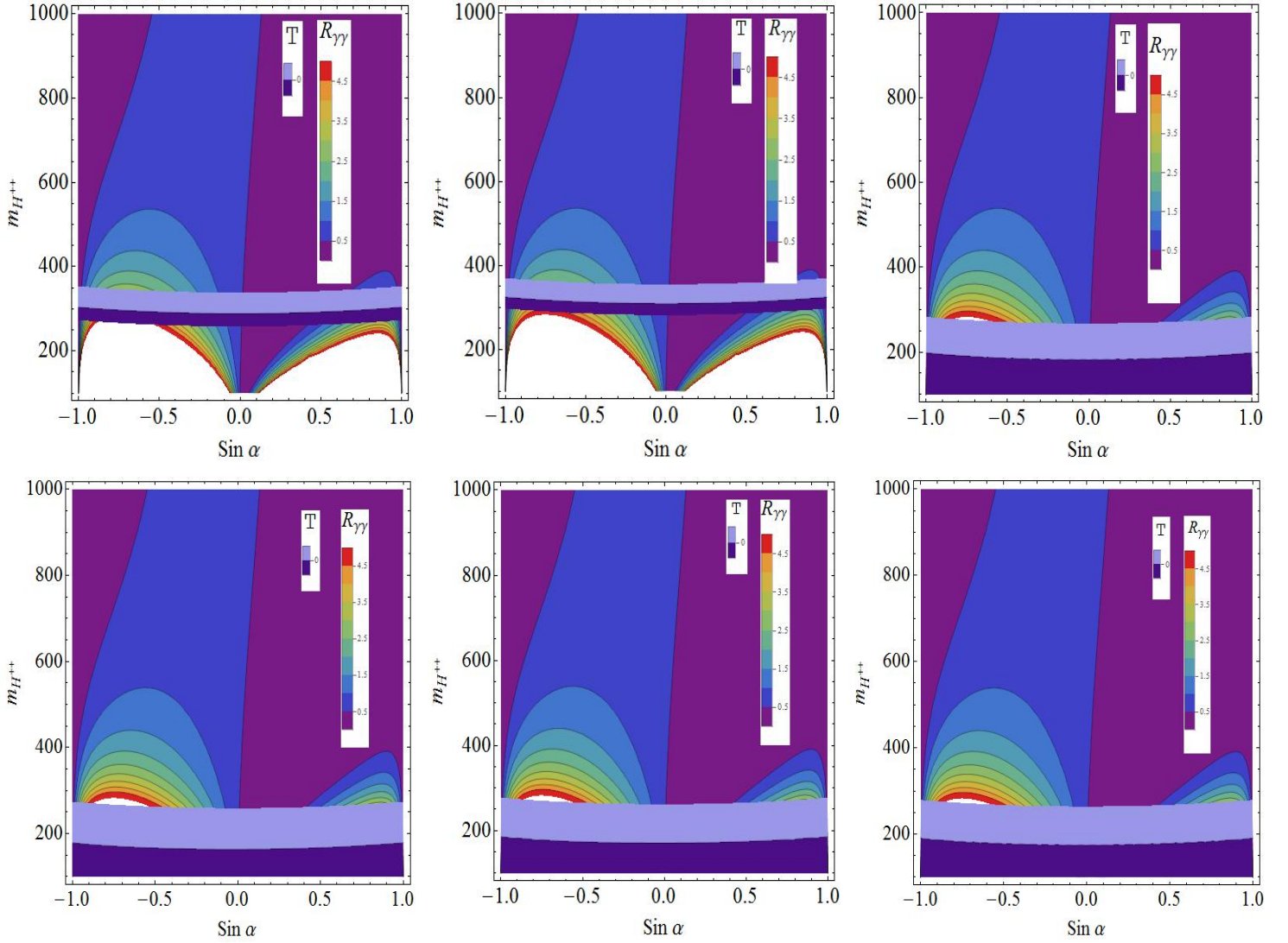


Figure 5.5: Contour graphs for the relative strength of the Higgs diphoton decay $R_{\gamma\gamma}$, including the restrictions of the T parameter in the HTM with vector-like quarks, as a function of the doubly charged Higgs boson mass $m_{H^{\pm\pm}}$ and the mixing in the CP-even neutral Higgs sector, $\sin \alpha$. We show plots for scenario \mathcal{D}_1 (upper left panel), scenario \mathcal{D}_X (upper middle panel), scenario \mathcal{D}_Y (upper right panel), scenario \mathcal{T}_X (lower left panel), scenario \mathcal{D}_2 (middle lower panel) and scenario \mathcal{U}_1 (lower right panel). Results for scenario \mathcal{T}_Y are not shown but summarized in the text. We took $M = 800$ GeV for all the graphs, and values for x_t, x_b consistent with a larger allowed range for $m_{H^{\pm\pm}}$.

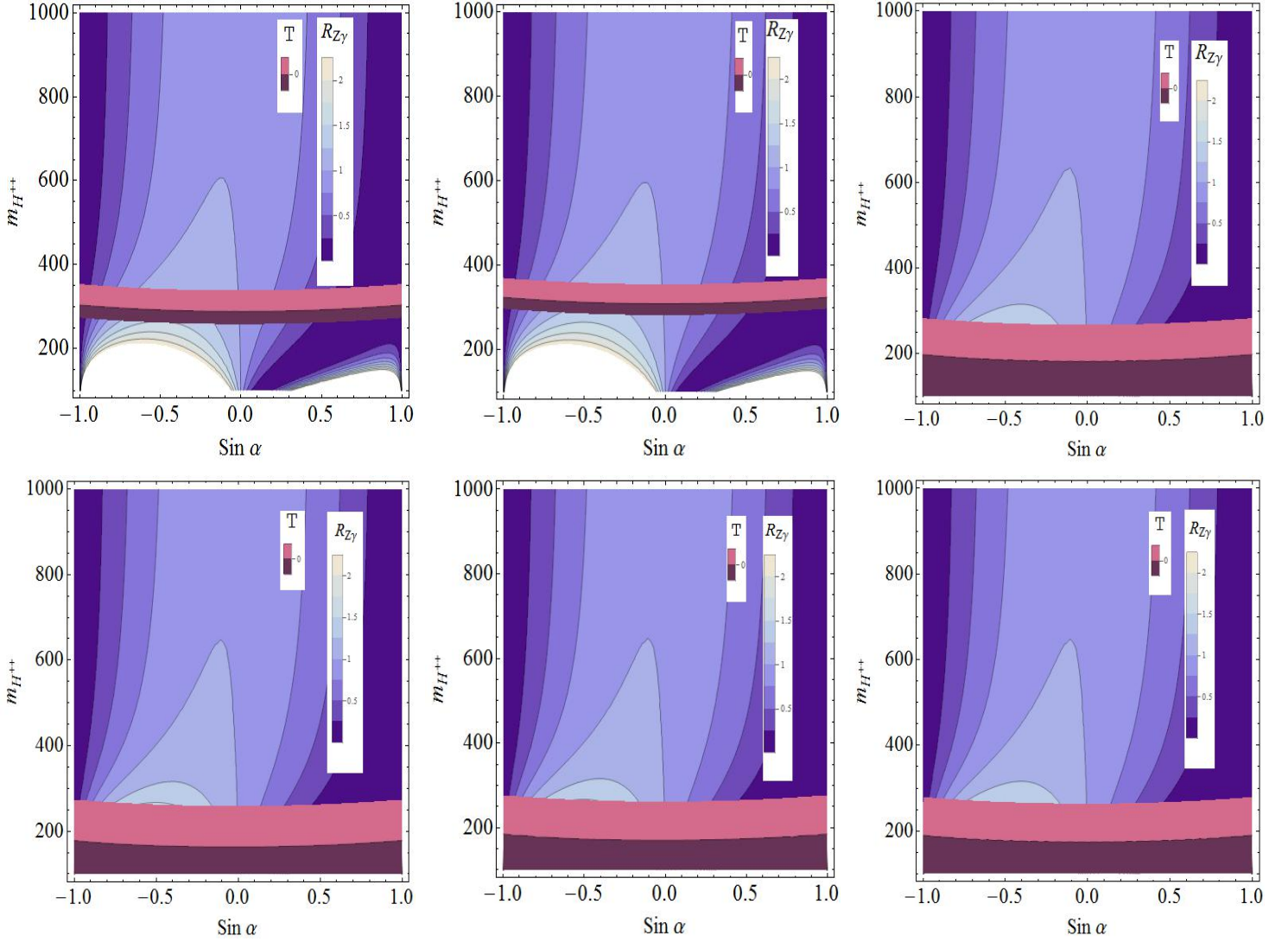


Figure 5.6: Contour graphs for the relative strength of the decay of the Higgs boson into a photon and a Z-boson, $R_{Z\gamma}$, including the restrictions of the T parameter in the HTM with vector-like quarks, as a function of the doubly charged Higgs boson mass $m_{H^{\pm\pm}}$ and the mixing in the CP-even neutral Higgs sector, $\sin\alpha$. We show plots for scenario \mathcal{D}_1 (upper left panel), scenario \mathcal{D}_X (upper middle panel), scenario \mathcal{D}_Y (upper right panel), scenario \mathcal{T}_X (lower left panel), scenario \mathcal{D}_2 (middle lower panel) and scenario \mathcal{U}_1 (lower right panel). Results for scenario \mathcal{T}_Y (not shown) are summarized in the text. We choose the same parameters as in Fig. 5.5.

than that for $R_{\gamma\gamma}$. We investigate the dependence in Fig. 5.6 on the parameter space of $\sin \alpha - m_{H^{\pm\pm}}$ through restrictions on the T parameter. Contour plots for the T parameter restrictions are shown in the (almost) horizontal bands, while values for $R_{Z\gamma}$ are shown in purple contours. Scales for both are included on the right panels. We have drawn plots for the same scenarios and the same order as for $R_{\gamma\gamma}$: \mathcal{D}_1 , \mathcal{D}_X , \mathcal{D}_Y , \mathcal{T}_X , \mathcal{D}_2 , \mathcal{U}_1 . The features for $R_{Z\gamma}$ resemble those for $R_{\gamma\gamma}$. Distinguishing signs among models come from restrictions on the values of the doubly charged Higgs boson mass. The relative branching ratios $R_{Z\gamma}$ are also sensitive to values of $\sin \alpha$. In the \mathcal{D}_1 model, in the regions allowed by $m_{H^{\pm\pm}}$ bands, an enhancement of the branching ratios in the $Z\gamma$ decay of 1.25 – 2 is possible for negative $\sin \alpha \in (-0.61, -0.17)$. In the \mathcal{D}_X model, an enhancement of $R_{Z\gamma}$ of 1.25 is obtained for negative $\sin \alpha \in (-0.72, -0.17)$. In the \mathcal{D}_2 model an enhancement of $R_{Z\gamma}$ of 1.25 – 2 is possible for negative $\sin \alpha \in (-0.74, -0.16)$, and the same holds for the other models, \mathcal{D}_Y , \mathcal{T}_X , \mathcal{U}_1 and \mathcal{T}_Y . Decays into $Z\gamma$ are correlated to those into $\gamma\gamma$ —that is, they are likely to be larger in the same regions of the parameter space and for low doubly charged Higgs boson masses.

5.5 Appendix

We list in Table 5.5 the W and Z couplings in vector-like quark models used to restrict masses and mixings in the \mathcal{D}_1 and \mathcal{D}_X models.

We list in Table 5.6 the Higgs boson couplings in vector-like quark models

Table 5.5: Couplings to the W and Z bosons

<i>Light-light couplings to the W boson</i>				
<i>model / matrix element</i>	V_{tb}^L		V_{tb}^R	
\mathcal{D}_1	c_L^d		0	
\mathcal{D}_X	c_L^u		0	
<i>Heavy-heavy couplings to the W boson</i>				
<i>model / matrix element</i>	V_{Xt}^L		V_{Xt}^R	
\mathcal{D}_X	c_L^u		c_R^u	
<i>Heavy-light couplings to the W boson</i>				
<i>model / matrix element</i>	V_{Xt}^L	V_{Xt}^R	V_{Tb}^L	V_{Tb}^R
\mathcal{D}_X	$-s_L^u$	$-s_R^u$	s_L^u	0
<i>Light-heavy couplings to the W boson</i>				
<i>model / matrix element</i>	V_{tB}^L		V_{tB}^R	
\mathcal{D}_1	s_L^d		0	
<i>Light-heavy couplings to the Z boson</i>				
<i>model / matrix element</i>	U_{tT}^L	U_{tT}^R	D_{bB}^L	D_{bB}^R
\mathcal{D}_1			$s_L^d c_L^d$	0
\mathcal{D}_X	$2s_L^u c_L^u$	$s_R^u c_R^u$		

Table 5.6: Couplings to the Higgs bosons

<i>Light-light couplings to the Higgs boson</i>		
<i>model / matrix element</i>	Y_{tt}	Y_{bb}
\mathcal{U}_1	$c_L^u{}^2$	1
\mathcal{D}_1	1	$c_L^d{}^2$
\mathcal{D}_X	$c_R^u{}^2$	1
\mathcal{D}_2	$c_R^u{}^2$	$c_R^d{}^2$
\mathcal{D}_Y	1	$c_R^d{}^2$
\mathcal{T}_X	$c_L^u{}^2$	$c_L^d{}^2$
\mathcal{T}_Y	$c_L^u{}^2$	$c_L^d{}^2$
<i>Heavy-heavy couplings to the Higgs boson</i>		
<i>model / matrix element</i>	Y_{TT}	Y_{BB}
\mathcal{U}_1	$s_L^u{}^2$	
\mathcal{D}_1		$s_L^d{}^2$
\mathcal{D}_X	$s_R^u{}^2$	
\mathcal{D}_2	$s_R^u{}^2$	$s_R^d{}^2$
\mathcal{D}_Y		$s_R^d{}^2$
\mathcal{T}_X	$s_L^u{}^2$	$s_L^d{}^2$
\mathcal{T}_Y	$s_L^u{}^2$	$s_L^d{}^2$

5.6 Conclusions

we analyzed the effects of introducing vector-like quarks in the Higgs Triplet Model, allowed to be U -type or D -type singlets (\mathcal{U}_1 , \mathcal{D}_1), SM-like or non SM, U -type or D -type doublets (\mathcal{D}_2 , \mathcal{D}_X , and \mathcal{D}_Y), and U -type or D -type triplets (\mathcal{T}_X and \mathcal{T}_Y). To conserve flavor, the only restriction we imposed was weak mixing with only the third family of ordinary quarks.

We posed the question: how does the introduction of these states affect the electroweak precision variables of the HTM? We were particularly interested in constraints on the mixing of the CP-even neutral Higgs bosons, the masses of the vector-like quarks and the mixing parameters with the ordinary quarks; and the mass of the doubly charged Higgs boson. We review here the constraints obtained in order.

First, the oblique parameters S , T and U were not all equally sensitive to mass parameters.

We concentrated on the T parameter, which showed significant variations with the doubly charged Higgs mass, in the absence of vector-like fermions. The doubly charged mass was restricted in a band around (100-280) GeV, varying very slightly with the triplet VEV, and about 10% with the mixing angle in the neutral Higgs sector. And the contributions of the HTM model to the T parameter were found to be always positive. Addition of vector-like quarks also affects the T parameter. While in models \mathcal{U}_1 , \mathcal{D}_2 , \mathcal{D}_Y , \mathcal{T}_X and \mathcal{T}_Y their contribution is always positive, in models \mathcal{D}_1 , \mathcal{D}_X , there is a region of parameter space where the contribution is negative, thus subtracting from the contribution from the doubly charged Higgs bosons and raising the bound on their masses. We have investigated this in detail for models \mathcal{D}_1 and \mathcal{D}_X , as the negative contribution to the T parameter occurs for a large range of the mixing parameter x_b and x_t . The \mathcal{D}_1 and \mathcal{D}_X models are then distinguishable in this framework, as they require doubly charged Higgs boson masses in the $\sim 280 - 370$ GeV region to satisfy electroweak constraints, while the other models require significantly lighter doubly charged Higgs bosons in the $\sim 100 - 280$ GeV region, some of which are already ruled out by measurements at the LHC. Electroweak precision data also restricts the mixing parameters to $x_b \in (117 - 538)$ GeV for vector-like quark masses $M \sim 1000$ GeV. The lower limit comes from $Zb\bar{b}$ constraints. A different restriction occurs for x_t . First, the Wtb vertex does not impose a lower limit, and second, the range of this parameter decreases when the mass of the vector-like quark mass increases, and $x_t \in (0, 550)$ GeV for $M \sim 1000$ GeV.

The effects of vector-like quark parameters on limits on the doubly charged Higgs boson masses are as follows. In the models \mathcal{U}_1 , \mathcal{D}_2 , \mathcal{D}_Y , \mathcal{T}_X , increasing M and decreasing $x_{t(b)}$ yields a slightly higher upper bound for doubly charged Higgs bosons mass. In the \mathcal{T}_Y model, on the other hand, where very light x_t values are required, decreasing these mixing parameters increases the doubly charged mass bound, and in \mathcal{D}_1 and \mathcal{D}_X models, higher upper limits for $m_{H^{\pm\pm}}$ are obtained for lighter vector-like quark masses M . The overall predictions are nevertheless quite robust with varying the vector-like quark masses.

While the production and decay mechanisms of the vector-like quarks are not modified by the particles in the HTM (as the only new particles, the triplet Higgs bosons, do not couple to quarks), loop-induced decays of the neutral Higgs bosons are affected. Interestingly, while the masses and mixing parameters of the vector-like quarks have little effect on the $H \rightarrow \gamma\gamma$ and $H \rightarrow Z\gamma$ decays, the effects of vector-like quarks come from combining these with constraints from electroweak precision observables.

These observables restrict the doubly charged Higgs boson mass to be in the range of 280-370

GeV for models \mathcal{D}_1 and \mathcal{D}_X , and about 100-280 GeV for the rest of the models. Thus the former two representations are favored by restrictions on the doubly charged mass at ATLAS and CMS. Enhancement of the rates $R_{\gamma\gamma}$ and $R_{Z\gamma}$ are more likely to occur at negative values of $\sin \alpha$, the mixing angle in the neutral Higgs sector. Thus in the HTM, scenarios \mathcal{D}_1 and \mathcal{D}_X stand out as distinguishable from the rest (from doubly charged Higgs boson mass restrictions) and from each other (from regions and strength of possible enhancements in loop dominated Higgs decays).

As a result, introducing vector-like quarks in the Higgs Triplet Model alters the electroweak constraints on the parameters of the model and yields tighter predictions for the enhancement of loop-dominated Higgs decays, expected to be measured even more precisely at the LHC operating at 13 TeV.

Chapter 6

Dark Matter in the Higgs Triplet Model

Abstract

The inability to predict neutrino masses and the existence of the dark matter are two essential shortcomings of the Standard Model. The Higgs Triplet Model provides an elegant resolution of neutrino masses via the seesaw mechanism. We show here that introducing vector-like leptons in the model also provides a resolution to the problem of Dark Matter. We investigate constraints, including the invisible decay width of the Higgs boson and the electroweak precision variables, and impose restrictions on model parameters. We analyze the effect of the relic density constraint on the mass and Yukawa coupling of DM. We also calculate the cross sections for indirect and direct DM detection and show our model predictions for the neutrino and muon fluxes from the Sun, and the restrictions they impose on the parameter space. With the addition of vector-like leptons, the model is completely consistent with DM constraints, in addition to improving electroweak precision and doubly charged mass restrictions, which are rendered consistent with present experimental data.

6.1 Introduction

The LHC discovery of the Higgs boson [29, 154] with properties consistent with that of the Standard Model (SM) Higgs, while providing a spectacular experimental confirmation of the SM, continues to raise questions about SM completeness and about scenarios responsible for

new physics beyond the SM. In addition, noncollider experimental results confront the SM with two major puzzles: neutrino masses and the existence of dark matter.

The phenomenon of neutrino oscillations shows that at least two neutrinos have nonzero but small masses, located around sub-eV scale [36]. The fact that the neutrino flavor structure is so different from that of quarks and leptons is a puzzle and may indicate that neutrinos are Majorana particles. Many models have been proposed to explain tiny neutrino masses. The seesaw mechanism, in which right-handed neutrinos are introduced with large Majorana masses [122, 282–287], is perhaps the simplest way to explain tiny neutrino masses. The most direct way for implementation of this mechanism for generating neutrino masses is to enlarge the particle content of the SM by a complex triplet scalar field, yielding the so-called Higgs Triplet Model (HTM) [120, 121, 123–128, 130, 132–134, 219–222, 237, 288–293]. The neutrino mass problem is resolved at the cost of introducing only this additional Higgs representation, together with its associated vacuum expectation value (VEV), but without extending the symmetry of the model. The triplet scalar field also plays a role in leptogenesis [294].

At the same time, evidence from astrophysics and cosmology indicate that the ordinary baryonic matter is not dominant in the Universe. Rather, about 25% of energy density of the Universe is comprised of a nonluminous and nonabsorbing matter, called dark matter (DM). While current observations indicate that most of the matter in the Universe is nonbaryonic dark matter, they do not provide information on what this dark matter consists of. Since the SM, which has been extremely successful in describing all current collider data, does not contain any dark matter candidates, a great deal of effort has gone into providing viable candidates, or alternatives scenarios (models which include a DM candidate naturally). The latter type of models do so at the expense of extra symmetries and a much enriched particle content. For models lacking natural candidates, a common method is to consider the simplest additions to the SM that can account for the dark matter. In these models, the SM particle content is extended by a small number of fields, and a new discrete symmetry is introduced to guarantee the stability of the dark matter particle. Several variations can be obtained depending on the number and type of new fields [e.g. a scalar, a fermion, or a vector, a singlet or a doublet under $SU(2)_L$, etc.] and on the discrete symmetry imposed (Z_2, Z_3, \dots).

In this chapter, we look at the Higgs Triplet Model for a resolution to both neutrino masses and dark matter problems. The resolution to neutrino masses, alluded to in the above, is well-known [120, 121, 237, 288, 289]. The complex triplet couples to left-handed leptons, yielding Majorana masses for the neutrinos through $L = 2$ lepton flavor violating terms [123–

128, 130, 132–134, 219–222, 290–293], while also contributing to type II leptogenesis [295, 296]. In addition, extra degrees of freedom that couple to the SM Higgs at the tree-level insure cancellation of quadratic divergences to the Higgs mass [297], a mechanism where scalars are favored. Additional support for the model comes from the observation that heavy particles with strong couplings to the Higgs field can strengthen the electroweak phase transition, through the entropy release mechanism from both bosons and fermions [298].

Unfortunately, as it stands, the Higgs Triplet Model lacks a dark matter candidate. Resolutions to this problems were proposed: some with additional Higgs triplets, where the neutral component of the additional (real) Higgs representation can act as a DM candidate [238–241], another where an *additional* $SU(2)_L$ triplet scalar field with hypercharge $Y = 1$ is added [299]. In this chapter, we investigate the possibility that the DM candidate is provided through the introduction of a complete fourth generation of vector-like leptons, comprised of $SU(2)_L$ doublets plus charged and neutral $SU(2)_L$ singlets [97, 300]. A simpler extension of the SM with only one fourth generation vector-like lepton doublet coupling to a triplet Higgs field, which gives Majorana mass to a pseudo-Dirac fourth neutrino has been considered in [202].

Vector-like pairs of fermions, unlike their chiral counterparts, are able to have mass explicitly through the gauge-invariant bilinear interaction in the Lagrangian $M_f f^\dagger f$. There is no reason why such pairs of vector-like fermions do not exist, and many theories—such as string theories and D-brane theories—often give rise generically to vector-like states [245, 246]. Since the mass of the vector-like fermions are not generated through the Yukawa couplings, the loop contributions involving the Higgs decouple faster than for chiral fermions. Thus the constraints from the current Higgs data, precision electroweak observables, and direct searches are less severe for vector-like fermions than for chiral fermions.

Originally, there has been a great deal of interest in vector-like leptons as a resolution to preliminary data indicating an enhanced Higgs decay rate to diphotons, while the Higgs production cross section was in agreement with expectations from the SM. The diphoton rate is increased through loops of mixed vector-like leptons. A vector-like doublet and a vector-like singlet allow for both Yukawa couplings and Dirac masses. The resulting mixing leads to a sign flip of the coupling of the lightest lepton to the Higgs field, yielding constructive interference with the SM amplitude for $h \rightarrow \gamma\gamma$.

This does not have to be so in the Higgs Triplet Model, where contributions from vector-like leptons can be offset by contributions from charged and doubly charged Higgs bosons. However new effects of vector-like leptons can arise. Previous analyses have shown that their

presence affects the mass bounds and decay patterns of the doubly charged Higgs boson [2, 3], improving consistency with the present experimental data.

We extend our previous considerations in Chapters 3 and 4 to explore the possibility that, introducing a new parity symmetry making all new vector-like leptons odd and prohibiting the mixing with the ordinary SM leptons, the lightest particle which is odd under this symmetry (a singlet neutrino) becomes stable on cosmological time scales and could have properties consistent with it being a candidate for the dark matter of the universe. Note that in a simple heavy fourth generation extension of SM, the heavy neutrino does not qualify as a dark matter due to its rapid annihilation to SM particles via Z boson exchange [301]. Leptonic dark matter candidates with unsuppressed couplings to the Z boson, such as ordinary fourth generation neutrinos are also excluded by limits from direct detection [302]. This constraint can be relaxed in the model considered here, as the two singlet neutrinos in the model have no couplings or very small couplings— to the Z boson.

Suppression of the lightest neutrino couplings to the Z boson can also evade present experimental limits from LEP on masses of new charged and neutral particles [36]. Measurements of the Z boson width restrict the number of active neutrinos to three, which further restrict the mass of the new neutrino to $M_N > 39$ GeV for a Majorana, and $M_N > 45$ GeV for a Dirac neutrino, precluding the viability of a neutrino which couples to the Z boson as a candidate for light dark matter. While, as we will show, we can relax these constraints here, the new states will have an effect on the precision electroweak parameters, which we calculate and use to restrict the parameter space. We then analyze the consequences of the model by requiring consistency with the invisible Higgs width and noncollider experimental data, particularly with direct and indirect dark matter searches. The relic density— an indication of the abundance of dark matter in the early universe, as measured by PLANCK satellite [303]— is one of the most stringent constraints on any model of DM, as well as direct detection experiments search for spin-independent (SI) or spin-dependent (SD) interactions with target nuclei, which can be detected by nuclear recoil experiments. Indirect detection experiment searches looking for gamma ray excesses measure the annihilation products of DM, and their predictions must also be tested in a model of DM. Finally, ultrahigh energy neutrino experiments measure the neutrino flux and flavor composition at astrophysical sources. We analyze the predictions for all of these in our model and indicate the constraints on vector-like neutrino mass and coupling which restrict our parameter space.

This chapter is organized as follows. In the next section, Sec. 6.2, we summarize the basic

features of the Higgs Triplet Model with vector-like leptons. We proceed by examining the electroweak precision constraints in the HTM in Sec. 6.3, where we present a numerical analysis on restrictions coming from the oblique parameters on the masses of the doubly charged Higgs bosons and relevant Yukawa coupling. We discuss the invisible decay width of the Higgs boson in Sec. 6.4. Then in Sec. 6.5, we calculate the dark matter relic density and indicate the restrictions it imposes on the mass of the dark matter and on the Yukawa couplings. These restrictions are then applied to the evaluation of the spin-dependent and spin-independent cross sections in the direct detection of dark matter in Sec. 6.6, and of the annihilation cross section of dark matter in Sec. 6.7. We discuss detection of DM at colliders in Sec. 6.8, and then investigate the fluxes of muons and neutrinos from the Sun in Sec. 6.9.

6.2 The Higgs Triplet Model with Vector-like Leptons

Here we review briefly the HTM with vector-like leptons, a more detailed version which has appeared in Chapter 5. The symmetry group of the HTM is the same as that of the SM, with the particle content enriched by (a) the addition of one triplet scalar field Δ with hypercharge $Y = 1$, and with VEV v_Δ :

$$\Delta = \begin{bmatrix} \frac{\Delta^+}{\sqrt{2}} & \Delta^{++} \\ \frac{1}{\sqrt{2}}(\delta + v_\Delta + i\eta) & -\frac{\Delta^+}{\sqrt{2}} \end{bmatrix}, \quad (6.1)$$

and (b) a vector-like fourth generation of leptons¹, to include: one $SU(2)_L$ left-handed lepton doublet $L'_L = (\nu'_L, e'_L)$, right-handed charged and neutral lepton singlets, ν'_R and e'_R ; and the mirror right-handed lepton doublet, $L''_R = (\nu''_R, e''_R)$ and left-handed charged and neutral lepton singlets ν''_L and e''_L , as listed in Table 6.1. Note that v_Δ is kept small by the seesaw mechanism, which requires a generation of small neutrino masses, and by the ρ parameter. In general we can assume, conservatively, $v_\Delta \lesssim 5$ GeV [134, 220].

Table 6.1: Representations of vector-like leptons, together with their quantum numbers under $SU(3)_C \times SU(2)_L \times U(1)_Y$.

Name	\mathcal{L}'_L	\mathcal{L}''_R	e'_R	e''_L	ν'_R	ν''_L
Quantum Number	$(\mathbf{1}, \mathbf{2}, -1/2)$	$(\mathbf{1}, \mathbf{2}, -1/2)$	$(\mathbf{1}, \mathbf{1}, -1)$	$(\mathbf{1}, \mathbf{1}, -1)$	$(\mathbf{1}, \mathbf{1}, 0)$	$(\mathbf{1}, \mathbf{1}, 0)$

¹We assume vector-like quarks to be heavy [36] and decouple them from the spectrum.

The Lagrangian density for this model contains, in addition to the SM terms, kinetic, Yukawa for ordinary leptons, explicit terms for the vector-like leptons, and potential terms:

$$\mathcal{L}_{\text{HTM}} = \mathcal{L}_{\text{kin}} + \mathcal{L}_Y + \mathcal{L}_{\text{VL}} - V(\Phi, \Delta), \quad (6.2)$$

where

$$\mathcal{L}_Y = - [\bar{L}_L^i h_e^{ij} \Phi e_R^j + \text{h.c.}] - [h_{ij} \bar{L}_L^{ic} i\tau_2 \Delta L_L^j + \text{h.c.}], \quad (6.3)$$

are the Yukawa interaction terms for the ordinary leptons, with h_e^{ij} a 3×3 complex matrix, and h_{ij} a 3×3 complex symmetric Yukawa matrix. Additionally, with the vector-like family of leptons as defined above,

$$\begin{aligned} \mathcal{L}_{\text{VL}} = & - [M_L \bar{L}'_L L''_R + M_E \bar{e}'_R e''_L + M_\nu \bar{\nu}'_R \nu''_L + \frac{1}{2} M'_\nu \bar{\nu}'_R{}^c \nu'_R + \frac{1}{2} M''_\nu \bar{\nu}''_L{}^c \nu''_L + h'_E (\bar{L}'_L \Phi) e'_R \\ & + h''_E (\bar{L}''_R \Phi) e''_L + h'_\nu (\bar{L}'_L \tau \Phi^\dagger) \nu'_R + h''_\nu (\bar{L}''_R \tau \Phi^\dagger) \nu''_L + h'_{ij} \bar{L}'_L{}^c i\tau_2 \Delta L'_L + h''_{ij} \bar{L}''_R{}^c i\tau_2 \Delta L''_R \\ & + \lambda^i_E (\bar{L}'_L \Phi) e^i_R + \lambda^i_L (\bar{L}'_L \Phi) e^i_R + \lambda'_{ij} \bar{L}'_L{}^c i\tau_2 \Delta L'_L + \lambda''_{ij} \bar{L}''_R{}^c i\tau_2 \Delta L''_R + \text{h.c.}], \end{aligned} \quad (6.4)$$

is the Yukawa interaction term for vector-like leptons and their interactions with ordinary leptons, and

$$\begin{aligned} V(\Phi, \Delta) = & m^2 \Phi^\dagger \Phi + M^2 \text{Tr}(\Delta^\dagger \Delta) + [\mu \Phi^T i\tau_2 \Delta^\dagger \Phi + \text{h.c.}] + \lambda_1 (\Phi^\dagger \Phi)^2 \\ & + \lambda_2 [\text{Tr}(\Delta^\dagger \Delta)]^2 + \lambda_3 \text{Tr}[(\Delta^\dagger \Delta)^2] + \lambda_4 (\Phi^\dagger \Phi) \text{Tr}(\Delta^\dagger \Delta) + \lambda_5 \Phi^\dagger \Delta \Delta^\dagger \Phi, \end{aligned} \quad (6.5)$$

is the scalar potential for the SM doublet Φ ($\langle \Phi \rangle = \frac{v_\Phi}{\sqrt{2}}$) and triplet Δ Higgs fields. The triplet and doublet Higgs VEVs are related through $v^2 = v_\Phi^2 + 2v_\Delta^2 \simeq (246 \text{ GeV})^2$. The scalar potential in Eq. (6.5) induces mixing among the physical states for the singly charged, the CP-odd, and the CP-even neutral scalar sectors, which are always small $\mathcal{O}(v_\Delta/v_\Phi)$ for the first two sectors, but not necessarily so for the latter one,

$$\begin{pmatrix} \varphi \\ \delta \end{pmatrix} = \begin{pmatrix} \cos \alpha & -\sin \alpha \\ \sin \alpha & \cos \alpha \end{pmatrix} \begin{pmatrix} h \\ H \end{pmatrix}, \quad (6.6)$$

where the mixing angle is given in terms of the parameters in $V(\Phi, \Delta)$ as

$$\tan 2\alpha = \frac{v_\Delta}{v_\Phi} \frac{2v_\Phi^2(\lambda_4 + \lambda_5) - 4(v_\Phi^2 \mu / \sqrt{2} v_\Delta)^2}{2v_\Phi^2 \lambda_1 - (v_\Phi^2 \mu / \sqrt{2} v_\Delta)^2 - 2v_\Delta^2(\lambda_2 + \lambda_3)}. \quad (6.7)$$

In Chapter 3, we showed that the Higgs masses and coupling strengths are consistent with choosing h to be the SM-like state at 125 GeV, while the state H a lighter state, perhaps the

state observed at LEP [111]². The masses of the neutral h and H are given by:

$$m_h^2 = 2v_\Phi^2 \lambda_1 \cos^2 \alpha + \left[(v_\Phi^2 \mu / \sqrt{2} v_\Delta)^2 + 2v_\Delta^2 (\lambda_2 + \lambda_3) \right] \sin^2 \alpha + \left[\frac{v_\Phi^3 \mu^2}{v_\Delta} - v_\Phi v_\Delta (\lambda_4 + \lambda_5) \right] \sin 2\alpha, \quad (6.8)$$

$$m_H^2 = 2v_\Phi^2 \lambda_1 \sin^2 \alpha + \left[(v_\Phi^2 \mu / \sqrt{2} v_\Delta)^2 + 2v_\Delta^2 (\lambda_2 + \lambda_3) \right] \cos^2 \alpha - \left[\frac{v_\Phi^3 \mu^2}{v_\Delta} - v_\Phi v_\Delta (\lambda_4 + \lambda_5) \right] \sin 2\alpha. \quad (6.9)$$

The expressions relating the λ_1 - λ_5 parameters to the Higgs masses can be found in [1]. In particular, the doubly charged Higgs boson mass is:

$$m_{H^{++}}^2 = \frac{v_\Phi^2 \mu}{\sqrt{2} v_\Delta} - v_\Delta^2 \lambda_3 - \frac{\lambda_5}{2} v_\Phi^2 \simeq \left(\frac{\mu}{\sqrt{2} v_\Delta} - \frac{\lambda_5}{2} \right) v_\Phi^2, \quad (6.10)$$

where we used $v_\Delta \ll v_\Phi$. As we choose $v_\Delta = 1$ GeV for consistency with the value of the ρ parameter, the doubly charged mass is approximately $m_{H^{++}} \simeq \left(\mu - \lambda_5 / \sqrt{2} \right)^{1/2}$ (207 GeV). The coupling λ_5 is expected to be ≤ 1 and for light doubly charged masses, the μ parameter is small,³ $\mu \sim v_\Delta \sim \mathcal{O}(\text{GeV})$.

New symmetries can be introduced to restrict the interactions of the vector leptons. For instance, we can impose (i) a symmetry under which all the new $SU(2)$ singlet fields are odd, while the new $SU(2)$ doublets are even, which forces all Yukawa couplings involving new leptons to vanish, $h'_E = h''_E = h'_\nu = h''_\nu = h'_{ij} = h''_{ij} = 0$, and the vector lepton masses arise only from explicit terms in the Lagrangian [97, 300]; and/or (ii) impose a new parity symmetry which disallows mixing between the ordinary leptons and the new lepton fields, under which all the mirror fields are odd, while the others are even [224], such that $\lambda_E^i = \lambda_L^i = \lambda'_{ij} = \lambda''_{ij} = \lambda''_{ij} = 0$. The latter are important for light vector-like leptons, as this scenario would satisfy restrictions from lepton-flavor-violating decays, which otherwise would either force the new leptons to be very heavy, $\sim 10 - 100$ TeV, or reduce the branching ratio for the Higgs into dileptons to 30-40% of the SM prediction. In addition, if all vector-like leptons are odd under this symmetry, the lightest particle can become stable and act as all, or part of, the dark matter in the universe. Thus the assumption (ii) has all the attractive features we like for this analysis, and we adopt it here, while allowing $h'_E, h''_E, h'_\nu, h''_\nu, h'_{ij}, h''_{ij} \neq 0$.

As we concentrate on the possibility that the lightest neutral component of the new vector-like leptons is a dark matter candidate, we are primarily interested in light states. The 2×2

²This scenario was imposed by the requirement of an enhanced diphoton signal for the Higgs of mass 125 GeV, so it can be relaxed here.

³Specifically, for our parameter space $\mu = 0.2$ GeV and $\lambda_5 < 0$.

mass matrix \mathcal{M}_E for the charged sector is defined as [3, 97, 300]

$$(\bar{e}'_L \quad \bar{e}''_L) (\mathcal{M}_E) \begin{pmatrix} e'_R \\ e''_R \end{pmatrix}, \quad \text{with} \quad \mathcal{M}_E = \begin{pmatrix} m'_E & M_L \\ M_E & m''_E \end{pmatrix}, \quad (6.11)$$

with $m'_E = h'_E v_\Phi / \sqrt{2}$ and $m''_E = h''_E v_\Phi / \sqrt{2}$, from the Lagrangian Eq. (6.4). The mass matrix can be diagonalized by two unitary matrices, U^L and U^R as follows:

$$U^{L\dagger} \mathcal{M}_E U^R = \begin{pmatrix} M_{E_1} & 0 \\ 0 & M_{E_2} \end{pmatrix}. \quad (6.12)$$

The mass eigenvalues are (by convention the order is $M_{E_1} > M_{E_2}$)

$$M_{E_1, E_2}^2 = \frac{1}{2} \left[(M_L^2 + m'^2_E + M_E^2 + m''^2_E) \pm \sqrt{(M_L^2 + m'^2_E - M_E^2 - m''^2_E)^2 + 4(m''_E M_L + m'_E M_E)^2} \right], \quad (6.13)$$

while in the neutral sector the mass matrix is

$$\frac{1}{2} (\bar{\nu}'_L \quad \bar{\nu}'_R \quad \bar{\nu}''_R \quad \bar{\nu}''_L) (\mathcal{M}_\nu) \begin{pmatrix} \nu'_L{}^c \\ \nu'_R \\ \nu''_R \\ \nu''_L{}^c \end{pmatrix}, \quad \text{with} \quad \mathcal{M}_\nu = \begin{pmatrix} 0 & m'_\nu & M_L & 0 \\ m'_\nu & M'_\nu & 0 & M_\nu \\ M_L & 0 & 0 & m''_\nu \\ 0 & M_\nu & m''_\nu & M''_\nu \end{pmatrix}, \quad (6.14)$$

with $m'_\nu = h'_\nu v_\Phi / \sqrt{2}$ and $m''_\nu = h''_\nu v_\Phi / \sqrt{2}$. This mass matrix can be diagonalized by a unitary matrix V :

$$V^\dagger \mathcal{M}_\nu V = \begin{pmatrix} M_{\nu_1} & 0 & 0 & 0 \\ 0 & M_{\nu_2} & 0 & 0 \\ 0 & 0 & M_{\nu_3} & 0 \\ 0 & 0 & 0 & M_{\nu_4} \end{pmatrix}. \quad (6.15)$$

In the limit where the explicit mass terms M_L , M_E and M_ν in the interaction Lagrangian vanish, after electroweak symmetry breaking there are two charged leptons with masses m'_E and m''_E , and four Majorana neutrinos with masses:

$$M_{\nu_{1,2}} = \sqrt{\frac{M'^2_\nu}{4} + m'^2_\nu} \pm \frac{M'_\nu}{2} \quad (6.16)$$

$$M_{\nu_{3,4}} = \sqrt{\frac{M''^2_\nu}{4} + m''^2_\nu} \pm \frac{M''_\nu}{2}. \quad (6.17)$$

The lightest of these eigenvalues will be the dark matter candidate and, as it is odd under the additional parity symmetry (*ii*), it is stable. For vanishing h'_ν , h''_ν Yukawa couplings, the two singlet vector-like neutrinos have vanishing couplings with the Z boson. Lifting the

Yukawa couplings slightly from 0 allows mixing between the singlet neutrinos and the neutral components of the doublet vector-like leptons, inducing a (small) coupling to the Z boson. For simplicity, we adopt the scenario in [97, 300] where $h'_\nu \neq 0$, but $h''_\nu = 0$, as well as setting the explicit neutrino mass in the Lagrangian $M_\nu = 0$. This scenario is sufficient to provide a single DM candidate and a single Yukawa coupling, and transparent enough to yield consequences. It corresponds to one neutrino state which does not mix and is sterile [the mirror $SU(2)_L$ doublet ν''_L], while the remaining neutral sector consists of three neutrinos which mix, with mixing matrix in the $(\nu'^c_L, \nu'_R, \nu''_R)$ basis given by

$$\mathcal{M}_{3\nu} = \begin{pmatrix} 0 & m'_\nu & M_L \\ m'_\nu & M'_\nu & 0 \\ M_L & 0 & 0 \end{pmatrix}. \quad (6.18)$$

The Yukawa coupling h'_ν must remain small to insure smallness of couplings to the Z boson. In the limit $h'_\nu = 0$, the matrix has two degenerate eigenvalues of mass M_L , predominantly $SU(2)_L$ doublets, and one state with mass M'_ν and predominantly singlet. For $h'_\nu \neq 0$, these three states mix, generating a small mixing coupling to the Z boson. The lightest neutrino state M_{ν_1} emerges as being dominantly ν'_R and is the dark matter candidate. For the charged lepton sector, we take $M_L = 205$ GeV and $M_E = 300$ GeV and $h'_E = h''_E = 0.8$ [97, 300]. In this case the lightest charged lepton will be $M_{E_2} \sim 108$ GeV, close to the LEP limit, $M_E > 102.6$ GeV [36]— which imposes an upper limit on the mass of the dark matter candidate, $M_{DM} \equiv M_{\nu_1} < M_{E_2}$.

Next, we analyze the effects of the new states on electroweak precision observables in the HTM and, consequently the restrictions imposed on its parameter space.

6.3 Vector-like lepton contributions to the S and T parameters

Adding new particles to the model spectrum affects quantum corrections on the propagators of W and Z bosons. The corrections are parametrized by two oblique parameters, S and T ,⁴ which encapsulate the model restrictions coming from electroweak precision data. For a

⁴We set $U = 0$.

Higgs state with mass $m_h = 125$ GeV, the allowed ranges are [134, 220]

$$\begin{aligned}\Delta S &= S - S_{\text{SM}} = 0.05 \pm 0.09, \\ \Delta T &= T - T_{\text{SM}} = 0.08 \pm 0.07,\end{aligned}\tag{6.19}$$

with errors correlated by a factor of 0.88. The explicit expressions for the S , T and U parameters for the HTM are given in Chapter 5. The addition of vector-like leptons modifies these by the following contributions. For the S parameter [97, 300]:

$$\begin{aligned}S &= \frac{1}{\pi} \left\{ \sum_{j,k=1}^2 (|U_{1j}^L|^2 |U_{1k}^L|^2 + |U_{2j}^R|^2 |U_{2k}^R|^2) b_2(M_{E_j}, M_{E_k}, 0) + \sum_{j,k=1}^2 \text{Re}(U_{1j}^L U_{1k}^{L*} U_{2j}^{R*} U_{2k}^R) f_3(M_{E_j}, M_{E_k}) \right. \\ &+ \sum_{j,k=1}^3 (|V_{1j}|^2 |V_{1k}|^2 + |V_{3j}|^2 |V_{3k}|^2) b_2(M_{\nu_j}, M_{\nu_k}, 0) + \sum_{j,k=1}^3 \text{Re}(V_{1j} V_{1k}^* V_{3j} V_{3k}^*) f_3(M_{\nu_j}, M_{\nu_k}) \\ &\left. - 2 \sum_{j=1}^2 (|U_{1j}^L|^2 + |U_{2j}^R|^2) b_2(M_{E_j}, M_{E_j}, 0) + \frac{1}{3} \right\},\end{aligned}\tag{6.20}$$

while the oblique correction parameter T for vector-like leptons is [97, 300]:

$$\begin{aligned}T &= \frac{1}{4\pi s_W^2 c_W^2 M_Z^2} \left\{ -2 \sum_{j=1}^2 \sum_{k=1}^3 (|U_{1j}^L|^2 |V_{1k}|^2 + |U_{2j}^R|^2 |V_{3k}|^2) b_3(M_{\nu_k}, M_{E_j}, 0) \right. \\ &+ 2 \sum_{j=1}^2 \sum_{k=1}^3 \text{Re}(U_{1j}^L U_{2j}^{R*} V_{1k} V_{3k}^*) M_{E_j} M_{\nu_k} b_0(M_{E_j}, M_{\nu_k}, 0) \\ &+ \sum_{j,k=1}^3 (|V_{1j}|^2 |V_{1k}|^2 + |V_{3j}|^2 |V_{3k}|^2) b_3(M_{\nu_j}, M_{\nu_k}, 0) \\ &- \sum_{j,k=1}^3 \text{Re}(V_{1j} V_{1k}^* V_{3j} V_{3k}^*) M_{\nu_j} M_{\nu_k} b_0(M_{\nu_j}, M_{\nu_k}, 0) \\ &+ (|U_{11}^L|^4 + |U_{21}^R|^4) M_{E_1}^2 b_1(M_{E_1}, M_{E_1}, 0) + (|U_{12}^L|^4 + |U_{22}^R|^4) M_{E_2}^2 b_1(M_{E_2}, M_{E_2}, 0) \\ &+ (2|U_{11}^L|^2 |U_{21}^L|^2 + 2|U_{12}^R|^2 |U_{22}^R|^2) b_3(M_{E_1}, M_{E_2}, 0) \\ &\left. - \sum_{j,k=1}^2 \text{Re}(U_{1j}^L U_{1k}^{L*} U_{2j}^{R*} U_{2k}^R) M_{E_j} M_{E_k} b_0(M_{E_j}, M_{E_k}, 0) \right\},\end{aligned}\tag{6.21}$$

where the Passarino-Veltman functions are

$$b_0(M_1, M_2, q^2) = \int_0^1 \log\left(\frac{\Delta}{\Lambda^2}\right) dx, \quad (6.22)$$

$$b_1(M_1, M_2, q^2) = \int_0^1 x \log\left(\frac{\Delta}{\Lambda^2}\right) dx, \quad (6.23)$$

$$b_2(M_1, M_2, q^2) = \int_0^1 x(1-x) \log\left(\frac{\Delta}{\Lambda^2}\right) dx = b_2(M_2, M_1, q^2), \quad (6.24)$$

$$b_3(M_1, M_2, 0) = \frac{M_2^2 b_1(M_1, M_2, 0) + M_1^2 b_1(M_2, M_1, 0)}{2}, \quad (6.25)$$

$$f_3(M_1, M_2) = M_1 M_2 \frac{M_2^4 - M_1^4 + 2M_1^2 M_2^2 \log\left(\frac{M_1^2}{M_2^2}\right)}{2(M_1^2 - M_2^2)^3}. \quad (6.26)$$

We defined $\Delta = M_2^2 x + M_1^2(1-x) - x(1-x)q^2$ and, in the above, Λ^2 is an arbitrary regularization scale that will not affect physical observables. The function $f_3(M_1, M_2) = -1/6$ remains well defined in the limit $M_2 \rightarrow M_1$. As in the HTM without vector-like leptons, the S parameter does not impose any restrictions on the parameter space of the model, while the T parameter is very restrictive. The reason is that T depends quadratically on mass differences, while S only logarithmically.

We proceed to analyze restrictions on the relevant masses and couplings in the model coming from the T parameter. In Fig. 6.1 we show the effects on the T parameter as a contour in a $m_{H^{\pm\pm}} - \sin \alpha$ plane (with $\sin \alpha$ being the mixing angle in the neutral Higgs sector) for two values of dark matter masses, $M_{DM} = 30$ GeV and $M_{DM} = 50$ GeV. The allowed values for this parameter, $-0.2 < \Delta T < 0.4$, are given in the code bars (colored contours in the figure). The maximum doubly charged mass values allowed are $m_{H^{\pm\pm}} \sim (280 - 290)$ GeV for dark matter masses in 24-30 GeV and 70-90 GeV regions, and approximately 250-270 GeV for dark matter masses in 30-70 and 90-103 GeV range. We have selected the particular values for $M_{DM} = 30$ GeV and $h'_\nu = 0.65$ (left panel) and $M_{DM} = 50$ GeV and $h'_\nu = 0.28$ (right panel) to belong to the parameter space where the relic density is within experimental bounds, as explained in detail in Sec. 6.5. As the figure indicates, the T parameter depends only slightly on $\sin \alpha$, but is extremely sensitive to the mass of the doubly charged Higgs boson. In our model, we set $m_h = 125$ GeV, $m_H = 98$ GeV and $v_\Delta = 1$ GeV as we discussed in Chapter 3.

In Fig. 6.2 we show the variation of the T parameter as a contour in an $m_{H^{\pm\pm}} - h'_\nu$ plane (left panel) and $h'_\nu - \sin \alpha$ (middle and right panels). For the left panel, we chose an illustrative example with $M_{DM} = 30$ GeV and $\sin \alpha = 0.5$; the T parameter does not depend sensitively on varying these, but again it is very sensitive to the mass of the doubly charged Higgs boson,

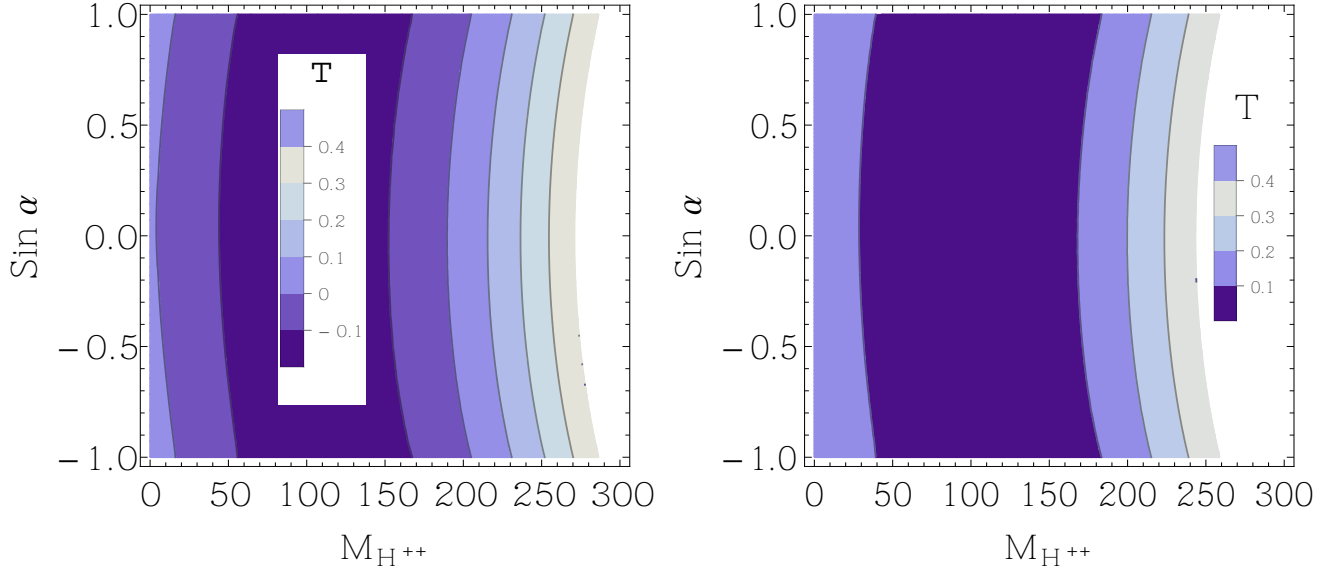


Figure 6.1: Contour graphs showing the contribution to the T parameter in the HTM (as given in the code bars) with vector-like leptons, as a function of the doubly charged Higgs mass $m_{H^{\pm\pm}}$ and the mixing angle $\sin \alpha$, for fixed values of the neutrino Yukawa coupling h'_ν . We take (left panel) $M_{DM} = 30$ GeV, $h'_\nu = 0.65$, (right panel) $M_{DM} = 50$ GeV, $h'_\nu = 0.28$. The allowed range of T parameter is $-0.2 < \Delta T < 0.4$. The white region represents the parameter region ruled out by the constraints.

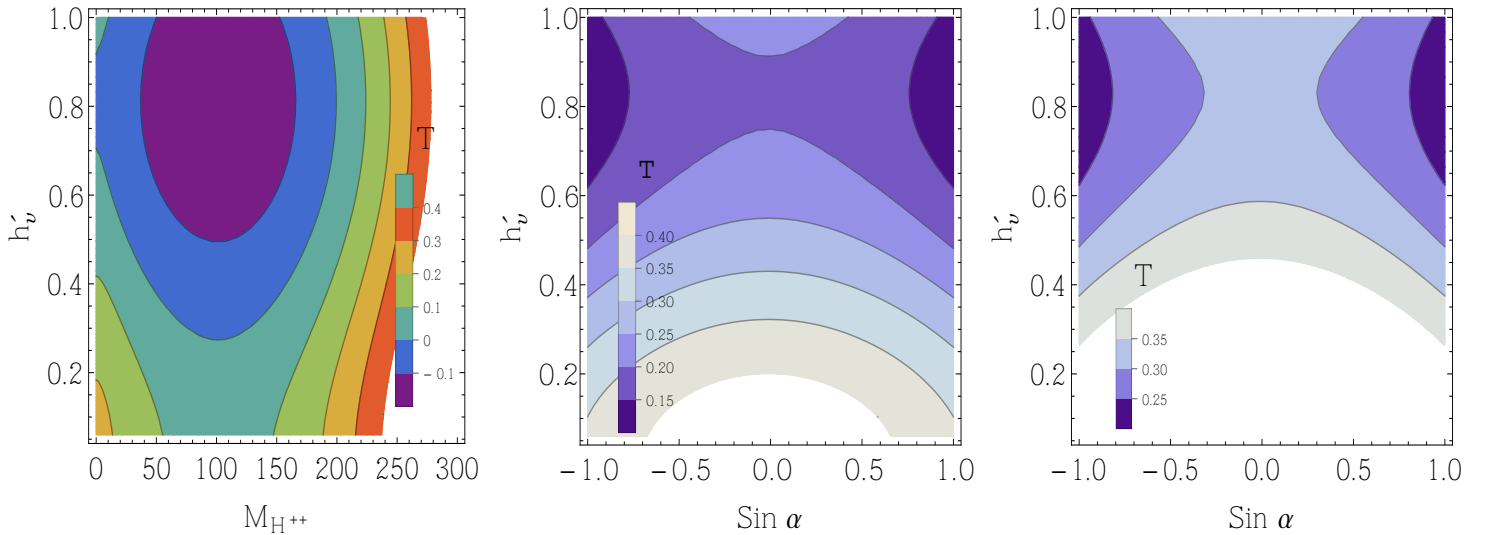


Figure 6.2: Contour graphs showing the contribution to the T parameter in the HTM with vector-like leptons (values as given in the code bars, within the allowed range $-0.2 < \Delta T < 0.4$.) as a function of the parameters of the model. In the left plot, we show the combined dependence on h'_ν and $m_{H^{\pm\pm}}$ (for $M_{DM} = 30$ GeV and $\sin \alpha = 0.5$); in the middle (right) panel, the dependence on h'_ν and $\sin \alpha$ for $M_{DM} = 50$ GeV and $m_{H^{\pm\pm}} = 240$ GeV ($m_{H^{\pm\pm}} = 260$ GeV). The white region represents the parameter region ruled out by the constraints.

as shown in the middle and right side panels, where increasing the value of $m_{H^{\pm\pm}}$ from 240 to 260 GeV places significant restrictions on the T parameter. Increasing the mass of the doubly charged Higgs boson and decreasing $\sin \alpha$ (the mixing angle) impose restrictions on h'_ν (the vector-like neutrino Yukawa coupling) from the T parameter. Note that the T parameter is not sensitive to the mass of the dark matter candidate and it affects it only indirectly, through the restrictions on the Yukawa couplings.

6.4 Invisible decay width of the Higgs boson

The existence of the vector-like neutrino ν_1 as a dark matter candidate will have an effect on the branching ratio of the Higgs boson, if $m_h \geq 2M_{\nu_1}$. Given that ν_1 is stable, the decays $h \rightarrow \nu_1\nu_1$, $h \rightarrow \nu_1\bar{\nu}_1$ will contribute to the invisible Higgs branching ratio, which is constrained by combined CMS and ATLAS measurements to be $BR_{\text{inv}} < 58\%$ for a SM Higgs with a mass of 125 GeV [304–307], and more stringently by global fits to be $BR_{\text{inv}} < 29\%$ with 95% C.L. [308, 309].

In the Higgs Triplet Model, the tree-level decay width of the Higgs boson into vector-like neutrinos is [1, 310]

$$[\Gamma(h \rightarrow \nu_1\bar{\nu}_1)]_{HTM} = \frac{G_F m_h (M_{\nu_1} C_{\nu_1\bar{\nu}_1}^h)^2}{2\pi\sqrt{2}} \left(1 - \left(\frac{2M_{\nu_1}}{m_h}\right)^2\right)^{\frac{3}{2}} \cos^2 \alpha, \quad (6.27)$$

where

$$C_{\nu_1\bar{\nu}_1}^h = \sqrt{2} h'_\nu \text{Re}(V_{11}V_{21}) \quad (6.28)$$

is the Higgs coupling to the lightest vector-like neutrino (ν_1). In addition, the component from the neutral triplet Higgs field violates lepton number and can decay into two neutrinos as

$$\begin{aligned} [\Gamma(h \rightarrow \nu_1\nu_1)]_{HTM} &\equiv \Gamma(h \rightarrow \nu_1^c\bar{\nu}_1) + \Gamma(h \rightarrow \bar{\nu}_1^c\nu_1) \\ &= \frac{1}{2} |h'_{\nu_1\nu_1}|^2 \frac{m_h}{4\pi} \left(1 - 2\frac{M_{\nu_1}^2}{m_h^2}\right) \left(1 - 4\frac{M_{\nu_1}^2}{m_h^2}\right)^2 \sin^2 \alpha, \end{aligned} \quad (6.29)$$

where $h'_{\nu_1\nu_1}$ is the triplet coupling constant from Eq. (6.4). The invisible branching ratio of the Higgs boson is defined as

$$BR_{\text{inv}} = \frac{[\Gamma(h \rightarrow \nu_1\bar{\nu}_1)]_{HTM} + [\Gamma(h \rightarrow \nu_1\nu_1)]_{HTM}}{[\Gamma(h \rightarrow \nu_1\bar{\nu}_1)]_{HTM} + [\Gamma(h \rightarrow \nu_1\nu_1)]_{HTM} + [\Gamma(h)]_{HTM}}, \quad (6.30)$$

where $[\Gamma(h)]_{HTM}$ is the total Higgs decay width in the HTM without vector-like leptons.

In Fig. 6.3, we show the invisible branching ratio of the Higgs boson (BR_{inv}) in the HTM with vector-like leptons as a contour plot in an $M_{DM} - h'_\nu$ plane, for triplet Yukawa coupling $h'_{\nu_1\nu_1} = 0.01$. We compare the calculation with the upper limit on BR_{inv} derived from global fits to ATLAS and CMS data [308, 309].⁵ As expected, the region restricted is only for $M_{DM} < m_h/2$, where the Higgs can decay to pairs of dark matter with a sizeable width. The left panel depicts the invisible width for the mixing angle in the neutral CP-even Higgs sector, $\sin \alpha = 0.1$, the middle panel for $\sin \alpha = 0.5$ and the right panel for $\sin \alpha = 0.8$. The figures show that increasing the Yukawa coupling (h'_ν) results in an increase of the invisible branching ratio of Higgs boson (BR_{inv}) as the decay into DM is enhanced, while decreasing $\sin \alpha$ imposes more restrictions on h'_ν in order to get the correct BR_{inv} , indicating that both the doublet and triplet Higgs components play an important role in the invisible decay.

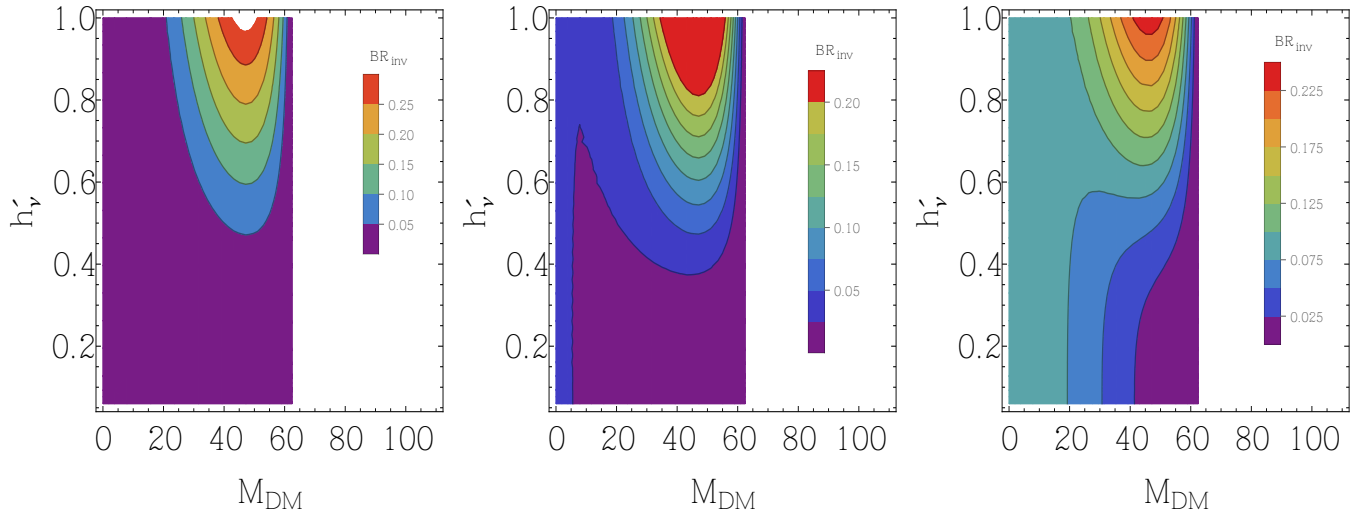


Figure 6.3: Contour graphs showing the invisible branching ratio of Higgs boson (BR_{inv}) in the HTM with vector-like leptons, as functions of the dark matter mass $M_{DM} = M_{\nu_1}$ (GeV) and the neutrino Yukawa coupling h'_ν , for $h'_{\nu_1\nu_1} = 0.01$. We compare our results to the upper limit of $BR_{\text{inv}} = 29\%$ from global fits to ATLAS and CMS data [308, 309] and we chose $\sin \alpha = 0.1$ (left panel), $\sin \alpha = 0.5$ (middle panel), $\sin \alpha = 0.8$ (right panel). If the mass of DM neutrino is in the white region, it does not contribute to the Higgs invisible decay width.

⁵These global fits, though more restrictive, are completely consistent with our analyses and do not restrict the parameter space unnecessarily.

6.5 Dark Matter Relic Density

Global fits to a number of cosmological data (cosmic microwave background, large scale structure and type Ia supernovae) determine very precisely the amount of non-baryonic DM in the energy content of the universe at $\Omega_{DM}h^2 = 0.1123 \pm 0.0035$ [311], where Ω_{DM} is the energy density of the DM with respect to the critical energy density of the universe, and h is the reduced Hubble parameter. Any analysis of DM must correctly replicate this value.

To this end, we used CalcHEP [312] to implement the Lagrangian of the HTM with vector-like leptons into micrOMEGAs [313], which we used to calculate the relic density ($\Omega_{DM}h^2$), spin-dependent cross section (σ^{SD}), spin-independent cross section (σ^{SI}), annihilation cross section ($\langle\sigma v\rangle$), and the flux of neutrino and muon predicted by the model. For the purpose of comparison with the data, we consider the 2σ allowed range of relic density: $0.1144 \leq \Omega_{DM}h^2 \leq 0.1252$, as constrained by WMAP [311] and Planck [303].

In Fig. 6.4, we present the allowed range of relic density of dark matter as a function of the dark matter mass M_{DM} (GeV) and the Yukawa coupling h'_ν , for two different values of the mixing angle, $\sin\alpha = 0$ (left panel) and $\sin\alpha = 0.8$ (right panel). Because of resonant annihilation into Z bosons or Higgs boson h respectively, we can see two dips at $M_{DM} \sim 45$ GeV and $M_{DM} \sim 62$ GeV. For a fixed Yukawa coupling (h'_ν) the cross sections becomes enhanced at the Z pole and similarly at the Higgs pole, with a dominant decay into quark/antiquark. As the dark matter relic density is inversely proportional to the annihilation cross section, the relic density decreases in these regions. Thus, in order to produce the correct dark matter relic density, we need to decrease the value of Yukawa coupling h'_ν to compensate for the effects of Z and h resonances, which produces the two dips at $M_{DM} = M_Z/2$ and $M_{DM} = m_h/2$. Above $M_{DM} = 80$ GeV annihilation into W^+W^- pairs (and later also Z bosons) becomes kinematically accessible. Finally, the relic density becomes dramatically suppressed for $M_{DM} \sim 100$ GeV due to coannihilation with the lightest charged vector-like lepton [97, 300, 310]. The effect of the Higgs resonance at $M_{DM} \sim 62$ GeV is slightly more pronounced for $\sin\alpha = 0$ than for $\sin\alpha = 0.8$ (this is the effect of increasing the triplet component contribution) and, above $M_{DM} = 80$ GeV, for $\sin\alpha = 0.8$, the relic abundance decrease is slightly more pronounced than in the case with $\sin\alpha = 0$, but the changes are small. Overall, the graph for $\sin\alpha = 0.8$ shows no marked difference from the one with $\sin\alpha = 0$. The results shown are for $m_{H^{\pm\pm}} = 240$ GeV. We calculated relic density for different values of the doubly charged Higgs boson mass and found that it is insensitive to variations in this parameter. Relic density constraints restrict the dark matter mass to be heavier than 23 GeV and lighter than 103

GeV in our model, independent of any other parameters, such as Yukawa couplings or mixing angles.

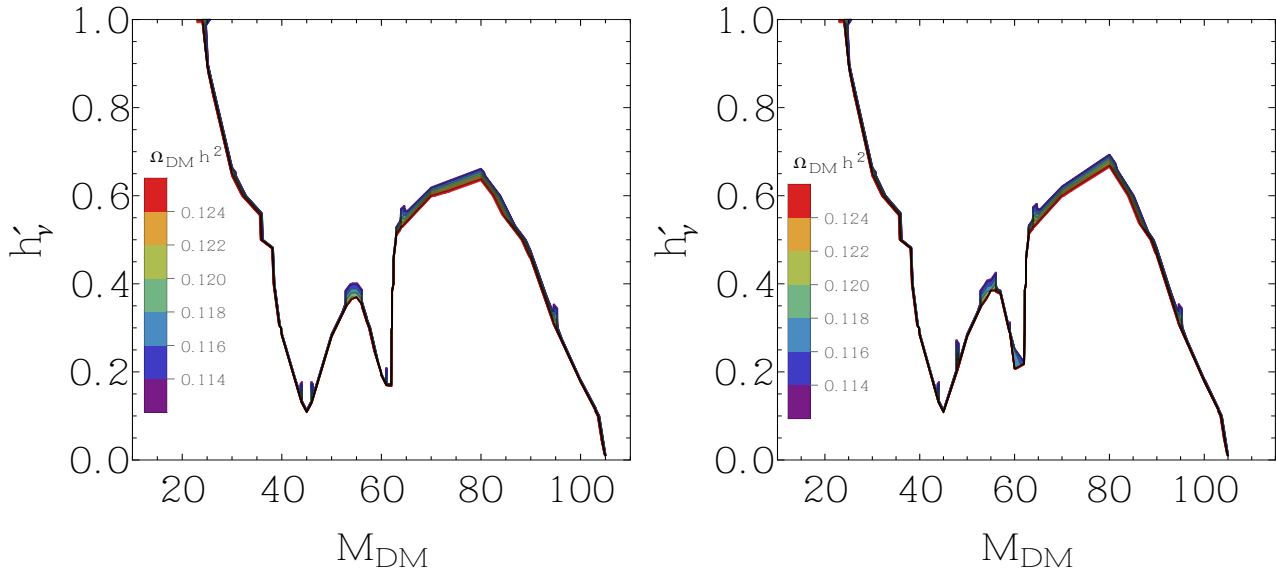


Figure 6.4: Contour graphs showing the correct relic density of dark matter, as a function of the dark matter mass M_{DM} (in GeV) and the neutrino Yukawa coupling h'_ν in the HTM with vector-like leptons, for $\sin \alpha = 0$ (left panel), and $\sin \alpha = 0.8$ (right panel). We impose the restriction $0.1144 \leq \Omega_{DM} h^2 \leq 0.1252$. The relic density is insensitive to the doubly charged Higgs boson mass, chosen here to be 240 GeV.

6.6 Direct Detection

Dark Matter is spread over the whole universe. This provides the opportunity to detect it as it passes through and scatters off normal matter (neutrons or protons), producing detectable signals. Though direct detection is the most straightforward method of detecting DM, such events are very rare, the deposited energies very small; and thus direct detection requires very sensitive detectors with highly accurate background rejection. The expected signals depend on the nature of the DM. For vector-like neutrinos, annihilation through the Higgs or Z boson exchange is expected to yield significant rates for direct detection. The interaction of DM with nuclear matter can be classified as elastic or inelastic, and as spin-dependent or spin-independent.

In elastic scattering the DM interacts with the nucleus as a whole, causing the nucleus to recoil, while in inelastic scattering some of the energy goes into recoil and some is used to excite the nucleus to a higher energy state, from where it decays by emitting a photon. The dark

matter detection experiments (DAMA/LIBRA [314], CoGeNT [315] and CRESST-II [316]) have reported signals consistent with a light DM candidate and with an elastic cross section with nucleons of $\mathcal{O}(10^{-41} - 10^{-40}\text{cm}^2)$.

In spin-dependent (axial vector) scattering, the DM spin couples with the spin of the nucleon, while in spin-independent (scalar) scattering, the cross section does not depend on spin, and thus it is larger for larger nuclei because of the coherence of DM interacting with the nucleus as a whole. We analyze the predictions of our model for the spin-dependent and spin-independent cross sections in turn, and compare them with the experimental constraints.

In Fig. 6.5, in the upper panels, we present the SD cross section of dark matter scattering off nucleons, as a function of the dark matter mass M_{DM} for $\sin \alpha = 0$. The left panel is for the proton, the right one for the neutron. The red lines show points of the parameter space, with restricted M_{DM} and h'_{ν} values, which reproduce acceptable relic density. The areas above the pink dashed line and green dashed-dotted line are ruled out by the COUPP [317] and XENON100 [318] measurements, respectively. As the plots show, to obtain the correct relic density, the resonantly enhanced annihilation rate implies a suppressed Yukawa coupling for the neutrino DM, which leads to a suppressed cross section. Here again we observe the two dips surrounding the Z resonance and the h resonance. The limits on the SD cross section from COUPP and XENON100 results do not restrict the parameter space of our model. In the bottom panel, we plot contour graphs for the spin-dependent cross sections of the nucleon as functions of the dark matter mass M_{DM} and Yukawa coupling h'_{ν} , for $\sin \alpha = 0$. Again we show the spin-dependent cross section of the proton and neutron in the left and right panel, respectively. All points are consistent with experimental bounds from XENON100 on the spin-dependent nucleon cross sections, as indicated by the color-coded panels, but only parameter points situated along the dash-dotted yellow lines in the bottom panels give the correct dark matter relic density. These cross sections are not sensitive to variations in $\sin \alpha$.

In Fig. 6.6, we plot the SI cross section of nucleon, as a function of the dark matter mass M_{DM} (in GeV) for $\sin \alpha = 0$ (left panel). The red line includes all points yielding consistent relic density. The regions above dash-dotted black line, dash-dotted green line, dash-dotted orange line, dash-dotted blue line, dash-dotted purple line, dash-dotted pink line are ruled out by XENON100 [319,320], XENON100 with 2σ expected sensitivity, CRESST-II [316], CDMS-II [321], TEXONO [322] and DAMIC100 (expected for 2014) [323] results, respectively. The cross section is enhanced at the Z pole and h pole and there, for a suppressed direct rate,

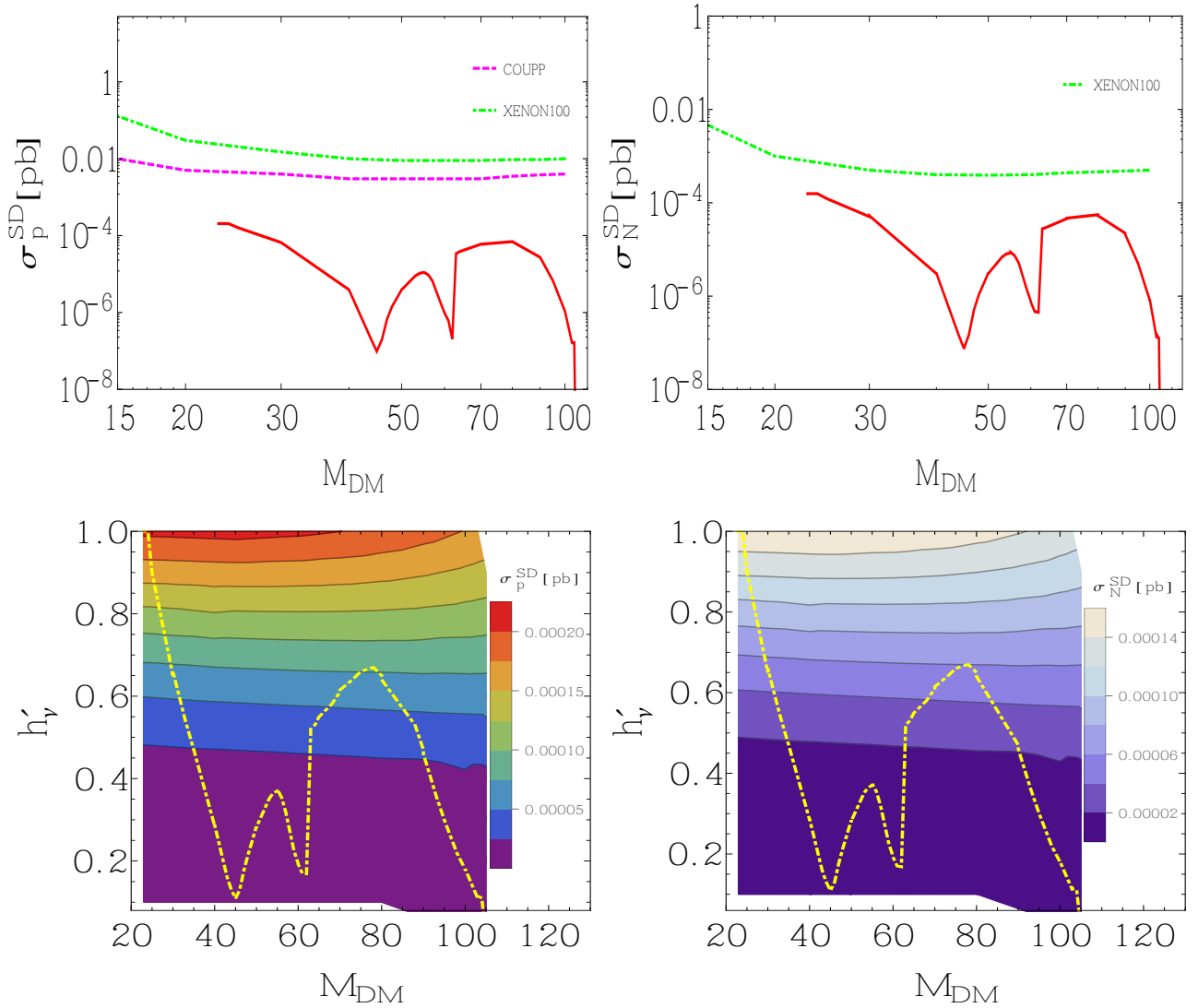


Figure 6.5: (Top panel) The spin-dependent cross section of the nucleon in the HTM with vector-like leptons, as a function of the dark matter mass M_{DM} (GeV) for $\sin \alpha = 0$. We show (left panel) the spin-dependent cross section of the proton (red line) with XENON100 (dash-dotted green) and COUPP (dashed pink) [318] results, (right panel) the spin-dependent cross section of the neutron (red line) with XENON100 (dash-dotted green) results [318]. The area above the pink dashed line and green dash-dotted line are ruled out by the COUPP and XENON100 results, respectively. (Bottom panels) Contour plots showing the spin-dependent cross section of the nucleons in the HTM with vector-like leptons, as functions of the dark matter mass M_{DM} and Yukawa coupling h'_ν , for $\sin \alpha = 0$. We show the spin-dependent cross section of the proton (left panel) and the spin-dependent cross section of the neutron (right panel). The panels at the right indicate the color-coded values of the cross section along each slice, and the dash-dotted yellow line represents the only parameter points with acceptable relic density, $0.1144 \leq \Omega_{DM} h^2 \leq 0.1252$.

the Yukawa coupling must be suppressed to compensate for the resonant production effect. This is seen as two dips at $M_{DM} \sim M_Z/2$ and $M_{DM} \sim m_h/2$. The limit on the SI cross section from XENON100 strongly constrains our model, while the updated results from the other experimental results do not restrict the parameter space. As the left panel of the figure shows, XENON100 results (with 2σ expected sensitivity) restrict the dark matter mass to be in the 37-52 GeV, or 57-63 GeV ranges, or heavier than 95 GeV. In the middle panel, we show the spin-independent cross section of the proton as a graph in $M_{DM} - h'_\nu$ space, constrained by all the experiments with the exception of XENON100, while in the right panel we include XENON100 (with 2σ expected sensitivity) measurements. The latter rules out large regions of parameter space (in white), while in both panels colored contours (as coded in the attached bars) are allowed by the spin-independent experiments. In both the middle and right panels, the dash-dotted line represents the only parameter points with acceptable relic density. Note here that, in agreement with the left panel, there are regions of the parameter space where no combination of M_{DM} and h'_ν satisfy *both* relic density *and* XENON100 SI cross section restrictions. Here too, the cross sections are not sensitive to the mixing angle or to other parameters in the model.

6.7 Indirect Detection

Pairs of dark matter particles annihilate, producing high-energy particles (antimatter, neutrinos or photons). Indirect detection experiments for dark matter look for signatures of annihilations of DM originating from particles in the flux of cosmic rays and are sensitive to DM interactions with all the SM particles. The most stringent constraints on DM annihilation cross sections have been derived from the Fermi Gamma-ray Space telescope (Fermi-LAT) [324], used to search for DM annihilation products from dwarf spheroidal galaxies and the Galactic Center, which probe annihilation cross sections into photons of $\langle\sigma v\rangle \sim 3 \times 10^{-26} \text{cm}^3/\text{s}$. These searches have attracted a lot of attention due to the unexpected high flux of cosmic ray positrons observed by the PAMELA experiment [325], and confirmed by AMS [326].

We test our model predictions and compare them to the experimental results.

In Fig. 6.7, we present the annihilation cross section of DM as a function of the dark matter mass M_{DM} and compare it with the constraints on the dark matter annihilation cross section for the e^+e^- channel, $\mu^+\mu^-$ channel, $\tau^+\tau^-$ channel, $u\bar{u}$, $b\bar{b}$ channel, and W^+W^- channel at 95% CL, derived from a combined analysis of 15 dwarf spheroidal galaxies from Fermi-LAT

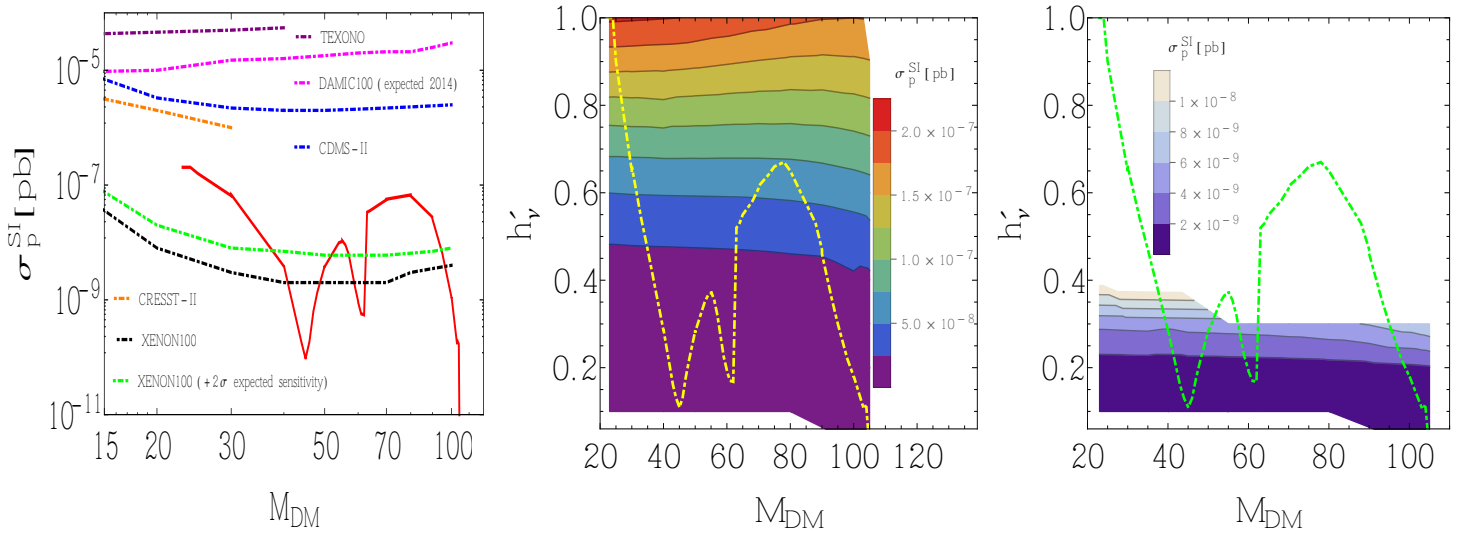


Figure 6.6: (Left panel) The spin-independent cross section of the proton as a function of the dark matter mass M_{DM} (GeV) in the HTM (red line). We also show restrictions from XENON100 [319] (dash-dotted black) XENON100 with 2σ expected sensitivity (dash-dotted green), CRESST-II [316] (dash-dotted orange), CDMS-II [321] (dash-dotted blue), TEXONO [322] (dash-dotted purple) and DAMIC100 (expected in 2014) [323] (dash-dotted pink) results. (Middle panel) Contour graph showing the spin-independent cross section of nucleon in the HTM with vector-like leptons, as function of the dark matter mass M_{DM} and h'_ν , for $\sin \alpha = 0$, considering all experimental constraints except XENON100. (Right panel) Same as the middle panel, but including constraints for XENON100 (with $+2\sigma$ expected sensitivity) [319] upper limit. The values of the cross section are indicated on the attached color bar. The contours indicate points consistent with the respective experimental constraints, while the dash-dotted line includes only points with acceptable relic density, $0.1144 \leq \Omega_{DM} h^2 \leq 0.1252$, some of which are ruled out by XENON100.

Collaboration results [327] (left panel). As the figure shows, the limit on the annihilation cross section from Fermi-LAT Collaboration results imposes some restrictions on our model parameters. Again, the annihilation cross section is enhanced at the Z pole around $M_{DM} = M_Z/2$. The regions around $M_{DM} = M_Z/2$ can be brought into agreement with the relic density constraint by modifying the Yukawa coupling h'_ν . In order to include the regions where the annihilation cross section is enhanced, we need to decrease the value of Yukawa coupling. A suppressed coupling leads to suppression of the annihilation rates [97, 300, 310]. The effect of the Higgs pole at $M_{DM} \sim m_h/2$ is more dramatic than the effect of the Z pole. The dominant annihilation modes of dark matter pair in this region are coming from decays into quark/antiquark (mainly $b\bar{b}$, which gives a relative contribution of $\sim 77\%$ to $1/\Omega_{DM}h^2$) and also a small contribution from $c\bar{c}$ and $\tau\bar{\tau}$ to obtain the correct dark matter relic density. In the right panel, we show the annihilation cross section as a contour plot in the dark matter mass M_{DM} and Yukawa coupling h'_ν plane. Here, as in the previous figures, the contours, according to the color-coding in the attached bar, represent the regions of the parameter space consistent with the experimental results, while the white regions are excluded. Only points along the dash-dotted line have acceptable relic density.

6.8 Detection at Particle Colliders

If dark matter has significant coupling to nuclear matter it can be produced in high energy collisions at LHC or at future colliders. Once produced, as it is neutral and weakly interacting, DM will not be observed directly, but it could be inferred from missing transverse momentum. Collider searches provide the opportunity to study DM production in a controlled environment. They are particularly sensitive to the region of low mass dark matter, where backgrounds are smaller. At the LHC, dark matter can be produced directly, together with additional radiation from the quarks or gluons participating in the reaction, which results in a single jet (monojet) plus missing momentum. High energy lepton colliders could create dark matter through a similar process. Assuming DM couples to quarks and gluons and couplings the order of the electroweak size, LHC excludes DM masses up to 500 GeV and for DM coupling to electrons with the same-size couplings, LEP excludes DM with mass below 90 GeV. Neither of these restrictions are applicable here, as vector-like neutrinos do not couple directly to either quarks or leptons.

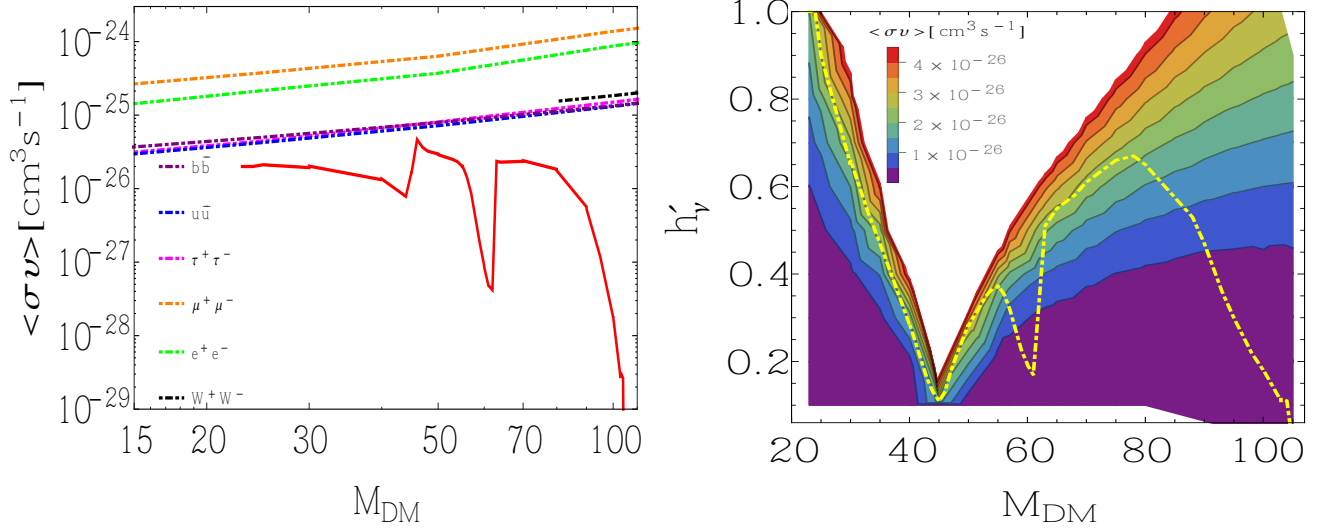


Figure 6.7: (Left panel) The annihilation cross section of DM as a function of the dark matter mass M_{DM} (GeV) (red line). We show the constraints on the dark matter annihilation cross section for the e^+e^- channel (dash-dotted green), $\mu^+\mu^-$ channel (dash-dotted orange), $\tau^+\tau^-$ channel (dash-dotted pink), $u\bar{u}$ (dash-dotted blue), $b\bar{b}$ channel (dash-dotted purple) and W^+W^- channel (dash-dotted black) at 95% C.L. derived from the combined analysis from Fermi-LAT Collaboration [327]. (Right panel) Contour plot showing the annihilation cross section as a function of the dark matter mass M_{DM} and its Yukawa coupling h'_ν . The contours are consisted with the experimental values for the cross sections, indicated by the color-coded bar, while the white regions are ruled out. Only points along the dash-dotted yellow line give the correct dark matter relic density, $0.1144 \leq \Omega_{DM} h^2 \leq 0.1252$.

6.9 The Flux of Muons and Neutrinos from the Sun

DM particles captured by the Sun/Earth, concentrate in the center of the Sun/Earth and then annihilate into SM particles. These SM particles further decay producing neutrinos that can be observed at the Earth [328]. The recent observations of ultra-high energy neutrino events at IceCube [329] seem to indicate a possible deficit in the muon track (known as the muon deficit problem) and an apparent energy gap in the three-year high energy neutrino data, challenging a simple explanation in terms of atmospheric neutrinos and suggesting an extraterrestrial origin. These astrophysical neutrinos are assumed to have originated from the decays of charged particles produced in pp or $p\gamma$ collisions. While the data obtained is largely consistent with SM predictions, the flux shows a mild deficiency in muons at high energies, prompting alternative explanations involving dark matter.

In Fig. 6.8, we show the neutrino (left panel) and muon (right panel) fluxes as functions of the dark matter mass M_{DM} (GeV). In the top graphs, we plot our results as a red curve, and include the upper limits on the neutrino and muon flux for the $b\bar{b}$ channel, $\tau^+\tau^-$ channel, and the $\nu_e\bar{\nu}_e$, $\nu_\mu\bar{\nu}_\mu$, $\nu_\tau\bar{\nu}_\tau$ channels from the Baikal NT200 detector results [330]. While the limit on the muon flux from Baikal results does not impose restrictions on our model,⁶ the neutrino flux excludes DM particles with mass in the 74-85 GeV region. The figures show again the two dips at $M_{DM} \sim 45$ GeV and $M_{DM} \sim 62$ GeV. Unlike for the annihilation cross section, here the effect of the Z pole is more dramatic than that of the Higgs pole at $M_{DM} \sim m_h/2$. The bottom panels show the fluxes of neutrino and muon as contour plots in the dark matter mass M_{DM} and the Yukawa coupling h'_ν . Note that here, as before, the contours are consistent with the experimental values for the measured flux of muons and neutrinos. However only points along the dash-dotted yellow line are consistent with the dark matter relic density exclusion limit.

6.10 Conclusions

We analyzed the effects of introducing vector-like leptons in the Higgs Triplet Model. Our aim was to provide a scenario that can explain both neutrino masses and provide a DM candidate, problems unresolved in the SM. We chose a full generation of vector-like leptons (one left-

⁶Due to limited space on the figure, we only show the recent results of Baikal NT200. But our results are also consistent with those from the Baksan Neutrino Observatory [331].

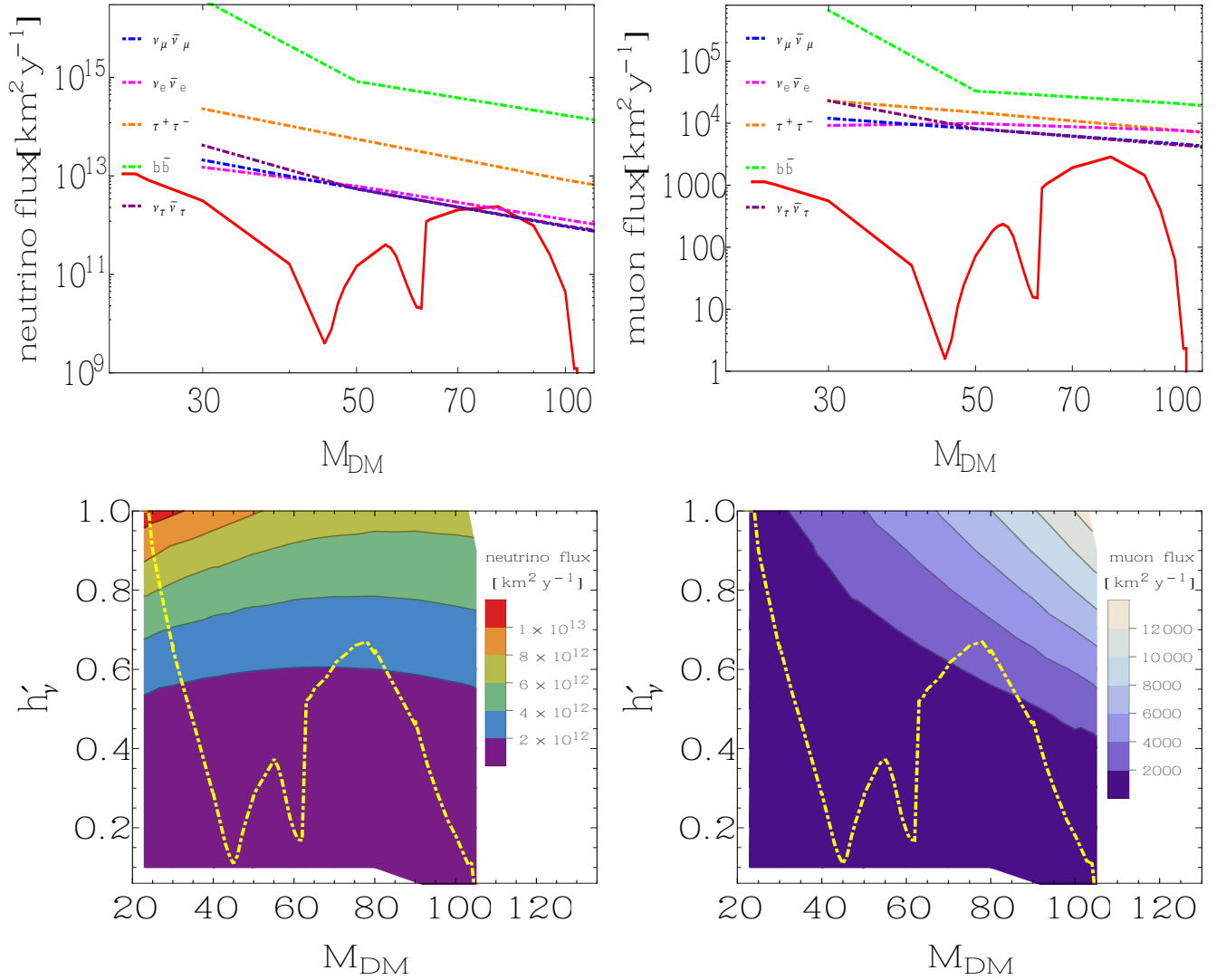


Figure 6.8: (Top panels) The fluxes of neutrinos (left panel) and muons (right panel) in the HTM with vector-like leptons, as functions of the dark matter mass M_{DM} (GeV) (the red line). We also show the upper limits on the neutrino and muon flux for the $b\bar{b}$ channel (dash-dotted green), $\tau^+ \tau^-$ channel (dash-dotted orange), $\nu_e \bar{\nu}_e$ channel (dash-dotted pink), $\nu_\mu \bar{\nu}_\mu$ channel (dash-dotted blue) and $\nu_\tau \bar{\nu}_\tau$ channel (dash-dotted purple) from the Baikal NT200 detector results [330]. (Bottom panel) Contour plots showing the flux of neutrinos (left panel) and muons (right panel) in the HTM with vector-like leptons, as functions of the dark matter mass M_{DM} and Yukawa coupling h'_ν . The flux values are color coded as in the bar attached. The contours indicate points consistent with the respective experimental constraints, while the dash-dotted yellow line includes the only points with acceptable relic density, $0.1144 \leq \Omega_{DM} h^2 \leq 0.1252$.

handed doublet and two right-handed singlets, together with their mirror representations). We ensured that a new symmetry differentiates between ordinary leptons and the new states, forbidding unwanted lepton flavor violation. Opting for a simplified Yukawa coupling structure, a mostly singlet right-handed vector-like neutrino emerges as a single DM candidate. Introducing vector-like leptons in the HTM relaxes the severe constraints on the mass of the doubly charged Higgs boson coming from electroweak precision tests. We revisited precision observables in this thesis, and showed that while the S parameter does not impose constraints on the parameter space, the T parameter is restrictive, allowing only certain combinations of doubly charged Higgs mass, Yukawa couplings, and mixing angles between the neutral Higgs bosons. Of these, the most sensitive parameter is the mass of the doubly charged Higgs boson, required to be less than about 280 GeV, but here, this boson has different branching ratios than in the minimal HTM. The T parameter is insensitive to the mass of the dark matter candidate.

We verified that the invisible decay width of the Higgs boson is consistent not only with the experimental data, but with the more restrictive limits imposed by global fits to the Higgs data. The invisible width is a relevant constraint for dark matter masses less than one half of the Higgs mass, and all of these survive. More stringent constraints come from direct detection experiments, especially from restriction on spin-independent nucleon cross section, and from the relic density. The latter restricts the combination between dark matter mass and its Yukawa coupling to narrow bands in the parameter space, and it disallows entirely regions where the DM candidate is lighter than 23 or heavier than 103 GeV. If one includes constraints from XENON100 on spin-independent scattering of dark matter off nucleons, these further restrict the dark matter mass to be in the the ranges: 37-52 GeV, or 57-63 GeV, or heavier than 95 GeV, all for points satisfying relic density constraints. In addition, consistent with direct detection experiments, the neutrino flux excludes DM particles with mass in the 74-85 GeV range. These are the most stringent restrictions, and they are insensitive to other model parameters, such as other masses (particularly the doubly charged Higgs boson) and the mixing angle between the neutral Higgs bosons.

To summarize, we presented a simple model that accounts for neutrino masses and dark matter and is consistent with the relic density and all direct and indirect searches. This model assumes a single dark matter particle, and the experimental data restricts its mass to be confined to limited regions in the parameter space. If the dark matter is as light as 1 or a few GeV, as some experiments suggest, this scenario is ruled out. However for DM mass around 30 GeV, allowing small deviations from direct detection, the HTM with vector-like

leptons provides a viable explanation. This analysis assumed the DM candidate to be light and set an upper bound on its mass of 108 GeV, by the choice of the mass of the lightest vector-like charged lepton.

Chapter 7

Conclusions and Outlook

In this thesis, we presented an analysis of one of the simplest extensions of the SM, the Higgs Triplet Model (HTM), with non-trivial mixing in the neutral Higgs sector and with vector-like fermions. We proposed a simple model that accounts for neutrino masses and dark matter, two problems unresolved in the SM. Perhaps the simplest way to explain tiny neutrino masses is the seesaw mechanism, in which right-handed neutrinos are introduced with large Majorana masses. In the Higgs Triplet Model, the particle content of the SM is extended by a complex triplet scalar field in order to implement this mechanism for generating neutrino masses. Introducing only this additional Higgs representation, together with its associated vacuum expectation value can solve the neutrino mass problem. In our model, the mixing in the CP-even neutral bosons is non-negligible, and both states are mixtures of doublet and triplet Higgs representations.

We study the tree-level and loop-induced ($\gamma\gamma$ and $Z\gamma$) decays of the two bosons for the case in which $m_{H_1} = 125$ GeV, $m_{H_2} = 136$ GeV (motivated by the CMS data); for the case where $m_{H_1} = 98$ GeV, $m_{H_2} = 125$ GeV (motivated by the LEP excess); and for the case where the two Higgs bosons are degenerate in mass and $m_{H_1} = m_{H_2} = 125$ GeV, which is motivated by the case where there is a single boson observed at the LHC. However the LEP/LHC scenario is favored by the data, and consistent with all other measurements. In our model, while the decay of the heavier Higgs boson (at 125 GeV) can be enhanced significantly with respect to the SM, the lighter boson signal is always reduced with respect to the SM which can also explain a lighter Higgs H that is missed by colliders because of significantly reduced decay into $\gamma\gamma$. For mixing angle below 0.2, the decay of the heavier Higgs boson is suppressed, however for other regions, the ratio can be reduced or enhanced depending on the value of the

mass splittings and doubly charged Higgs boson masses. However, all the tree-level branching ratios are suppressed with respect to the same ones in the SM and independent of the mass splitting values. In the SM the decay $Z\gamma$ is similar to the one for $\gamma\gamma$, but with a smaller rate and a further reduced branching ratio. Our model predicts only one enhanced signal for the decay of the heavier Higgs boson to $Z\gamma$ in scenario 2.

An extension of the SM via additional vector-like leptons is not ruled out experimentally, and has been shown to provide a dark matter candidate. The presence of the vector-like leptons affects the loop-dominated decays of the neutral Higgs ($\gamma\gamma$ and $Z\gamma$), while leaving the production cross section and tree-level decays largely unchanged. The model presents a mechanism for (modestly) enhancing one loop-decay $\gamma\gamma$ not for $Z\gamma$ for small mixing angles and light doubly charged Higgs bosons $m_{H^{\pm\pm}} \lesssim 300$ GeV. The relative branching ratios are very sensitive to the values of the doubly charged Higgs mass, mixing in the neutral Higgs sector and mixing in the vector-like lepton sector. The doubly charged Higgs boson with intermediate values of mass can decay significantly into vector-like leptons, which, if light enough, would modify the decays of the doubly charged Higgs bosons further. As a result, these decay modes could be observable at the LHC with significant enough cross sections times branching ratios. Our model restricts the mass of doubly charged Higgs boson to be around 200-600 GeV.

Introduction of vector-like quarks also imposes different constraints on the HTM as it can affect both the production and decay of the Higgs bosons at the LHC. We were particularly interested in constraints on the mixing of the CP-even neutral Higgs bosons, the masses of the vector-like quarks and the mixing parameters with the ordinary quarks; and the mass of the doubly charged Higgs boson. The oblique parameter, T , imposes some restrictions on the parameter space of the model. The contribution to the T parameter in the HTM from some representations of vector-like quarks could relax the severe constraint on the doubly charged Higgs mass and bring it in closer agreement with present experimental constraints. The doubly charged Higgs boson mass are required to be in the (about) 280-370 GeV and (about) 100-280 GeV depending on the models that we have considered to satisfy electroweak constraints. The mixing parameters are also restricted to be $x_b \in (117 - 538)$ GeV and $x_t \in (0, 550)$ GeV for vector-like quark masses $M \sim 1000$ GeV. While the masses and mixing parameters of the vector-like quarks have little effect on the $H \rightarrow \gamma\gamma$ and $H \rightarrow Z\gamma$ decays, as in the SM, the effects of vector-like quarks come from combining these with constraints from electroweak precision observables.

The HTM with vector-like leptons accounts for both neutrino masses and dark matter, and is consistent with the relic density and all direct and indirect DM searches. Assuming a single vector-like neutrino dark matter particle, the experimental data restricts the DM candidate to be light: in the 37-52 GeV, or 57-63 GeV range, or heavier than 95 GeV, all for points satisfying relic density constraints. In addition, the neutrino flux excludes DM particles with mass in the 74-85 GeV range. The T parameter is insensitive to the mass of the dark matter candidate. However it can restrict doubly charged mass, Yukawa couplings, and mixing angles between the neutral Higgs bosons. The most sensitive parameter is the mass of the doubly charged Higgs boson, required to be less than about 280 GeV.

Despite no new signals of physics beyond the SM at the LHC, the SM cannot be the complete theory of particle interactions. My thesis focused on a model beyond the SM, the HTM and extension of this model by adding fermionic particles. One can extend this scenario to a more complicated one, involving several DM particles. This model would be less constrained, but it loses the predictability of the simple scenario presented here. A possible avenue of research is to extend my current work on Dark matter, to other models beyond the SM for instance the left-right symmetric model. We could study the collider (LHC) aspects of the model, constraints from vacuum stability as well as the Electroweak precision data (EWPD) in the model. Given the importance of DM in understanding the universe, and the effort going into direct and indirect detection, and into collider experiments, simple models such as this one can help elucidate the nature of Dark Matter.

Bibliography

- [1] F. Arbabifar, S. Bahrami, and M. Frank, “Neutral Higgs Bosons in the Higgs Triplet Model with nontrivial mixing,” *Phys. Rev.*, vol. D87, no. 1, p. 015020, 2013, 1211.6797.
- [2] S. Bahrami and M. Frank, “Dark matter in the Higgs triplet model,” *Phys. Rev. D*, vol. 91, p. 075003, Apr 2015.
- [3] S. Bahrami and M. Frank, “Vector Quarks in the Higgs Triplet Model,” *Phys. Rev.*, vol. D90, no. 3, p. 035017, 2014, 1405.4245.
- [4] S. Bahrami and M. Frank, “Vector Leptons in the Higgs Triplet Model,” *Phys. Rev.*, vol. D88, p. 095002, 2013, 1308.2847.
- [5] S. Bahrami and M. Frank, “Neutrino Dark Matter in the Higgs Triplet Model,” in *Proceedings, Meeting of the APS Division of Particles and Fields (DPF 2015)*, 2015, 1509.04763.
- [6] G. Aad *et al.*, “Observation of a new particle in the search for the Standard Model Higgs boson with the ATLAS detector at the LHC,” *Phys. Lett.*, vol. B716, pp. 1–29, 2012, 1207.7214.
- [7] S. Weinberg, “A Model of Leptons,” *Phys. Rev. Lett.*, vol. 19, pp. 1264–1266, Nov 1967.
- [8] A. Salam, “Weak and Electromagnetic Interactions,” *Conf. Proc.*, vol. C680519, pp. 367–377, 1968.
- [9] S. L. Glashow and S. Weinberg, “Breaking Chiral Symmetry,” *Phys. Rev. Lett.*, vol. 20, pp. 224–227, Jan 1968.
- [10] A. Degee, *Scalar and fermionic extensions of the Standard Model*. Dissertations and theses : Doctoral thesis, Universite de Liege, October 2013.

- [11] S. Weinberg, “The Making of the standard model,” *Eur. Phys. J.*, vol. C34, pp. 5–13, 2004, hep-ph/0401010. [,99(2005)].
- [12] W. Hollik, “Quantum field theory and the Standard Model,” in *High-energy physics. Proceedings, 17th European School, ESHEP 2009, Bautzen, Germany, June 14-27, 2009*, 2010, 1012.3883.
- [13] A. Djouadi, “The Anatomy of electro-weak symmetry breaking. I: The Higgs boson in the standard model,” *Phys. Rept.*, vol. 457, pp. 1–216, 2008, hep-ph/0503172.
- [14] F. J. Hasert *et al.*, “Observation of Neutrino Like Interactions Without Muon Or Electron in the Gargamelle Neutrino Experiment,” *Phys. Lett.*, vol. B46, pp. 138–140, 1973.
- [15] F. Hasert *et al.*, “Search for elastic muon-neutrino electron scattering,” *Physics Letters B*, vol. 46, pp. 121–124, Sept. 1973.
- [16] J. J. Aubert, U. Becker, P. J. Biggs, J. Burger, M. Chen, G. Everhart, P. Goldhagen, J. Leong, T. McCarriston, T. G. Rhoades, M. Rohde, S. C. C. Ting, S. L. Wu, and Y. Y. Lee, “Experimental Observation of a Heavy Particle J ,” *Phys. Rev. Lett.*, vol. 33, pp. 1404–1406, Dec 1974.
- [17] J. E. Augustin *et al.*, “Discovery of a Narrow Resonance in e^+e^- Annihilation,” *Phys. Rev. Lett.*, vol. 33, pp. 1406–1408, 1974. [Adv. Exp. Phys.5,141(1976)].
- [18] G. Arnison *et al.*, “Experimental Observation of Isolated Large Transverse Energy Electrons with Associated Missing Energy at $s^{**}(1/2) = 540\text{-GeV}$,” *Phys. Lett.*, vol. B122, pp. 103–116, 1983. [,611(1983)].
- [19] G. Arnison *et al.*, “Experimental Observation of Lepton Pairs of Invariant Mass Around $95\text{-GeV}/c^{**2}$ at the CERN SPS Collider,” *Phys. Lett.*, vol. B126, pp. 398–410, 1983.
- [20] J. Ellis, M. K. Gaillard, and D. V. Nanopoulos, “An Updated Historical Profile of the Higgs Boson,” 2015, 1504.07217.
- [21] M. Sundaresan, *Handbook of Particle Physics*, vol. 1. CRC Press, illustrated ed., April 2001.
- [22] S. F. Novaes, “Standard model: An Introduction,” in *Particles and fields. Proceedings, 10th Jorge Andre Swieca Summer School, Sao Paulo, Brazil, February 6-12, 1999*, 1999, hep-ph/0001283.

- [23] F. Englert and R. Brout, “Broken Symmetry and the Mass of Gauge Vector Mesons,” *Phys. Rev. Lett.*, vol. 13, pp. 321–323, Aug 1964.
- [24] P. W. Higgs, “Broken Symmetries and the Masses of Gauge Bosons,” *Phys. Rev. Lett.*, vol. 13, pp. 508–509, Oct 1964.
- [25] P. Higgs, “Broken symmetries, massless particles and gauge fields,” *Physics Letters*, vol. 12, no. 2, pp. 132 – 133, 1964.
- [26] G. S. Guralnik, C. R. Hagen, and T. W. B. Kibble, “Global Conservation Laws and Massless Particles,” *Phys. Rev. Lett.*, vol. 13, pp. 585–587, Nov 1964.
- [27] P. W. Higgs, “Spontaneous Symmetry Breakdown without Massless Bosons,” *Phys. Rev.*, vol. 145, pp. 1156–1163, May 1966.
- [28] J. Ellis, M. K. Gaillard, and D. V. Nanopoulos, “A Historical Profile of the Higgs Boson,” 2012, 1201.6045.
- [29] S. Chatrchyan *et al.*, “Observation of a new boson at a mass of 125 GeV with the CMS experiment at the LHC,” *Phys. Lett.*, vol. B716, pp. 30–61, 2012, 1207.7235.
- [30] D. Hooper, “Particle Dark Matter,” in *Proceedings of Theoretical Advanced Study Institute in Elementary Particle Physics on The dawn of the LHC era (TASI 2008)*, pp. 709–764, 2010, 0901.4090.
- [31] G. B. Gelmini, “TASI 2014 Lectures: The Hunt for Dark Matter,” in *Theoretical Advanced Study Institute in Elementary Particle Physics: Journeys Through the Precision Frontier: Amplitudes for Colliders (TASI 2014) Boulder, Colorado, June 2-27, 2014*, 2015, 1502.01320.
- [32] “Johar Ashfaque, From MACHOs to WIMPsmeet the top five candidates for 'dark matter'. 15 December 2015. < <http://phys.org/news/2015-12-machos-wimpsmeet-candidates-dark.html> >.”
- [33] P. de Aquino, *Beyond Standard Model Phenomenology at the LHC*. Springer Theses, Springer International Publishing, 2013.
- [34] “The Nobel Prize in Physics 2015. Nobelprize.org. Nobel Media AB 2014. Web. 19 Feb 2016. < <http://www.nobelprize.org/nobel-prizes/physics/laureates/2015/> >.”
- [35] F. Suekane, *Neutrino Oscillations: A Practical Guide to Basics and Applications*. Lecture Notes in Physics, Springer Japan, 2015.

- [36] K. A. Olive *et al.*, “Review of Particle Physics,” *Chin. Phys.*, vol. C38, p. 090001, 2014.
- [37] A. Falkowski, D. M. Straub, and A. Vicente, “Vector-like leptons: Higgs decays and collider phenomenology,” *JHEP*, vol. 05, p. 092, 2014, 1312.5329.
- [38] O. Lebedev, H. P. Nilles, S. Raby, S. Ramos-Snchez, M. Ratz, P. K. Vaudrevange, and A. Wingerter, “A mini-landscape of exact {MSSM} spectra in heterotic orbifolds ,” *Physics Letters B*, vol. 645, no. 1, pp. 88 – 94, 2007.
- [39] F. del Aguila, L. Ametller, G. L. Kane, and J. Vidal, “Vector Like Fermion and Standard Higgs Production at Hadron Colliders,” *Nucl. Phys.*, vol. B334, p. 1, 1990.
- [40] B. Martin and G. Shaw, *Particle Physics*. Manchester Physics Series, Wiley, 2013.
- [41] R. Mann, *An Introduction to Particle Physics and the Standard Model*. Taylor & Francis, 2011.
- [42] L. Zeune, *Constraining Supersymmetric Models: Using Higgs Physics, Precision Observables and Direct Searches*. Springer Theses, Springer International Publishing, 2015.
- [43] G. Dvali and M. Redi, “Black Hole Bound on the Number of Species and Quantum Gravity at LHC,” *Phys. Rev.*, vol. D77, p. 045027, 2008, 0710.4344.
- [44] G. Dvali, “Black Holes and Large N Species Solution to the Hierarchy Problem,” *Fortsch. Phys.*, vol. 58, pp. 528–536, 2010, 0706.2050.
- [45] G. R. Dvali, G. Gabadadze, M. Kolanovic, and F. Nitti, “Scales of gravity,” *Phys. Rev.*, vol. D65, p. 024031, 2002, hep-th/0106058.
- [46] X. Calmet, M. Graesser, and S. D. H. Hsu, “Minimum length from first principles,” *Int. J. Mod. Phys.*, vol. D14, pp. 2195–2200, 2005, hep-th/0505144.
- [47] X. Calmet, M. Graesser, and S. D. H. Hsu, “Minimum length from quantum mechanics and general relativity,” *Phys. Rev. Lett.*, vol. 93, p. 211101, 2004, hep-th/0405033.
- [48] X. Calmet, S. D. H. Hsu, and D. Reeb, “Quantum gravity at a TeV and the renormalization of Newton’s constant,” *Phys. Rev.*, vol. D77, p. 125015, 2008, 0803.1836.
- [49] P. de Aquino, *Beyond Standard Model Phenomenology at the LHC*. PhD thesis, Louvain U., New York, 2012.

- [50] “*LHCb* experiment observes new matter-antimatter difference. 24 Apr 2013. < <http://press.web.cern.ch/press-releases/2013/04/lhcb-experiment-observes-new-matter-antimatter-difference> >.”
- [51] “Cian O’Luanaigh, *LHCb* experiment observes new matter-antimatter difference. 24 Apr 2013. < <http://press.web.cern.ch/press-releases/2013/04/lhcb-experiment-observes-new-matter-antimatter-difference> >.”
- [52] R. D. Peccei and H. R. Quinn, “Constraints imposed by CP conservation in the presence of pseudoparticles,” *Phys. Rev. D*, vol. 16, pp. 1791–1797, Sep 1977.
- [53] R. D. Peccei and H. R. Quinn, “CP Conservation in the Presence of Pseudoparticles,” *Phys. Rev. Lett.*, vol. 38, pp. 1440–1443, Jun 1977.
- [54] D. Griffiths, *Introduction to Elementary Particles*. Physics textbook, Wiley, 2008.
- [55] K. Hashimoto, *D-Brane: Superstrings and New Perspective of Our World*. SpringerLink : Bücher, Springer Berlin Heidelberg, 2012.
- [56] E. Gardi, N. Glover, and A. Robson, *LHC Phenomenology*. Scottish Graduate Series, Springer International Publishing, 2014.
- [57] C. Merino, *Lectures on Particle Physics, Astrophysics and Cosmology: Proceedings of the Third IDPASC School, Santiago de Compostela, Spain, January 21 – February 2, 2013*. Springer Proceedings in Physics, Springer International Publishing, 2014.
- [58] P. Langacker, *The Standard Model and Beyond*. Series in High Energy Physics, Cosmology and Gravitation, Taylor & Francis, 2009.
- [59] G. Petrucciani, *Observation of a New State in the Search for the Higgs Boson at CMS*. Publications of the Scuola Normale Superiore, Scuola Normale Superiore, 2014.
- [60] F. Halzen and A. Martin, *QUARK & LEPTONS: AN INTRODUCTORY COURSE IN MODERN PARTICLE PHYSICS*. Wiley India Pvt. Limited, 2008.
- [61] N. Cabibbo, “Unitary Symmetry and Leptonic Decays,” *Phys. Rev. Lett.*, vol. 10, pp. 531–533, Jun 1963.
- [62] M. Kobayashi and T. Maskawa, “CP Violation in the Renormalizable Theory of Weak Interaction,” *Prog. Theor. Phys.*, vol. 49, pp. 652–657, 1973.
- [63] L.-L. Chau and W.-Y. Keung, “Comments on the Parametrization of the Kobayashi-Maskawa Matrix,” *Phys. Rev. Lett.*, vol. 53, pp. 1802–1805, Nov 1984.

- [64] L. Wolfenstein, “Parametrization of the Kobayashi-Maskawa Matrix,” *Phys. Rev. Lett.*, vol. 51, pp. 1945–1947, Nov 1983.
- [65] A. J. Buras, M. E. Lautenbacher, and G. Ostermaier, “Waiting for the top quark mass, $K^+ \rightarrow \pi^+$ neutrino anti-neutrino, $B_s^0-\overline{B}_s^0$ mixing and CP asymmetries in B decays,” *Phys. Rev.*, vol. D50, pp. 3433–3446, 1994, hep-ph/9403384.
- [66] J. Charles, A. Hocker, H. Lacker, S. Laplace, F. R. Le Diberder, J. Malcles, J. Ocariz, M. Pivk, and L. Roos, “CP violation and the CKM matrix: Assessing the impact of the asymmetric B factories,” *Eur. Phys. J.*, vol. C41, pp. 1–131, 2005, hep-ph/0406184.
- [67] T. Schorner-Sadenius, *The Large Hadron Collider: Harvest of Run 1*. Springer International Publishing, 2015.
- [68] V. Lindahl, “Detection Prospects of Doubly Charged Higgs Bosons from the Higgs Triplet Model at the LHC,” 2011.
- [69] K. Yagyu, *Studies on Extended Higgs Sectors as a Probe of New Physics Beyond the Standard Model*. PhD thesis, Toyama U., 2012, 1204.0424.
- [70] N. Ilic, “ATLAS physics prospects for the upgraded LHC,” *EPJ Web Conf.*, vol. 95, p. 04031, 2015.
- [71] LHC Higgs Cross Section Working Group, S. Heinemeyer, C. Mariotti, G. Passarino, and R. Tanaka (Eds.), “Handbook of LHC Higgs Cross Sections: 3. Higgs Properties,” *CERN-2013-004*, CERN, Geneva, 2013, 1307.1347.
- [72] R. Wolf, *The Higgs Boson Discovery at the Large Hadron Collider*. Springer Tracts in Modern Physics, Springer International Publishing, 2015.
- [73] A. Straessner, *Electroweak Boson Physics at LEP and LHC*. 2009.
- [74] S. Chatrchyan and others., “Measurement of the properties of a Higgs boson in the four-lepton final state,” *Phys. Rev. D*, vol. 89, p. 092007, May 2014.
- [75] V. Khachatryan *et al.*, “Observation of the diphoton decay of the Higgs boson and measurement of its properties,” *Eur. Phys. J.*, vol. C74, no. 10, p. 3076, 2014, 1407.0558.
- [76] G. Aad *et al.*, “Observation and measurement of Higgs boson decays to WW^* with the ATLAS detector,” *Phys. Rev.*, vol. D92, no. 1, p. 012006, 2015, 1412.2641.
- [77] G. Aad *et al.*, “Evidence for the Higgs-boson Yukawa coupling to tau leptons with the ATLAS detector,” *JHEP*, vol. 04, p. 117, 2015, 1501.04943.

- [78] S. Chatrchyan *et al.*, “Evidence for the 125 GeV Higgs boson decaying to a pair of τ leptons,” *JHEP*, vol. 05, p. 104, 2014, 1401.5041.
- [79] G. Aad *et al.*, “Search for the $b\bar{b}$ decay of the Standard Model Higgs boson in associated $(W/Z)H$ production with the ATLAS detector,” *JHEP*, vol. 01, p. 069, 2015, 1409.6212.
- [80] S. Chatrchyan *et al.*, “Search for the standard model Higgs boson produced in association with a W or a Z boson and decaying to bottom quarks,” *Phys. Rev. D*, vol. 89, p. 012003, Jan 2014.
- [81] “Search for resonances decaying to photon pairs in 3.2 fb⁻¹ of pp collisions at $\sqrt{s} = 13$ TeV with the ATLAS detector,” Tech. Rep. ATLAS-CONF-2015-081, CERN, Geneva, Dec 2015.
- [82] “Search for new physics in high mass diphoton events in proton-proton collisions at $\sqrt{s} = 13$ TeV,” Tech. Rep. CMS-PAS-EXO-15-004, CERN, Geneva, 2015.
- [83] K. Fujikawa, “A Vector - like extension of the standard model,” *Prog. Theor. Phys.*, vol. 92, pp. 1149–1160, 1994, hep-ph/9411258.
- [84] T. Yoshikawa, “The Effects of a vector - like doublet as the fourth generation to R(b),” *Prog. Theor. Phys.*, vol. 96, pp. 269–274, 1996, hep-ph/9512251.
- [85] K. Ishiwata and M. B. Wise, “Phenomenology of heavy vectorlike leptons,” *Phys. Rev.*, vol. D88, no. 5, p. 055009, 2013, 1307.1112.
- [86] G. Aad *et al.*, “Search for production of vector-like quark pairs and of four top quarks in the lepton-plus-jets final state in pp collisions at $\sqrt{s} = 8$ TeV with the ATLAS detector,” *JHEP*, vol. 08, p. 105, 2015, 1505.04306.
- [87] N. Kumar and S. P. Martin, “Vectorlike leptons at the Large Hadron Collider,” *Phys. Rev.*, vol. D92, no. 11, p. 115018, 2015, 1510.03456.
- [88] J. Beringer *et al.*, “Review of Particle Physics (RPP),” *Phys. Rev.*, vol. D86, p. 010001, 2012.
- [89] D. Abercrombie *et al.*, “Dark Matter Benchmark Models for Early LHC Run-2 Searches: Report of the ATLAS/CMS Dark Matter Forum,” 2015, 1507.00966.
- [90] “Dark matter. 28 Feb 2016. < <http://home.cern/about/physics/dark-matter> >.”
- [91] G. Aad *et al.*, “Search for new phenomena in events with a photon and missing transverse momentum in pp collisions at $\sqrt{s} = 8$ TeV with the ATLAS detec-

- tor,” *Phys. Rev.*, vol. D91, no. 1, p. 012008, 2015, 1411.1559. [Erratum: *Phys. Rev.*D92,no.5,059903(2015)].
- [92] T. Aaltonen *et al.*, “Evidence for a Particle Produced in Association with Weak Bosons and Decaying to a Bottom-Antibottom Quark Pair in Higgs Boson Searches at the Tevatron,” *Phys. Rev. Lett.*, vol. 109, p. 071804, Aug 2012.
- [93] M. Carena, S. Gori, N. R. Shah, and C. E. M. Wagner, “A 125 GeV SM-like Higgs in the MSSM and the $\gamma\gamma$ rate,” *JHEP*, vol. 03, p. 014, 2012, 1112.3336.
- [94] J.-J. Cao, Z.-X. Heng, J. M. Yang, Y.-M. Zhang, and J.-Y. Zhu, “A SM-like Higgs near 125 GeV in low energy SUSY: a comparative study for MSSM and NMSSM,” *JHEP*, vol. 03, p. 086, 2012, 1202.5821.
- [95] M. Carena, S. Gori, N. R. Shah, C. E. M. Wagner, and L.-T. Wang, “Light Stau Phenomenology and the Higgs $\gamma\gamma$ Rate,” *JHEP*, vol. 07, p. 175, 2012, 1205.5842.
- [96] H. An, T. Liu, and L.-T. Wang, “125 GeV Higgs boson, enhanced diphoton rate, and gauged $U(1)_{PQ}$ -extended MSSM,” *Phys. Rev. D*, vol. 86, p. 075030, Oct 2012.
- [97] A. Joglekar, P. Schwaller, and C. E. M. Wagner, “Dark Matter and Enhanced Higgs to Di-photon Rate from Vector-like Leptons,” *JHEP*, vol. 12, p. 064, 2012, 1207.4235.
- [98] B. Batell, D. McKeen, and M. Pospelov, “Singlet Neighbors of the Higgs Boson,” *JHEP*, vol. 10, p. 104, 2012, 1207.6252.
- [99] G. F. Giudice, P. Paradisi, A. Strumia, and A. Strumia, “Correlation between the Higgs Decay Rate to Two Photons and the Muon $g - 2$,” *JHEP*, vol. 10, p. 186, 2012, 1207.6393.
- [100] A. Urbano, “Higgs boson decay into photons through a spin-2 loop,” *Phys. Rev.*, vol. D87, no. 5, p. 053003, 2013, 1208.5782.
- [101] M. Chala, “ $h \rightarrow \gamma\gamma$ excess and Dark Matter from Composite Higgs Models,” *JHEP*, vol. 01, p. 122, 2013, 1210.6208.
- [102] U. Ellwanger, “A Higgs boson near 125 GeV with enhanced di-photon signal in the NMSSM,” *JHEP*, vol. 03, p. 044, 2012, 1112.3548.
- [103] V. Barger, P. Huang, M. Ishida, and W.-Y. Keung, “Flavor-tuned 125 GeV supersymmetric Higgs boson at the LHC: Test of minimal and natural supersymmetric models,” *Phys. Rev. D*, vol. 87, p. 015003, Jan 2013.

- [104] K. Schmidt-Hoberg and F. Staub, “Enhanced $h \rightarrow \gamma\gamma$ rate in MSSM singlet extensions,” *JHEP*, vol. 10, p. 195, 2012, 1208.1683.
- [105] K. Schmidt-Hoberg, F. Staub, and M. W. Winkler, “Enhanced diphoton rates at Fermi and the LHC,” *JHEP*, vol. 01, p. 124, 2013, 1211.2835.
- [106] A. Arhrib, R. Benbrik, and C.-H. Chen, “ $H \rightarrow \gamma\gamma$ in the Complex Two Higgs Doublet Model,” 2012, 1205.5536.
- [107] “Evidence for a new state decaying into two photons in the search for the standard model Higgs boson in pp collisions,” Tech. Rep. CMS-PAS-HIG-12-015, CERN, Geneva, 2012.
- [108] “Search for a standard model Higgs bosons decaying to tau pairs in pp collisions,” Tech. Rep. CMS-PAS-HIG-12-018, CERN, Geneva, 2012.
- [109] “Updated Combination of CDF and D0 Searches for Standard Model Higgs Boson Production with up to 10.0 fb^{-1} of Data,” 2012, 1207.0449.
- [110] S. Schael *et al.*, “Search for neutral MSSM Higgs bosons at LEP,” *Eur. Phys. J.*, vol. C47, pp. 547–587, 2006, hep-ex/0602042.
- [111] R. Barate *et al.*, “Search for the standard model Higgs boson at LEP,” *Phys. Lett.*, vol. B565, pp. 61–75, 2003, hep-ex/0306033.
- [112] M. Carena, I. Low, and C. E. M. Wagner, “Implications of a Modified Higgs to Diphoton Decay Width,” *JHEP*, vol. 08, p. 060, 2012, 1206.1082.
- [113] W.-F. Chang, J. N. Ng, and J. M. S. Wu, “Constraints on new scalars from the LHC 125 GeV Higgs signal,” *Phys. Rev. D*, vol. 86, p. 033003, Aug 2012.
- [114] C.-W. Chiang and K. Yagyu, “Higgs boson decays to $\gamma\gamma$ and $Z\gamma$ in models with Higgs extensions,” *Phys. Rev.*, vol. D87, no. 3, p. 033003, 2013, 1207.1065.
- [115] I. Dorsner, S. Fajfer, A. Greljo, and J. F. Kamenik, “Higgs Uncovering Light Scalar Remnants of High Scale Matter Unification,” *JHEP*, vol. 11, p. 130, 2012, 1208.1266.
- [116] G. Belanger, U. Ellwanger, J. F. Gunion, Y. Jiang, and S. Kraml, “Two Higgs Bosons at the Tevatron and the LHC?,” 2012, 1208.4952.
- [117] G. Belanger, U. Ellwanger, J. F. Gunion, Y. Jiang, S. Kraml, and J. H. Schwarz, “Higgs Bosons at 98 and 125 GeV at LEP and the LHC,” *JHEP*, vol. 01, p. 069, 2013, 1210.1976.

- [118] J. F. Gunion, Y. Jiang, and S. Kraml, “Diagnosing Degenerate Higgs Bosons at 125 GeV,” *Phys. Rev. Lett.*, vol. 110, no. 5, p. 051801, 2013, 1208.1817.
- [119] P. M. Ferreira, R. Santos, H. E. Haber, and J. P. Silva, “Mass-degenerate Higgs bosons at 125 GeV in the two-Higgs-doublet model,” *Phys. Rev.*, vol. D87, p. 055009, 2013, 1211.3131.
- [120] T. P. Cheng and L.-F. Li, “Neutrino masses, mixings, and oscillations in $SU(2) \times U(1)$ models of electroweak interactions,” *Phys. Rev. D*, vol. 22, pp. 2860–2868, Dec 1980.
- [121] J. Schechter and J. W. F. Valle, “Neutrino masses in $SU(2) \times U(1)$ theories,” *Phys. Rev. D*, vol. 22, pp. 2227–2235, Nov 1980.
- [122] R. N. Mohapatra and G. Senjanovic, “Neutrino masses and mixings in gauge models with spontaneous parity violation,” *Phys. Rev. D*, vol. 23, pp. 165–180, Jan 1981.
- [123] A. G. Akeroyd, M. Aoki, and H. Sugiyama, “Probing Majorana phases and the neutrino mass spectrum in the Higgs triplet model at the CERN LHC,” *Phys. Rev. D*, vol. 77, p. 075010, Apr 2008.
- [124] A. G. Akeroyd, M. Aoki, and H. Sugiyama, “Lepton flavor violating decays $\tau \rightarrow \bar{l}ll$ and $\mu \rightarrow e\gamma$ in the Higgs triplet model,” *Phys. Rev. D*, vol. 79, p. 113010, Jun 2009.
- [125] T. Fukuyama, H. Sugiyama, and K. Tsumura, “Constraints from muon g-2 and LFV processes in the Higgs Triplet Model,” *JHEP*, vol. 03, p. 044, 2010, 0909.4943.
- [126] S. T. Petcov, H. Sugiyama, and Y. Takanishi, “Neutrinoless double beta decay and $H^{\pm\pm} \rightarrow l'^{\pm}l^{\pm}$ decays in the Higgs triplet model,” *Phys. Rev. D*, vol. 80, p. 015005, Jul 2009.
- [127] T. Fukuyama, H. Sugiyama, and K. Tsumura, “Phenomenology in the Higgs triplet model with the A_4 symmetry,” *Phys. Rev. D*, vol. 82, p. 036004, Aug 2010.
- [128] A. G. Akeroyd, C.-W. Chiang, and N. Gaur, “Leptonic signatures of doubly charged Higgs boson production at the LHC,” *JHEP*, vol. 11, p. 005, 2010, 1009.2780.
- [129] A. Arhrib, R. Benbrik, M. Chabab, G. Moulataka, and L. Rahili, “Higgs boson decay into 2 photons in the type II Seesaw Model,” *JHEP*, vol. 04, p. 136, 2012, 1112.5453.
- [130] A. Arhrib, R. Benbrik, M. Chabab, G. Moulataka, M. C. Peyranere, L. Rahili, and J. Ramadan, “Higgs potential in the type II seesaw model,” *Phys. Rev. D*, vol. 84, p. 095005, Nov 2011.

- [131] E. J. Chun, H. M. Lee, and P. Sharma, “Vacuum Stability, Perturbativity, EWPD and Higgs-to-diphoton rate in Type II Seesaw Models,” *JHEP*, vol. 11, p. 106, 2012, 1209.1303.
- [132] A. Melfo *et al.*, “Type II neutrino seesaw mechanism at the LHC: The roadmap,” *Phys. Rev. D*, vol. 85, p. 055018, Mar 2012.
- [133] M. Aoki, S. Kanemura, and K. Yagyu, “Testing the Higgs triplet model with the mass difference at the LHC,” *Phys. Rev. D*, vol. 85, p. 055007, Mar 2012.
- [134] S. Kanemura and K. Yagyu, “Radiative corrections to electroweak parameters in the Higgs triplet model and implication with the recent Higgs boson searches,” *Phys. Rev. D*, vol. 85, p. 115009, Jun 2012.
- [135] M. Aoki, S. Kanemura, M. Kikuchi, and K. Yagyu, “Radiative corrections to the Higgs boson couplings in the triplet model,” *Phys. Rev.*, vol. D87, no. 1, p. 015012, 2013, 1211.6029.
- [136] A. G. Akeroyd and M. Aoki, “Single and pair production of doubly charged Higgs bosons at hadron colliders,” *Phys. Rev. D*, vol. 72, p. 035011, Aug 2005.
- [137] A. G. Akeroyd and S. Moretti, “Enhancement of $H \rightarrow \gamma\gamma$ from doubly charged scalars in the Higgs triplet model,” *Phys. Rev. D*, vol. 86, p. 035015, Aug 2012.
- [138] A. G. Akeroyd and C.-W. Chiang, “Phenomenology of large mixing for the CP-even neutral scalars of the Higgs triplet model,” *Phys. Rev. D*, vol. 81, p. 115007, Jun 2010.
- [139] L. Wang and X.-F. Han, “Recent Higgs boson data and Higgs triplet model with vectorlike quarks,” *Phys. Rev. D*, vol. 86, p. 095007, Nov 2012.
- [140] G. Aad *et al.*, “Search for doubly-charged Higgs bosons in like-sign dilepton final states at $\sqrt{s} = 7$ TeV with the ATLAS detector,” *Eur. Phys. J.*, vol. C72, p. 2244, 2012, 1210.5070.
- [141] S. Chatrchyan *et al.*, “A search for a doubly-charged Higgs boson in pp collisions at $\sqrt{s} = 7$ TeV,” *Eur. Phys. J.*, vol. C72, p. 2189, 2012, 1207.2666.
- [142] V. M. Abazov and others., “Search for Doubly Charged Higgs Boson Pair Production in the Decay to $\mu^+\mu^+\mu^-\mu^-$ in $p\bar{p}$ Collisions at $\sqrt{s} = 1.96$ TeV,” *Phys. Rev. Lett.*, vol. 93, p. 141801, Sep 2004.

- [143] V. M. Abazov *et al.*, “Search for Pair Production of Doubly Charged Higgs Bosons in the $H^{++}H^{--} \rightarrow \mu^+\mu^+\mu^-\mu^-$ Final State,” *Phys. Rev. Lett.*, vol. 101, p. 071803, Aug 2008.
- [144] D. Acosta *et al.*, “Search for Doubly Charged Higgs Bosons Decaying to Dileptons in $p\bar{p}$ Collisions at $\sqrt{s} = 1.96$ TeV,” *Phys. Rev. Lett.*, vol. 93, p. 221802, Nov 2004.
- [145] T. Aaltonen *et al.*, “Search for Doubly Charged Higgs Bosons with Lepton-Flavor-Violating Decays Involving τ Leptons,” *Phys. Rev. Lett.*, vol. 101, p. 121801, Sep 2008.
- [146] A. G. Akeroyd and C.-W. Chiang, “Doubly charged Higgs bosons and three-lepton signatures in the Higgs triplet model,” *Phys. Rev. D*, vol. 80, p. 113010, Dec 2009.
- [147] C.-W. Chiang, T. Nomura, and K. Tsumura, “Search for doubly charged Higgs bosons using the same-sign diboson mode at the LHC,” *Phys. Rev. D*, vol. 85, p. 095023, May 2012.
- [148] E. J. Chun, K. Y. Lee, and S. C. Park, “Testing Higgs triplet model and neutrino mass patterns,” *Phys. Lett.*, vol. B566, pp. 142–151, 2003, hep-ph/0304069.
- [149] J. S. Gainer, W.-Y. Keung, I. Low, and P. Schwaller, “Looking for a light Higgs boson in the $Z\gamma \rightarrow \bar{l}l\gamma$ channel,” *Phys. Rev. D*, vol. 86, p. 033010, Aug 2012.
- [150] C.-S. Chen, C.-Q. Geng, D. Huang, and L.-H. Tsai, “New scalar contributions to $h \rightarrow Z\gamma$,” *Phys. Rev. D*, vol. 87, p. 075019, Apr 2013.
- [151] C.-S. Chen, C.-Q. Geng, D. Huang, and L.-H. Tsai, “Correlation of and $Z\gamma$ in Type-II seesaw neutrino model ,” *Physics Letters B*, vol. 723, no. 13, pp. 156 – 160, 2013.
- [152] P. Achard *et al.*, “Search for doubly charged Higgs bosons at LEP,” *Phys. Lett.*, vol. B576, pp. 18–28, 2003, hep-ex/0309076.
- [153] P. S. Bhupal Dev, D. K. Ghosh, N. Okada, and I. Saha, “125 GeV Higgs Boson and the Type-II Seesaw Model,” *JHEP*, vol. 03, p. 150, 2013, 1301.3453. [Erratum: JHEP05,049(2013)].
- [154] G. Aad *et al.*, “Observation of a new particle in the search for the Standard Model Higgs boson with the ATLAS detector at the LHC,” *Phys. Lett.*, vol. B716, pp. 1–29, 2012, 1207.7214.
- [155] T. Aaltonen *et al.*, “Search for New Bottomlike Quark Pair Decays $Q\bar{Q} \rightarrow (tW^\mp)(\bar{t}W^\pm)$ in Same-Charge Dilepton Events,” *Phys. Rev. Lett.*, vol. 104, p. 091801, Mar 2010.

- [156] A. Lister, “Search for Heavy Top-like Quarks $t' \rightarrow Wq$ Using Lepton Plus Jets Events in 1.96-TeV $p\bar{p}$ Collisions,” in *Proceedings, 34th International Conference on High Energy Physics (ICHEP 2008)*, 2008, 0810.3349.
- [157] K. Agashe, G. Perez, and A. Soni, “Flavor structure of warped extra dimension models,” *Phys. Rev. D*, vol. 71, p. 016002, Jan 2005.
- [158] K. Agashe, G. Perez, and A. Soni, “Collider signals of top quark flavor violation from a warped extra dimension,” *Phys. Rev. D*, vol. 75, p. 015002, Jan 2007.
- [159] A. Carmona and J. Santiago, “The Effective Lagrangian for Bulk Fermions in Models with Extra Dimensions,” *JHEP*, vol. 01, p. 100, 2012, 1110.5651.
- [160] G.-Y. Huang, K. Kong, and S. C. Park, “Bounds on the Fermion-Bulk Masses in Models with Universal Extra Dimensions,” *JHEP*, vol. 06, p. 099, 2012, 1204.0522.
- [161] C. Biggio, F. Feruglio, I. Masina, and M. Perez-Victoria, “Fermion generations, masses and mixing angles from extra dimensions,” *Nucl. Phys.*, vol. B677, pp. 451–470, 2004, hep-ph/0305129.
- [162] D. E. Kaplan and T. M. P. Tait, “Supersymmetry breaking, fermion masses and a small extra dimension,” *JHEP*, vol. 06, p. 020, 2000, hep-ph/0004200.
- [163] H.-C. Cheng, “Doublet-triplet splitting and fermion masses with extra dimensions,” *Phys. Rev. D*, vol. 60, p. 075015, Sep 1999.
- [164] T. Moroi and Y. Okada, “Radiative corrections to Higgs masses in the supersymmetric model with an extra family and antifamily,” *Mod. Phys. Lett.*, vol. A7, pp. 187–200, 1992.
- [165] T. Moroi and Y. Okada, “Upper bound of the lightest neutral Higgs mass in extended supersymmetric Standard Models,” *Phys. Lett.*, vol. B295, pp. 73–78, 1992.
- [166] K. S. Babu, I. Gogoladze, M. U. Rehman, and Q. Shafi, “Higgs boson mass, sparticle spectrum, and the little hierarchy problem in an extended MSSM,” *Phys. Rev. D*, vol. 78, p. 055017, Sep 2008.
- [167] S. P. Martin, “Extra vectorlike matter and the lightest Higgs scalar boson mass in low-energy supersymmetry,” *Phys. Rev. D*, vol. 81, p. 035004, Feb 2010.

- [168] P. W. Graham, A. Ismail, S. Rajendran, and P. Saraswat, “Little solution to the little hierarchy problem: A vectorlike generation,” *Phys. Rev. D*, vol. 81, p. 055016, Mar 2010.
- [169] S. P. Martin, “Raising the Higgs mass with Yukawa couplings for isotriplets in vectorlike extensions of minimal supersymmetry,” *Phys. Rev. D*, vol. 82, p. 055019, Sep 2010.
- [170] J. Kang, P. Langacker, and B. D. Nelson, “Theory and phenomenology of exotic isosinglet quarks and squarks,” *Phys. Rev. D*, vol. 77, p. 035003, Feb 2008.
- [171] B. A. Dobrescu and C. T. Hill, “Electroweak Symmetry Breaking via a Top Condensation Seesaw Mechanism,” *Phys. Rev. Lett.*, vol. 81, pp. 2634–2637, Sep 1998.
- [172] R. S. Chivukula, B. A. Dobrescu, H. Georgi, and C. T. Hill, “Top quark seesaw theory of electroweak symmetry breaking,” *Phys. Rev. D*, vol. 59, p. 075003, Mar 1999.
- [173] H. Collins, A. Grant, and H. Georgi, “Phenomenology of a top quark seesaw model,” *Phys. Rev. D*, vol. 61, p. 055002, Jan 2000.
- [174] H.-J. He, C. T. Hill, and T. M. P. Tait, “Top quark seesaw model, vacuum structure, and electroweak precision constraints,” *Phys. Rev. D*, vol. 65, p. 055006, Feb 2002.
- [175] C. T. Hill and E. H. Simmons, “Strong dynamics and electroweak symmetry breaking,” *Phys. Rept.*, vol. 381, pp. 235–402, 2003, hep-ph/0203079. [Erratum: *Phys. Rept.*390,553(2004)].
- [176] R. Contino, L. Da Rold, and A. Pomarol, “Light custodians in natural composite Higgs models,” *Phys. Rev. D*, vol. 75, p. 055014, Mar 2007.
- [177] K. Kong, M. McCaskey, and G. W. Wilson, “Multi-lepton signals from the top-prime quark at the LHC,” *JHEP*, vol. 04, p. 079, 2012, 1112.3041.
- [178] A. Carmona, M. Chala, and J. Santiago, “New Higgs Production Mechanism in Composite Higgs Models,” *JHEP*, vol. 07, p. 049, 2012, 1205.2378.
- [179] M. Gillioz, R. Grober, C. Grojean, M. Muhlleitner, and E. Salvioni, “Higgs Low-Energy Theorem (and its corrections) in Composite Models,” *JHEP*, vol. 10, p. 004, 2012, 1206.7120.
- [180] N. Arkani-Hamed, A. G. Cohen, E. Katz, and A. E. Nelson, “The Littlest Higgs,” *Journal of High Energy Physics*, vol. 2002, no. 07, p. 034, 2002.

- [181] T. Han, H. E. Logan, B. McElrath, and L.-T. Wang, “Phenomenology of the little Higgs model,” *Phys. Rev. D*, vol. 67, p. 095004, May 2003.
- [182] M. Perelstein, M. E. Peskin, and A. Pierce, “Top quarks and electroweak symmetry breaking in little Higgs models,” *Phys. Rev. D*, vol. 69, p. 075002, Apr 2004.
- [183] M. Schmaltz and D. Tucker-Smith, “LITTLE HIGGS THEORIES,” *Annual Review of Nuclear and Particle Science*, vol. 55, no. 1, pp. 229–270, 2005, <http://dx.doi.org/10.1146/annurev.nucl.55.090704.151502>.
- [184] M. Carena, J. Hubisz, M. Perelstein, and P. Verdier, “Collider signatures for new T -parity-odd quarks in little Higgs models,” *Phys. Rev. D*, vol. 75, p. 091701, May 2007.
- [185] S. Matsumoto, T. Moroi, and K. Tobe, “Testing the littlest Higgs model with T parity at the CERN Large Hadron Collider,” *Phys. Rev. D*, vol. 78, p. 055018, Sep 2008.
- [186] A. Davidson and K. C. Wali, “Family mass hierarchy from universal seesaw mechanism,” *Phys. Rev. Lett.*, vol. 60, pp. 1813–1816, May 1988.
- [187] K. S. Babu and R. N. Mohapatra, “Solution to the strong CP problem without an axion,” *Phys. Rev. D*, vol. 41, pp. 1286–1291, Feb 1990.
- [188] B. Grinstein, M. Redi, and G. Villadoro, “Low Scale Flavor Gauge Symmetries,” *JHEP*, vol. 11, p. 067, 2010, 1009.2049.
- [189] D. Guadagnoli, R. N. Mohapatra, and I. Sung, “Gauged Flavor Group with Left-Right Symmetry,” *JHEP*, vol. 04, p. 093, 2011, 1103.4170.
- [190] A. Azatov, M. Toharia, and L. Zhu, “Higgs mediated flavor changing neutral currents in warped extra dimensions,” *Phys. Rev. D*, vol. 80, p. 035016, Aug 2009.
- [191] “Search for Type III Seesaw Model Heavy Fermions in Events with Four Charged Leptons using 5.8 fb^{-1} of $\sqrt{s} = 8 \text{ TeV}$ data with the ATLAS Detector,” Tech. Rep. ATLAS-CONF-2013-019, CERN, Geneva, Mar 2013.
- [192] S. Chatrchyan *et al.*, “Search for heavy lepton partners of neutrinos in proton-proton collisions in the context of the type III seesaw mechanism,” *Phys. Lett.*, vol. B718, pp. 348–368, 2012, 1210.1797.
- [193] F. del Aguila, J. de Blas, and M. Perez-Victoria, “Effects of new leptons in electroweak precision data,” *Phys. Rev. D*, vol. 78, p. 013010, Jul 2008.

- [194] S. Dawson and E. Furlan, “A Higgs conundrum with vector fermions,” *Phys. Rev. D*, vol. 86, p. 015021, Jul 2012.
- [195] S. Dawson, E. Furlan, and I. Lewis, “Unravelling an extended quark sector through multiple Higgs production?,” *Phys. Rev. D*, vol. 87, p. 014007, Jan 2013.
- [196] J. Kearney, A. Pierce, and N. Weiner, “Vectorlike fermions and Higgs couplings,” *Phys. Rev. D*, vol. 86, p. 113005, Dec 2012.
- [197] H. Davoudiasl, H.-S. Lee, and W. J. Marciano, “Dark side of Higgs diphoton decays and muon $g - 2$,” *Phys. Rev. D*, vol. 86, p. 095009, Nov 2012.
- [198] K. J. Bae, T. H. Jung, and H. D. Kim, “125 GeV Higgs boson as a pseudo-Goldstone boson in supersymmetry with vectorlike matters,” *Phys. Rev. D*, vol. 87, p. 015014, Jan 2013.
- [199] M. B. Voloshin, “ CP violation in Higgs boson diphoton decay in models with vectorlike heavy fermions,” *Phys. Rev. D*, vol. 86, p. 093016, Nov 2012.
- [200] D. McKeen, M. Pospelov, and A. Ritz, “Modified Higgs branching ratios versus CP and lepton flavor violation,” *Phys. Rev. D*, vol. 86, p. 113004, Dec 2012.
- [201] H. M. Lee, M. Park, and W.-I. Park, “Axion-mediated dark matter and Higgs diphoton signal,” *JHEP*, vol. 12, p. 037, 2012, 1209.1955.
- [202] C. Arina, R. N. Mohapatra, and N. Sahu, “Co-genesis of Matter and Dark Matter with Vector-like Fourth Generation Leptons,” *Phys. Lett.*, vol. B720, pp. 130–136, 2013, 1211.0435.
- [203] B. Batell, S. Jung, and H. M. Lee, “Singlet Assisted Vacuum Stability and the Higgs to Diphoton Rate,” *JHEP*, vol. 01, p. 135, 2013, 1211.2449.
- [204] H. Davoudiasl, I. Lewis, and E. Ponton, “Electroweak phase transition, Higgs diphoton rate, and new heavy fermions,” *Phys. Rev. D*, vol. 87, p. 093001, May 2013.
- [205] J. Fan and M. Reece, “Probing Charged Matter Through Higgs Diphoton Decay, Gamma Ray Lines, and EDMs,” *JHEP*, vol. 06, p. 004, 2013, 1301.2597.
- [206] A. Carmona and F. Goertz, “Custodial Leptons and Higgs Decays,” *JHEP*, vol. 04, p. 163, 2013, 1301.5856.
- [207] C. Cheung, S. D. McDermott, and K. M. Zurek, “Inspecting the Higgs for New Weakly Interacting Particles,” *JHEP*, vol. 04, p. 074, 2013, 1302.0314.

- [208] W.-Z. Feng and P. Nath, “Higgs diphoton rate and mass enhancement with vectorlike leptons and the scale of supersymmetry,” *Phys. Rev. D*, vol. 87, p. 075018, Apr 2013.
- [209] C. Englert and M. McCullough, “Modified Higgs Sectors and NLO Associated Production,” *JHEP*, vol. 07, p. 168, 2013, 1303.1526.
- [210] K. Ishiwata and M. B. Wise, “Higgs properties and fourth generation leptons,” *Phys. Rev. D*, vol. 84, p. 055025, Sep 2011.
- [211] S. K. Garg and C. S. Kim, “Vector like leptons with extended Higgs sector,” 2013, 1305.4712.
- [212] A. Joglekar, P. Schwaller, and C. E. M. Wagner, “A Supersymmetric Theory of Vector-like Leptons,” *JHEP*, vol. 07, p. 046, 2013, 1303.2969.
- [213] G. F. Giudice and O. Lebedev, “Higgs-dependent Yukawa couplings,” *Phys. Lett.*, vol. B665, pp. 79–85, 2008, 0804.1753.
- [214] E. Del Nobile, R. Franceschini, D. Pappadopulo, and A. Strumia, “Minimal Matter at the Large Hadron Collider,” *Nucl. Phys.*, vol. B826, pp. 217–234, 2010, 0908.1567.
- [215] “Updated measurements of the Higgs boson at 125 GeV in the two photon decay channel,” 2013.
- [216] “Combination of standard model Higgs boson searches and measurements of the properties of the new boson with a mass near 125 GeV,” Tech. Rep. CMS-PAS-HIG-13-005, CERN, Geneva, 2013.
- [217] G. Aad *et al.*, “Measurements of Higgs boson production and couplings in diboson final states with the ATLAS detector at the LHC,” *Phys. Lett.*, vol. B726, pp. 88–119, 2013, 1307.1427. [Erratum: *Phys. Lett.*B734,406(2014)].
- [218] “Study of the spin of the Higgs-like boson in the two photon decay channel using 20.7 fb⁻¹ of pp collisions collected at $\sqrt{s} = 8$ TeV with the ATLAS detector,” Tech. Rep. ATLAS-CONF-2013-029, CERN, Geneva, Mar 2013.
- [219] A. Arhrib, R. Benbrik, M. Chabab, G. Moulhaka, and L. Rahili, “ $h\gamma\gamma$ Coupling in Higgs Triplet Model,” 2012, 1202.6621.
- [220] M. Aoki, S. Kanemura, M. Kikuchi, and K. Yagyu, “Radiative corrections to the Higgs boson couplings in the triplet model,” *Phys. Rev. D*, vol. 87, p. 015012, Jan 2013.

- [221] E. J. Chun and P. Sharma, “A light triplet boson and Higgs-to-diphoton in supersymmetric type II seesaw,” *Phys. Lett.*, vol. B722, pp. 86–93, 2013, 1301.1437.
- [222] L. Wang and X.-F. Han, “130 GeV gamma-ray line and enhancement of $h \rightarrow \gamma\gamma$ in the Higgs triplet model plus a scalar dark matter,” *Phys. Rev. D*, vol. 87, p. 015015, Jan 2013.
- [223] R. Dermisek and A. Raval, “Explanation of the muon $g-2$ anomaly with vectorlike leptons and its implications for Higgs decays,” *Phys. Rev. D*, vol. 88, p. 013017, Jul 2013.
- [224] K. Ishiwata and M. B. Wise, “Phenomenology of heavy vectorlike leptons,” *Phys. Rev. D*, vol. 88, p. 055009, Sep 2013.
- [225] S. Chatrchyan *et al.*, “Search for a Higgs boson decaying into a Z and a photon in pp collisions at $\sqrt{s} = 7$ and 8 TeV,” *Phys. Lett.*, vol. B726, pp. 587–609, 2013, 1307.5515.
- [226] “Search for the Standard Model Higgs boson in the $H \rightarrow Z\gamma$ decay mode with pp collisions at $\sqrt{s} = 7$ and 8 TeV,” Tech. Rep. ATLAS-CONF-2013-009, CERN, Geneva, Mar 2013.
- [227] G. Abbiendi *et al.*, “Search for doubly charged Higgs bosons with the OPAL detector at LEP,” *Phys. Lett.*, vol. B526, pp. 221–232, 2002, hep-ex/0111059.
- [228] G. Abbiendi *et al.*, “Measurement of heavy quark forward backward asymmetries and average B mixing using leptons in hadronic Z decays,” *Phys. Lett.*, vol. B577, pp. 18–36, 2003, hep-ex/0308051.
- [229] J. Abdallah *et al.*, “Search for doubly charged Higgs bosons at LEP-2,” *Phys. Lett.*, vol. B552, pp. 127–137, 2003, hep-ex/0303026.
- [230] J. Sztuk-Dambietz, “Multi-lepton production and a search for doubly-charged Higgs at HERA,” *Journal of Physics: Conference Series*, vol. 110, no. 7, p. 072042, 2008.
- [231] A. Aktas *et al.*, “Search for doubly-charged Higgs boson production at HERA,” *Phys. Lett.*, vol. B638, pp. 432–440, 2006, hep-ex/0604027.
- [232] V. M. Abazov *et al.*, “Search for Doubly Charged Higgs Boson Pair Production in $p\bar{p}$ Collisions at $\sqrt{s} = 1.96$ TeV,” *Phys. Rev. Lett.*, vol. 108, p. 021801, Jan 2012.

- [233] S. Chatrchyan *et al.*, “Searches for long-lived charged particles in pp collisions at $\sqrt{s}=7$ and 8 TeV,” *JHEP*, vol. 07, p. 122, 2013, 1305.0491.
- [234] G. Aad *et al.*, “Search for long-lived, multi-charged particles in pp collisions at using the ATLAS detector,” *Physics Letters B*, vol. 722, no. 45, pp. 305 – 323, 2013.
- [235] S. Kanemura, K. Yagyu, and H. Yokoya, “First constraint on the mass of doubly-charged Higgs bosons in the same-sign diboson decay scenario at the LHC,” *Phys. Lett.*, vol. B726, pp. 316–319, 2013, 1305.2383.
- [236] M. Muhlleitner and M. Spira, “Note on doubly charged Higgs boson pair production at hadron colliders,” *Phys. Rev. D*, vol. 68, p. 117701, Dec 2003.
- [237] M. Magg and C. Wetterich, “Neutrino Mass Problem and Gauge Hierarchy,” *Phys. Lett.*, vol. B94, p. 61, 1980.
- [238] P. Fileviez Perez, H. H. Patel, M. J. Ramsey-Musolf, and K. Wang, “Triplet scalars and dark matter at the LHC,” *Phys. Rev. D*, vol. 79, p. 055024, Mar 2009.
- [239] T. Araki, C. Q. Geng, and K. I. Nagao, “Dark matter in inert triplet models,” *Phys. Rev. D*, vol. 83, p. 075014, Apr 2011.
- [240] Y. Kajiyama, H. Okada, and K. Yagyu, “Two Loop Radiative Seesaw Model with Inert Triplet Scalar Field,” *Nucl. Phys.*, vol. B874, pp. 198–216, 2013, 1303.3463.
- [241] P. V. Dong, T. P. Nguyen, and D. V. Soa, “3-3-1 model with inert scalar triplet,” *Phys. Rev. D*, vol. 88, p. 095014, Nov 2013.
- [242] S. Banerjee, M. Frank, and S. K. Rai, “Higgs data confronts sequential fourth generation fermions in the Higgs triplet model,” *Phys. Rev. D*, vol. 89, p. 075005, Apr 2014.
- [243] S. Gopalakrishna, T. Mandal, S. Mitra, and G. Moreau, “LHC Signatures of Warped-space Vectorlike Quarks,” *JHEP*, vol. 08, p. 079, 2014, 1306.2656.
- [244] J. Berger, J. Hubisz, and M. Perelstein, “A Fermionic Top Partner: Naturalness and the LHC,” *JHEP*, vol. 07, p. 016, 2012, 1205.0013.
- [245] T. P. T. Dijkstra, L. R. Huiszoon, and A. N. Schellekens, “Supersymmetric standard model spectra from RCFT orientifolds,” *Nucl. Phys.*, vol. B710, pp. 3–57, 2005, hep-th/0411129.

- [246] O. Lebedev, H. P. Nilles, S. Raby, S. Ramos-Sanchez, M. Ratz, P. K. S. Vaudrevange, and A. Wingerter, “A Mini-landscape of exact MSSM spectra in heterotic orbifolds,” *Phys. Lett.*, vol. B645, pp. 88–94, 2007, hep-th/0611095.
- [247] C. Anastasiou, E. Furlan, and J. Santiago, “Realistic composite Higgs models,” *Phys. Rev. D*, vol. 79, p. 075003, Apr 2009.
- [248] N. Vignaroli, “Discovering the composite Higgs through the decay of a heavy fermion,” *JHEP*, vol. 07, p. 158, 2012, 1204.0468.
- [249] N. Bonne and G. Moreau, “Reproducing the Higgs boson data with vector-like quarks,” *Phys. Lett.*, vol. B717, pp. 409–419, 2012, 1206.3360.
- [250] D. Carmi, A. Falkowski, E. Kuflik, and T. Volansky, “Interpreting LHC Higgs Results from Natural New Physics Perspective,” *JHEP*, vol. 07, p. 136, 2012, 1202.3144.
- [251] S. Fajfer, A. Greljo, J. F. Kamenik, and I. Mustac, “Light Higgs and Vector-like Quarks without Prejudice,” *JHEP*, vol. 07, p. 155, 2013, 1304.4219.
- [252] S. A. R. Ellis, R. M. Godbole, S. Gopalakrishna, and J. D. Wells, “Survey of vector-like fermion extensions of the Standard Model and their phenomenological implications,” *JHEP*, vol. 09, p. 130, 2014, 1404.4398.
- [253] J. A. Aguilar-Saavedra, R. Benbrik, S. Heinemeyer, and M. Perez-Victoria, “Handbook of vectorlike quarks: Mixing and single production,” *Phys. Rev. D*, vol. 88, p. 094010, Nov 2013.
- [254] J. A. Aguilar-Saavedra, “Mixing with vector-like quarks: constraints and expectations,” *EPJ Web Conf.*, vol. 60, p. 16012, 2013, 1306.4432.
- [255] G. Moreau, “Constraining extra fermion(s) from the Higgs boson data,” *Phys. Rev. D*, vol. 87, p. 015027, Jan 2013.
- [256] A. Azatov, O. Bondu, A. Falkowski, M. Felcini, S. Gascon-Shotkin, D. K. Ghosh, G. Moreau, A. Y. Rodríguez-Marrero, and S. Sekmen, “Higgs boson production via vectorlike top-partner decays: Diphoton or multilepton plus multijets channels at the LHC,” *Phys. Rev. D*, vol. 85, p. 115022, Jun 2012.
- [257] H. Cai, “Mono Vector-Quark Production at the LHC,” *JHEP*, vol. 02, p. 104, 2013, 1210.5200.

- [258] G. Cacciapaglia, A. Deandrea, D. Harada, and Y. Okada, “Bounds and Decays of New Heavy Vector-like Top Partners,” *JHEP*, vol. 11, p. 159, 2010, 1007.2933.
- [259] S. Schael *et al.*, “Precision electroweak measurements on the Z resonance,” *Phys. Rept.*, vol. 427, pp. 257–454, 2006, hep-ex/0509008.
- [260] “Search for heavy top-like quarks decaying to a Higgs boson and a top quark in the lepton plus jets final state in pp collisions at $\sqrt{s} = 8$ TeV with the ATLAS detector,” 2013.
- [261] G. Aad and B. Acharya, “Search for pair production of heavy top-like quarks decaying to a high- p_T W boson and a b quark in the lepton plus jets final state at $\sqrt{s} = 7$ TeV with the ATLAS detector,” *Phys.Lett. B*, vol. 718, pp. 1284–1302, 1 2013.
- [262] S. Chatrchyan and others., “Search for a Vectorlike Quark with Charge $2/3$ in $t + Z$ Events from pp Collisions at $\sqrt{s} = 7$ TeV,” *Phys. Rev. Lett.*, vol. 107, p. 271802, Dec 2011.
- [263] G. Aad *et al.*, “Search for pair and single production of new heavy quarks that decay to a Z boson and a third-generation quark in pp collisions at $\sqrt{s} = 8$ TeV with the ATLAS detector,” *JHEP*, vol. 11, p. 104, 2014, 1409.5500.
- [264] S. Chatrchyan *et al.*, “Search for heavy, top-like quark pair production in the dilepton final state in pp collisions at ,” *Physics Letters B*, vol. 716, no. 1, pp. 103 – 121, 2012.
- [265] T. A. collaboration, “Search for pair production of heavy top-like quarks decaying to a high- p_T W boson and a b quark in the lepton plus jets final state in pp collisions at $\sqrt{s} = 8$ TeV with the ATLAS detector,” 2013.
- [266] “Search for vector-like top quark partners produced in association with Higgs bosons in the diphoton final state,” Tech. Rep. CMS-PAS-B2G-14-003, CERN, Geneva, 2014.
- [267] “Search for heavy top-like quarks decaying to a Higgs boson and a top quark in the lepton plus jets final state in pp collisions at $\sqrt{s} = 8$ TeV with the ATLAS detector,” Tech. Rep. ATLAS-CONF-2013-018, CERN, Geneva, Mar 2013.
- [268] S. Chatrchyan *et al.*, “Inclusive search for a vector-like T quark with charge in pp collisions at $\sqrt{s} = 8$ TeV,” *Physics Letters B*, vol. 729, pp. 149 – 171, 2014.

- [269] “Search for anomalous production of events with same-sign dileptons and b jets in 14.3 fb^{-1} of pp collisions at $\sqrt{s} = 8 \text{ TeV}$ with the ATLAS detector,” Tech. Rep. ATLAS-CONF-2013-051, CERN, Geneva, May 2013. Not published in the proceedings.
- [270] “Search for pair-produced vector-like quarks of charge $-1/3$ in dilepton+jets final state in pp collisions at $\sqrt{s} = 8 \text{ TeV}$,” Tech. Rep. CMS-PAS-B2G-12-021, CERN, Geneva, 2013.
- [271] “Search for pair-produced vector-like quarks of charge $-1/3$ in lepton+jets final state in pp collisions at $\sqrt{s} = 8 \text{ TeV}$,” Tech. Rep. CMS-PAS-B2G-12-019, CERN, Geneva, 2012.
- [272] “Search for pair production of new heavy quarks that decay to a \mathbf{Z} boson and a third generation quark in pp collisions at $\sqrt{s} = 8 \text{ TeV}$ with the ATLAS detector,” Tech. Rep. ATLAS-CONF-2013-056, CERN, Geneva, Jun 2013.
- [273] S. Chatrchyan *et al.*, “Search for Top-Quark Partners with Charge $5/3$ in the Same-Sign Dilepton Final State,” *Phys. Rev. Lett.*, vol. 112, p. 171801, Apr 2014.
- [274] M. E. Peskin and T. Takeuchi, “Estimation of oblique electroweak corrections,” *Phys. Rev. D*, vol. 46, pp. 381–409, Jul 1992.
- [275] K. Hagiwara, S. Matsumoto, D. Haidt, and C. S. Kim, “A Novel approach to confront electroweak data and theory,” *Z. Phys.*, vol. C64, pp. 559–620, 1994, hep-ph/9409380. [Erratum: *Z. Phys.*C68,352(1995)].
- [276] Z. Kang, J. Li, T. Li, Y. Liu, and G.-Z. Ning, “Light Doubly Charged Higgs Boson via the WW^* Channel at LHC,” *Eur. Phys. J.*, vol. C75, no. 12, p. 574, 2015, 1404.5207.
- [277] L. Lavoura and J. P. Silva, “Oblique corrections from vectorlike singlet and doublet quarks,” *Phys. Rev. D*, vol. 47, pp. 2046–2057, Mar 1993.
- [278] M. Baak, M. Goebel, J. Haller, A. Hoecker, D. Ludwig, K. Moenig, M. Schott, and J. Stelzer, “Updated Status of the Global Electroweak Fit and Constraints on New Physics,” *Eur. Phys. J.*, vol. C72, p. 2003, 2012, 1107.0975.
- [279] J. Cao, L. Wu, P. Wu, and J. M. Yang, “The Z +photon and diphoton decays of the Higgs boson as a joint probe of low energy SUSY models,” *JHEP*, vol. 09, p. 043, 2013, 1301.4641.

- [280] C.-W. Chiang and K. Yagyu, “Higgs boson decays to $\gamma\gamma$ and $Z\gamma$ in models with Higgs extensions,” *Phys. Rev. D*, vol. 87, p. 033003, Feb 2013.
- [281] Y. Okada and L. Panizzi, “LHC signatures of vector-like quarks,” *Adv. High Energy Phys.*, vol. 2013, p. 364936, 2013, 1207.5607.
- [282] P. Minkowski, “ $\mu \rightarrow e\gamma$ at a rate of one out of 109 muon decays?,” *Physics Letters B*, vol. 67, no. 4, pp. 421 – 428, 1977.
- [283] T. Yanagida, “in Proceedings of the Workshop on the Unified Theories and the Baryon Number in the Universe, Tsukuba, Japan, 1979, edited by O. Sawada and A. Sugamoto (KEK, Tsukuba, Japan, 2004),” p. 95.
- [284] A. S. Joshipura and K. M. Patel, “Horizontal symmetries of leptons with a massless neutrino,” *Phys. Lett.*, vol. B727, pp. 480–487, 2013, 1306.1890.
- [285] P. R. M. Gell-Mann and R. Slansky, “in Supergravity, edited by D. Z. Freedman and P. van Nieuwenhuizen (North- Holland, Amsterdam, 1979),”
- [286] S. L. Glashow, “The future of elementary particle physics, NATO Secur. Sci., Ser. B 59, 687 (1980),”
- [287] R. N. Mohapatra and G. Senjanovic, “Neutrino Mass and Spontaneous Parity Nonconservation,” *Phys. Rev. Lett.*, vol. 44, pp. 912–915, Apr 1980.
- [288] W. Konetschny and W. Kummer, “Nonconservation of Total Lepton Number with Scalar Bosons,” *Phys. Lett.*, vol. B70, p. 433, 1977.
- [289] G. Lazarides, Q. Shafi, and C. Wetterich, “Proton Lifetime and Fermion Masses in an $SO(10)$ Model,” *Nucl. Phys.*, vol. B181, pp. 287–300, 1981.
- [290] T. Fukuyama, H. Sugiyama, and K. Tsumura, “Constraints from LFV processes in the Higgs triplet model,” *Journal of High Energy Physics*, vol. 2010, no. 3, pp. 1–18, 2010.
- [291] A. Arhrib, R. Benbrik, M. Chabab, G. Moulhaka, and L. Rahili, “Higgs boson decay into 2 photons in the type II Seesaw model,” *Journal of High Energy Physics*, vol. 2012, no. 4, pp. 1–20, 2012.
- [292] E. J. Chun, H. M. Lee, and P. Sharma, “Vacuum stability, perturbativity, EWPD and Higgs-to-diphoton rate in type II seesaw models,” *Journal of High Energy Physics*, vol. 2012, no. 11, pp. 1–15, 2012.

- [293] P. Dey, A. Kundu, and B. Mukhopadhyaya, “Some consequences of a Higgs triplet,” *Journal of Physics G: Nuclear and Particle Physics*, vol. 36, no. 2, p. 025002, 2009.
- [294] T. Hambye and G. Senjanovic, “Consequences of triplet seesaw for leptogenesis,” *Phys. Lett.*, vol. B582, pp. 73–81, 2004, hep-ph/0307237.
- [295] E. Ma and U. Sarkar, “Neutrino Masses and Leptogenesis with Heavy Higgs Triplets,” *Phys. Rev. Lett.*, vol. 80, pp. 5716–5719, Jun 1998.
- [296] T. Hambye, E. Ma, and U. Sarkar, “Supersymmetric triplet Higgs model of neutrino masses and leptogenesis,” *Nucl. Phys.*, vol. B602, pp. 23–38, 2001, hep-ph/0011192.
- [297] I. Chakraborty and A. Kundu, “Triplet-extended scalar sector and the naturalness problem,” *Phys. Rev. D*, vol. 89, p. 095032, May 2014.
- [298] X. Chang and R. Huo, “Electroweak baryogenesis in the MSSM with vectorlike superfields,” *Phys. Rev. D*, vol. 89, p. 036005, Feb 2014.
- [299] S. Kanemura and H. Sugiyama, “Dark matter and a suppression mechanism for neutrino masses in the Higgs triplet model,” *Phys. Rev. D*, vol. 86, p. 073006, Oct 2012.
- [300] M. Fairbairn and P. Grothaus, “Baryogenesis and Dark Matter with Vector-like Fermions,” *JHEP*, vol. 10, p. 176, 2013, 1307.8011.
- [301] W.-Y. Keung and P. Schwaller, “Long Lived Fourth Generation and the Higgs,” *JHEP*, vol. 06, p. 054, 2011, 1103.3765.
- [302] J. Angle, E. Aprile, *et al.*, “Limits on Spin-Dependent WIMP-Nucleon Cross Sections from the XENON10 Experiment,” *Phys. Rev. Lett.*, vol. 101, p. 091301, Aug 2008.
- [303] P. A. R. Ade *et al.*, “Planck 2013 results. XVI. Cosmological parameters,” *Astron. Astrophys.*, vol. 571, p. A16, 2014, 1303.5076.
- [304] C. Lange, “Beyond Standard Model Higgs,” 2014, 1411.7279.
- [305] G. Aad *et al.*, “Search for Invisible Decays of a Higgs Boson Produced in Association with a Z Boson in ATLAS,” *Phys. Rev. Lett.*, vol. 112, p. 201802, May 2014.
- [306] S. Chatrchyan *et al.*, “Search for invisible decays of Higgs bosons in the vector boson fusion and associated ZH production modes,” *Eur. Phys. J.*, vol. C74, p. 2980, 2014, 1404.1344.

- [307] N. Zhou, Z. Khechadorian, D. Whiteson, and T. M. P. Tait, “Bounds on Invisible Higgs Boson Decays Extracted from LHC $t\bar{t}H$ Production Data,” *Phys. Rev. Lett.*, vol. 113, p. 151801, Oct 2014.
- [308] G. Belanger, B. Dumont, U. Ellwanger, J. F. Gunion, and S. Kraml, “Global fit to Higgs signal strengths and couplings and implications for extended Higgs sectors,” *Phys. Rev. D*, vol. 88, p. 075008, Oct 2013.
- [309] J. R. Espinosa, M. Muhlleitner, C. Grojean, and M. Trott, “Probing for Invisible Higgs Decays with Global Fits,” *JHEP*, vol. 09, p. 126, 2012, 1205.6790.
- [310] M. Heikinheimo, K. Tuominen, and J. Virkajarvi, “Invisible Higgs and Dark Matter,” *JHEP*, vol. 07, p. 117, 2012, 1203.5766.
- [311] E. Komatsu *et al.*, “Seven-year Wilkinson Microwave Anisotropy Probe (WMAP) Observations: Cosmological Interpretation,” *The Astrophysical Journal Supplement Series*, vol. 192, no. 2, p. 18, 2011.
- [312] A. Belyaev, N. D. Christensen, and A. Pukhov, “CalcHEP 3.4 for collider physics within and beyond the Standard Model,” *Comput. Phys. Commun.*, vol. 184, pp. 1729–1769, 2013, 1207.6082.
- [313] G. Belanger, F. Boudjema, A. Pukhov, and A. Semenov, “micrOMEGAs 3: A program for calculating dark matter observables,” *Comput. Phys. Commun.*, vol. 185, pp. 960–985, 2014, 1305.0237.
- [314] R. Bernabei *et al.*, “New results from DAMA/LIBRA,” *Eur. Phys. J.*, vol. C67, pp. 39–49, 2010, 1002.1028.
- [315] C. E. Aalseth *et al.*, “Results from a Search for Light-Mass Dark Matter with a p -Type Point Contact Germanium Detector,” *Phys. Rev. Lett.*, vol. 106, p. 131301, Mar 2011.
- [316] G. Angloher *et al.*, “Results on low mass WIMPs using an upgraded CRESST-II detector,” *Eur. Phys. J.*, vol. C74, no. 12, p. 3184, 2014, 1407.3146.
- [317] E. Behnke *et al.*, “First dark matter search results from a 4-kg CF_3I bubble chamber operated in a deep underground site,” *Phys. Rev. D*, vol. 86, p. 052001, Sep 2012.
- [318] E. Aprile *et al.*, “Limits on Spin-Dependent WIMP-Nucleon Cross Sections from 225 Live Days of XENON100 Data,” *Phys. Rev. Lett.*, vol. 111, p. 021301, Jul 2013.

- [319] L. S. Lavina, “Latest results from XENON100 data,” in *24th Rencontres de Blois on Particle Physics and Cosmology Blois, Loire Valley, France, May 27-June 1, 2012*, 2013, 1305.0224.
- [320] E. Aprile *et al.*, “Dark Matter Results from 225 Live Days of XENON100 Data,” *Phys. Rev. Lett.*, vol. 109, p. 181301, Nov 2012.
- [321] R. Agnese *et al.*, “Silicon detector results from the first five-tower run of CDMS II,” *Phys. Rev. D*, vol. 88, p. 031104, Aug 2013.
- [322] H. B. Li *et al.*, “Limits on Spin-Independent Couplings of WIMP Dark Matter with a p -Type Point-Contact Germanium Detector,” *Phys. Rev. Lett.*, vol. 110, p. 261301, Jun 2013.
- [323] A. E. Chavarria *et al.*, “DAMIC at SNOLAB,” *Phys. Procedia*, vol. 61, pp. 21–33, 2015, 1407.0347.
- [324] M. Ackermann *et al.*, “Dark matter constraints from observations of 25 Milky Way satellite galaxies with the Fermi Large Area Telescope,” *Phys. Rev. D*, vol. 89, p. 042001, Feb 2014.
- [325] O. Adriani *et al.*, “An anomalous positron abundance in cosmic rays with energies 1.5-100 GeV,” *Nature*, vol. 458, pp. 607–609, 2009, 0810.4995.
- [326] L. Accardo *et al.*, “High Statistics Measurement of the Positron Fraction in Primary Cosmic Rays of 0.5-500 GeV with the Alpha Magnetic Spectrometer on the International Space Station,” *Phys. Rev. Lett.*, vol. 113, p. 121101, Sep 2014.
- [327] M. Ackermann *et al.*, “Dark matter constraints from observations of 25 Milky Way satellite galaxies with the Fermi Large Area Telescope,” *Phys. Rev.*, vol. D89, p. 042001, 2014, 1310.0828.
- [328] G. Belanger, F. Boudjema, and A. Pukhov, “micrOMEGAs : a code for the calculation of Dark Matter properties in generic models of particle interaction,” in *The Dark Secrets of the Terascale*, pp. 739–790, 2013, 1402.0787.
- [329] M. G. Aartsen *et al.*, “First Observation of PeV-Energy Neutrinos with IceCube,” *Phys. Rev. Lett.*, vol. 111, p. 021103, Jul 2013.
- [330] A. D. Avrorin *et al.*, “Search for neutrino emission from relic dark matter in the Sun with the Baikal NT200 detector,” *Astropart. Phys.*, vol. 62, pp. 12–20, 2014, 1405.3551.

- [331] M. Boliev, S. Demidov, S. Mikheyev, and O. Suvorova, “Search for muon signal from dark matter annihilations in the Sun with the Baksan Underground Scintillator Telescope for 24.12 years, journal=Journal of Cosmology and Astroparticle Physics,” vol. 2013, no. 09, p. 019, 2013.